Analysis of LmxMPK4 and LmxMPK6, two mitogen-activated protein kinases of *Leishmania mexicana*

DISSERTATION

Submitted for the doctoral degree in natural sciences
- Dr. rer. nat. -
Department of Biology
Faculty of Mathematics, Informatics and Natural Sciences
University of Hamburg, Germany

by
Simona John von Freyend

Glasgow, UK, May 2010

Genehmigt vom Department Biologie
der Fakultät für Mathematik, Informatik und Naturwissenschaften
an der Universität Hamburg
auf Antrag von Frau Professor Dr. I. BRUCHHAUS
Weiterer Gutachter der Dissertation:
Priv.-Doz. Dr. M. WIESE
Tag der Disputation: 23. Juli 2010

Hamburg, den 08. Juli 2010

Professor Dr. Axel Temming
Leiter des Departments Biologie

The goal of science is to build better mousetraps.
The goal of nature is to build better mice.

Table of Contents

Abbreviations

-/-	double-allele deletion
HCl	hydrochloric acid
NaOH	sodium hydroxide
NaCl	sodium chloride
+/-	single-allele deletion
× g	times gravity
℃	degree Celsius
1NA	1-naphthyl-pyrazolo[3,4*d*]pyrimidine
A	ampère
aa	amino acids
ADP	adenosine diphosphate
Amp	ampicillin
AMP	adenosine monophosphate
AP	alcaline phosphatase
APS	ammonium persulfate
ATP	adenosine triphosphate
BNI	Bernhard Nocht Institute for Tropical Medicine
bp	base pairs
BSA	bovine serum albumin
C. elegans	*Caenorhabditis elegans*
C. reinhardtii	*Chlamydomonas reinhardtii*
CaBP	Ca^{2+}-binding proteins
cAMP	cyclic adenosine monophosphate
CD-domain	common docking domain
cGMP	cyclic guanosine monophosphate
CL	cutaneous leishmaniasis
CPB	cysteine protease B
cpm	counts per minute
CSPD	disodium 3-(4-methoxyspiro{1,2-dioxetane-3,2'-(5'-chloro)tricyclo [3.3.1.1]decan}-4-yl)phenyl phosphate
C-terminus	carboxy terminus
Da	Dalton
DABCO	1,4-diazabicyclo[2.2.2]octane
DAG	diacylglycerol
DAPI	4′,6-diamidino-2-phenylindole dilactate
DB	database
DCL	diffuse cutaneous leishmaniasis

ddH_2O	double distilled water
D-domain	docking domain
DHFR-TS	dihydrofolate reductase-thymidylate synthase
DIG	digoxigenin
DMF	N,N-dimethylformamide
DMSO	dimethyl sulfoxide
DNA	deoxyribonucleic acid
dNTP	deoxyribonucleotide triphosphate
DTT	1,4-dithiothreitol
E. coli	*Escherichia coli*
EDTA	ethylenediamine tetraacetic acid
EGF	epidermal growth factor
EGTA	ethylene glycol bis(β-aminoethylether) tetraacetic acid
ER	endoplasmic reticulum
ERK	extracellular signal-related kinase
EtBr	ethidium bromide
F	Farad
FACS	fluorescence-activated cell sorting
FCS	fetal calf serum
g	gramme
gDNA	genomic DNA
GFP	green fluorescent protein
GIPL	glycoinositol phospholipids
gRNA	guide RNA
GS	glutamine synthetase
GSK	glycogen synthase kinase
GST	glutathione-S-transferase
GTP	guanosine triphosphate
h	hours
HEPES	N-2-hydroxyethylpiperazine-N′-2-ethanesulfonic acid
His	hexahistidine
HPLC	high performance liquid chromatography
HRE	hormone response element
HRP	horse radish peroxidase
HSP	heat-shock protein
HYG	hygromycin B resistance marker gene
iFCS	heat-inactivated FCS
IgG	immunoglobulin G
iNOS	inducible nitric oxide synthase

InsP	Inositol phosphate
InsP3	inositol 1,4,5-triphosphate
IPS	*myo*-inositol-1-phosphate synthase
IPTG	isopropyl-β-D-thiogalactopyranoside
IR	intergenic region
JNK	c-Jun N-terminal kinase
kb	kilo base pairs
kDa	kilo Dalton
kDNA	kinetoplast DNA
l	litres
L.	*Leishmania*
LB	Luria-Bertani (broth)
LPG	lipophosphoglycan
M	molar
m/z	mass-to-charge ratio
MALDI-TOF	matrix-assisted laser desorption/ionisation - time of flight
MAP	mitogen-activated protein
MAP2K	MAP kinase kinase
MAP3K	MAP kinase kinase kinase
MAPK	MAP kinase
MBP	myelin basic protein
MCL	mucocutaneous leishmaniasis
MCS	multiple cloning sites
MES	morpholinoethane sulfonic acid
min	minutes
MOPS	morpholinopropane sulfonic acid
mRNA	messenger RNA
MS	mass spectrometry
MS/MS	tandem MS
NEO	neomycin resistance marker gene
N-terminus	amino-terminus
OD	optical density
ORF	open reading frame
PAC	puromycin resistance marker gene
PBS	phosphate-buffered saline
PCR	polymerase chain reaction
PH	pleckstrin homology
PhD	*Philosophiae Doctor*
PHLEO	phleomycin resistance marker gene

PKA	protein kinase A
PKDL	post kala-azar dermal leishmaniasis
PM	peritrophic membrane
PMSF	phenylmethyl sulfonyl fluoride
PSG	promastigote secretory gel
PTB	phosphotyrosine binding
PtdIns	phosphatidylinositol
PtdInsP	phosphatidylinositol phosphate
PV	parasitophorous vacuoles
PVDF	polyvinylidene fluoride
RNA	ribonucleic acid
RNAi	RNA interference
rpm	revolutions per minute
rRNA	ribosomal RNA
RT	room temperature
RTK	receptor tyrosine kinases
s	seconds
SAP	shrimp alkaline phosphatase
SDR	substrate-determining residue
SDS	sodium dodecyl sulphate
SDS-PA	SDS-polyacrylamide
SDS-PAGE	SDS-PA gel electrophoresis
SH	Src homology
SL	spliced leader
SSC	standard saline citrate
T.	*Trypanosoma*
TBS	Tris-buffered saline
TBV	transmission-blocking vaccines
TEM	transmission electron microscopy
TEMED	N,N,N′,N′-tetramethylethylenediamine
TLCK	Nα-tosyl-L-lysine chloromethyl ketone hydrochloride
Tris	tris(hydroxymethyl)aminomethane
TRP	transient receptor potential
U	units
UTR	untranslated region
UV	ultraviolet
V	volt
v/v	volume per volume
VL	visceral leishmaniasis

w/v	weight per volume
WHO	World Health Organisation
X-Gal	5-Bromo-4-chloro-3-indolyl-β-D-galactopyranoside

1. Introduction

1.1 *Leishmania* and Leishmaniasis

In 1903 William Leishman of Glasgow, professor of pathology at Netley, UK, published an article in the British Medical Journal, identifying several small round or oval bodies in the spleen and liver of a patient suffering from what he called “Dum-Dum fever” (Leishman, W. B. 1903). He associated the bodies with similar ones found in the blood, liver and spleen of rats which had died of trypanosomiasis. His findings were confirmed by Charles Donovan through observations he had made in smears taken from patients in Madras, India (Donovan, C. 1903). The described bodies were consequently named Leishman-Donovan bodies and the parasite whose intracellular stage the bodies constitute was named *Leishmania donovani* (*L. donovani*) (Bailey, H. et al. 1959). In subsequent years it became evident that parasites of the genus *Leishmania* are responsible for a wide range of diseases known as leishmaniasis.

1.1.1 Taxonomy

The genus *Leishmania* comprises about 30 different species that infect mammals and reptiles, which are further subdivided into the subgenera *Leishmania* (*L.*) and *L. (Viannia).* This classification is based on observations that the species of the subgenus *L.*, to which *L. mexicana* belongs, develop exclusively in the midgut and foregut of the sand fly host, while *L.* (*Viannia*) develop in an additional phase in the hindgut (Lainson, R. et al. 1987). The protists *Leishmania* group within the order Trypanosomatida of the class kinetoplastida. One of the most characterising features of the kinetoplastida is the possession of a region of unique, highly condensed mitochondrial DNA known as the kinetoplast. There are, however, many more striking features shared by members of this group, like intricate RNA-editing and trans-splicing of all mRNA transcripts, which will be discussed in more detail later. The kinetoplastids contain a wide range of free-living organisms and parasites of plants and vertebrates, with parasitism having evolved separately at least four times (Simpson, A. G. et al. 2006). The most important parasites from a human perspective are found within the genera *Trypanosoma* (*T.*) and *Leishmania*, which consist of flagellated cells with a digenetic life cycle. *T. brucei* is the cause of African sleeping sickness, whereas *T. cruzi* is responsible for the American Chagas disease. Twenty species of *Leishmania* are known to be pathogenic in humans.

1.1.2 Life cycle of *Leishmania*

Leishmania parasites alternate in their digenetic life cycle between the profoundly different basic cell forms of extracellular promastigotes and intracellular amastigotes within the phlebotomine sand fly hosts and vertebrate hosts, respectively (Fig. 1).

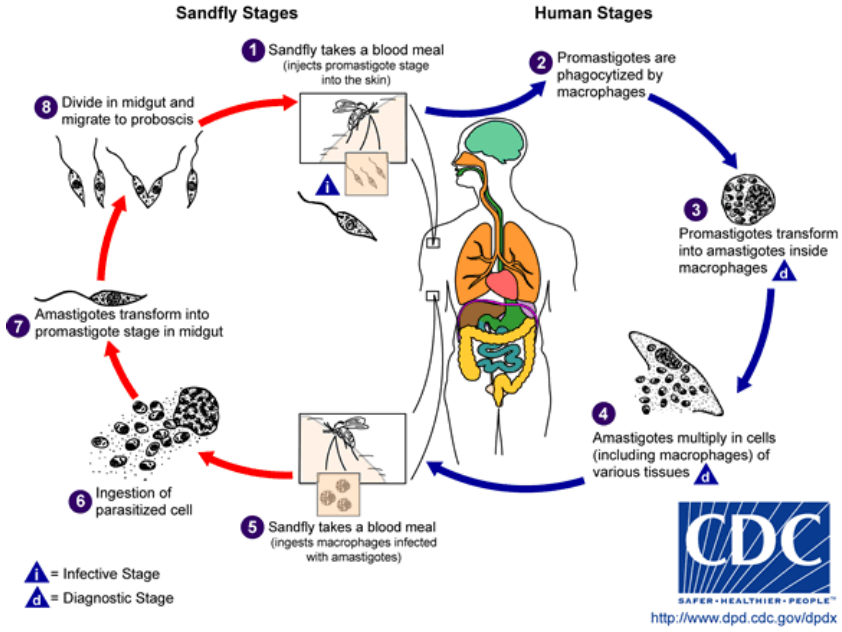

Figure 1, Life cycle of *Leishmania*
1, blood meal of an infected sand fly, transfers promastigotes to the mammalian host; 2, promastigotes are phagocytosed by leukocytes; 3, differentiation of promastigotes into amastigotes within the parasitophorous vacuoles; 4, intracellular proliferation of amastigotes; 5, sand fly blood meal on infected mammalian host; 6, ingestion of the blood meal releases amastigotes; 7, amastigotes differentiate into the insect stage promastigotes; 8, progression through numerous promastigote forms, migration to proboscis.
Source: **http://www.dpd.cdc.gov/dpdx**

The following addresses the life cycle involving humans as mammalian hosts. Although there have been few reports on congenital (Eltoum, I. A. et al. 1992) or venereal (Symmers, W. S. 1960) transmission of leishmaniasis as well as transmission by blood transfusions (Bruce-Chwatt, L. J. 1972) or needles of drug addicts (Cruz, I. et al. 2006), the most common path of transmission of the disease is by the bite of an infected sand fly. The small, two to three millimetre long sand flies of the order Diptera and the subfamily Phlebotominae are referred to as phlebotomine sand flies and include all known vectors of leishmaniasis in the genera *Phlebotomus* (*P.*) in the Old World (Swaminath, C. S. et al. 1942) and *Lutzomyia* (*Lu.*) in the New World. There are 500 known phlebotomine species but only 31 have been confirmed as vectors of *Leishmania* with a further 43 being suspected vectors (Killick-Kendrick, R. 1999). *Lu. olmeca olmeca* is the natural vector of *L. mexicana*, which was the focus of this study (Bates, P. A. 2007). All sand flies naturally feed on sugar sources like plant saps and honeydew of aphids (Cameron, M. M. et al. 1995), but during the production of eggs female sand flies additionally feed on blood.

Parasites are taken up with the blood meal from an infected vertebrate host and are released from ruptured macrophages in the digestive tract of the sand flies, where they undergo differentiation into several distinct promastigote stages (Bates, P. A. et al. 2004). There have been reports on the rare event of a genetic exchange taking place within a sexual cycle in the sand fly (Akopyants, N. S. et al. 2009). Within less than 12 hours of ingestion the blood meal bolus is enclosed by a peritrophic matrix (PM, previously peritrophic membrane). This acellular coating, composed of chitinous microfibrils, proteoglycans and proteins is produced by epithelial cells and lines the gut lumen of most insects, protecting against rough food particles and pathogens (Shao, L. et al. 2001). The production of type 1 PMs of hematophagous insects is directly caused by gut distension after a blood meal (Tellam, R. L. et al. 1999). In the case of *Leishmania* the PM curiously does not prevent pathogen infection, but instead provides protection for the differentiating promastigotes, which are highly susceptible to gut proteases (Pimenta, P. F. et al. 1997). Released amastigotes differentiate into slow-moving, small procyclic promastigotes with short flagella, replicating expeditiously within the PM. The following transformation of procyclics into long and thin nectomonads coincides with the disintegration of the PM, causing the release of nectomonads into the gut lumen. It is still a matter of debate if the chitinases, which instigate the degeneration of the PM, are produced by the sand fly or the parasite itself and it is possible that there are differences between *Leishmania* species (Rogers, M. E. et al. 2008; Sadlova, J. et al. 2009). As soon as nectomonads are released into the midgut lumen they attach between microvilli of epithelial cells to avoid elimination from the midgut during digestion. It was shown for *L. major* that the abundant surface molecule lipophosphoglycan (LPG) specifically binds to the midgut galectin receptor PpGalec of the sand fly vector *P. papatasi* (Kamhawi, S. et al. 2004). The binding mechanism of *Leishmania* to the epithelial cells seems to be responsible for the classification of sand fly vectors into specific hosts, supporting the development of only one *Leishmania* species which attaches to the midgut by LPG, and permissive hosts, capable of transmitting a wide range of *Leishmania* species, which bind to the epithelium with a lectin-like protein, independent of LPG (Myskova, J. et al. 2007). Nectomonads migrate towards the anterior midgut and differentiate into the shorter leptomonads, which go through the second round of multiplication in the insect host, leading to a massive infection of the anterior midgut. Leptomonads produce the promastigote secretory gel (PSG), a matrix structure composed mainly of filamentous proteophosphoglycan, which is thought to trigger metacyclogenesis and is responsible for the ‘blocked fly’ effect (Rogers, M. E. et al. 2002). The transformation of leptomonads into non-dividing metacyclics gives rise to a large number of these small, agile and highly infective promastigote forms at the stomodeal valve, which separates the midgut from the foregut and the proboscis. The other parasite form found at the stomodeal valve was named haptomonads. It is unclear whether this non-motile promastigote form arises from nectomonads or leptomonads, but

they have been shown to attach at the stomodeal valve and to each other, forming a parasite plug and to produce chitinases which damage the stomodeal valve (Rogers, M. E. et al. 2008). This pathology together with the physical force of the PSG causes the opening of the stomodeal valve, allowing parasites access to the foregut and proboscis. The damaged stomodeal valve, in combination with the 'blocked fly' effect additionally instigate an impaired feeding by the fly. Flies ingest smaller amounts of blood, probe more, feed longer and transmit *Leishmania* parasites by regurgitation (Kamhawi, S. 2006). An overview of the different promastigote stages within the phlebotomine sand fly is given in Fig. 2.

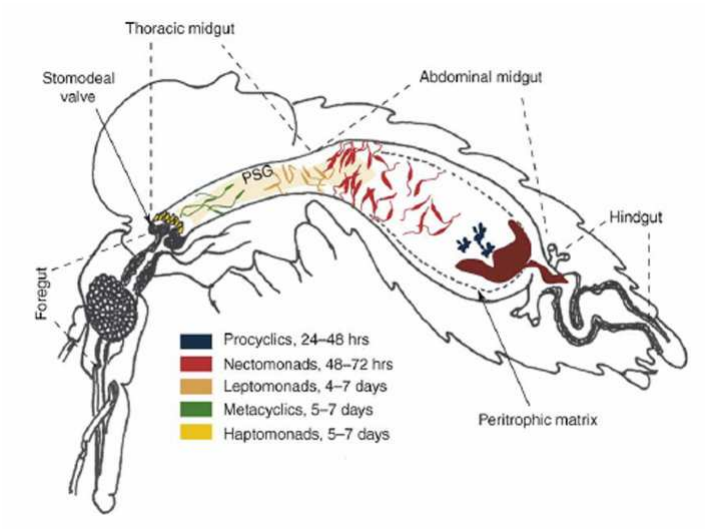

Figure 2, The different *Leishmania* promastigote forms in the phlebotomine sand fly vector
Source: (Kamhawi, S. 2006)

Depending on the causative *Leishmania* species and circumstances of infection, leishmaniasis can be an anthroponosis, transmitted solely between humans, or a zoonosis, which additionally infects domestic or wild animals as reservoir hosts. The bite of a female phlebotomine sand fly delivers parasites together with a mixture of sand fly saliva and PSG into the skin of the vertebrate host. Both PSG and sand fly saliva play a role as disease exacerbating factors by influencing the immune system and thus promoting parasite survival and replication. Lysates from sand fly saliva were shown to decrease the levels of interferon γ (IFN-γ), tumour necrosis factor α (TNF-α) and interleukin 6 (IL-6), among several other effects on the immune system (Rohousova, I. et al. 2006). A single *Leishmania* antigen LACK (*Leishmania* homologue of receptor for activated C-kinase) leads to the production of IL-4. All these factors favour the development of a Th2 immune response, which supports the development of the disease, whereas a Th1 immune response leads to the clearing of *Leishmania* from the host organism (Rogers, K. A. et al. 2002). A Th1 response involves among other events the production of nitric oxide by activated macrophages to kill *Leishmania* parasites.

Activation of macrophages is promoted by IFN-γ and TFN-α and indirectly by IL-12. IL-4 circumvents macrophage activation by blocking IL-12 binding to cells and incidentally inhibiting IFN-γ production. Intracellular amastigotes play an additional role in the establishment and maintenance of a Th2 response, by influencing macrophage signalling accordingly (Kima, P. E. 2007). Metacyclic promastigotes deposited by sand flies also need to avoid complement-mediated lysis to successfully invade phagocytic cells and establish infection. The serine/threonine protein kinase, LPK-1, which is homologous to MAP2Ks was shown to play a role in circumventing the activation of the alternative complement pathway by inhibiting through phosphorylation the activating cleavage of the complement factors C3, C5 and C9 (Hermoso, T. et al. 1991; Li, S. et al. 1996). The shedding of C5b-C9 complexes from the parasite surface also seems to have a part in the evasion of complement-mediated lysis (Puentes, S. M. et al. 1990). *Leishmania* parasites however require a certain opsonisation to effectuate invasion of their host cells by phagocytosis. This is partly achieved through the inactivation of the bound complement factor C3b by the leishmanial surface metallo-protease gp63, which obviates complement activation and instead promotes phagocytic clearance (Schlagenhauf, E. et al. 1998). The serum component C-reactive protein (CRP) also binds to the surface of metacyclic promastigotes and enhances their uptake by macrophages (Culley, F. J. et al. 1996). Phagocytosis by macrophages is initiated by the binding of parasites to the cell surface, which can occur on several receptors, including not only the complement receptors, but also receptors for mannose-fucose, fibronectin and CRP (Solbach, W. et al. 2000). Entry into macrophages seems to occur also through the phagocytosis of infected, apoptotic polymorphonuclear neutrophil granulocytes, which are the first leukocytes to reach the site of infection (van, Zandbergen G. et al. 2004). Phagocytosis leads to the localisation of *Leishmania* in phagosomal vesicles, which fuse with endocytic organelles, thus forming a parasitophorous vacuole (PV). Depending on *Leishmania* species, PVs either envelop all parasites together (*L. mexicana* complex) or tightly enclose separate parasites within their own PV (*L. donovani* complex). Within the PV parasites differentiate to amastigotes, the small, immobile intracellular form with a very short flagellum that hardly extends beyond the flagellar pocket. Differentiation was originally thought to be triggered by the acidic pH in the PV and temperature differences between the mammalian and insect hosts alone (Zilberstein, D. et al. 1994) and these factors can indeed prompt the *in vitro* differentiation of promastigotes into axenic amastigotes. However, it has become clear in recent years that other factors like the binding of CRP (Bee, A. et al. 2001) and proteins of the heat shock response (Wiesgigl, M. et al. 2001b) also play an important role in the differentiation of metacyclic promastigotes to amastigotes *in vivo*. Amastigotes proliferate in macrophages, which eventually leads to the lysis of the host cell and the fresh infection of nearby macrophages. The long-term persistence of *Leishmania* in vertebrate hosts is a

frequent phenomenon and has been associated with the localisation of parasites in fibroblasts (Bogdan, C. et al. 2000).

1.1.3 Epidemiology and Clinical manifestation

Leishmania parasites are responsible for a whole complex of diseases with various manifestations, ranging from cutaneous and mucocutaneous to visceral forms of leishmaniasis. The distribution of leishmaniasis is closely connected with the prevalence of the insect vector. Phlebotomine sand flies are found in many of the world's inter-tropical and temperate regions, being most prevalent in developing countries. The World Health Organization (WHO) estimates that approximately 14 million people in 88 countries are affected by leishmaniasis, with a further 350 million people at risk of infection and 1.5 – 2 million new cases each year. This makes the leishmaniases the world-wide third most important vector-borne disease (Reithinger, R. et al. 2007), but as only 32 of the 88 affected countries require cases of leishmaniasis be reported, the actual number of cases could be even higher. In 33 of the 88 affected countries, leishmaniasis is endemic (Desjeux, P. 2004). The only continents not affected by leishmaniasis are Australia and Antarctica. On the American continent, leishmaniasis occurs from Texas, USA, to northern Argentina with the exception of Uruguay and Chile. Large parts of Africa are just as affected by various forms of the disease as south-west Europe and many countries in the middle east and Asia, notably India, Bangladesh, Sudan and Nepal. Over 90% of the world's cases of visceral leishmaniasis (VL) occur in those four countries and Brazil, whereas 90% of cutaneous leishmaniasis (CL) cases are found in Afghanistan, Algeria, Brazil, Iran, Peru, Saudi Arabia and Syria (Desjeux, P. 2004). Fig. 3 shows a map of the world wide distribution of leishmaniasis.

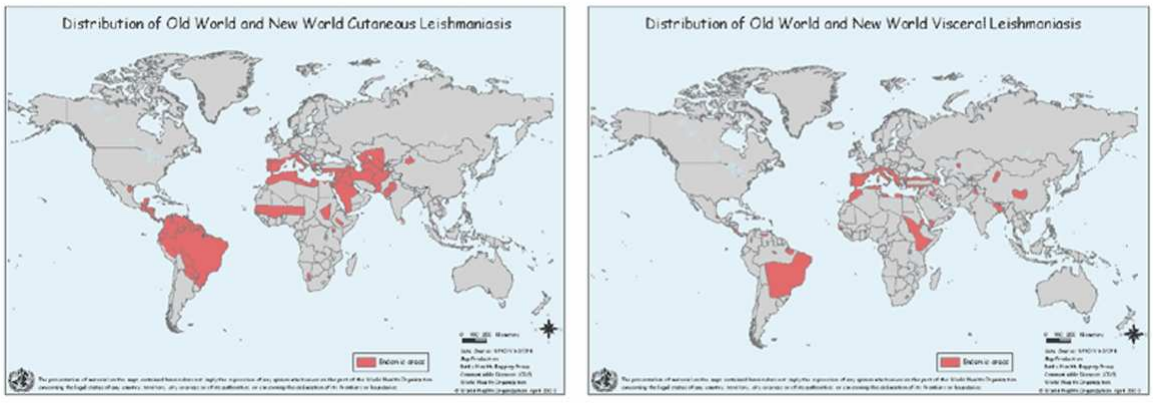

Figure 3, world wide distribution of cutaneous and visceral leishmaniasis
Source: WHO (http://www.who.int/leishmaniasis/leishmaniasis_maps/en/index.html)

Outbreaks of the disease in different areas of the world have dramatically increased in recent years (Desjeux, P. 2004). Although part of this increase in numbers is certainly due

to a more stringent control and better diagnosis, there are many factors which contribute to a spread of leishmaniases. Large migrations of people due to economic reasons, occupation or civil unrest as well as poor living conditions leading to malnutrition facilitate outbreaks of the disease (Cerf, B. J. et al. 1987; Desjeux, P. 2004). Deforestation, colonisation of previously rural areas and urbanisation equally play a role in the rise of leishmaniasis cases (Desjeux, P. 2001). Another important factor has been the co-infection of patients with HIV and leishmaniasis. High parasitaemia, together with a high tendency of relapsing and low therapeutic success rates in cases with HIV/*Leishmania* co-infections lead to higher numbers of human reservoirs (Cruz, I. et al. 2006). Diseases caused by the parasite *Leishmania* can be divided according to symptoms into two major types, cutaneous and visceral leishmaniasis (Fig. 4). Clinical manifestation and severity of symptoms are determined by several factors, like the immune status and genotype of the infected patients, as well as the species of infecting *Leishmania* and the transmitting vector (Murray, H. W. et al. 2005).

Cutaneous leishmaniasis (CL)

The mildest form of the leishmaniases is generally a result of infection with parasite species of the subgenus *Viannia*, *L. major*, *L. aethiopica*, species of the *L. tropica* complex and *L. mexicana,* but can be caused by all *Leishmania* species which infect humans. Clinical symptoms of CL, also known as Bagdad boil, oriental boil or Aleppo boil, are restricted to the skin of patients in the form of lesions, which usually occur on exposed body parts at the site of the insect bite. In the old world CL lesions appear mostly in the form of papules, nodules and nodule-ulcers, but new world CL manifests mainly with ulcerative lesions. Lesions are generally self healing, but can lead to permanent scarring and consequently to social stigmatism. Diffuse CL (DCL) can develop in patients suffering from CL, who have an impaired cell-mediated immune response and are infected by some members of the *L. mexicana* complex and *L. aethiopica*. DCL leads to a high number of chronic, not self-healing skin lesions which can cover the entire body of a patient and are difficult to treat. Post kala-azar dermal leishmaniasis (PKDL) occurs in east Africa and the Indian subcontinent in patients several years after seemingly successful treatment of VL. Lesions of PKDL are usually localised around the mouth before they become more generalised. The most severe form of CL is mucocutaneous leishmaniasis (MCL), which arises in 1 – 10 % of infections with *L. braziliensis, L. panamensis* and *L. guyanensis* 1 – 5 years after the original CL lesion has healed. Lesions of MCL spread to mucosal tissues predominantly of the nose and mouth, where they cause perforation of the nasal septum, destructive inflammatory lesions of the nasal, pharyngeal and laryngeal mucosa and thereby severe disfigurement of the patient. Inflammatory infections associated with MCL can be potentially life threatening. An estimated 1 – 1.5 million new cases of CL occur each year.

Visceral leishmaniasis (VL)

Known as kala-azar, this severe form of leishmaniasis is generally lethal when left untreated. The most important *Leishmania* species causing VL are *L. donovani* on the Indian subcontinent, in Asia and Africa and *L. infantum* or *L. chagasi* in south Western Europe, southwest and central Asia and South America. *L. tropica* and *L. amazonensis* can at times also induce VL. Typical symptoms of VL are fever, anaemia, substantial weight loss and severe hepatosplenomegaly.

Figure 4, Different forms of cutaneous leishmaniasis and visceral leishmaniasis
A, prominent facial lesion of cutaneous leishmaniasis; B, typical lesion (Chiclero ulcer) evoked by *L. mexicana* infection; C, hepatosplenomegaly and wasting in a case of visceral leishmaniasis; D, diffuse cutaneous leishmaniasis induced by *L. panamensis*; E, post kala-azar dermal leishmaniasis in a man in India; F, severe facial disfigurement caused by mucocutaneous leishmaniasis.
Source: (Murray, H. W. et al. 2005)

1.1.4 Treatment and prevention of Leishmaniasis

Physical treatments like irradiation, freezing with liquid nitrogen, infrared and photodynamic climatotherapy are used successfully against milder cases of CL (Le, Pape P. 2008). Additionally there are several antileishmanial drugs currently in use. In most countries pentavalent antimonials (SbV) like N-methyl meglumine antimonite (Glucantime®) or sodium stibogluconate (Pentostam®) are used as first-line treatment. These compounds have been used against leishmaniasis for about 75 years but their mode of action is still not fully understood. SbV is generally regarded as a pro-drug that is converted into the highly active form trivalent antimony (SbIII) within the parasite (Wyllie,

S. et al. 2004), but SbV itself also possesses antileishmanial activity (Ephros, M. et al. 1999). SbV interferes with glucose catabolism and macromolecular biosynthesis, like fatty acid β-oxidation (Berman, J. D. et al. 1987), but specific targets have not been identified. Antimonials additionally provoke the production of reactive oxygen species like superoxide, nitric oxide and hydrogen peroxide in the parasitophorous vacuoles. This common host cell defence mechanism, known as respiratory burst, ultimately leads to the death of amastigotes in an apoptosis-like mechanism (Sudhandiran, G. et al. 2003). *Leishmania* rely on a functioning trypanothione system in the defence against oxidative stress as they lack catalase and metabolise hydrogen peroxide using trypanothione-dependent peroxidases. Observations that SbIII inhibits trypanothione reductase *in vitro* and most likely *in vivo* and causes efflux of trypanothione and glutathione *in vivo* have linked effects of SbIII in the parasite with the initiation of apoptosis (Wyllie, S. et al. 2004). Despite the wide usage of antimonials, they are no ideal treatment for leishmaniasis, as they display high toxicity and various side effects and resistance against them is on the rise (Rijal, S. et al. 2003). First-line treatment in the Indian state of Bihar has already been changed from pentavalent antimony to amphotericin B, as failure rate of the former had risen to 65 % (Sundar, S. et al. 2000). Amphotericin B deoxycholate (Fungizone®), originally developed as an antifungal, is highly effective especially against Indian kala-azar. However, it requires lengthy administrations in the form of infusions and leads to serious adverse reactions like renal toxicity. Consequently admission to hospital for the duration of treatment is required, which is mostly inapplicable for patients in developing countries. Amphotericin B leads to parasite lysis by binding to membrane ergosterol, thereby inducing pores in the cell membrane. The major cause for toxicity of Amphotericin B is its high affinity for low density lipoproteins, which can be prevented by change to a liposomal formulation. Liposomal Amphotericin B (AmBisome®) cures leishmaniasis with a rate of up to 100% during a 3 to 5 day treatment and is consequently the drug of choice in southern Europe (Maltezou, H. C. 2010). Its high cost, however, makes it unaffordable in developing countries. Efforts are being made to create new cheaper formulations and to reduce the cost of liposomal Amphotericin B (Croft, S. L. et al. 2006). Miltefosine (Impavido®), which is currently licensed in India, Colombia and Germany, is the only available oral treatment and the most promising antileishmanial drug to date. The hexadecylphosphocholine is believed to interfere with a number of cellular processes. It has been proposed to affect the synthesis of glycophosphatidylinositol (GPI) anchors that link proteins like LPG to the membrane, by perturbing ether-remodelling through the inhibition of acyl-coenzyme A acyl-transferase (Lux, H. et al. 2000). It additionally seems to affect ether lipid metabolism and signal transduction (Le, Pape P. 2008; Lux, H. et al. 1996). Miltefosine is highly efficient especially against Indian VL, but displays teratogenic adverse effects in test animals (Sindermann, H. et al. 2006). It is therefore not indicated for use in pregnant women and requires efficient birth control for women of child-bearing

age during and 2 months after treatment. The aminoglycoside antibiotic paromomycin (Humatin®) was licensed for treatment of VL in India in 2007 and effectively kills both promastigotes and amastigotes. It is the cheapest treatment available to date and entails low adverse effects, yet requires a 21 day treatment of intramuscular injections (Davidson, R. N. et al. 2009). Resistance against paromomycin was readily induced in promastigotes *in vitro* and constitutes a possible future predicament (Maarouf, M. et al. 1998). Combination therapies of the described drugs are used to avoid the emergence of resistance, shorten treatment length, lower costs and generally enhance treatment efficiency (van, Griensven J. et al. 2010). The threat of growing and emerging resistances and the various inadequacies of existing drugs, however, demonstrate the urgency for the development of new drugs against leishmaniasis.

1.2 Genome organisation and gene regulation in *Leishmania*

Leishmania parasites are diploid organisms and hold a genome of about 34 Mb with chromosomes ranging in size from 0.3 to 2.8 Mb. Old World species have 36 chromosomes and New World parasites of the *L. braziliensis* complex have 35, while those of the *L. mexicana* complex have 34 (Myler, P. J. et al. 2000). Up to date the genomes of *L. braziliensis* (strain MHOM/BR/75/M2904), *L. infantum* (strain JPCM5), *L. major* (strain Friedlin) and, only recently, *L. mexicana* (strain MHOM/GT/2001/U1103) have been successfully sequenced. The G/C content of *Leishmania* genomes was revealed to be comparatively high (*L. major*, 63%; human, 40-45%). Micro array analyses of RNA levels in *L. major*, *L. infantum*, *L. mexicana* and *L. braziliensis* revealed a mostly constitutive expression of genes, with only around 10% of genes showing significant alterations of mRNA levels (Depledge, D. P. et al. 2009; Holzer, T. R. et al. 2006; Leifso, K. et al. 2007b; Rochette, A. et al. 2009). Studies of mRNA levels of *L. major*, *L. infantum* and *L. braziliensis* have similarly shown that only a maximum of 6% of compared genes are differentially expressed between the species (Depledge, D. P. et al. 2009). The genomes of these parasites also show a very high synteny with more than 99% of genes conserved and high amino acid identity within genes (Peacock, C. S. et al. 2007). All these findings demonstrate that the highly divergent disease patterns that *L. major*, *L. infantum* and *L. braziliensis* evoke are not due to large differences in the genome or in transcriptional regulation but either depend on a small number of genes, on translational regulation or on different factors than the genome. *Leishmania* transcription leads to polycistronic precursor RNAs and regulation takes place at the mRNA level, mainly through mRNA processing and stability. Consequently, RNA polymerase II promotors are almost lacking in kinetoplastids, with the only exception of the promotor for the spliced leader (SL) sequence. The occurrence of transcription factors in *Leishmania* is equally

lower than in most other eukaryotes (Ivens, A. C. et al. 2005). A high number of proteins with CCCH-type zinc finger domains typical for RNA-binding proteins, on the other hand, further supports the notion of regulation on mRNA level (Ivens, A. C. et al. 2005). Precursor RNAs are processed by *trans*-splicing, a process which adds the 39-nucleotide SL sequence to the 5'-end of transcripts, generally at the first AG di-nucleotide downstream of regulating U-rich polypyrimidine tracts in the 5'-untranslated region (UTR). Each SL is capped at the 5'-end with 7-methylguanosine. Polyadenylation of the 3'-end of each transcript is coupled with *trans*-splicing, releasing a monocistronic, capped and polyadenylated mRNA. Polyadenylation is not depending on consensus poly(A) signal sequences, like in higher eukaryotes, as it simply occurs 100 to 400 nucleotides upstream of the splice acceptor site of the downstream gene, depending on species (Clayton, C. E. 2002). *Cis*-splicing, as it is the common occurrence in higher eukaryotes, exists in *Trypanosoma*, but plays a minor role as the genome contains virtually no introns (Liang, X. H. et al. 2003). No introns have so far been discovered in *Leishmania* (Myler, P. J. et al. 2000). Members of the order kinetoplastida are characterised by the existence of a kinetoplast, a term for the highly condensed, circular DNA of the single, large mitochondrion. The kinetoplast DNA (kDNA) makes up 10 to 15% of the total DNA, contains high copy numbers of genes and appears in the microscope as a strongly DAPI-stainable bean shape near the flagellum. The kinetoplast contains two types of circular DNA molecules. 5,000 – 10,000 non-identical copies of minicircles encode so-called guide RNAs (gRNA). Maxicircles on the other hand occur as 25 to 50 identical copies, with a size from 20 to 39 kb (minicircles: 0.5 – 2.8 kb) and encode mitochondrial proteins alongside rRNAs and some gRNAs. The transcripts for mitochondrial proteins undergo extensive sequence modification during a process called RNA editing, which in this form is typical for kinetoplastids. An editosome catalyses the RNA editing, which is initiated by the specific binding of gRNAs to the unedited transcript. Using the sequence of gRNAs as template, uridines are inserted into or deleted from the primary transcript, generating mature mRNA ready for translation. RNA interference (RNAi) does not exist in most *Leishmania* species with the possible exception of *L. braziliensis* (Peacock, C. S. et al. 2007). Null mutants in *Leishmania* can be generated by the replacement of genes with resistance marker genes through homologous recombination (Cruz, A. et al. 1991).

1.3 Metabolism in kinetoplastids

The metabolism of trypanosomatids reflects the circumstances dictated by their unique life cycles and has proven to be a fascinating source in the search of potential drug targets. It has not been possible so far to fully elucidate all metabolic pathways of trypanosomatids, but recent methodical advances have led to a large amount of new information on this topic (Opperdoes, F. R. et al. 2007; Saunders, E. C. et al. 2010; Scheltema, R. A. et al.

2010). Despite the expected similarities between the metabolism of *Leishmania* and *Trypanosoma* a number of intriguing differences have also been found, which arise most likely from divergences in the parasites environment. The insect stages of *T. brucei* and *Leishmania* for example have to deal with vastly different carbon sources for their energy metabolism, depending on the food sources of their respective hosts. Tsetse flies feed on blood all the time, whereas sand flies additionally ingest nectar. *T. brucei* procyclics are therefore mainly confronted with a protein-rich environment, because the carbohydrates originally included in the blood meal are not replenished after consumption by insect host and parasites (Bringaud, F. et al. 2006). *Leishmania* promastigotes on the other hand reside in an environment containing plant starch and disaccharides (Bringaud, F. et al. 2006). The constant and abundant presence of glucose within the bloodstream of vertebrate hosts, allows *T. brucei* bloodstream forms to contain the simplest form of energy metabolism of the trypanosomatid life forms, relying solely on glycolysis as ATP source (Hellemond, J. J. et al. 2005). *T. brucei* procyclics, as well as *Leishmania* promastigotes and amastigotes on the other hand cannot rely on the continuous presence of glucose, due to their respective environments and therefore use a much more elaborate range of pathways for their energy metabolism, although they prefer glucose when available (Bringaud, F. et al. 2006; Opperdoes, F. R. et al. 2007; Saunders, E. C. et al. 2010). *Leishmania* amastigotes must scavenge their essential nutrients from the amino acid rich phagolysosome of macrophages where they reside. In addition to scavenging essential amino acids, glycoproteins and sugars, *Leishmania* also scavenge purine, haem, vitamins and cations (iron, magnesium) from the phagolysosome and integrate host-derived glycosphingolipids in their cell membranes (Burchmore, R. J. et al. 2001; McConville, M. J. et al. 2007). It has been suggested that amastigotes use fatty acids as their major carbon source for energy metabolism (Hart, D. T. et al. 1982), but this now seems unlikely since it has transpired that they lack two essential enzymes of the glyoxylate pathway (Opperdoes, F. R. et al. 2007). The glyoxylate cycle of plants and bacteria converts acetyl-CoA, the end product of fatty acid β-oxidation, into malate and oxaloacetate, the precursors for gluconeogenesis. All enzymes of the citric acid cycle or tricarboxylic acid (TCA) cycle are present in *Leishmania* (Opperdoes, F. R. et al. 2007), but it is a matter of debate whether trypanosomatids use the complete cycle to fully oxidise pyruvate and other metabolic intermediates like malate and fumarate to CO_2 (Saunders, E. C. et al. 2010). Indeed it was shown for *T. brucei* that the enzymes of the TCA cycle are mainly involved in non-cyclic pathways, like amino acid degradation via α-ketoglutarate and succinate, fatty acid biosynthesis via acetyl-CoA and citrate and gluconeogenesis via malate (Bringaud, F. et al. 2006; van Weelden, S. W. et al. 2005). The proposed functions of the TCA-cycle as well as other essential pathways of trypansomatid energy metabolism are depicted in Fig. 5. One of the central enzymes in the TCA-cycle is malate dehydrogenase, which converts malate to oxaloacetate.

Trypanosomatids contain three versions of this enzyme, one located in the mitochondrion, one in the cytoplasm and one in the glycosomes. Malate can be transported through organelle membranes and therefore links the mitochondrial TCA-cycle with the gluconeogenesis which occurs partially in the cytoplasm and in the glycosomes. The expression of malate dehydrogenase is differentially regulated in *T. brucei*, with only the cytosolic malate dehydrogenase expressed in bloodstream forms, which lack gluconeogenesis, relying solely on glycolysis for their energy metabolism (Aranda, A. et al. 2006).

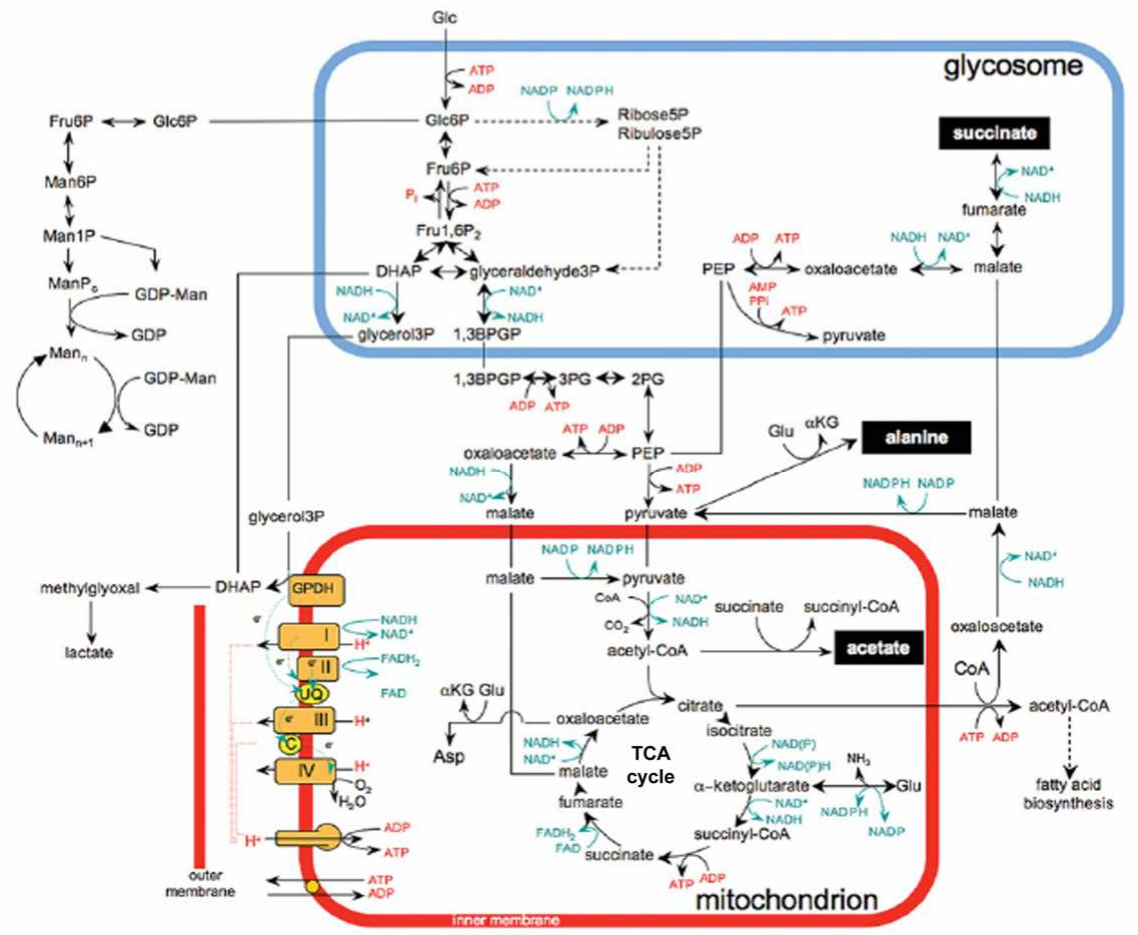

Figure 5, Schematic depiction of central carbon metabolism in *Leishmania* promastigotes
The metabolites depicted inside a black box are the major secreted end-products; dotted arrows depict pathway steps including multiple enzymes, which are not shown in this figure; I – IV, complexes of the respiratory chain; αKG, α-ketoglutarate; Glu, glutamate; GPDH, FAD-dependent glycerol 3-phosphate dehydrogenase; Glc6P, glucose-6-phosphate; Man6P, mannose-6-posphate; ManPc, Mannose-1,4-cyclic-phosphate; Man_x, mannogen oligomers; PEP, phosphoenolpyruvate; 2PG, 2-phosphogylcerate; 3PG, 3-phosphoglycerate.
Source: (Saunders, E. C. et al. 2010)

Glycosomes are special modified peroxisomes of kinetoplastids, which harbour the first steps of glycolysis and the main reactions of gluconeogenesis. This causes the compartmentalisation of energy metabolism which compensates in trypanosomatids for the lack of negative feedback regulation of the early steps of glycolysis (Haanstra, J. R. et

al. 2008). The ATP and NAD consumed by early steps of glycolysis are regenerated by the import of phosphoenolpyruvate (PET) into glycosomes and its conversion to succinate or pyruvate. Another route to generate NADPH in glycosomes is the generation of pentose phosphate sugars from hexose-phosphates by the pentose phosphate pathway (Maugeri, D. A. et al. 2003). In *Leishmania* but not in *Trypanosoma* hexose-phosphates are also used to generate mannogen in the cytosol (Ralton, J. E. et al. 2003). These short mannose chains accumulate in stationary phase promastigotes and amastigotes, where they function as the major short-term carbohydrate storage material (Saunders, E. C. et al. 2010). NADH and succinate generated by mitochondrial metabolism are reoxidised via an electron transport chain, consisting of the complexes I – IV in the inner mitochondrial membrane (Bringaud, F. et al. 2006; van Hellemond, J. J. et al. 1997a). The resultant proton gradient leads to the generation of ATP via a F_0F_1-ATP synthase. *Leishmania* can survive under anaerobic conditions, but undergo a metabolic arrest (van Hellemond, J. J. et al. 1997a). This rapid, yet reversible arrest is also brought about by starvation or the inhibition of the respiratory complex IV with cyanide, demonstrating that substrate-level phosphorylation is not sufficient to supply the cells with enough ATP for regular growth, even in the presence of high glucose levels (Saunders, E. C. et al. 2010; van Hellemond, J. J. et al. 1997a). The procyclic stages of some *T. brucei* strains depend likewise on mitochondrial oxidative phosphorylation for ATP synthesis (Bringaud, F. et al. 2006; Zikova, A. et al. 2009), while other strains grow normally under inhibition of oxidative phosphorylation (Lamour, N. et al. 2005). In the absence of sufficient amounts of glucose, amino acids are used as alternative carbon sources for energy metabolism. In *T. brucei* the principal source of carbon and energy in the absence of glucose is proline (Lamour, N. et al. 2005), while *Leishmania* on the other hand do not display this preference (Hart, D. T. et al. 1982; Saunders, E. C. et al. 2010). The amino acids histidine, leucine, isoleucine, lysine, phenylalanine, tryptophane, tyrosine, valine and arginine are essential in all trypanosomatids and consequently need to be scavenged from the environment (McConville, M. J. et al. 2007; Opperdoes, F. R. et al. 2007). Gene analyses have shown that *L. major* should be able to synthesise methionine and threonine starting from aspartate semialdehyde, unlike both *T. cruzi* and *T. brucei* which lack the required enzymes (Opperdoes, F. R. et al. 2007). Amino acids used for energy metabolism (glutamine/glutamate, proline, asparagine/aspartate, alanine, serine, glycine, threonine, isoleucine, methionine, valine and cysteine) are catabolised to intermediates of the TCA-cycle, which are subsequently used for the generation of NADH, fatty acid biosynthesis or gluconeogenesis via PEP carboxykinase (Opperdoes, F. R. et al. 2007; Saunders, E. C. et al. 2010). A large family of amino acid permeases are responsible for the uptake of amino acids into the parasites and have partly been shown to be regulated in a stage-specific manner and depending on circumstances (Akerman, M. et al. 2004; Darlyuk, I. et al. 2009; Jackson, A. P. 2007; Mazareb, S. et al. 1999; Shaked-Mishan, P. et al. 2006).

The specific arginine transporter LdAAP3 for instance was highly expressed as a consequence of arginine depletion, but showed no difference in protein abundance when arginine levels were high (Darlyuk, I. et al. 2009). The ensuing low level of arginine transport seemed rather to be a consequence of down regulation of transporter activity, suggesting the presence of a signalling pathway which senses intracellular concentrations of arginine and inhibits LdAAP3 activity (Darlyuk, I. et al. 2009). This reflects the regulation of the *S. cerevisiae* arginine transporter CAN1, which is negatively regulated by the binding of the small G protein Rheb (Urano, J. et al. 2000). In trypanosomatids arginine serves as a precursor for polypeptide biosynthesis and polyamine biosynthesis. In *Trypanosoma*, but not in *Leishmania*, it also functions as energy reservoir in the form of phospho-arginine, produced from arginine by arginine kinase (Pereira, C. A. et al. 2000; Pereira, C. A. et al. 2002). As part of the urea cycle, arginine is hydrolysed to ornithine, producing urea and therefore attaining the removal of toxic ammonia. *L. major*, *T. brucei* and *T. cruzi* only contain a rudimentary urea cycle with homologues of the enzymes argininosuccinate-lyase, which catabolises argininosuccinate to arginine and fumarate, and ornithine transcarbamoylase, which produces citrulline from ornithine and carbamoyl phosphate, missing from all three genomes (Opperdoes, F. R. et al. 2007). The polyamines putrescine, spermidine and spermine are generated from ornithine, with arginine as the sole precursor, and play a central role in many eukaryotic cells in growth, differentiation and macromolecular biosynthesis (Tabor, C. W. et al. 1984). The drug eflornithine® (α-difluoromethylornithine or DFMO) irreversibly inhibits the enzyme ornithine decarboxylase which generates putrescine from ornithine in *T. gambiense* (Garofalo, J. et al. 1982; Muller, S. et al. 2001). The selectivity for the parasitic enzyme over the homologue of the mammalian host is intriguingly based on the high turn-over rate of mammalian ornithine decarboxylase rather than differences in structure or binding (Persson, L. et al. 2003; Tabor, C. W. et al. 1984). DFMO is not effective against *T. rhodesiense* and *Leishmania,* possibly due to poor uptake of the drug and low affinity to the targeted enzymes (Muller, S. et al. 2001). Inhibitors of S-adenosylmethionine decarboxylase, the enzyme which provides S-adenosyl-methioninamine for the synthesis of spermidine and spermine have also been shown to be effective against trypanosomes, further underlining the importance of polyamines in the parasites (Bacchi, C. J. et al. 1992; Bitonti, A. J. et al. 1990). Spermidine is also used to generate trypanothione, a metabolite of two molecules of glutathione linked by spermidine, which forms the trypanosomatid specific redox-buffer system and has been implicated in the defence against oxidative stress (Bocedi, A. et al. 2010). In conclusion, the parasitic metabolism is a fascinating field for further research and provides many potential drug targets. Metabolic enzymes in trypanosomatids seem to be for the most part constitutively expressed, due to the absence of transcriptional regulation and to provide the parasites with the possibility of rapid reaction to fluctuations in available nutrients (Leifso, K. et al. 2007a; Saunders, E. C.

et al. 2010). It is therefore to be expected that posttranslational regulation of metabolism plays an important role in trypanosomatids and it is highly likely that signal transduction cascades are involved in this regulation.

1.4 Metabolomics

Metabolomics, the study of all metabolites within a given system, is a rapidly emerging field in addition to the classical “omics”, genomics and proteomics (Fernie, A. R. et al. 2004). Metabolomics involves sampling, sample preparation, which has to be carried out with great care to quench all or most metabolic activity in the sample and to ensure reproducibility, sample analysis and data processing. Sample analysis must be highly selective and sensitive and can be conducted by a range of techniques, mainly involving mass spectrometry (MS). The analysis of an organism’s metabolome is technically extremely challenging as metabolites include a wide range of chemically different molecules of varying sizes and concentrations, such as low molecular weight polar volatiles like ethanol or metabolites of high molecular weight like polar carbohydrates or non-polar lipids (Han, J. et al. 2008). It is essential that the employed mass analysers achieve high resolutions and mass accuracies of about 1ppm, meaning the mass of a molecule can be accurately solved up to the 6th decimal place and even only slightly different molecules in mass but of different formulae can be correctly distinguished (Breitling, R. et al. 2006b). Currently only two types of analysers conform to these requirements, by trapping ionised metabolite mixtures in an orbital flight path (Breitling, R. et al. 2006a). The Fourier transform ion cyclotron resonance mass spectrometry (FTICR-MS) employs a strong magnetic field for this purpose, which requires superconducting magnets and consequently leads to high maintenance costs (Breitling, R. et al. 2006a). The Orbitrap analyser uses instead a radial magnetic field to trap ions between two special spindle-shaped electrodes, so that they circle around the central one (Breitling, R. et al. 2006a; Hu, Q. et al. 2005). The frequency of ion oscillations around the centre is detected and processed by fast Fourier transformation, equal to the data in FTICR-MS, and is proportional to the mass-over-charge ratio (Hu, Q. et al. 2005). To further enhance the quality of obtained data, mass spectrometry is usually combined with liquid chromatography (LC-MS) (Dunn, W. B. et al. 2005). Compounds are first separated by LC-MS and successively passed into mass spectrometry. This provides an additional characteristic retention time for each metabolite and has the advantage of less complex mass spectra and the potential separation of isomers. The combination of the two methods also reduces an effect known as ion suppression, in which several compounds can affect each others signals in mass spectrometry. Continuous improvements of technology led to high accuracies in detection and will keep expanding the possibilities of detection, but will also lead to increasingly large amounts of the already large data sets.

Bioinformatics approaches, like the matching of signals to databases like LeishCyc (Doyle, M. A. et al. 2009), LipidMAPS (Fahy, E. et al. 2007), KEGG (Kanehisa, M. 2002), Metlin (Smith, C. A. et al. 2005), the Human Metabolome Database (Wishart, D. S. et al. 2007) or PubChem (Wang, Y. et al. 2009), allow for the analysis of these large amounts of data. In experiments with *Leishmania* up to 60% of detected signals were found to be derivates of metabolites, which were irrelevant for the biological interpretation of data and need to be identified in data sets (Scheltema, R. A. et al. 2010). The availability of metabolomics gives rise to many applications, one of them being systems analysis, the complete prediction of an organism's metabolic network (Chavali, A. K. et al. 2008; Doyle, M. A. et al. 2009; Fernie, A. R. et al. 2004). Other approaches use metabolomics to identify pathways which are for instance specifically involved in drug resistance in *Leishmania* (Scheltema, R. A. et al. 2010).

1.5 Signal transduction in higher eukaryotes

Free-living cells as well as cells of multicellular organisms require the possibility to react to conditions and changes in their environment. This involves the recognition, relay and conversion of extracellular signals. Signalling pathways in the cells use phosphorylations, ubiquitinations, acetylations and phosphoinositides to relay extracellular signals. Cells of multicellular eukaryotes can detect a multitude of different signals like proteins, peptides, amino acids, nucleotides, steroids, retinoids, fatty acids and even solute gases like nitric oxide (NO) and carbon monoxide (CO). Intercellular signal types of multicellular organisms are differentiated by the distance and type of elicitor cells. Autocrine signals control the elicitor cell itself, juxtacrine signals directly affect neighbouring cells through gap junctions, paracrine signalling describes extracellular signals which influence cells in the vicinity and endocrine signals, the hormones, take effect over long distances. Receptor molecules bind the respective signal molecules and trigger the intracellular signal transduction which eventually leads to the appropriate cellular response. Different types of receptors exist in mammals, which can be generally grouped as intracellular receptor molecules and cell-surface receptors. Intracellular receptors can be localised in the nucleus or in the cytoplasm and bind all lipophilic signalling molecules which can cross the cell membrane by passive diffusion, including steroid hormones, NO, CO and retinoids. The soluble gas NO, for example, originates from the desamination of arginine by the enzyme NO-synthase and activates a cytosolic guanylate cyclase, which produces the messenger molecule cyclic guanosine monophosphate (cGMP). Lipophilic hormones bind to their cytosolic receptor molecules, provoking a translocation of the complex into the nucleus. In the nucleus the ligand-activated transcription factors influence gene expression by binding to specific nucleotide sequences, the so-called hormone response elements (HREs). The three most important types of cell-surface receptors are ligand

gated ion channels, G-protein coupled receptors and receptors with enzymatic activity. Some neurotransmitters entail the opening of ligand gated ion channels, situated on the post-synaptic membrane, and mediate a rapid influx of ions, to change the membrane potential and influence the transmission of the electrical signal. Ligand gated ion channels on the myoceptor of skeletal muscles, for instance, open after binding of acetylcholine. The subsequent influx of cations polarises the membrane and leads to muscle contraction. G-protein coupled receptors are integral membrane proteins with seven trans-membrane domains, which relay the signal by means of a separate membrane bound trimeric GTP-binding protein (G-protein). Non-activated G-proteins bind GDP to their α-subunit. The binding of a signal to G-protein coupled receptors leads to a conformational change of the receptor which entails a binding and a subsequent conformational change of the G-protein. Hereupon the α-subunit releases the bound GDP, which leads to the binding of GTP and subsequently to the dissociation of the G-protein into its two active components, the α-subunit and the $\beta\gamma$-complex. The conformational change of the subunits and the dissociation of the components both effect the activation of target proteins by the α-subunit and the $\beta\gamma$-complex, respectively. The α-subunit additionally has GTP-ase activity and hydrolyses GTP to GDP after a short time, thereby facilitating the re-association of the three subunits to the inactive trimeric G-protein. As the G-protein coupled receptor remains active as long as the signal ligand is bound, it can activate G-proteins repeatedly. Many G-protein coupled receptors relay their signal by activating the membrane-bound adenylate cyclase which synthesises cyclic adenosine monophosphate (cAMP). This major signalling molecule exists in all eukaryotes and is known to mainly activate protein kinase A (PKA). PKA phosphorylates different substrates, largely depending on the cell type, which explains why the outcome of cAMP signalling differs between cell types. The third major class of membrane receptors are those with their own enzymatic activity. In humans this class compasses receptors with the activity of tyrosine kinases, tyrosine phosphatases, serine/threonine kinases and guanylate cyclases. Receptor tyrosine kinases are the most common receptors with enzymatic activity and are oligomers of transmembrane peptides. The ligand either causes the building of an oligomer or the re-orientation of oligomeric subunits, which directly enables the kinase domains to activate each other by autophosphorylation on tyrosine moieties. Proteins which bind intracellularly to phosphorylated receptor tyrosine kinases are characterised by highly conserved binding domains, known as SH2- (Src-homologous region) or PTB-domains (phosphotyrosine binding). Proteins with these domains can either extenuate the signal via negative feedback or relay the signal further by binding to other proteins through additional domains like SH3-domains. Some signalling proteins consist almost only of SH2- and SH3-domains and function as adaptors to link receptor tyrosine kinases with downstream proteins without SH2-domains, like the central signalling protein Ras. The monomeric GTPase Ras is active when it is bound to GTP and inactive when linked to

GDP. It acts as a cross-over point in a great number of highly diverse signalling pathways, like apoptosis, proliferation, differentiation and cell adhesion. One type of signalling pathway activated by Ras is a mitogen-activated protein (MAP) kinase cascade.

1.5.1 Protein kinases

Protein kinases transfer the γ-phosphate of ATP to alcohol groups of serine or threonine amino acid residues or phenolic groups of tyrosine, generating phosphate monoesters. Phosphorylations are highly common posttranslational modifications, inducing conformational changes in proteins and generating or masking binding motifs. This affects the enzymatic activity, binding properties, protein stability or subcellular localisation of the phosphorylated protein. Protein kinases are hugely important components in cell signalling. This is illustrated by 1.5 – 2.5% of eukaryotic genomes coding for kinases, which regulate several major cellular processes like proliferation, differentiation, metabolism and gene expression (Chang, L. et al. 2001; Hanks, S. K. 2003; Johnson, G. L. et al. 2002). Protein kinases can be roughly divided into the two basic groups eukaryotic protein kinases (ePK), which share a conserved catalytic domain (Fig. 7), and atypical protein kinases (aPK) that lack strong sequence homology but have been experimentally shown to possess kinase activity (Manning, G. et al. 2002a). The group of ePKs can be further subdivided into Ca^{2+}/Calmodulin-dependent kinases (CAMK), homologues of casein kinase 1 (CK1), cyclic nucleotide- and calcium-phospholipid-dependent kinases (AGC), homologues of yeast sterile kinases 7, 11 and 20 (STE), tyrosine kinases (TK), tyrosine kinase-like kinases (TKL) and the CMGC-group, comprising cyclin-dependent kinases (CDKs), MAP kinases, glycogen synthase kinases (GSK) and CDK-like kinases (Manning, G. 2005). Another possibility of distinguishing protein kinases is by the amino acid residues that they phosphorylate. This leads to the distinction between serine/threonine kinases, tyrosine kinases and dual-specificity kinases that typically accept the amino acid residues serine, tyrosine and threonine as substrates. The phosphorylation of serine, threonine and tyrosine diverges greatly with ratios of 1800:200:1 (Hubbard, M. J. et al. 1993). Tyrosine phosphorylation by dual-specificity kinases seems to be very stringent and specific to physiological substrates, whereas non-specific tyrosine phosphorylation is usually weak (Crews, C. M. et al. 1992; Featherstone, C. et al. 1991; Lindberg, R. A. et al. 1992; Menegay, H. J. et al. 2000). The conserved catalytic domain of ePKs comprises twelve subdomains of regions uninterrupted by large amino acid insertions, which contain fundamental motifs of conserved residues (Fig. 7) (Hanks, S. K. 2003). The catalytic domains of protein kinases have a threefold role, mediating the binding and orientation of the phosphate donor as a complex with a divalent cation (generally Mg^{2+} or Mn^{2+}), as well as the binding and orientation of the protein substrate and the transfer of the γ-phosphate from the donor to the acceptor residue

(Hanks, S. K. et al. 1995). Crystal structure analysis of the catalytic core of several protein kinases has revealed a common 3-dimensional structure, comprising a N-terminal lobe of five β-strands and one α-helix, called the C-helix, and a mainly α-helical C-terminal lobe, conjoined by a hinge region (Fig. 6) (Krupa, A. et al. 2004).

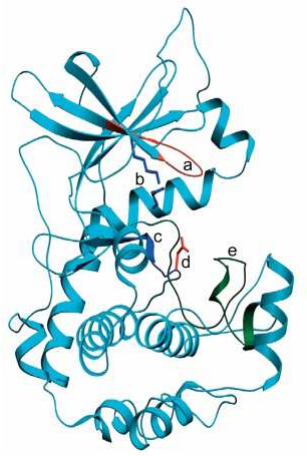

Figure 6, The three-dimensional structure of the catalytic domain of an exemplary serine/threonine or tyrosine kinase
Key functional elements are labelled with lower case letters; a, phosphate anchor ribbon; b, lysine-glutamate pair; c, catalytic loop; d, catalytic base; e, activation segment;
Source: (Krupa, A. et al. 2004)

The N-terminal lobe includes the subdomains I – IV, while the C-terminus encompasses the subdomains VIA to XI (Fig. 7). The N-terminal lobe is generally defined to commence 7 positions upstream of the conserved GxGxxG motif with a hydrophobic residue, whereas the C-terminal lobe ends 9 – 13 positions downstream of the invariant arginine residue in subdomain XI (Hanks, S. K. et al. 1995). The N-terminal lobe and the hinge region are mainly responsible for the binding and orientation of complexed ATP, while the binding and orientation of the substrate occurs in the C-terminal lobe of the catalytic domain (Hanks, S. K. 2003). All residues responsible for the catalytic activity are located around the cleft between the two lobes (Fig. 6). They include the phosphate-anchor ribbon, a glycine-rich loop of GxGxxG in subdomain I, and a lysine residue in subdomain II which is positioned by a salt-bridge with a glutamate in subdomain III within the C-helix, and Mg^{2+} ions. Both of these regions are involved in accurately positioning the ATP for phosphotransfer, together with the aspartate residue of the DFG motif in subdomain VII and the asparagine of the catalytic loop in subdomain VIB. Exchange of the lysine residue within the lysine-glutamate salt bridge to a methionine renders the kinase inactive as it is unable to align ATP into a functional position (Gibbs, C. S. et al. 1991). The catalytic loop with the consensus motif HRDLKxxN (reduced to the invariant DxxxxN in Fig. 7) in subdomain VIB contains the invariant aspartate which acts as the catalytic base by accepting a proton of the attacking substrate hydroxyl group during the phosphotransfer. The APE motif in subdomain VIII and the DxxxxG motif in subdomain IX act stabilising on

the C-terminal lobe. Most protein kinases require for activation the phosphorylation of a threonine and/or tyrosine residue within the activation segment, the region starting at the conserved DFG motif until the conserved APE motif (see Fig. 6 and 7) (Johnson, L. N. et al. 2001). The activation segment is part of the substrate-binding pocket and phosphorylation of its residues leads to a conformational change, allowing the substrate and ATP to bind (Johnson, L. N. et al. 2001; Krupa, A. et al. 2004).

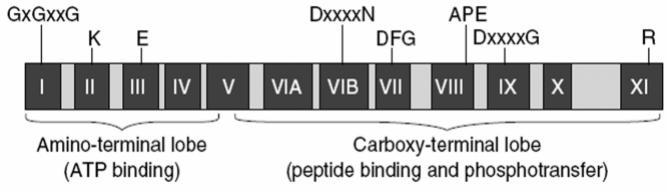

Figure 7, The conserved catalytic domain of eukaryotic protein kinases
The conserved subdomains are numbered with Roman numerals and highly conserved amino acid motifs are displayed above their position in the subdomains (x: arbitrary amino acid); the common amino-terminal and carboxy-terminal lobe as identified by crystal structures are indicated below the subdomains; Source: (Hanks, S. K. 2003)

1.5.1.1 Mitogen-activated protein kinases

Mitogen-activated protein (MAP) kinase cascades are a type of signalling pathway that is highly conserved in all eukaryotes. Most mammalian cell surface receptors effectuate the activation of at least one MAP kinase cascade. The cascade typically comprises a core module of three consecutively activated kinases. A serine/threonine kinase MAP kinase kinase kinase (MAP3K) phosphorylates and thereby activates a dual-specificity MAP kinase kinase (MAP2K), which in turn specifically and highly selectively activates a MAP kinase by phosphorylation. The activating phosphorylation of MAP3Ks takes place by small GTP-binding proteins of the Ras or Rho family or by Ste20-like kinases. The N-terminus of MAP2Ks typically contains a docking site (D-site), which binds to the common docking or CD-domain of the downstream MAP kinase and plays a role in regulating the phosphorylation reaction and its specificity (Tanoue, T. et al. 2003). The D-site with the consensus motif $[K/R]_{2-3}$-X_{1-6}-[L/I]-X-[L/I] has been found in most eukaryotic MAP2Ks (Grewal, S. et al. 2006). Scaffold proteins likewise prevent unspecific crosstalk between MAP kinase cascades, in addition to bringing together the separate units of the cascade to facilitate their activation (Scott, J. D. et al. 2009). Characteristic for MAP kinases is the unusual activation by double phosphorylation on the threonine and tyrosine residue of the TXY motif within the activation loop in subdomain VIII (Fig. 8). MAP kinases belong to the family of serine/threonine kinases and their ideal substrate phosphorylation site displays the consensus sequence P-X-[S/T]-P, even though some identified substrates concur only with the reduced consensus sequence of [S/T]-P (Clark-Lewis, I. et al. 1991; Davis, R. J. 1993). Final substrates of MAP kinase pathways in mammals are generally transcription

factors. The first MAP kinase cascade to be elucidated was a mammalian signalling pathway activated by Ras, which phosphorylates a MAP3K named Raf. Raf activates the MAP2K MAP/ERK kinase (MEK1/2), whose substrate is ERK1/2, an activator of transcription factors that affect cell differentiation and proliferation. In mammals exist at least four subfamilies of MAP kinases, the extracellular signal-regulated kinases 1 and 2 (ERK1/2), activated by MEK1/2, the p38 proteins (p38 α, β, γ, δ), activated by MKK3 and MKK6, c-Jun N-terminal kinases/stress-activated protein kinases (JNK/SAPK1, 2, 3), activated by MKK4 and MKK7, and ERK 5, activated by MEK5. Extracellular signals triggering MAP kinase cascades are manifold. Signal cascades involving ERK kinases tend to be involved in cell differentiation, proliferation and development, while p38 kinases play a key role in the regulation of inflammatory cytokine expression. JNK/SAPKs are, as the name "stress-activated protein kinases" implies, activated in response to environmental stress, as well as radiation and growth factors. JNK/SAPKs phosphorylate c-Jun, a subunit of the AP-1 transcription complex, increasing among others the expression of many cytokine genes. A total of 22 MAP kinases, 7 MAP2Ks and 20 MAP3Ks have been identified in mammals up to date (Pearson, G. et al. 2001). The genome of *Saccharomyces cerevisia* encodes for 6 MAP kinases (Hunter, T. et al. 1997) whereas *Caenorhabditis elegans* features 14 member of the MAP kinase family (Plowman, G. D. et al. 1999).

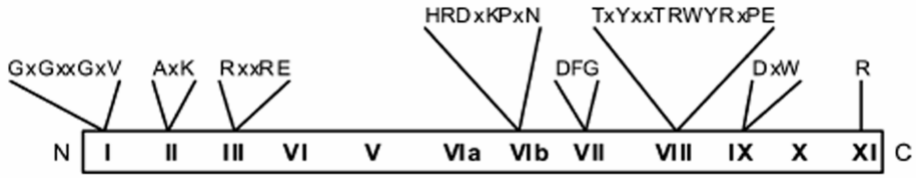

Figure 8, The conserved catalytic domain of mitogen-activated protein kinases
The Roman numerals denote the 12 conserved subdomains; conserved consensus motifs are indicated above. Source: (Wiese, M. et al. 2003b)

As MAP kinases play such a central role in many signal transduction pathways, their malfunctioning is ultimately involved in the origination of several diseases, like Alzheimer's disease, Parkinson's disease and various cancers (Kim, E. K. et al. 2010). MAP kinases are consequently promising targets for the development of new drugs. Up to date 10 inhibitors of protein kinases have been approved for the treatment of cancers and considerable research is undertaken to elucidate the functionality of MAP kinases and other protein kinases in the treatment of inflammatory diseases (Cohen, P. 2009).

1.6 Signal transduction in kinetoplastids

Signal transduction pathways are expected to play a central role in kinetoplastids, as they undergo substantial biochemical and morphological changes in response to their differing environment. Kinetoplastids possess a large number of protein kinases, a sign of the importance of phosphorylations in their signalling processes (Parsons, M. et al. 2005). However, due to the transcription of polycistronic mRNAs and the prevalence of posttranscriptional regulation of expression, kinetoplastid signalling pathways are expected to differ largely from higher eukaryotes, where for instance MAP kinases mainly use transcription factors as substrates. Protein kinases in *Trypanosoma* and *Leishmania* are therefore thought to regulate mRNA turnover instead, as well as metabolic and cell cycle specific functions. The comparison of the kinomes of *T. brucei*, *T. cruzi* and *L. major* revealed the existence of members of all major kinase families in these kinetoplastids (Parsons, M. et al. 2005). However, in comparison to the human kinome the CAMK and AGC groups were underrepresented, while there were proportionally more members of the CMGC, STE and NEK (NIMA (never in mitosis/Aspergillus)-related kinase) groups (Parsons, M. et al. 2005). Not much is known about NEKs in trypanosomatids, apart from one being differentially regulated during development and one playing a role in basal body duplication (Parsons, M. et al. 2005). Some NEKs of trypanosomatids are unusual as they contain PH domains. The activation of kinetoplastid signalling cascades is still ambiguous. The most common receptors in mammals which detect extracellular signals and activate intracellular signalling cascades are receptor tyrosine kinases (Manning, G. et al. 2002b), but all known receptors of plants are serine/threonine kinases (Shiu, S. H. et al. 2004). The genome of kinetoplastids does not encode any tyrosine kinases, tyrosine-like kinases, SH2- or SH3-domain proteins or receptor guanylyl cyclases, thus raising the question how are extracellular signals recognised and translated into intracellular changes (Parsons, M. et al. 2005)? Ten genes, which encode products with both serine/threonine kinase domains and transmembrane domains have, however, been identified in the *T. brucei* genome (Parsons, M. et al. 2005). Five of the identified potential receptors belong to the STE11 family of kinases, one to the family of elongation factor 2 kinases (PEK), three are unique kinases not assignable to any family and one is a member of the CAMK family. All three unique kinases contain MAP2K related domains, but one additionally possesses structural features related to calcium ion binding and to galactose oxidase and one is predicted to be without catalytical function. All STE11 family members display a domain related to MAP2Ks and one also possesses a catalytical domain of adenylyl cyclases (Parsons, M. et al. 2005). Kinetoplastids feature a comparatively large number of adenylyl cyclases (AC), most of which are integral membrane proteins and differ considerably in structure from their mammalian counterparts, as they belong to class II cyclases which are exclusive to protozoa (Laxman, S. et al. 2007). They consist of a transmembrane domain,

which links the highly diverse extracellular ligand-binding domains with a cytoplasmic adenylate cyclase. It has been proposed that ACs are the primary signal receptors in kinetoplastids (Seebeck, T. et al. 2004). The activation of ACs seems to require dimerisation (Naula, C. et al. 2001), and occurs, unlike in mammals, independent of G-proteins (Laxman, S. et al. 2007). The main function of cAMP in mammals is the activation of protein kinase A (PKA). Putative PKA homologues have been identified in *T. brucei* (Huang, H. et al. 2006; Laxman, S. et al. 2007), along with phosphodiesterase homologues, which are responsible for the degradation of cAMP (Kunz, S. et al. 2006). The ultimate outcome of cAMP signalling has not been completely elucidated, but it seems to regulate flagellar function (Oberholzer, M. et al. 2007) and osmotic homeostasis (Laxman, S. et al. 2007), as well as proliferation and differentiation (Seebeck, T. et al. 2001). In *T. brucei* a protein has also been identified, which contains cAMP-binding domains along with Ca^{2+}-dependent membrane targeting domains, suggesting a possible role as a cAMP-responsive scaffolding protein (Laxman, S. et al. 2007). The universal eukaryotic signalling molecule Ca^{2+} also plays an important role in kinetoplastid signalling. Kinetoplasts encode a large number of proteins belonging to the calpain superfamily, a family of intracellular Ca^{2+}-dependent cysteine proteases or Ca^{2+}-binding proteins (CaBP) (Ersfeld, K. et al. 2005). Calpains are differentially expressed, contain acetylation motifs and, although their exact function is not known, they have been shown to contain motifs which can bind a potential PKA binding protein, suggesting a possible scaffold function (Ersfeld, K. et al. 2005). A CAMK has been proposed to play a central role in the differentiation of *T. cruzi* from blood forms to epimastigotes (Souza, C. F. et al. 2009). Homeostasis of low cytoplasmic Ca^{2+} levels is maintained with the help of energy-dependent transport of Ca^{2+} ions by the endoplasmatic reticulum, the plasma membrane, the mitochondrion and the acidocalcisomes (Zilberstein, D. 1993). Acidocalcisomes, which are also involved in osmoregulation and maintenance of intracellular pH are suspected to play the most important role in Ca^{2+} homeostasis (Docampo, R. et al. 2005). Heat shock proteins (HSP), which are expressed in kinetoplastids in large numbers dependent on life cycle stages, have also been proposed to regulate signal transduction pathways (Folgueira, C. et al. 2007; Wiesgigl, M. et al. 2001a). In accordance with this is the observation that the survival and transformation of *L. donovani* parasites in the mammalian host depends on the ability to respond to heat-stress with an increased dephosphorylation of proteins, possibly due to the increased activity of phosphatases (Salotra, P. et al. 2000). Elements of the phosphoinositol cascade have also been identified in kinetoplastids. This signalling cascade, involving the phosphorylation of membrane-bound phosphatidylinositol (PtdIns) by phosphatidylinositol 3-kinase (PI3K), is one of the major pathways inducing proliferation in higher eukaryotes. Phosphatidylinositol phosphates (PtdInsPs) bind intracellular proteins with PH (pleckstrin homology) domains to signal complexes, which relay the extracellular signal of growth factors. Genes for PI3K,

PH domain proteins and phospholipase C (PIPLC), which cleaves PtdInsPs, have been identified in *T. brucei* and *T. cruzi* (Bringaud, F. et al. 1998; Docampo, R. et al. 1991; Nozaki, T. et al. 1999), but the consequent release of Ca^{2+} does not take place in trypanosomes, like it does in higher eukaryotes (Parsons, M. et al. 2000).

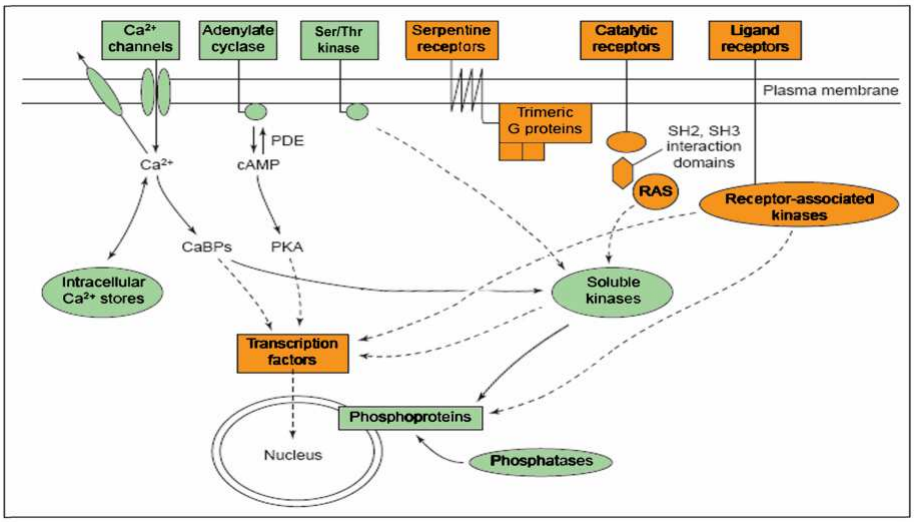

Figure 9, Comparison of cell signalling in trypanosomatids and higher eukaryotes
Green elements indicate cell signalling events also found in trypanosomatids, orange elements indicate cell signalling events only found in higher eukaryotes; solid arrows indicate known connections, dashed arrows indicate missing connections; adapted from (Parsons, M. et al. 2000)

Fig. 9 displays a simplified diagram of cell signalling events in trypanosomatids in comparison with higher eukaryotes. Trypanosomatids require a tight cell cycle control, as they are highly polarised cells with a single mitochondrion. The eukaryotic cell cycle can generally be divided into two periods: the interphase, during which cells grow, and duplicate their DNA and mitosis, during which the actual cell division takes place. The interphase is further divided into three general phases. Fig. 10 shows a diagram of the typical eukaryotic cell cycle.

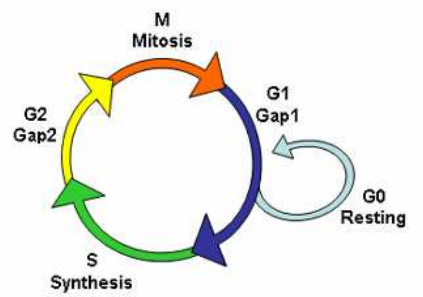

Figure 10, Typical eukaryotic cell cycle
Each phase of the cell cycle is indicated in a different colour and labelled in the diagram.

During the first gap phase (G0/G1), cells take up nutrients, express enzymes needed for cell division and grow. The replication of DNA takes place during the S phase and is divided during mitosis (M phase), adjacent to the second gap phase (G2), in which microtubules are synthesised and protein synthesis is reduced. The kinetoplast in trypanosomatids passes through its own cell cycle which is shorter than the nuclear one, so that segregation is completed before the start of mitosis. The regulation of the cell cycle in *Trypanosoma* seems to vary between different life cycle stages (McKean, P. G. 2003). Kinases of the CDK family play a vital role in cell cycle control in higher eukaryotes and seemingly also in trypanosomatids. CDKs require the binding of specific cyclin proteins for their activity. Trypanosomatids contain a relatively large complement of CDKs, with 11 CDKs and 10 cyclins in *T. brucei*. CRK3 is so far the only *T. brucei* CDK which has been shown to be cyclin-dependent and is one of two CDKs essential for cell cycle control. When bound to the cyclin CYC2, CRK3 is an essential regulator of G1 phase progression (Hammarton, T. C. et al. 2004). The interaction of CRK3 with CYC6 is essential for G2/M phase progression in trypanosomatids (Hammarton, T. C. et al. 2003; Hammarton, T. C. 2007; Hassan, P. et al. 2001). CRK1 also controls G1 phase progression with functional differences between bloodstream and procyclic forms of *T. brucei* (Tu, X. et al. 2005).

1.6.1 Mitogen-activated protein kinases in kinetoplastids

The genome of *Leishmania* encodes enzymes of all three levels of the MAP kinase cascade. Sequence homology analyses identified 23 potential MAP3K homologues, belonging to the STE11 family, seven MAP2K homologues, all of the STE7 family of protein kinases, and 15 putative MAP kinase homologues in *Leishmania* (Ivens, A. C. et al. 2005; Parsons, M. et al. 2005; Wiese, M. 2007). Only one member of the STE20 family to which the mammalian MAP3Ks belong was found in *L. major* (Parsons, M. et al. 2005). Not much data is available concerning the trypanosomatid MAP3Ks. The only MAP3K which has been examined to date in trypanosomatids was MRK1. It was deemed essential in *L. major* promastigotes, as all attempts to delete the gene failed (Agron, P. G. et al. 2005), and displayed upregulated mRNA levels in *T. brucei* bloodstream forms (Koumandou, V. L. et al. 2008). All MAP2Ks of *L. mexicana* were cloned, and to some extent analysed in our laboratory. LmxMKK3 shows characteristics that classify it close to CAMKs (Parsons, M. et al. 2005). LmxMKK2, LmxMKK6 and LmxMKK7 are all rather large proteins with molecular masses of 120 kDa, 176 kDa and 116 kDa, respectively. In the case of LmxMKK6 and LmxMKK7 this is due to an N-terminal extension, while LmxMKK2 displays an unusually long C-terminus. All three of these MAP2Ks transpired to be rather difficult to express as recombinant protein and showed no innate phospho-transferase activity towards MBP in a radioactive kinase assay (Melzer, I. M., PhD thesis,

2007). LmxMKK5 on the other hand was easy to express as recombinant protein and showed a strong phosphotransferase activity towards MBP {Melzer, 2007 156 /id;John von Freyend, 2010 162 /id}. LmxMKK4 (previously LmxPK4) seems to play a role in the differentiation of promastigotes to amastigotes. It is not essential in promastigotes, but the deletion of its gene leads to an impaired lesion development in mouse infection experiments, although the protein is only expressed in promastigotes and during the differentiation to axenic amastigotes (Kuhn, D. et al. 2005). The deletion mutants also display an elongated flagellum, suggesting a role of LmxMKK4 in flagellar-length control (Kuhn, D., PhD thesis, 2004). The MAP2K LmxMKK was equally found to be involved in the regulation of flagellar length, as its deletion led to promastigotes with a flagellum reduced to one fifth of its normal length and no paraflagellar rod (Wiese, M. et al. 2003a). Deletion mutants of LmxMKK caused delayed lesion development in mouse infection experiments, but protein expression of LmxMKK was restricted to promastigotes (Wiese, M. et al. 2003a). The examination of phylogenetic relationships with a radial tree showed that LmxMKK5 and LmxMKK4 cluster together with four stress-activated MAP2Ks from *Arabidopsis thaliana* (AtMKK1, AtMKK2, AtMKK3, AtMKK6) and the single MAP2Ks found in *Chlamydomonas rheinhardtii* and *Dictyostelium discoideum* (Fig. 11). All other *L. mexicana* MAP2Ks can be found together with the human MAP2K T-cell originated protein kinase (TOPK) on a separate branch of the tree.

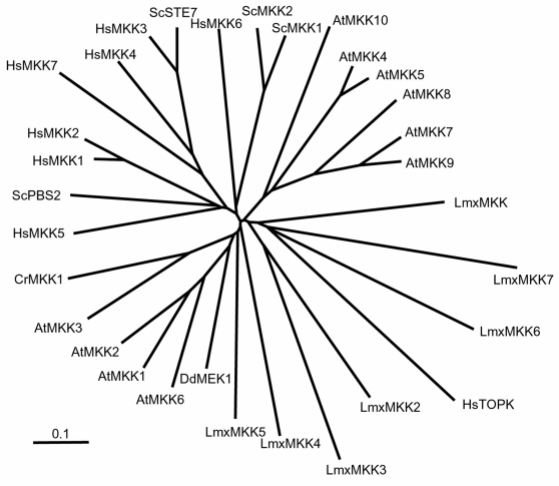

Figure 11, Radial phylogenetic tree of the catalytic domain of all MAP2Ks of *L. mexicana* and other organisms
At, *Arabidopsis thaliana*; Cr, *Chlamydomonas rheinhardtii*; Dd, *Dictyostelium discoideum*; Hs, *Homo sapiens*; Lmx, *L. mexicana*; Sc, *Saccharomyces cerevisiae*.
Source: (John von Freyend, S. et al. 2010)

The finding that LmxMKK activates the MAP kinase LmxMPK3 *in vitro* and *in vivo* was the first identification of two consecutive members of a MAPK signalling cascade in *Leishmania* (Erdmann, M. et al. 2006). LmxMPK3 deletion led, analogous to LmxMKK, to a drastically reduced flagellum and although parasites still contained PFR it was shown to

be not appropriately assembled (Erdmann, M. et al. 2006). Although functional LmxMPK3 is not essential for lesion development in mouse infection experiments it is required to establish infection of the sand fly host (Erdmann, M., PhD thesis, 2009). LmxMPK3 *in vitro* displays autophosphorylation on the tyrosine of the TXY motif, but requires the phosphorylation of both tyrosine and threonine in its activation motif for *in vivo* activity (Erdmann, M., PhD thesis, 2009). The second possible identification of two consecutive members of a MAPK signalling cascade in *Leishmania* was the demonstration that co-expression with LmxMKK4 generates an activated recombinant LmxMPK13 (Scholz, A., PhD thesis, 2008). Just as described for LmxMKK4, deletion mutants of LmxMPK13 display elongated flagella, indicating that LmxMKK4 could also be the activator of LmxMPK13 *in vivo* (Scholz, A., PhD thesis, 2008). Deletion studies of LmxMPK14 and LmxMPK9 have likewise implicated these kinases in the regulation of flagellar length (Bengs, F. et al. 2005; Scholz, A., PhD thesis, 2008). LmxMPK9, LmxMPK13 and LmxMPK14 are all related members of a subfamily of kinases which was named MAP kinase – related kinases (Miyata, Y. et al. 1999; Wiese, M. 2007). It is intriguing that such a large number of MAP kinases in *Leishmania* seem to be involved in the regulation of flagellar length. The findings underline the importance of flagellar control during the trypanosomatid life cycle. Some MAP kinases have been shown to be essential or important in *Leishmania*. LmxMPK1, the first MAP kinase to be identified in *Leishmania*, is essential for the survival of amastigotes in mammalian macrophages (Wiese, M. 1998). Its homologue in *T. brucei*, TbKFR1, is essential in procyclics in the insect host and it was found to be involved in the regulation of interferon γ-induced proliferation of bloodstream forms in the mammalian host (Hua, S. B. et al. 1997). LmxMPK1 is therefore an interesting drug target. LmxMPK2 also presents a potential drug target, as deletion analyses showed it to be essential for lesion development in mouse infection studies (Wiese, M., unpublished data). The deletion of *LmxMPK5* produced *Leishmania* mutants that persisted in Balb/c mice, but had an impaired ability to cause lesions (Wanders, P., MD thesis, 2004). The homologue of LmxMPK5 in *T. brucei*, TbMAPK5, is not essential in life cycle stages in the insect host, but regulates the differentiation of bloodstream forms in the mammalian host (Domenicali, Pfister D. et al. 2006). LmxMPK11 and LmxMPK12 on the other hand are not essential for *Leishmania* promastigotes or amastigotes, as deletion mutants displayed infectivity in Balb/c mice (Windelberg, M., MD thesis, 2007). LmxMPK7 and LmxMPK8 are the only MAP kinases found in *Leishmania* that do not have any homologues in *Trypanosoma*. Transgenic *L. donovani* parasites, expressing a GFP-fusion protein of the *L. major* protein LmaMPK7 caused delayed lesion development and proliferated slowly in Balb/c mice, dependent on kinase activity (Morales, M. A. et al. 2010). The *L. mexicana* MAP kinases LmxMPK4 and LmxMPK6 were investigated in the context of this dissertation. The obvious importance of protein kinases in various

intracellular events in trypanosomatids renders them ideal targets for the development of anti-trypanosomatid drugs (Naula, C. et al. 2005).

1.7 State of knowledge and research objectives, LmxMPK4

The main part of this thesis was concerned with the analysis of the *L. mexicana* MAP kinase LmxMPK4. The gene coding for LmxMPK4 was first isolated from genomic *L. mexicana* DNA with the help of degenerate oligonucleotide primers, corresponding to the phosphorylation lip of protein kinases (Wiese, M. et al. 2003b). The identified gene was corroborated by the release of the *L. major* Friedlin genome sequencing project and published in the NCBI Entrez database as AJ293282. The 1089 bp long open reading frame of *LmxMPK4* encodes a protein of 363 amino acids and a calculated molecular mass of 41.5 kDa and is contained in the *L. mexicana* genome as a single copy gene (Wang, Q. et al. 2005; Wiese, M. et al. 2003b). LmxMPK4 shows high conservation within the different *Leishmania* species (*L. major* 98.9%, *L. panamensis* 98.6 %, *L. donovani* 97.5%, *L. infantum* 97.5% amino acid identities). The homologue in *T. brucei*, TbMAPK2, is not as highly conserved, but still displays an amino acid identity of 67.2% with LmxMPK4. The LmxMPK4 homologue in *T. cruzi* equally has an amino acid identity of 67.4%. Homologues in other organisms include *C. rheinhardtii* (43.9%) and *D. discoideum* (45%). With only 42% amino acid identity LmxMPK4 shows a significant amino acid divergence from its closest human homologues ERK1/2. The kinase domain of LmxMPK4 extends from tyrosine 17 to phenylalanine 318 and takes up most of the protein with a 16 amino acids long N-terminal and 45 residues long C-terminal region. The kinase domain contains the twelve typical kinase subdomains and several amino acid residues, which are highly conserved in kinases (Wang, Q. et al. 2005). A potential common docking domain (DAAEE) is contained in the C-terminal region. The conserved lysine residue in subdomain II which is involved in accurate substrate phosphorylation has been mutated to methionine, generating the kinase-dead mutant LmxMPK4K59M (Wang, Q. et al. 2005). The conserved TXY-motif in the activation loop curiously contains a glutamine in LmxMPK4, which is rather unusual for MAP kinases. No previously found human MAP kinase homologues display the TQY phosphorylation motif, but another *L. mexicana* MAP kinase, LmxMPK12 (accession number DQ026026), and kinases from *Aedes aegypti* (accession number EAT39586) and *Caenorhabditis elegans* (pmk-3, accession number NP_501363 and mpk-2, accession number NP_494947) also contain a glutamine as the central amino acid in their activation motif. The kinases of the latter two organisms have been classified as JNK and p38 kinases, respectively, due to sequence homology. Although LmxMPK4 shows its highest homology to human ERK and not SAPKs, it can be argued that it could play a role as SAPK in *Leishmania*, whose kinome lacks typical SAPKs containing TGY and TPY motifs (Kultz, D. 1998; Wiese, M. 2007). *In vitro*

phosphotransferase activity of recombinant LmxMPK4, expressed as GST-fusion protein in *E. coli*, was demonstrated to be low and consists mainly of autophosphorylation activity (Wang, Q. et al. 2005). The *L. major* homologue LmaMPK4 was over-expressed in *L. major* promastigotes and shown to display phosphotransferase activity towards MBP after immuno-purification (Morales, M. A. et al. 2007). The phosphotransferase activity of GFP-LmaMPK4 was significantly higher when the protein was purified from *L. major* promastigotes that had been subjected to 34°C and pH 5.5 for 12 hours, which would trigger the start of differentiation to axenic amastigotes in *L. mexicana*. *L. major* parasites over-expressing GFP-LmaMPK4 also showed a cytosolic distribution for the fusion protein when analysed with confocal microscopy (Morales, M. A. et al. 2007). Parasites over-expressing GFP-LmaMPK4 showed a strong virulence defect in mouse infection experiments (Morales, M. A. et al. 2007). Deletion experiments in *L. mexicana* promastigotes only succeeded in replacing the genomic copies of *LmxMPK4* after an additional extrachromosomal copy of the gene had been introduced into the parasites (Wang, Q. et al. 2005). The generated *L. mexicana* mutants were used in prolonged mouse infection studies, after which the presence of the extrachromosomal copy of *LmxMPK4* was verified in all isolated parasites capable of proliferation (Wang, Q. et al. 2005). LmxMPK4 was consequently deemed essential in promastigotes and amastigotes. Protein and mRNA levels of LmxMPK4 *in vivo* were lower in amastigotes than in promastigotes, indicating a down-regulation in amastigotes, which obviously does not correlate with reduced importance of the protein (Wang, Q. et al. 2005). Interestingly, analysis and deletion experiments of the *T. brucei* homologue TbMAPK2 showed the protein to be essential in procyclics, but not in bloodstream forms (Muller, I. B. et al. 2002). Bloodstream forms, in which *TbMAPK2* had been deleted showed no visible phenotype, but differentiated into procyclics with a considerable delay. The originating procyclic cells displayed a mostly normal morphology and were motile, but did not proliferate. Despite the observed growth arrest, which was shown not to result from a specific arrest in the cell cycle, procyclic cell lines survived for rather long periods in culture. Wild type bloodstream forms nevertheless upregulate mRNA levels of TbMAPK2, indicating either functional redundancy or compensation for the loss of TbMAPK2 in bloodstream forms (Muller, I. B. et al. 2002). These findings show that TbMAPK2 and LmxMPK4 either play different roles in *L. mexicana* and *T. brucei* or that their function is essential in *Leishmania* amastigotes and promastigotes, as well as in *T. brucei* procyclics, but not in *T. brucei* bloodstream forms. In conclusion, LmxMPK4 presents itself as an interesting research object and a possible target for the development of anti-leishmanial drugs. Accordingly, one of the objectives of this thesis was to generate active recombinant LmxMPK4, which could be used for drug screening. Although the discussed complementary genetic approach, adapted by Morales et al. generates active protein for *in vitro* kinase assays and is excellent for studying the *in vivo* activation status of the

kinase, it is not an easy to use method for generating suitable amounts of active protein (Morales, M. A. et al. 2007), particularly if high-throughput drug screening is envisaged. The work of this thesis should investigate whether the GST-tag, previously used for purification of recombinant LmxMPK4, influences kinase activity. Other approaches to establish higher phosphotransferase activity were going to be the search for better substrates than MBP, expression of the kinase using another tag and the search for a possible activating MAP2K of *L. mexicana*. Another research objective of this thesis was to continue analysing the role LmxMPK4 plays in *Leishmania* and the identification of its *in vivo* target. On grounds of the essentiality of the protein this investigation could not be based on the analysis of deletion mutants. To overcome this obstacle an inhibitor-sensitised mutant of LmxMPK4 was created (Bishop, A. C. et al. 2001). In this mutant the gatekeeper residue methionine111 was exchanged to glycine, creating an additional pocket within the ATP-binding site that should permit the specific binding of the synthetic inhibitor 1-naphthyl-pyrazolo[3,4d]pyrimidine (1NA), but not affect the function of the kinase (Puls, G., diploma thesis, 2005). The inhibitor-sensitised LmxMPK4ISMG mutant should be able to substitute the function of wild type LmxMPK4 in *Leishmania*, permitting the investigation of the immediate effects of LmxMPK4 inhibition in vivo. This thesis aimed to elucidate the role of LmxMPK4 in vivo with the help of the inhibitor-sensitised mutant system.

1.8 State of knowledge and research objectives, LmxMPK6

The other research objective of this thesis was the analysis of the *L. mexicana* MAP kinase LmxMPK6. This kinase was, just as LmxMPK4, cloned from genomic DNA of *L. mexicana* by conducting a PCR with degenerate oligonucleotides, corresponding to the phosphorylation lip of MAP kinases (Wiese, M. et al. 2003b). The open reading frame was confirmed by sequencing and published in the NCBI Entrez database with the accession number AJ293284. The open reading frame of *LmxMPK6* comprises 3318 bp and encodes a protein of 1106 amino acids with an estimated molecular weight of 118.9 kDa. The activation motif of LmxMPK6 contains an aspartate, flanked by the conserved threonine and tyrosine residues. The kinase displays all twelve typical kinase subdomains, characteristic conserved amino acid moieties and a common docking domain of the sequence DGFRD (Wiese, M. et al. 2003b). A distinctive feature of LmxMPK6 is its extremely prolonged C-terminus of 775 bp. The only other MAP kinase of *L. mexicana* with a similar, even longer, C-terminal extension is LmxMPK8, which phylogenetically clusters with LmxMPK6 (Wiese, M. 2007). The C-terminal extension of LmxMPK6 contains four possible SH3-binding sites with the consensus sequence PXXP and two possible monopartite nuclear localisation signals, consisting of four or five basic amino acids (Wiese, M. et al. 2003b). LmxMPK6 was classified as a *Leishmania* MAP kinase,

but its kinase domain additionally displays attributes of cyclin-dependent protein kinases. It contains for instance a threonine and tyrosine residue at position 14 and 15, which are typically phosphorylated in the ATP binding sites of CDKs to promote negative regulation, but do not exist in MAP kinases. One of the diagnostic motifs for MAP kinases F-X_{10}-RE is only partially present in LmxMPK6, where the phenylalanine is exchanged to glutamate. No functional cyclin-binding site is present in LmxMPK6 on the other hand, as the motif PQTALRE typical for kinetoplastid CDKs (Mottram, J. C. 1994) is replaced by the sequence RKTSSRE in LmxMPK6. The closest homologues of LmxMPK6 are found in other *Leishmania* species (*L. major* 87%, *L. infantum* 88%, *L. braziliensis* 67% amino acid identities) and in *T. cruzi* (68% amino acid identity) and *T. brucei* (60% amino acid identity). Homologues to proteins of other organisms are rather weak (*Schistosoma mansoni* 48%, *D. discoideum* 40%, *S. cerevisiae* 36% amino acid identities). The closest human homologue of LmxMPK6 is the CDC2-related kinase 2 with 49% amino acid identities. Apart from the fact that LmxMPK6 mRNA was upregulated in stationary phase promastigotes, nothing was known of LmxMPK6 *in vivo* or *in vitro* at the start of this thesis (Wiese, M. et al. 2003b). The closest homologue of LmxMPK6 from *T. brucei*, TbECK1, was found to be constitutively expressed during both life cycle stages, both in regard to mRNA and protein levels (Ellis, J. et al. 2004). It was not possible to repress the expression of TbECK1 via RNA interference in either life cycle stage, indicating that the protein might be essential in both stages. Extrachromosomal over-expression of several mutants of TbECK1, which were either truncated and/or carried point mutations, demonstrated a severe growth arrest with a high amount of aberrant karyotypes. The phenotype was not displayed when the wild type protein TbECK1 was over-expressed. Instead it was only apparent when truncated mutants, lacking the C-terminus, were over-expressed and then only when these truncated mutants contained at least one of the phosphorylation residues in the TXY-motif and possessed ATP-binding ability (Ellis, J. et al. 2004). This dependence on the presence of an active, yet truncated mutant, indicated that the phenotype resulted from an aberrant activity of the truncated kinase, and not from inactivity due to the lack of the C-terminal extension. The C-terminus of TbECK1 therefore seems to negatively regulate the kinase. One aim of this thesis was to investigate the role of the C-terminal extension of LmxMPK6, by constructing truncated versions of the protein and subjecting them to *in vitro* kinase assays. It was furthermore aspired to test the phosphotransferase activity of recombinant wild type LmxMPK6, generate a kinase-dead mutant of LmxMPK6 and determine via deletion experiments whether LmxMPK6 is essential for *L. mexicana*.

2. Materials

2.1 Laboratory equipment

Centrifuges

Centrifuge 5415C/D/R	Eppendorf, Hamburg, Germany
GS-6KR Centrifuge (Rotor: GH3.8)	Beckman Instruments, Munich, Germany
HERMLE Z 400 K	Hermle Labortechnik, Wehingen, Germany
Optima TL Ultracentrifuge (Rotor: TLA 55)	Beckman Coulter, Krefeld, Germany
ProFuge 10 K	Stratagene, La Jolla, CA, USA
Sorvall RC-5B Refrigerated (Rotors: SS-34, GSA)	Kendro Laboratory Products, Hanau, Germany

CO_2 incubator

BBK 6220	Kendro Laboratory Products, Hanau, Germany

Electrophoresis equipment

Minigel(-Twin)	Biometra, Göttingen, Germany
Power supply: Consort E734	Consort, Turnhout, Belgium
Power supply: Gene Power Supply GPS 200/400	Amersham Biosciences, Freiburg, Germany

Immunoblotting equipment

Fastblot B33 / B34	Biometra, Göttingen, Germany

FACS Sorter

FACSCalibur Flow Cytometer	BD Biosciences, San Jose, CA, USA

Heat block

Thermomixer comfort	Eppendorf, Cambridge, UK

Microscopes

Axiovert 25	Carl Zeiss, Jena, Germany
Axioskop 2 plus	Carl Zeiss, Jena, Germany
Digital camera: C4742-95	Hamamatsu Photonics, Herrsching am Ammersee, Germany
Axiostar plus	Carl Zeiss, Jena, Germany

pH Meter

HI221 Microprocessor pH meter	Hanna Instruments, Leighton Buzzard, UK

Photometer

BioPhotometer 6131	Eppendorf, Hamburg, Germany
Pharmacia LKB Ultrospec III	Pharmacia, Milton Keynes, UK

Safety cabinet

HERAsafe HS15 (Heraeus)	Kendro Laboratory Products, Hanau, Germany

Shaking incubators

Innova 44	New Brunswick Scientific, Edison, NJ, USA

Shaking water baths

GFL 1083	GFL, Burgwedel, Germany
mgw LAUDA M3	Heidolph Electro, Kehlheim, Germany

Sonifier

Branson Sonifier 250	Branson, Danbury, CT, USA

Thermocycler

Gene Amp PCR System 9700	PE Applied Biosystems, Weiterstadt, Germany
Gene Amp PCR System 2400	PE Applied Biosystems, Weiterstadt, Germany

Transfectors

Nucleofector II	Amaxa Biosystems, Gaithersburg, MD, USA

UV linker

UV Stratalinker 1800	Stratagene, La Jolla, CA, USA

Vortex

IKA-VIBRO-FIX VF2	IKA Labortechnik, Staufen, Germany

2.2 Glassware, plastics, other materials

Plastic consumables	Eppendorf (Cambridge, UK) Sarstedt (Leicester, UK) Greiner Bio-One (Solingen, Germany) Nunc (Langenselbold, Germany) VWR International (Lutterworth, UK)
Neubauer counting chambers	VWR International (Darmstadt, Germany)
Biodyne A nylon membrane	Pall (Dreieich, Germany)
Immobilon-P PVDF membrane	Millipore (Schwalbach, Germany)
CEA medical X-ray, screenfilm blue, sensitive	Supplier: Ernst Christiansen GmbH, Planegg, Germany Manufacturer: CEA, Strängnäs, Sweden
HiTrap desalting sephadex G-25 column	GE Healthcare Life Sciences, Little Chalfont, UK
Parafilm M	Brand GmbH, Wertheim, Germany
Complete EDTA-free protease inhibitor tablets	Roche Diagnostics, Burgess Hill, UK
Gel drying frames	Carl Roth, Karlsruhe, Germany
Whatman cellulose blotting paper 3MM chr 58 cm x 68 cm	Whatman plc, Maidstone, UK

2.3 Chemicals

[γ-^{32}P]-ATP	Perkin Elmer, Rodgau, Germany Hartmann Analytic GmbH, Braunschweig, Germany
Acetic acid	Carl Roth, Karlsruhe, Germany
Acrylamide 30% (w/v) /Bis-acrylamide 0.8% (w/v)	Merck Chemicals, Nottingham, UK
Adenosine triphosphate (ATP)	Roche Diagnostics, Mannheim, Germany
Agar-Agar	Carl Roth, Karlsruhe, Germany
Agarose (electrophoresis grade)	Carl Roth, Karlsruhe, Germany
Ammonium chloride	Sigma-Aldrich, Steinheim, Germany
Ammonium persulfate (APS)	Merck Chemicals, Nottingham, UK
Ampicillin	Sigma-Aldrich, Steinheim, Germany
Bacto Tryptone	Becton Dickinson, Heidelberg, Germany
Blocking reagent	Roche Diagnostics, Mannheim, Germany
Boric acid	Carl Roth, Karlsruhe, Germany
Bovine serum albumine (BSA)	Sigma-Aldrich, Steinheim, Germany

Bromophenol blue	Sigma-Aldrich, Steinheim, Germany
Calcium chloride	Carl Roth, Karlsruhe, Germany
Chelating sepharose fast flow	GE Healthcare, Little Chalfont, UK
Chloroform	Carl Roth, Karlsruhe, Germany
Cobalt chloride hexahydrate	Sigma-Aldrich, Gillingham, UK
Coomassie Brilliant Blue G250	Carl Roth, Karlsruhe, Germany
Coomassie Brilliant Blue R250	Carl Roth, Karlsruhe, Germany
CSPD	Roche Diagnostics, Mannheim, Germany
DABCO	Sigma-Aldrich, Steinheim, Germany
DAPI	Sigma-Aldrich, Steinheim, Germany
Disodium hydrogen phosphate dihydrate	Carl Roth, Karlsruhe, Germany
DMF	Merck, Darmstadt, Germany
DMSO	Carl Roth, Karlsruhe, Germany
DNA, MB grade (from fish sperm)	Roche Diagnostics, Mannheim, Germany
dNTP mix	Roche Diagnostics, Mannheim, Germany
DTT	Biomol, Hamburg, Germany
EDTA disodium dihydrate	Sigma-Aldrich, Gillingham, UK
EGTA	Carl Roth, Karlsruhe, Germany
Ethanol	Carl Roth, Karlsruhe, Germany
Ethidium bromide	Sigma-Aldrich, Steinheim, Germany
FCS	PAN Biotech, Aidenbach, Germany
Formaldehyde 37% (Formaline)	Carl Roth, Karlsruhe, Germany
Formamide	Carl Roth, Karlsruhe, Germany
Glucose	Carl Roth, Karlsruhe, Germany
Glutaraldehyde	Merck, Darmstadt, Germany
Glutathione, reduced	Sigma-Aldrich, Steinheim, Germany
Glutathione Uniflow Resin	BD Biosciences, Oxford, UK
Glycerol	Carl Roth, Karlsruhe, Germany
Glycine	Carl Roth, Karlsruhe, Germany
Hemin	Sigma-Aldrich, Steinheim, Germany
HEPES	Carl Roth, Karlsruhe, Germany
Hydrochloric acid	Carl Roth, Karlsruhe, Germany
Hygromycin B	Merck Biosciences, Schwalbach, Germany
Imidazole	Carl Roth, Karlsruhe, Germany
IPTG	Gerbu Biochemicals, Gaiberg, Germany
Isoamyl alcohol	Carl Roth, Karlsruhe, Germany
Isopropanol	Carl Roth, Karlsruhe, Germany
Kanamycin sulfate	VWR, Lutterworth, UK
Leupeptin	Sigma-Aldrich, Steinheim, Germany

L-Glutamine	PAN Biotech, Aidenbach, Germany
Lithium chloride	Merck Chemicals, Nottingham, UK
Magnesium chloride hexahydrate	Carl Roth, Karlsruhe, Germany
Magnesium sulfate	Merck, Darmstadt, Germany
Maleic acid	Carl Roth, Karlsruhe, Germany
Manganese chloride	Merck, Darmstadt, Germany
MBP dephosphorylated	Millipore,
MES	Fischer Scientific (Serva), Loughborough, UK
Methanol	Carl Roth, Karlsruhe, Germany
Milk powder	Carl Roth, Karlsruhe, Germany
MOPS	Sigma-Aldrich, Gillingham, UK
Mowiol 4-88	Merck, Darmstadt, Germany
Neomycin (G418)	Roche Diagnostics, Mannheim, Germany
N-Lauroyl sarcosine sodium salt	VWR, Lutterworth, UK
Okadaic acid	Merck, Darmstadt, Germany
ortho-Phenanthroline	Sigma-Aldrich, Steinheim, Germany
ortho-Phosphoric acid	Carl Roth, Karlsruhe, Germany
Paraformaldehyde	VWR, Lutterworth, UK
Penstrep (1000 U/ml Penicillin, 10 mg/ml Streptomycin)	Life Technologies, Carlsbad, USA
Phenol, equilibrated in TE buffer pH 7.5-8.0	Carl Roth, Karlsruhe, Germany
Phleomycin (Bleomycin)	Merck Biosciences, Schwalbach, Germany
PMSF	Sigma-Aldrich, Steinheim, Germany
Poly-L-Lysine hydrobromide	Sigma-Aldrich, Steinheim, Germany
Potassium acetate	Carl Roth, Karlsruhe, Germany
Potassium chloride	Sigma-Aldrich, Gillingham, UK
Potassium dihydrogen phosphate	Merck, Darmstadt, Germany
Puromycin dihydrochloride	Carl Roth, Karlsruhe, Germany
Rubidium chloride	Sigma-Aldrich, Gillingham, UK
Saponin	Carl Roth, Karlsruhe, Germany
Schneider's Drosophila medium	Generon Ltd., Maidenhead, UK
SDM medium	Generon Ltd., Maidenhead, UK
Silver nitrate	Carl Roth, Karlsruhe, Germany
Sodium acetate trihydrate	Carl Roth, Karlsruhe, Germany
Sodium carbonate	Carl Roth, Karlsruhe, Germany
Sodium chloride	Sigma-Aldrich, Gillingham, UK
Sodium dihydrogen phosphate	Merck, Darmstadt, Germany
Sodium dodecyl sulfate (SDS)	Fischer Scientific, Loughborough, UK
Sodium fluoride	Merck, Darmstadt, Germany

Sodium hydroxide	Carl Roth, Karlsruhe, Germany
Sodium orthovanadate	Sigma-Aldrich, Steinheim, Germany
Sodium thiosulfate pentahydrate	Carl Roth, Karlsruhe, Germany
S-protein agarose	Merck Chemicals, Nottingham, UK
TEMED	Sigma-Aldrich, Steinheim, Germany
Tetracycline	Sigma-Aldrich, Steinheim, Germany
Trisodium citrate	Carl Roth, Karlsruhe, Germany
TLCK	Sigma-Aldrich, Steinheim, Germany
Triton X-100	Carl Roth, Karlsruhe, Germany
Trizma	Sigma-Aldrich, Gillingham, UK
Tween 20	Carl Roth, Karlsruhe, Germany
X-Gal	Roche Diagnostics, Mannheim, Germany
Xylenecyanol	Sigma-Aldrich, Steinheim, Germany
Yeast extract	Fluka, Gillingham, UK
2-mercaptoethanol	Carl Roth, Karlsruhe, Germany

All chemicals from Carl Roth ordered in the UK were supplied by Techmate Ltd (Milton Keyes, UK).

2.4 Culture media, stock and buffer solutions

Agarose gel loading buffer (10x)	0.1 M EDTA pH 8.0 0.1% (w/v) bromophenol blue 0.1% (w/v) xylenecyanol 0.5x TBE 50% (v/v) glycerol
Bradford reagent	5% (v/v) ethanol 0.01% (w/v) Coomassie Brilliant Blue G250 10% (v/v) phosphoric acid filtered, stored at 4°C, in opaque container
Chloroform/isoamyl solution	98% (v/v) chloroform 2% (v/v) isoamyl alcohol
Complete EDTA-free protease inhibitor cocktail	1 tablet complete EDTA-free (Roche) in 2 ml PBS
Coomassie R250 destaining solution	30% (v/v) methanol 10% (v/v) acetic acid

Coomassie R250 staining solution	0.1% (w/v) Coomassie Brilliant Blue R250 40% (v/v) methanol 10% (v/v) acetic acid filtered through fluted filter
Cryo medium for *Leishmania*	90% (v/v) iFCS 10% (v/v) DMSO
DAPI stock solution	160 µg/ml in methanol
Equilibration buffer for HiTrap desalting	40 mM Tris-HCl pH 7.0 0.1% (v/v) 2-mercaptoethanol 0.1 mM EGTA 0.1% Triton X-100
Fixing solution for *Leishmania* cell counting	10% (v/v) formaldehyde in 1x PBS
Fixing solution for *Leishmania* FACS analysis	70% (v/v) methanol in 1x PBS
Gel drying solution	20% (v/v) ethanol 10% (v/v) glycerol
GST elution buffer	10 mM reduced glutathione 50 mM Tris-HCl pH 8.0
Hemin stock solution	2.5 mg/ml in 50 mM NaOH
His-purification binding buffer	50 mM Tris-HCl pH 8.0 1 M NaCl 10% (v/v) glycerol 20 mM imidazole
His-purification elution buffer	50 mM Tris-HCl pH 8.0 300 mM NaCl 10% (v/v) glycerol 500 mM imidazole 1 mM PMSF
His-purification washing buffer	50 mM Tris-HCl pH 8.0 1 M NaCl 10% (v/v) glycerol 10 mM imidazole
iFCS	FCS inactivated for 45 min at 56°C filter-sterilised
Immunoblot blocking solution (secondary antibody: anti-rabbit)	5% (w/v) milk powder 20 mM Tris-HCl pH 7.5 in PBST
Immunoblot blocking solution (secondary antibody: anti-mouse)	3% (w/v) BSA in TBST

Immunoblot stripping solution	62.5 mM Tris-HCl pH 6.7 2% (w/v) SDS 0.78% (v/v) 2-mercaptoethanol
Immunoblot transfer buffer	25 mM Trizma 150 mM glycine 10% (v/v) methanol
Kinase reaction buffer LmxMPK4 (10x)	100 mM $MnCl_2$ 500 mM MOPS pH 7.0 1 M NaCl
Kinase reaction buffer standard (10x)	20 mM $MnCl_2$ 100 mM $MgCl_2$ 500 mM MOPS pH 7.2 1 M NaCl
LB agar	1.5% (w/v) agar-agar in LB medium autoclaved for sterilisation (if required, antibiotics were added after LB agar had cooled to ca. 50°C)
LB medium	1% (w/v) bacto tryptone 0.5% (w/v) yeast extract 1% (w/v) NaCl autoclaved for sterilisation (if required, antibiotics were added after LB medium had cooled to ca. 50°C)
Leishmania lysis buffer for kinase assays	40 mM Tris-HCl pH 7.0 2.5 mM EDTA 15 mM DTT 1% Triton X-100 1 mM PMSF 10 µg/ml leupeptin 1 mM ortho-phenantroline
Metabolomics extraction buffer	80% (v/v) ethanol 20% (v/v) 20mM HEPES filter-sterilised
Mowiol/DABCO	2.4 g Mowiol 6 g glycerol 12 ml 0.2 M Tris-HCl pH 8.5 6 ml ddH_2O 2.5% (w/v) DABCO
PBS	137 mM NaCl 2.7 mM KCl 10.1 mM Na_2HPO_4 1.8 mM KH_2PO_4
PBST	0.2% (v/v) Tween 20 in 1x PBS

RF1	100 mM RbCl 50 mM $MnCl_2 \cdot 4H_2O$ 10 mM $CaCl_2 \cdot 2H_2O$ 30 mM potassium acetate 15% (v/v) glycerol adjusted to pH 5.8, filter-sterilised
RF2	10 mM RbCl 75 mM $CaCl_2 \cdot 2H_2O$ 10 mM MOPS 15% (v/v) glycerol Adjusted to pH 6.8, filter-sterilised
Schneider's Drosophila medium	complete 20% (v/v) iFCS (PAN) 1% (v/v) penstrep 1% (v/v) L-glutamine 3.9 mg/ml MES in Schneider's Drosophila medium filter-sterilised
SDM medium complete	10% (v/v) iFCS 1% (v/v) penstrep 7.5 µg/ml hemin in SDM medium filter-sterilised
SDS-PAGE electrophoresis buffer (10x)	0.25 M Trizma 1.92 M glycine 1% (w/v) SDS
SDS-PAGE sample buffer (5x)	62.5 mM Tris-HCl pH6.8 20% (v/v) glycerol 2% (w/v) SDS 0.001% (w/v) bromophenol blue 200 mM DTT
SDS-PAGE resolving gel buffer (4x)	1.5 M Tris base 0.4% (w/v) SDS adjusted to pH 8.8
SDS-PAGE stacking gel buffer (4x)	0.5 M Tris base 0.4% (w/v) SDS adjusted to pH 6.8
Silver staining developing solution	60 g/l Na_2CO_3 20 µl/l $Na_2S_2O_3$ 250 µl/l formaldehyde
Silver staining fixing solution	50% (v/v) methanol 12% (v/v) acetic acid 500 µl/l formaldehyde
Silver staining solution I	0.2 g/l $Na_2S_2O_3$
Silver staining solution II	2 g/l $AgNO_3$ 375 µl/l formaldehyde

Silver staining stopping solution	50% (v/v) methanol 12% (v/v) acetic acid
Silver staining storage solution	6% (v/v) glycerol
Silver staining washing solution I	50% (v/v) ethanol
Silver staining washing solution II	50% (v/v) methanol
Silver staining washing solution III	30% (v/v) methanol
Southern blot blocking reagent (10x)	100 mM maleic acid 150 mM NaCl pH adjusted to 7.5 10% (w/v) blocking reagent Store at -20°C
Southern blot denaturing solution	0.25 N HCl
Southern blot DIG I buffer	0.1 M maleic acid 0.15 M NaCl adjusted to pH 7.5 with NaOH
Southern blot DIG II buffer	10% (w/v) blocking reagent in DIG I buffer
Southern blot DIG III buffer	50 mM $MgCl_2$ 0.1 M NaCl 0.1 M Tris-HCl pH 9.5
Southern blot DIG washing buffer	0.3% (v/v) Tween 20 in DIG I buffer
Southern blot hybridising solution	0.02% (w/v) SDS 0.1% (w/v) N-Lauroyl sarcosine 20% (v/v) Southern blot blocking reagent (10x) 25% (v/v) SSC (20x) 50% (v/v) formamide
Southern blot neutralising solution	0.5 M NaOH 1.5 M NaCl
Southern blot pre-hybridising solution	100µg/ml DNA, MB grade (from fish sperm) in hybridising solution
Southern blot washing buffer 1	2x SSC 0.1% (w/v) SDS
Southern blot washing buffer 2	0.1x SSC, 0.1% SDS
SSC (20x)	3 M NaCl 0.34 M trisodium citrate pH adjusted to 7.0
S-tag purification binding/washing buffer (10x)	200 mM Tris-HCl pH 7.5 1.5 M NaCl

$T_{10}E_{0.1}$	10 mM Tris-HCl pH 8.0 0.1 mM EDTA pH 8.0
TBE (5x)	0.45 M Trizma 0.45 M boric acid 10 mM EDTA pH 8.0
TBS	20 mM Tris-HCl pH 7.5 150 mM NaCl
TBST	0.05% (v/v) Tween 20 in TBS
TELT	50 mM Tris-HCl pH 8.0 62.6 mM EDTA pH 8.0 2.5 M LiCl 4% Triton X-100
TENS	10 mM Tris-HCl pH 8.0 1 mM EDTA pH 8.0 100 mM NaOH 0.5% (w/v) SDS

2.5 Bacterial strains

Description	Genotype	Source
BL21 (DE3) [pAP*lac*IQ]	B F$^-$ *dcm ompT hsdS*(r_B^- m_B^-) *gal* λ(DE3) [pAP*lac*IQ]	Joachim Clos, Hamburg, Germany
OneShot TOP10F'	F´{*lac*I^q Tn*10* (Tet^R)} *mcr*A Δ(*mrr-hsd*RMS-*mcr*BC) Φ80*lacZ*ΔM15 Δ*lac*X74 *rec*A1 *ara*D139 Δ(*ara-leu*)7697 *gal*U *gal*K *rps*L *end*A1 *nup*G	Invitrogen Life Technologies, Karlsruhe, Germany
OneShot INV110	F´ {traΔ36 proAB lacI^q lacZΔM15} rpsL (Str^R) thr leu endA thi-1 lacY galK galT ara tonA tsx dam dcm supE44 Δ(lac-proAB) Δ(mcrC-mrr)102::Tn10 (Tet^R)	Invitrogen Life Technologies, Karlsruhe, Germany
XL1-Blue	*ecA endA gyrA96 thi-1 hsdR17 supE44 rel A1 lac* [F' *proAB lac^{q}ZΔM15* Tn*10* (Tet^R)]	Stratagene, La Jolla, CA, USA
BL21-CodonPlus(DE3)-RP	B F$^-$ *omp*T *hsd*S($r_B^-m_B^-$) *dcm*$^+$ Tet^r *gal* λ(DE3) *end*A Hte [*argU proL* Cam^r]	Stratagene, La Jolla, CA, USA
BL21(DE3)	B F$^-$ *dcm ompT hsdS*(r_B^- m_B^-) *gal* λ(DE3)	Stratagene, La Jolla, CA, USA

2.6 *Leishmania* strain

Leishmania mexicana mexicana MNYC/BZ/62/M379, clone 2

2.7 Mouse strain

Infection studies were performed with 6 to 10 weeks old, female BALB/c mice which had either been bred in the BNI (Hamburg, Germany) or were purchased from Charles River (Sulzfeld, Germany).

2.8 Oligonucleotids

description	oligonucleotide sequence
90	5' TCCCCGGCGGTTGGCCGAT 3'
91	5' AAACCGCTCGCGGTGTGTT 3'
4IS-GA.for:	5' CACTTTCCTGCCTTAAGGCCTCATGCGGC 3'
4IS-GA.rev:	5' ATTTAAATCTGTGTCATAAAGATCGGCCACCAAGTAAAT-GTCC 3'
abMPK6TY.for:	5 GGATCC GCGATCGC GCTCGACGTCCTATAG 3'
abMPK6TY.rev:	5' GATATCAAGCTTCAAGATCTGCCCGACATGTTGATGCCA-GTATCGGGGGA 3'
LmxMPK4i.for	5' GACATTTACTTGGTGGGAGATCTTTATGACACAGAT 3'
LmxMPK4i.rev	5' TGTGTCATAAAGATCTCCCACCAAGTAAATGTCCTC 3'
LmxMPK6delds.rev	5' CGCGATATCACACAATACCCGCACC 3'
LmxMPK6delup.for	5' CGCGATATCCACGGCCGCTTATCT 3'
mapkin15_1.rev	5' GATCTGACGAGCTCATCACT 3'
mapkin150505_2.for	5' TGCGGGAGATGGAGATAA 3'
mapkin150505_3.rev	5' CTTCGCAGTTAATCGTCTT 3'
mapkin150505c-term	5' CCCGATATCTCGAGCCTATTCGTTCAATTGTG 3'
mapkin150505n-term	5' CCCGATATCATGACTCAGCTCGTCCC 3'
mapkin24_12.for	5' GCTGCGTTGTTGCGTGTTT 3'
mpk4_1.for	5' GATGAAGCGTAAACCAATCT 3'
mpk4_6.for	5' TCGTAGTAAATATCCCATA 3'
MPK6Cterm.for	5' CATATGAGCGAACCACACATCTCGA 3'
MPK6Cterm.rev	5' GGTACCGATGCCAGTATCGGGGGA 3'
MPK6KM.rev	5' TCTGTTTAAACCGCATGATGGCGACAAGCTTCC 3'
MPK6KM.for	5' GCGGTTTAAACAGACAGAGCAGGATGAG 3'
MPK6NcoIAvrII.for	5' ACACCTAGGCCATGGACTTCAAGGCTCAGCTTG 3'
MPK6NheAvrII.rev	5' ACACCTAGGGCTAGCCAGCTTTGTGCCGTAATC 3'

MPK6Nterm.for	5' GGATCCGATGGATGGAGGCCTACGAGA 3'
MPK6Nterm.rev	5' GATATCAGCTGTTTTTGGCCGT 3'
MPK6short2.for	5' GGATCCACCATGGAGGCCTACGAGACA 3'
MPK6short2.rev	5' GATATCAAGCTTCAAGATCTGCCTGACATGTTGCTGTTT-TTGGCCGTGGG 3'
pJCLinker	5' P-AATTGCGGAATTCCACTAGTTAACA 3'
pJCLinker	5' P-AGCTTGTTAACTAGTGGAATTCCGC 3'
ScaI.for	5' CTGTGACTGGTGAGTACTCAACCAAG–3'
ScaI.rev	5' ATGACTTGGTTGAGTACTCACCAGTC– 3'

2.9 DNA vectors and plasmid constructs

pCR2.1-TOPO	Invitrogen Life Technologies, Karlsruhe
pJCduet	Clos J., BNI, Hamburg
pX63polPAC	(Bengs, F. et al. 2005)
pXpolNeo	Wiese M., BNI, Hamburg, Germany (unpublished)
pXpolPhleo	Wiese M., BNI, Hamburg, Germany (unpublished)
pBluescript II SK(+)	Stratagene, La Jolla, CA, USA,
pGEX-KG	(Guan, K. L. et al. 1991)
pCR2.1 TOPO	Invitrogen, Karlsruhe, Germany
pBmapkin240505	(Wiese, M. et al. 2003b)
pGEX-KG-LmxMPK4	(Wang, Q. et al. 2005)
pGEX-KG-LmxMPK4KM	(Wang, Q. et al. 2005)
pGEX-KGPK5	(Melzer, I. M., PhD thesis, 2007)
pXpolNeoMPK4IS	(Puls, G., diploma thesis, 2005)
pXpolPacMPK4	(Wang, Q. et al. 2005)
pB11mapkin150505delphleo	(Wiese, M. et al. 2003b)
pGEX-KG3-mapkin24-0505	(Wiese, M. et al. 2003b)
pGEX2TYMPK7KM	Bleicher N. M., BNI, Hamburg, Germany (unpublished)
pBE23mapkin24-0505P14	(Wiese, M. et al. 2003b)

The names and plasmid maps of all constructs generated throughout the course of this thesis are shown in the appendix.

2.10 Antibodies

Primary antibodies

Antigen / Name	Host	Dilution	Source
Digoxigenin (Fab fragments antibody AP-conjugated)	sheep	1:10000	Roche Diagnostics, Mannheim, Germany
Phosphotyrosine / 4G10 (hybridoma cell supernatant)	mouse	1:250	Bernhard Fleischer, BNI, Hamburg
anti-LmxMPK4	rabbit	1:250	(Wiese, M. et al. 2003b)
anti-LmxMPK6Cterm	rabbit	1:100	Wiese, M., unpublished
anti-LmxMPK6Nterm	rabbit	1:250	Wiese, M., unpublished

Secondary antibodies

Antigen / Name	Host	Dilution	Source
Mouse IgG (HRP-conjugated)	rabbit	1:2000	DAKO, Hamburg, Germany
Rabbit IgG (HRP-conjugated)	goat	1:5000	Dianova, Hamburg, Germany

2.11 Enzymes

Alkaline phosphatase, shrimp	Roche Diagnostics, Mannheim, Germany
Expand High Fidelity PCR System	Roche Diagnostics, Mannheim, Germany
Klenow enzyme	New England Biolabs, Hitchin, UK
Restriction endonucleases	New England Biolabs, Hitchin, UK
RNase A (bovine pancreas)	Roche Diagnostics, Mannheim, Germany
T4 DNA ligase	Roche Diagnostics, Mannheim, Germany
Thrombin	Amersham Biosciences, Freiburg, Germany
λ-phosphatase	New England Biolabs, Hitchin, UK

2.12 Molecular biology kits

Human T Cell Nucleofector Kit	Amaxa Biosystems, Gaithersburg, USA
M&N NucleoSpin Extract II Kit	Macherey & Nagel, Düren, Germany
M&N NucleoSpin Plasmid Kit	Macherey & Nagel, Düren, Germany
M&N NucleoBond Xtra Midi Kit	Macherey & Nagel, Düren, Germany
SuperSignal West Pico Chemiluminescent Substrate Kit	Pierce/Perbio Science, Bonn, Germany
TOPO TA Cloning Kit	Life Technologies, Carlsbad, USA formerly: Invitrogen Life Technologies
PCR Probe DIG Synthesis Kit	Roche Diagnostics, Burgess Hill, UK

2.13 DNA and protein molecular weight markers

1kb DNA Ladder	Carl Roth, Karlsruhe, Germany
PCR Marker	New England Biolabs, Hitchin, UK
Prestained Protein Marker, Broad Range	New England Biolabs, Hitchin, UK

3. Methods

3.1 Cell biology

3.1.1 Culturing of *E. coli*

3.1.1.1 Culturing on agar plates

A maximum of 150 µl of a suspension of *E. coli* cells were evenly distributed with a Drigalski spatula on LB agar plates, which contained the required antibiotics. Antibiotics were used to select positive clones at concentrations of 100 µg/ml (ampicillin), 50 µg/ml (kanamycin) and 20 µg/ml (tetracycline). The inoculated agar plates were incubated upside down over night at 37°C.

3.1.1.2 Culturing in liquid medium

An adequate volume of LB medium was inoculated with one colony of *E. coli,* taken with a sterile 100 µl pipette tip from freshly incubated agar plates, or with an aliquot of a liquid pre-culture to a final concentration of 1% (v/v). Antibiotics were, if required, added to the same concentrations as mentioned in 3.1.1.1. The cultures were incubated in a shaking incubator at 37°C and 120-250 rpm until they had reached the required optical density.

3.1.1.3 Preparation of glycerol stocks

A volume of 500 µl was taken from a freshly incubated liquid overnight culture and carefully mixed with 500 µl sterile glycerol in a sterile CryoTube. The mixture was incubated for 1 hour on ice and subsequently stored at -70°C.

3.1.2 Culturing of *Leishmania*

3.1.2.1 Culturing of *L. mexicana* promastigotes

L. mexicana promastigotes were cultivated at 27°C in SDM medium (Brun, R. et al. 1977), containing antibiotics if required. The antibiotics used were phleomycin (bleomycin) at 5 µg/ml, hygromycin B at 20 µg/ml, G418 (neomycin) at 10 µg/ml and puromycin at a concentration of 40 µM. Whenever possible, that is when mutations were considered stable, parasites were cultured without selection pressure by antibiotics. This was the case for double-allele knock-out mutants as well as for clones containing mutated versions of essential genes and no copy of the respective wild type gene. The standard method was to culture *L. mexicana* in 10 ml SDM medium in cell culture flasks (Sarstedt).

Cultures were inoculated with a ratio between 1:500 and 1:1000 from an early stationary or late logarithmic culture by using disposable plastic pastettes or pipettes with sterile filter-tips. Culture flasks containing *L. mexicana* were incubated lying down. Dependent on circumstances, parasites were also cultivated in 6-well, 12-well, 24-well and 96-well culture plates, which were wrapped in Parafilm M to prevent evaporation.

3.1.2.2 *In vitro* differentiation to and culturing of *L. mexicana* axenic amastigotes

Cells from a logarithmic promastigote culture (3-4·10^7 cells/ml) were used to inoculate 10 ml of Schneider's Drosophila medium to a density of 4×10^6 cells/ml. An adequate volume was taken from a promastigote culture and sedimented by centrifugation at 2,050 x g at 4°C for 1 min. The supernatant was removed and cells were suspended in Schneider's Drosophila medium and incubated at 34°C under 5% CO_2 (Bates, P. A. et al. 1992). Differentiation was regarded complete on the third day of cultivation. If cell clumps occurred, cultures were carefully and slowly passed 2 times through a syringe using a 23 gauge needle and 4 times using a 18 gauge needle.

3.1.2.3 *In vitro* differentiation to *L. mexicana* promastigotes

Lesion-derived amastigotes were washed with SDM medium and used to inoculate fresh SDM medium to a density of 1×10^7 cells/ml. Cultures were incubated at 27°C without CO_2 to induce differentiation into promastigotes.

3.1.2.4 *Leishmania* cryo stabilates

All cells from a 10 ml *L. mexicana* promastigote culture in its logarithmic growth phase were sedimented by centrifugation for 10 min at 4°C and 2,050 x g. The supernatant was removed and the pellets were resuspended in 1.5 ml cold cryo medium. Aliquots of 500 µl were distributed to 3 CryoTubes and incubated in the gas phase of a liquid nitrogen storage tank for 24 hours. The stabilates were subsequently stored submerged in liquid nitrogen. To start a new culture from a stabilate, the CryoTubes were removed from the liquid nitrogen storage tank, transported on ice and thawed in a 37°C water bath. The contents were transferred into fresh SDM medium, containing the required antibiotics, by using disposable pastettes. The cultures were incubated over night at 27°C after which they were used to inoculate a fresh culture (as described under 3.1.2.1).

3.1.3 Growth assays of *L. mexicana* under inhibitor influence

All promastigote growth curves presented in this work were assayed using 1 ml cultures, incubated in 24-well plates at 27°C. The cultures were inoculated to a density of

5×10^5 cells/ml and samples for cell counting were removed each day at the same time for a period of 5 – 10 days. Addition of the inhibitor 1Na or DMSO took place directly after inoculation of the cultures by using the lowest feasible volume (in general 1 – 2 µl). The cultures were mixed by pipetting after the addition of inhibitor and each time before a sample for cell counting was removed.

3.1.4 Counting of *Leishmania* cells

Samples were suspended in fixing solution for cell counting in appropriate dilutions, varying from 1:10 to 1: 50, and 10 µl were loaded on each side of a Neubauer counting chamber (0.1 mm, 0.0025 mm^2) to be counted by using a light microscope. The square areas of each side, each consisting of 25 smaller squares, were counted and the mean value used to calculate the cell density in cells/ml by multiplying it with the dilution factor and with the chamber factor 10^4.

3.1.5 Propidium-iodide labelling and fluorescence-activated cell sorting (FACS) of *L. mexicana* promastigotes

L. mexicana promastigotes from a logarithmic culture (1-2×10^7 cells/ml) were grown in SDM medium with the addition of 5 µM 1Na, 2.5 µM flavopiridol or a respective volume of DMSO for up to 10 hours. Samples were taken from the culture before the addition of adjuvant and subsequently after one, three, seven and ten hours. Samples consisted of 1 ml culture, which was washed in PBS once and suspended in 1 ml fixing solution for *Leishmania* FACS analysis. After incubation over night at 4°C, propidium iodide was added to a concentration of 10 µg/ml and samples were incubated at RT for 15 minutes and analysed. Flow cytrometry detected the fluorescence of propidium iodide in the FL3 channel.

3.1.6 Generation of metabolomics extracts of *L. mexicana* promastigotes

Buffers for the generation of extracts for metabolomic profiling analyses were always made up fresh using chemicals of the highest available analytical grade.

Promastigote cultures were inoculated from logarithmic cultures to densities of 5×10^6 cells/ml. The inhibitor 1Na or a respective volume of DMSO was added to the newly inoculated cultures, which were then incubated for 48 hours at 27°C. All samples were produced as biological triplicates, which were pooled at the end of 48 hours. The pooled cultures were washed once with PBS, resuspended in PBS and kept at 27°C while the cell densities were determined as quickly as possible by cell counting. For each sample group

three aliquots of 1×10^8 cells were distributed to centrifugation tubes (50 ml). The cells were harvested by centrifugation for 10 min at 3,500 x g at 0℃. Supernatants were discarded and the pellets were swiftly resuspended in 1 ml metabolomics extraction buffer that had been heated to 80℃ in 1.5 ml microcentrifuge tubes for at least 30 min. The cell extracts were quickly transferred back to the original pre-heated microcentrifuge tubes, vortexed shortly and incubated for 3 min at 80℃. After the incubation time the tubes were placed in a pre-chilled benchtop cooler and stored at -20℃ until processing of all samples was finished. To minimise delays in the extraction procedure a maximum of four samples was processed at once. When all samples were processed the microcentrifuge tubes were taken from the benchtop cooler and cellular fragments were sedimented by centrifugation at 0℃ and 16,110 x g for 10 min. The supernatant, containing the extracted metabolites, was carefully removed and transferred into a clean 1.5 ml microcentrifugation tube that had been pre-chilled at -20℃. The samples were stored at -70℃ and analysed by mass spectrometry as soon as possible, but always within the same day. Each extract was analysed 2 times by LC-MS, yielding technical replicate information.

3.2 Mouse foot pad infection studies

All footpad infection studies were conducted with female 6-10 weeks old BALB/c mice. *Leishmania* promastigotes from a culture in late log-phase (3-4$\times10^7$ cells/ml) were harvested by centrifugation at 5,600 x g for 20 s, washed with ice-cold PBS and resuspended in PBS to a final density of 3.3×10^8 cells/ml. Each mouse was infected into the left hind foot pad with 30 µl of the *Leishmania* cell suspension, equalling 1×10^7 cells. Both hind paws were measured regularly with the help of a caliper gauge to monitor lesion development.

3.2.1 Isolation of *L. mexicana* from mouse foot pads

The severed foot pads were sterilised with 70% ethanol, cut into pieces and transferred into 10 ml of ice-cold PBS. To disrupt tissues and liberate amastigotes from macrophages, the pieces were passed through a sterile metal grid. The resulting debris was collected in a sterile petri dish within the PBS used to rinse the grid. The suspension was transferred to sterile centrifugation tubes and cell debris was removed by centrifugation for 10 min at 150 x g and 4℃. The supernatant was again centrifuged at 1,500 x g at 4 ℃ for 10 min to sediment amastigotes, which were subsequently resuspended in 10 ml ice-cold PBS.

3.2.2 Microscopy of DAPI stained *Leishmania*

A 10-well microscope slide was coated with 20 µl 0.1 mg/ml poly-L-lysine in PBS for 15 min. The wells were washed twice with 50 µl PBS. 500 µl were taken from a log-phase

Leishmania culture and centrifuged at 5,600 x g for 20 s. The supernatant was discarded and cells were washed with 1 ml ice-cold PBS and resuspended in 300 µl ice-cold PBS. A mixture of 20 µl cell suspension and 20 µl 4% (v/v) paraformaldehyde was added to each prepared well on the microscope slide. After incubation for 15 min the slide was washed twice with ice-cold PBS. 20 µl of a DAPI solution (dilution 1:100 in PBS) was added to the slide, which was subsequently incubated for 20 min in the dark, followed by 3 washing steps with ice-cold PBS. The slide was dried in the dark for 5 min before it was covered with Mowiol/DABCO solution and a cover slip. Cells were viewed with a Zeiss fluorescence microscope and images were captured using a Hamamatsu digital camera and the Openlab software v 5.0.1 by Improvision.

3.3 Molecular biology

3.3.1 Preparation of competent *E. coli*

Glycerol stocks of cells of the required genotype were used to inoculate LB agar plates, containing the required antibiotic. XL1-Blue and INV110 cells contain resistance against the antibiotic tetracycline, which was used at a concentration of 40 µg/ml. To select BL21(DE3) [pAP*lac*IQ], kanamycin was added at a concentration of 50 µg/ml. BL21(DE3) do not contain any endogenous resistances. One *E. coli* colony was taken from the respective fresh agar plate and used to inoculate 2 ml LB. The culture was incubated at 37°C over night in a shaking incubator at 225 rpm. 500 µl of the over night culture was used to inoculate 100 ml LB medium, containing the required antibiotic. The culture was incubated at 37°C at 225 rpm until it reached an optical density (OD_{550}) of approximately 0.2, after which it was placed on ice for 15 min. The cell suspension was distributed to two 50 ml centrifugation tubes and sedimented for 15 min at 3,500 x g and 4°C. The supernatants were discarded and each pellet was resuspended in 16 ml RF1, respectively. The combined cell suspensions were incubated on ice for 1.5 hours before another centrifugation step at 3,500 x g and 4°C for 15 min. The supernatants were discarded once again and the cells were resuspended in RF2 and distributed to microcentrifugation tubes in 200 µl aliquots after 15 min incubation on ice. All aliquots were quick-frozen in liquid nitrogen and stored at -70°C.

3.3.2 Heat-shock transformation of *E. coli*

Competent cells were defrosted on ice and a maximum of 10 µl of the DNA to be transformed was added to the cells. If BL21(DE3) [pAP*lac*IQ] cells were transformed, only 20 µl of the competent cells were used. The suspension was left on ice for 30 min and then incubated for 1 min (40 s in the case of BL21(DE3) [pAP*lac*IQ] cells) in a water bath which had been pre-heated to 42 °C. 800 µl LB medium (500 µl in the case of BL21(DE3)

[pAP*lac*IQ] cells) without any antibiotics was added and the cell suspension was incubated in a thermomixer at 37°C for 1 hour. Cells were plated on agar plates containing the antibiotics required for plasmid selection in volumes according to the expected transformation efficiency. If the transformed plasmid allowed blue-white selection of accurately transformed cells, the agar plates were additionally plated with 40 µl X-Gal (40 mg/ml in DMF) and 40 µl IPTG (100 mM).

3.3.3 Transformation of *Leishmania* by electroporation

For each transformation 3×10^7 promastigotes were harvested from a *L. mexicana* culture in late-log stage ($3\text{-}4\times10^7$ cells/ml) by centrifugation for 1 min at 5,600 x g and 4°C and resuspended in 100 µl Human T Cell Nucleofector solution, supplemented according to the manufacturer's instructions. The DNA that was supposed to be transformed was added to the cell solution, which was then transferred into the provided electroporation cuvette that had been pre-chilled on ice. The cells were electroporated in the Amaxa Nucleofector II by using the programme V-033 and subsequently kept on ice for 10 min. The cell solution was transferred into fresh 10 ml SDM medium without any new antibiotics by using the small pastettes provided in the kit. The cells were incubated at 27°C for 24 hours, after which the appropriate selective antibiotic was added and the culture was distributed to two 96-well plates in a 1:4 and 1:40 dilution, respectively.

3.3.4 Isolation of plasmid DNA from *E. coli*

3.3.4.1 Mini-preparation of plasmid DNA (Zhou, C. et al. 1990)

One colony from an LB agar plate was used to inoculate 3 ml LB, which was incubated over night at 37°C and 225 rpm in a shaking incubator. 1.5 ml of the culture was subsequently pelleted by centrifugation at 15,800 x g at RT for 30 s. The main part of the supernatant was discarded and the cells were resuspended by vortexing in the remaining supernatant. 300 µl of TENS buffer was added to the cell suspension, which was vortexed at medium speed for 4 s and transferred to ice. 150 µl of 3 M sodium acetate (pH 5.2) was added to the suspension, followed by vortexing for 3 s. Cell debris was subsequently removed by two subsequent centrifugation steps for 10 min at 15,800 x g and 4°C. The supernatant was transferred into a fresh microcentrifugation tube and mixed with 900 µl ice-cold ethanol, followed by centrifugation for 15 min at 15,800 x g and 4°C. The supernatant was discarded and the DNA pellet was washed with 70% ice-cold ethanol, which was removed by centrifugation for 10 min at 15,800 x g and 4°C. The pellets were air-dried at RT and resuspended in 40 µl ddH_2O.

3.3.4.2 Mini-preparation of plasmid DNA using the NucleoSpin Plasmid Kit by Macherey & Nagel

One colony from an LB agar plate was used to inoculate 3 ml LB, which was incubated over night at 37°C and 225 rpm in a shaking incubator. 1.5 ml of the culture was subsequently pelleted by centrifugation at 15,800 x g at RT for 30 s. The remaining procedure followed the instructions of the manufacturer's manual in the chapter "Using a microcentrifuge".

3.3.4.3 Midi-preparation of plasmid DNA using the NucleoBond Xtra Midi Kit by Macherey & Nagel

The cells of a 100 ml overnight culture were harvested by centrifugation at 4,000 x g and 4°C for 15 min. The supernatant was discarded and the subsequent steps followed the instructions of the manufacturer's manual in the chapter "High-copy plasmid purification" until the elution of the plasmid DNA. The eluted DNA solution was distributed to microcentrifuge tubes in 833 µl aliquots and mixed with 583 µl 2-propanol by vortexing. The suspension was centrifuged for 30 min at 15,800 x g and 4°C. The supernatant was discarded and the DNA pellets were washed with 1 ml ice-cold 70% ethanol. The DNA was centrifuged for 10 min at 15,800 x g and 4°C and the supernatant was discarded once again. The DNA pellets were dried on air and when completely dry, resuspended and combined in a total volume of 120 µl ddH_2O.

3.3.5 Isolation of genomic DNA from *Leishmania*

3 ml of cells of a culture in stationary phase were harvested by centrifugation at 15,800 x g for 30 s. The supernatant was discarded and the sedimented cells were suspended in 400 µl fresh TELT buffer. After 5 min incubation at RT 400 µl cold phenol was added to the suspension, which was then rotated end-over-end for 5 min at 4°C, followed by centrifugation for 10 min at 15,800 x g and 4°C. The aqueous upper phase was carefully transferred to a fresh microcentrifugation tube and mixed with 400 µl chloroform/isoamyl alcohol (24:1) by rotating end-over-end for 5 min at 4°C. Another centrifugation step for 10 min at 15,800 x g and 4°C separated the solution into phases. The aqueous upper phase was again transferred to a fresh microcentrifugation tube and mixed with 1 ml ice-cold ethanol. The pellet that was generated by the subsequent centrifugation for 10 min at 15,800 x g and 4°C was washed once with 400 µl ice-cold 70% ethanol before it was dried on air at RT. After the evaporation of all residual alcohol, the DNA was carefully suspended in 100 µl $T_{10}E_{0.1}$ to avoid shearing of the genomic DNA. Storage took place at 4°C.

3.3.6 Phenol/chloroform extraction of DNA solutions

100 µl of a DNA solution (e. g. a restriction endonuclease digest) were mixed with 100 µl TE-equilibrated phenol by vortexing for 30 s. The mixture was separated into different phases by centrifugation for 5 min at 15,800 x g and RT. The aqueous upper phase was carefully removed, transferred into a fresh 1.5 ml microcentrifugation tube and mixed with 100 µl chloroform/isoamyl alcohol by vortexing for 30 s. Another centrifugation step at 15,800 x g for 5 min at RT separated the mixture again into phases and the aqueous upper phase was once again removed and transferred into a fresh microcentrifugation tube. The procedure was followed by an ethanol precipitation step.

3.3.7 Ethanol precipitation of DNA solution

2.5 volumes of ice-cold 100% ethanol and 1/9 volume of 3 M sodium acetate pH 5.2 were added to the DNA solution in question and mixed thoroughly. The mixture was incubated at -70°C for at least 30 min, after which it was centrifuged at 15,800 x g and 4°C for 15 min. 70% ethanol was added to wash the DNA pellet and removed completely after centrifugation for 10 min at 15,800 x g and 4°C. The DNA pellet was dried on air, after which it was dissolved in an appropriate amount of ddH_2O.

3.3.8 Reactions with DNA-modifying enzymes

3.3.8.1 Cleavage of DNA with type II restriction endonucleases

All restriction endonucleases were purchased from New England Biolabs and used according to the manufacturer's instructions in terms of buffer and incubation temperature. Analytical digests were conducted in a total volume of 15 µl using 1 µl of eluted plasmid DNA from mini-preparations and 5 - 10 U of the enzyme. Analytical digests were incubated for 1 hour at the appropriate temperature. Preparative digests of plasmid DNA were performed in a total volume of 100 µl using 10-20 µg DNA and 30 - 60 U of the appropriate enzyme. Preparative digests were generally incubated for three hours.

3.3.8.2 Complete fill-in of a 5'-overhang by Klenow enzyme to create blunt end DNA

DNA was extracted by phenol/chloroform, precipitated by ethanol and dissolved in 43.25 µl ddH_20. Added to this mixture were 1 µl dNTPs, 1.5 U Klenow enzyme and 5 µl 1 x EcoPol reaction buffer, followed by an incubation for 15 min at 25°C. The reaction was stopped by heating at 75 °C for 20 min.

3.3.8.3 Dephosphorylation of DNA 5'-ends

Linearised plasmid DNA was treated with shrimp alkaline phosphatase (SAP) to prevent religation of the fragments. The DNA was extracted by phenol/chloroform, precipitated by ethanol and dissolved in 25.5 µl ddH_2O. 3 µl of the provided SAP buffer was added together with 1.5 U SAP and the mixture was incubated at 37°C for 2 hours. The enzyme was inactivated by heating the reaction to 65°C for 20 min.

3.3.8.4 Ligation of DNA fragments

Approximately 50-100 ng vector was incubated with three times more insert DNA, 1.5 µl of the provided ligase buffer and 1.5 U T4 DNA ligase in a total volume of 15 µl. The mixture was incubated over night at 13°C in a PCR machine and subsequently used for bacterial transformation.

3.3.9 Agarose gel electrophoresis

Agarose gels were prepared at concentrations of 0.7 – 1.2% (w/v) agarose in 0.5 x TBE buffer and contained 0.3 µg/ml ethidium bromide (EtBr). The DNA samples were mixed with a 1/10 volume of 10 x agarose gel loading buffer, loaded into the gel pockets and separated at 1.4 – 10 V/cm. UV illumination visualised nucleic acids with intercalated EtBr. The use of a DNA marker allowed the estimation of length and concentration of separated DNA fragments.

3.3.10 DNA extraction from agarose gels using the NucleoSpin Extract II Kit by Macherey & Nagel

Agarose gelelectrophoresis was performed and the bands of interest were identified by UV illumination and excised with a clean scalpel under low intensity UV light (λ = 365 nm). The extraction of bands was conducted according to the instructions in the manufacturer's manual. The DNA was eluted with 15-50 µl ddH_2O.

3.3.11 Polymerase chain reaction (PCR)

PCRs were conducted using the Expand High Fidelity PCR System from Roche. Reactions were set up to a final volume of 50 µl in 200 µl PCR tubes and contained approximately 30 ng template DNA, 1.5 µl of each oligonucleotide primer solution (10 µM), 5 µl of the supplied PCR buffer that included 15 mM $MgCl_2$, 1 µl of a 20 mM dNTP solution and 0.75 µl of the supplied enzyme mix. The tubes were kept on ice during the set up and until the reaction was performed in a thermocycler. The program used depended largely on individual conditions. The annealing temperature was chosen as a few degrees under

the mean melting temperature of the oligonucleotides, while the elongation time depended on the length of the amplified DNA fragment and equated roughly to 1 min per each 1.5 kb of the expected product. The overall used program was constituted like the following:

DNA denaturation	5 min	95°C	
DNA denaturation	1 min	95°C	25-32 cycles
Primer annealing	1 min	45-65°C	
DNA elongation	1-3 min	72°C (for products over 3 kb : 68°C)	
Final DNA elongation	7 min	72°C (for products over 3 kb: 68°C)	

3.3.12 Cloning of a PCR product with the TOPO TA Cloning Kit

The kit supplies the plasmid vector pCR2.1 TOPO which is linearised with single 3'-thymidine overhangs and a covalently bound topoisomerase I. This permits without adding any other enzymes the quick and efficient ligation of PCR products which contain a single 3'-adenine overhang due to the terminal transferase activity of *Taq* polymerase. 4 µl fresh PCR product was incubated with 1 µl supplied salt solution and 0.5 µl of the supplied pCR2.1 TOPO vector. The reaction was incubated for 5 min at RT and subsequently transformed into competent *E. coli* TOP10F' cells following the instructions in the manufacturer's manual.

3.3.13 DNA sequencing

DNA sequencing reactions were performed by Agowa (Berlin, Germany) for all reactions commissioned before September 2007. All sequencing reactions after September 2007 were performed by Source Bioscience geneservice, Cambridge, UK. The samples were prepared according to the companies' instructions.

3.3.14 Southern blot analysis

Genomic DNA was isolated according to protocol (3.3.5) and digested with one or more restriction endonucleases to generate easy to distinguish DNA fragments of the sequence to be analysed. The digest was performed in a total volume of 100 µl and contained 5-10 µg genomic DNA, 60-80 U of the appropriate enzyme, the appropriate enzyme reaction buffer and 14 µg RNase A. It was important to select only restriction endonucleases that did not display any star activity as the digest was incubated over night rotating end-over-end at the appropriate temperature to ensure full cleavage of all genomic DNA. The cleaved DNA was precipitated by ethanol, dissolved in 15 µl $T_{10}E_{0.1}$

and separated by electrophoresis on a 0.7% (w/v) agarose gel at 80 V. The separated DNA was visualised together with a ruler by UV illumination to facilitate the localisation of marker bands on the final blots. The agarose gel was incubated in Southern blot denaturing solution on a benchtop shaker with low frequency for 20 min to denature the DNA double strands. Subsequently the gel was incubated in Southern blot neutralising solution for 30 min at RT. The transfer of DNA onto the Biodyne A membrane took place over night at 4°C by capillary blotting. This was ensured by the following set-up: 4 long (11.2 cm x 28 cm) strips of Whatman cellulose blotting paper were placed on a propped-up glass plate so that the ends reached down into a basin containing 20 x SSC buffer but the main area was raised above the buffer level. The agarose gel was inverted and placed on the blotting paper strips. All areas of blotting paper that were not covered by the agarose gel were covered with Parafilm M to ensure capillary blotting took place only through the agarose gel. A Biodyne A membrane was cut to the same size as the agarose gel and placed on top of it under 4 layers of Whatman cellulose blotting paper of the same size. A stack of at least 10 cm height of absorbent paper that had been cut to the same size as the agarose gel was placed on top of the construction and covered with a glass plate. A weight on the glass plate ensured an even distribution of pressure throughout the construction. After incubation over night at 4°C the construction was dissembled and the gel pockets were marked on the membrane. The DNA was linked to the membrane by UV illumination in a UV linker in the auto-cross-link mode. The cross-linked membrane was shrink-wrapped in thermoplastic foil together with 50 ml pre-hybridising solution and incubated in a shaking water bath at 42°C for at least 3 hours. The detection of the DNA sequence to be analysed in a Southern blot is carried out by a DNA probe which is homologous to the sequence in question and can consequently bind to it. This, however, requires the DNA probe to be single strand, which is why it was denatured at 98°C for 10 min before it was added to the hybridising solution. The labelling of the DNA probe was accomplished by using the PCR DIG Probe Synthesis Kit from Roche, according to the manufacturer's instructions. If the Southern blot was conducted with a pre-used hybridising solution the denaturing of the probe was achieved by placing the hybridising solution in a boiling water bath (on a bunsen burner, including boiling stones) for 10 min. The Southern blot membrane was shrink-wrapped with 50 ml hybridising solution containing the denatured DIG-labelled DNA probe and incubated over night in a shaking water bath at 42°C. The hybridising solution was removed, transferred into a 50 ml centrifugation tube and stored at -20°C. The membrane was washed twice at RT for 7 min by shaking in Southern blot washing buffer 1. The membrane was then washed twice for 10 min with Southern blot washing buffer 2 in a container which was placed in a shaking water bath that had been heated to 68°C. Subsequently the membrane was washed for 20 min by shaking at RT in Southern blot DIG washing buffer. The blocking took place by shrink-wrapping the membrane with 50 ml Southern blot DIG II buffer and incubating it by

shaking at 37℃ for 2 hours. The buffer was replaced by 40 ml DIG II buffer containing an AP-conjugated antibody against digoxigenin in a 1:10,000 dilution and the membrane was incubated shrink-wrapped in this buffer at 37℃ for 45 min. This was followed by two more 15 min washing steps in DIG washing buffer and an equilibration for 5 min in DIG III at RT. Each side of the membrane was then soaked for 2.5 min in DIG III buffer containing CSPD in a 1:100 dilution and the membrane was placed between two plastic foils in a radiographic cassette and, after pre-incubation for 10 min at 37℃, exposed to X-ray films for 15-120 min at 37℃.

3.4 Protein biochemistry

3.4.1 Expression of recombinant proteins in *E. coli*

E. coli cells were transformed with the required plasmid and spread on a LB agar plate including the appropriate antibiotics (100 µg/ml ampicillin, 20 µg/ml tetracycline, 50 µg/ml kanamycin). After incubation over night at 37℃ the plate was repeatedly rinsed with 1 ml LB medium, which was then used to inoculate 100 ml LB including the appropriate antibiotics. The culture was placed in a shaking incubator at 37℃ and at 225 rpm until it reached an optical density at 600 nm of approximately 0.9. After cooling the cell suspension to 18℃ the protein expression was induced by the addition of IPTG to a concentration of 100 µM. An over night incubation at 18℃ in a shaking incubator at 225 rpm, was followed by harvesting the cells by centrifugation at 3,500 x g and 4℃ for 15 min. The *E. coli* cell pellet was washed once with approximately 10 ml cold PBS and it was immediately followed-up with the preparation of cell lysates.

3.4.2 Preparation of cell lysates for protein purification

The cell suspension was centrifuged again for 15 min at 3,500 x g and 4℃ after being washed in PBS. The resulting cell pellet was resuspended in 5 ml PBS containing 200 µl complete EDTA-free protease inhibitor cocktail and transferred to a 15 ml centrifugation tube. The cell suspension was kept on ice during the entire process of sonification. Cell lysis was achieved by using a Branson sonifier with a 6 mm tip for two consecutive constant impulses of 20 s divided by a 20 s break at the programs 2, 3 and 4. If the cell lysate did not show a rather clear and not milky appearance after this treatment, another 20 s constant impulse on program 4 was distributed. 600 µl 10% (v/v) Triton X-100 was added to the lysate and the mixture was incubated rotating at 4℃ for 30 min. A centrifugation step of 10 min at 15,800 x g and 4℃ removed all cell debris and the supernatants were immediately used for protein purification.

3.4.3 Affinity purification of recombinant proteins

3.4.3.1 Purification of GST-tag fusion proteins

Glutathione Uniflow resin was provided as a 50% (v/v) solution. 400 µl of the resin was used per 100 ml of original *E. coli* culture expressing recombinant proteins. The resin was washed twice with 10 ml PBS and centrifuged at 500 x g for 2 min in between each wash step. The protein-containing supernatant was added to the washed resin and incubated rotating at 4°C for 1 hour to enable binding of GST-tag fusion proteins to the resin. The protein-bound resin was subsequently sedimented from the mixture by centrifugation at 500 x g and 4°C for 2 min and the supernatant was removed. The resin was washed 4 times with 5 ml ice-cold PBS. The solution was incubated rotating at 4°C for 10 min between each wash step and sedimentation was achieved by centrifugation at 4°C and 500 x g for 2 min. The supernatant was removed in each case with the help of a 1 ml syringe and a 23 gauge needle to minimise loss of resin. The recombinant protein was eluted after washing by incubating the resin rotating for 10 min at 4°C in 200 µl glutathione elution buffer and centrifugation at 500 x g and 4°C for 2 min. The supernatants containing the purified, eluted GST-tag fusion proteins were stored for a maximum of 3 days on ice at 4°C until further use.

Because of the poor expression levels experienced for GST-LmxMPK6 and GST-LmxMPK6K33M those proteins were expressed using 200 ml *E. coli* cultures. The cell suspensions were distributed to two 15 ml centrifugation tubes for the preparation of cell lysates but were then incubated with the same amount of Glutathione Uniflow Resin as other proteins from 100 ml cultures and subsequently treated exactly the same.

3.4.3.2 Purification of His-tag fusion proteins

Per 100 ml of original *E. coli* protein expression culture 400 µl of Chelating Sepharose Fast Flow were loaded with Co^{2+}. To achieve this, the sepharose was initially sedimented by centrifugation at 500 x g and 4°C for 2 min to facilitate the removal of the storage solution. The sepharose was subsequently washed twice with 1 ml H_2O, once with 200 µl 0.1 M $CoCl_2$ solution, once again three times with 1 ml H_2O and finally with 200 µl His-purification binding buffer. Between each washing step, the solutions were rotated at RT for 5 min, the sepharose was sedimented by centrifugation for 2 min at 500 x g and 4°C and the supernatant was removed with the help of a 1 ml syringe with a 23 gauge needle. The resulting Co^{2+}-loaded sepharose was mixed with the protein supernatant from step 3.4.2 and with 5 ml His-purification binding buffer and incubated rotating for 1 hour at 4°C. The sepharose was subsequently washed one time each with 6 ml His-purification washing buffer, 1 ml His-purification binding buffer and 1 ml His-purification washing

buffer. The solution was rotated at 4°C for 10 min between each washing step and each time sedimented by centrifugation at 500 x g and 4°C for 2 min. The purified protein was not eluted but remained bound to the resin and was stored on ice at 4°C in 200 µl His-purification washing buffer.

3.4.3.3 Purification of S-tag fusion proteins

The preparation of lysates for S-tag protein purification differed slightly from the method described in 3.4.2 as the harvested and washed cells were suspended in 10 ml S-tag purification binding/washing (B/W) buffer and afterwards incubated with 1 ml of 10% (v/v) Triton X-100. All other steps proceeded according to the protocol described above. The protein supernatants (3.4.2) were incubated with 200 µl S-protein agarose slurry rotating at RT for 45 min. The protein-bound resin was sedimented by centrifugation at 500 x g for 5 min and washed 5 times with 5 ml B/W buffer, interspersed with 10 min incubation on the roller at RT. The proteins were not eluted from the resin as this would require the addition of 3 M $MgCl_2$ and a subsequent dialysis against B/W buffer to remove $MgCl_2$. All this posed a high risk of protein loss by precipitation, which is why the protein was kept bound to the resin and was stored on ice at 4°C in 200 µl B/W buffer.

3.4.4 Thrombin cleavage of GST-tag fusion proteins

250 µg of GST-tag fusion protein was incubated over night at 20°C with 0.5 U thrombin.

3.4.5 Determination of protein concentration by Bradford assay

500 µl Bradford reagent was mixed with 10 µl protein sample and incubated for 2-3 min. The protein concentration was measured with the help of an Eppendorf BioPhotometer in the calibrated Bradford mode.

3.4.6 Discontinuous SDS polyacrylamide gel electrophoresis (SDS-PAGE)

SDS-PA gels were prepared at RT and consisted of 4% stacking gels and varying resolving gels of 8-15% concentrations. Protein samples were mixed with ¼ volume of 5 x SDS-PAGE sample buffer and incubated at 95°C for 10 min to denature proteins. After 5 min on ice a maximum of 30 µl per sample was loaded in the gel pockets. The proteins were separated at 20 mA while in the stacking gel and at 30 mA while in the resolving gel. If a double SDS-PAGE chamber was used the applied electrical current was doubled. Proteins of kinase assays were separated at 15 mA in the stacking gel and at 20 mA in the resolving gel to achieve a better separation of protein bands. A pre-stained NEB

protein molecular weight marker was used to estimate the molecular weight of separated proteins.

3.4.7 Staining of SDS-PA gels

3.4.7.1 Coomassie staining

After completion of gel electrophoresis the gels were incubated shaking at RT for approximately 1 h, but at least 30 min in Coomassie staining solution. The gels were subsequently washed several times with Coomassie destaining solution until the protein bands were distinctly visible and the blue background was sufficiently reduced. The gels were either dried or stored in ddH_2O.

3.4.7.2 Silver staining

The gel was incubated for 30 min in silver staining fixing solution and subsequently washed thrice with washing solution I for 10 min each. All steps took place on a benchtop shaker at RT. The gel was pre-treated with solution I for 5 min after which it was washed twice with ddH_2O for 1 min. Incubation with solution II took place for 10 min followed by two washing steps in ddH_2O for 1 min and the incubation in developing solution. When the gel bands were distinctly visible the developing solution was discarded and the reaction was brought to an end by the addition of stopping solution. Finally the gel was washed with washing solution II and III for 30 min each and left in storage solution until it was dried.

3.4.8 Drying of PA gels

Stained gels were incubated in gel drying solution for at least 30 min. Sheets of cellophane were soaked in water and the pre-incubated gels were placed between two cellophane sheets which were mounted within gel drying frames. The absence of air bubbles was crucial to dry gels without tearing. The construction was placed in a fume hood for 12-24 hours.

3.4.9 Immunoblot analysis

Proteins that had been separated by SDS-PAGE were transferred to an Immobilon-P PVDF membrane by semi-dry electroblotting. The stacking gel was removed from the resolving gel, which was then placed in transfer buffer. Eight Whatman cellulose blotting papers were cut to the same size as the resolving gel and soaked in transfer buffer. An Immobilon-P PVDF membrane of the same size was incubated 1 min in 100 % methanol and 10 min in transfer buffer. The blot was set up starting at the anode. Four Whatman

papers were stacked and the membrane was carefully and without inclusion of any air bubbles placed on top of the stack. The SDS-PA gel was positioned on top of the membrane under a stack of 4 Whatman papers. A plastic pipette was carefully rolled over the set-up to remove any remaining air bubbles. The protein transfer took place at 4 mA/cm^2 for 30 min, if one gel was blotted, or 45 min, if two gels were blotted.

The SDS PA gel was Coomassie-stained after completion of electroblotting and the membrane containing the transferred proteins was blocked by shaking in Immunoblot blocking solution for 1 hour at 37°C. The incubation with primary antibody was conducted by subsequently placing the membrane in a 50 ml centrifugation tube, which included an appropriate dilution of antibody in blocking solution, and rotating the tube over night at 4°C. The membrane was then washed four times with PBST (TBST in the case of 4G10) by shaking for 5 min at RT. The second antibody was also diluted in blocking solution and incubated with the membrane for 1 h at 37°C.This was followed by 3 washing steps in PBST (TBST) and 2 washing steps in PBS (TBS), lasting 5 min each. Detection of protein bands was achieved by soaking the membrane with equal measures of the two solutions of the SuperSignal West Pico Chemiluminescent Substrate Kit. The membrane was placed between two plastic foils in a radiographic cassette and X-ray films were exposed for 1 s to 30 min.

3.4.10 Stripping-off antibodies from an immunoblot

To be able to re-probe an immunoblot with a different antibody, the previous one had to be removed. This was achieved by incubating the membrane for 30 min in a container that was filled with 100 ml immunoblot stripping solution and that was placed in a 65°C hot water bath. The membrane was subsequently washed twice for 10 min with PBST or TBST before it was blocked with fresh blocking solution. The detection of protein bands using a different antibody could follow.

3.5 *In vitro* kinase assays

Approximately 1 µg of recombinant protein was incubated rotating end-over-end at 27°C or 34°C for 1 h with 5 µl 1mM ATP, containing 5 µCi [γ-^{32}P] ATP (6000 Ci/mmol) and 5 µg of MBP in a volume of 50 µl of the respective 1 x kinase buffer. To terminate the reaction the samples were mixed with 12.5 µl 5 x SDS sample buffer and heated for 10 min at 98°C. Thirty µl of each reaction were separated by SDS-PAGE, using 12% SDS-PA gels. The Coomassie-stained gels were dried and exposed to X-ray film in a radiographic cassette at -70°C for several hours or days.

3.5.1 *In vitro* kinase assays with *Leishmania* lysates

An appropriate volume containing 2×10^9 promastigotes or 4×10^9 amastigotes, respectively, was removed from a *L. mexicana* cell culture. The cells were sedimented by centrifugation at 15,800 x g for 30 s. The supernatants were discarded and the cells were resuspended in 2 ml *Leishmania* lysis buffer for kinase assays. Lysis of cells was achieved by two consecutive freeze-thaw-cycles in which the samples were frozen in liquid nitrogen for 2 min and then thawed on ice for approximately 45 min. Cell debris was removed by centrifugation at 15,800 x g and 4°C for 15 min. The cellular ATP still present in the supernatant was removed by HiTrap Desalting. The sephadex column was equilibrated with 25 ml equilibration buffer at 120 drops per min before the sample was slowly passed through the column. After completion of desalting the column was once again equilibrated with 25 ml equilibration buffer and stored containing 25 ml 20% (v/v) ethanol at 4°C.

If dephosphorylation of lysates was performed the lysates were incubated with 1200 U λ-phosphatase for 1 h at 30°C.

Approximately 20 µg of protein lysate was incubated in a general kinase assay with the addition of the phosphatase inhibitors Na-orthovanadate and sodium fluoride (10 mM each).

4. Results

4.1 LmxMPK4

Previous experiments have shown that recombinant LmxMPK4 expressed as a GST-tag fusion protein is only marginally activate towards MBP in an *in vitro* kinase assay but displays a low amount of autophosphorylation (Wang, Q. et al. 2005). Due to it being essential, LmxMPK4 has been identified as a potential drug target in *L. mexicana*, but it requires an active, inhibitable enzyme to develop efficient drug screening assays. This work therefore attempted to find an activating *L. mexicana* MAP2K for LmxMPK4. There are seven known MAP2Ks in *L. mexicana*. LmxMKK and LmxMKK4 (formerly LmxPK4) are involved in flagellar length control and are not essential in *Leishmania* (Erdmann, M. et al. 2006; Kuhn, D. et al. 2005). As LmxMPK4 is essential and shows no involvement in flagellar length both of these MAP2Ks are unlikely activators of LmxMPK4. LmxMKK3 possesses characteristics that classify it close to Ca^{2+}/Calmodulin kinases (Parsons, M. et al. 2005) and is therefore also an improbable activator of LmxMPK4. LmxMKK2, LmxMKK6 and LmxMKK7 are all rather large (120 kDa, 176 kDa and 116 kDa) and have been most difficult to express as recombinant protein in previous attempts in the Wiese laboratory. The small amounts of recombinant protein that were generated of these three MAP2Ks showed no phosphotransferase activity towards MBP when tested in kinase assays (Melzer, I. M., PhD thesis, 2007). LmxMKK5 on the other hand had been found to be easily expressable as recombinant protein and displayed phosphotransferase activity towards MBP (Melzer, I. M., PhD thesis, 2007). It was therefore investigated whether co-expression of LmxMPK4 with LmxMKK5 would lead to the purification of active recombinant LmxMPK4.

4.1.1 Activation of LmxMPK4 by LmxMKK5

4.1.1.1 Generation of co-expression constructs

To co-express LmxMPK4 with the MAP2K LmxMKK5, the dual expression vector pJCduet was used (John von Freyend, S. et al. 2010). The pJCduet vector allows a lac repressor-regulated simultaneous expression of two proteins, as it contains two multiple cloning sites (MCS). Each MCS is preceded by T7 RNA polymerase promoters with lac operator elements. The system was used to express both LmxMKK5 and LmxMPK4 simultaneously in *E. coli*, but purify solely LmxMPK4 via its hexahistidine tag. LmxMKK5 was liberated from pGEX-KGPK5 with *Eco*RI and *Sna*BI and ligated into pJCduet, which had been cleaved by *Mun*I and *Eco*RV. The resulting pJCLmxPK5 was provided with a linker sequence in the second expression site. This linker was integrated by ligating the

two annealed, phosphorylated oligonucleotides 5'-P-AATTGCGGAATTCCACTAGTTAAC-A-3' and 5'-P-AGCTTGTTAACTAGTGGAATTCCGC-3' into the *Eco*RI, *Hin*dIII cleaved pJCLmxPK5. The same strategy was used to generate pJCLinker. To express LmxMPK4 as a hexahistidine-tag fusion protein, the gene was excised from pGEX-KG-LmxMPK4 by *Eco*RI and *Hin*dIII and ligated in-frame into pJCLinker and pJCLmxPK5Linker. A co-expression construct of LmxMKK5 and the kinase-dead mutant LmxMPK4KM was also generated to control for unspecific kinase activity in the upcoming kinase assay. The sequence containing the K59M mutation was liberated from pGEX-KG-LmxMPK4KM with *Bst*BI and *Sac*II and cloned into the *Bst*BI/*Sac*II cleaved pJCLinkerLmxMPK4 and pJCLinkerLmxMPK4LmxPK5, respectively (see 8.3 for plasmid maps).

4.1.1.2 Recombinant co-expression and affinity purification of His-LmxMPK4

The plasmids pJCLinker, pJCLinkerLmxMPK4, pJCLinkerLmxMPK4LmxPK5 and pJCLinkerLmxMPK4KMLmxPK5 were transformed into *E. coli* BL21(DE3)[pAPlacIQ] cells and co-expressed over night at 18°C. LmxMPK4 was subsequently purified via its N-terminal hexahistidine tag on Co^{2+} sepharose. To compare the recombinant expression of LmxMPK4 as a his-tag fusion protein with the previously by Wang et al. employed expression as a GST-tag fusion protein, the plasmid pGEX-KG-LmxMPK4 was transformed into *E. coli* BL21(DE3) and purified on glutathione sepharose (Wang, Q. et al. 2005). The His-tag fusion proteins were not eluted from the sepharose but kept on beads in washing buffer, to avoid interference of the high amount of imidazole in the elution buffer with the enzyme activity in the ensuing assays. GST-LmxMPK4 was eluted with GST-elution buffer. SDS-PAGE separation of the purified proteins was used to assess the amount of LmxMPK4 and bacterial contaminants.

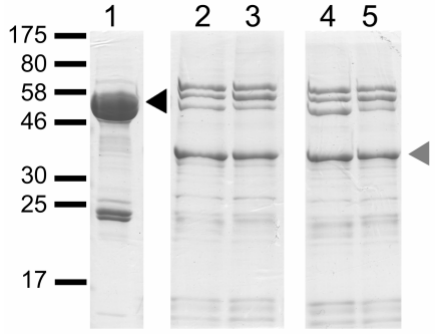

Figure 12. Coomassie-stained gel of recombinant GST-LmxMPK4 and various His-LmxMPK4 versions
lane 1, GST-LmxMPK4; lane 2, His-LmxMPK4, expressed alone; lane 3, His-LmxMPK4K59M, expressed alone; lane 4, His-LmxMPK4, co-expressed with LmxMKK5; lane 5, His-LmxMPK4K59M, co-expressed with LmxMKK5; black arrowhead indicates GST-LmxMPK4, grey arrowhead indicates His-LmxMPK4; all depicted lanes originate from the same Coomassie-stained gel; molecular masses of standard proteins are indicated in kDa.

Staining with Coomassie brilliant blue showed a distinct protein band at the expected molecular mass of 42.5 kDa, in all preparations containing the His-tagged LmxMPK4 (Fig. 12, lanes 2-5). Several other proteins, presumably of bacterial origin, were also present but less abundant than His-LmxMPK4 in the samples. The expression level of His-tagged LmxMPK4 was rather low compared to LmxMPK4 expressed as a GST-tag fusion protein (Fig. 12, lane 1).

4.1.1.3 Phosphotransferase activity of co-expressed LmxMPK4

About 1 µg of the different recombinant His-tagged proteins on beads was incubated rotating end-over-end for 1 h at 34°C in a kinase assay with 1 mM ATP, containing 5 µCi [γ^{32}]ATP (6000 Ci/mmol) and 5 µg MBP in 50 µl of a kinase buffer that had previously been found optimal for LmxMPK4, containing 50 mM 3(N-morpholino)propanesulfonic acid (MOPS), pH 7.0, 10 mM $MnCl_2$ and 0.1 M NaCl (Wang, Q. et al. 2005). Thirty µl of each reaction was separated by SDS-PAGE, the gel Coomassie-stained, dried and analysed by autoradiography. Unlike singly expressed His-LmxMPK4, His-LmxMPK4 co-expressed with LmxMKK5 showed a strong phosphorylation activity towards MBP, generating a distinct band in the autoradiograph after an exposure time of just 3 h (Fig. 13, lane 2').

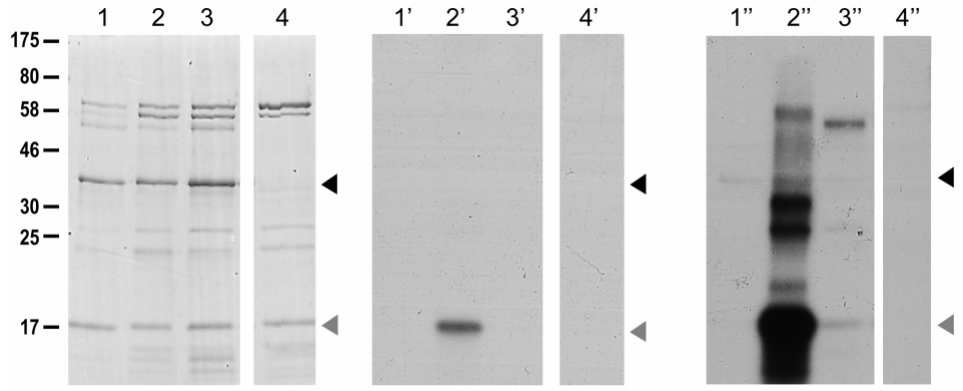

Figure 13. Kinase assay of His-LmxMPK4 and His-LmxMPK4K59M co-expressed with LmxMKK5
Left panel, Coomassie-stained gel; middle panel, autoradiograph after 3 h exposure; right panel, autoradiograph of the same experiment after 40 h exposure;
Lanes 1, 1' and 1'', wild type His-LmxMPK4, expressed on its own; lanes 2, 2' and 2'', wild type His-LmxMPK4, co-expressed with LmxMKK5; lanes 3, 3' and 3'', His-LmxMPK4K59M, co-expressed with LmxMKK5; lanes 4, 4' and 4'', mock control using the empty expression vector pJCLinker. Black arrowheads indicate His-LmxMPK4, grey arrowheads indicate myelin basic protein; molecular masses of standard proteins are indicated in kDa; all parts of the displayed autoradiographs originate from the same experiment.

The co-expressed kinase-dead mutant or the empty vector mock control did not display any comparably high phosphotransferase activity (Fig. 13, lane 3'). After longer exposure time, the kinase-dead mutant did, however, display a slight phosphorylation of MBP and a phosphorylation band at about 58 kDa (Fig. 13, lane 3''). The phosphorylation band at

58 kDa corresponds in size to co-purified LmxMKK5, which is most likely also responsible for the slight MBP phosphorylation. No phosphorylation at this size was detected in the sample of co-expressed wild type His-LmxMPK4 (Fig. 13, lane 2''). None of the samples displayed autophosphorylation activity of His-LmxMPK4 at the short exposure time (Fig. 13, middle panel), but a weak autophosphorylation of singly and co-expressed His-LmxMPK4 was visible after longer exposure times (Fig. 13, lanes 1'' and 2'').

In conclusion, Fig. 13 shows the *in vitro* activation of His-LmxMPK4 by co-expression with LmxMKK5. The activation of LmxMPK4 by LmxMKK5 permits the development of drug screening assays with LmxMPK4 as a drug target. Drug screens require an optimal function of the tested enzyme, not only regarding buffer and incubation conditions, but also with respect to the appropriate substrate. For this reason the commonly used kinase substrates Histone H1 and α–Casein were compared with MBP for their suitability as substrates for activated His-LmxMPK4. His-LmxMPK4 was expressed alone and co-expressed with LmxMKK5, purified and subjected to a kinase assay with the substrates in question. The empty vector pJCLinker was expressed and used as mock control under the same conditions. The Coomassie-stained gels and corresponding autoradiographs are shown in Fig. 14. His-LmxMPK4, co-expressed with LmxMKK5 showed no distinct phosphorylation activity towards Histone H1, but phosphorylated α–Casein stronger than MBP (Fig. 14, compare lanes 4' and 7'). Considering the exposure time of 30 h the activity of His-LmxMPK4 towards MBP is a lot weaker than in the assay shown in Fig. 13, above. The corresponding Coomassie-stained gel shows the amount of His-LmxMPK4 applied in the assay was comparatively low.

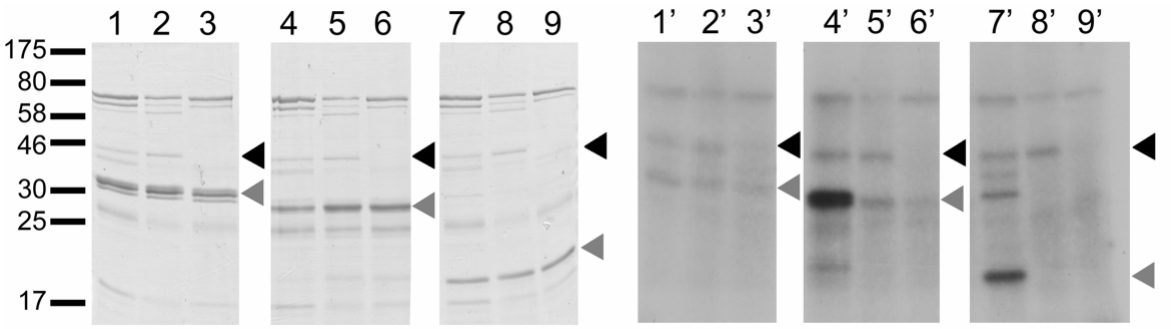

Figure 14. Kinase assay of singly and co-expressed His-LmxMPK4 with different substrates
left panel, Coomassie-stained gel; right panel, autoradiograph, 30 h exposure;
lanes 1,1', 4, 4', 7, 7', His-LmxMPK4, co-expressed with LmxMKK5; lanes 2, 2', 5, 5', 8, 8', His-LmxMPK4, expressed alone; lanes 3, 3', 6, 6', 9, 9', mock-control using the empty pJCLinker expression vector; lanes 1-3, 1'-3', kinase assay with the substrate histone H1; lanes 4-6, 4'-6', kinase assay with the substrate α-Casein; lanes 7-9, 7'-9', kinase assay with the substrate MBP; black arrowheads indicate His-LmxMPK4, grey arrowheads indicate the respective substrates; molecular masses of standard proteins are indicated in kDa; all parts of the displayed autoradiographs originate from the same experiment.

4.1.1.4 Analysis of the phosphorylation status of activated LmxMPK4

MAP2Ks typically activate MAP kinases by phosphorylation of the threonine and tyrosine residue of the TXY-motif in the activation loop. Thus, the phosphorylation status of LmxMPK4 after co-expression with LmxMKK5 was analysed, to establish whether LmxMKK5 phosphorylates LmxMPK4 in the expected manner. The initial analysis via immunoblot used the monoclonal antibody 4G10, which specifically detects phosphorylated tyrosine residues. LmxMPK4 and LmxMPK4K59M were expressed alone and together with LmxMKK5 and the empty vector pJCLinker was expressed and used as mock control. The recombinant expression in all samples was induced by IPTG over night at 18°C and His-LmxMPK4 and His-LmxMPK4K59M were purified on Co^{2+} sepharose and kept on beads for all subsequent analyses. Protein samples taken directly after purification were compared with samples of purified protein that had been subjected to a non-radioactive kinase assay, in which the proteins were incubated rotating end-over-end for 1 h at 34°C with 1 mM ATP in 50 µl of the kinase reaction buffer for LmxMPK4. Twenty-five µl of each sample was separated by SDS-PAGE and analysed by immunoblot. To make sure all samples contained the same amount of LmxMPK4, the immunoblots were stripped of all antibodies and reprobed with antiserum against LmxMPK4. Additionally the SDS-PA gels that had been used for immunoblotting were stained with Coomassie brilliant blue to show all proteins present in the analysed samples. The Coomassie stained gels as well as the LmxMPK4-probed immunoblots showed equal protein levels in all samples, illustrating that all observed differences in the 4G10 probed immunoblots were solely due to changes in the phosphorylation status. Both the LmxMPK4 antiserum as well as the 4G10 antibody show no cross-reaction with any other proteins than LmxMPK4. Without the non-radioactive kinase assay tyrosine phosphorylation was only detected in the co-expressed His-LmxMPK4 and His-LmxMPK4K59M (Fig. 15 A, lane 4 and 5), and not in the singly expressed proteins or the mock control (Fig. 15 A, lanes 1-3). A weak tyrosine phosphorylation of singly expressed His-LmxMPK4 appeared after the non-radioactive kinase assay was performed (Fig. 15 B, lane 2), whereas singly expressed His-LmxMPK4K59M never displayed any tyrosine phosphorylation (Fig. 15, lane 3). The tyrosine phosphorylation of His-LmxMPK4 and His-LmxMPK4K59M, co-expressed with LmxMKK5, did not change perceptibly after the kinase assay (compare Fig. 15 A, lane 4, 5 and Fig. 15 B, lane 4, 5).

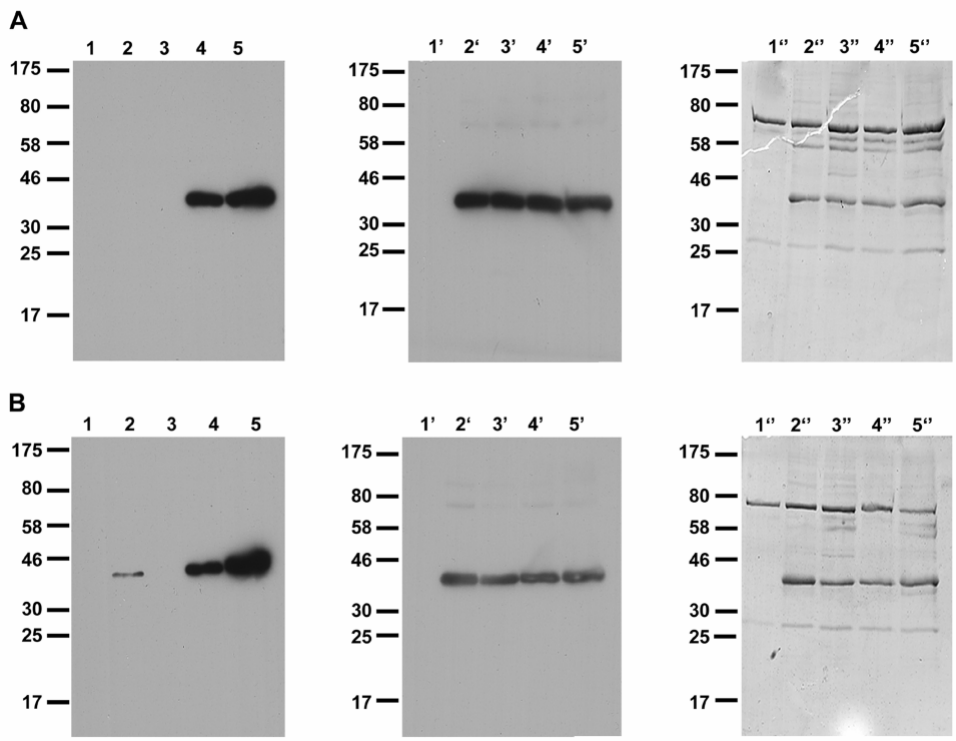

Figure 15. Immunoblot of phosphorylated tyrosine residues in recombinant His-LmxMPK4
Lanes 1, 1', 1'', mock control using the empty expression vector pJCLinker; lanes 2, 2', 2'', wild type His-LmxMPK4; lanes 3, 3', 3'', His-LmxMPK4K59M; lanes 4, 4', 4'', wild type His-LmxMPK4 co-expressed with LmxMKK5; lanes 5, 5', 5'', His-LmxMPK4K59M, co-expressed with LmxMKK5. Lanes 1-5, blot probed with monoclonal antibody 4G10 against phosphorylated tyrosine; lanes 1'-5', blot stripped and re-probed with antiserum against the carboxy-terminal peptide of LmxMPK4; lanes 1''-5'', gel Coomassie-stained after blotting. (A) Recombinant protein, as purified from *E. coli*; (B) recombinant protein after non-radioactive kinase assay. Blots for A and B were treated and developed simultaneously under exactly the same conditions to allow comparison. Molecular masses of standard proteins are indicated in kDa.

To gain information about the position of the phosphorylated tyrosine residue and the phosphorylation status of threonine, tandem mass spectrometry (MS/MS) analyses were performed to identify the sequence of any phosphorylated peptides. For this purpose 25 µl of purified His-LmxMPK4 and His-LmxMPK4K59M, after co-expression with LmxMKK5 or singly expressed, was separated on SDS-PAGE. The gel bands corresponding to the various forms of LmxMPK4 were excised and subjected to in-gel tryptic digests. Phospho-peptides were enriched by TiO_2 chromatography and samples were analysed by liquid chromatography-MS/MS (LC-MS/MS) with multistage analysis (MSA) on an LTQ-Orbitrap XL. Unlike the immunoblot analysis MS/MS detects tyrosine phosphorylation in the TQY motif in singly expressed His-LmxMPK4, illustrating the higher sensitivity of this method. Tyrosine 192 of the TQY-motif was the only phosphorylated residue detected in singly expressed His-LmxMPK4. For singly expressed His-LmxMPK4K59M on the other hand, no phosphorylated peptides could be detected. Co-expression with LmxMKK5 led to a significant change in the phosphorylation pattern of both His-LmxMPK4 and His-LmxMPK4K59M (Table 1).

Table 1. Phosphopeptides evaluated in MS/MS analysis
Oxidised methionine residues are listed in bold and phosphorylated residues in underlined bold. The table lists the scores assigned to the different phosphopeptides by Mascot, Ascore, and Post-Translational Modification score by MSQuant. Peptides were evaluated by their PTM- and Ascores as well as by manual validation. The scores highlighted grey, are considered significant. Manual validation supported identifications of all phosphorylation sites, however, was especially important in cases where the peak assignment for the PTM- and/or Ascore was deficient or in disagreement with that given by the Mascot score. For the peptides in question, conclusions on the manual assessments are included in the "Comments" column

Sample	Peptide	Mascot score	Ascore	PTM-score	Comments
LmxMPK4	DDQ**M**SSSDLTQ**Y**VVTR	104	30.78	203.5	
	DDQMSSSDLTQ**Y**VVTR	98	54.32	160.8	
LmxMPK4 (LmxMKK5)	DDQ**M**SSSDLTQ**Y**VVTR	66	41.50	147.4	
	DDQMSSSDLTQ**Y**VVTR	86	27.68	122.0	
	DDQMSSSDL**T**QYVVTR	83	29.17	88.8	
	DDQ**M**SSSDL**T**Q**Y**VVTR	42	T:12.22 Y:31.10	48.8	Confirmed by manual validation
	DDQMSSSDL**T**Q**Y**VVTR	48	T:10.64 Y:19.95	87.2	Confirmed by manual validation
	DDQV**M**SS**S**DLTQYVVTR	49	-	58.8	Confirmed by manual validation
	DDQVMS**S**SDLTQYVVTR	44	20.56	-	Confirmed by manual validation
	DDQVMSS**S**DLTQ**Y**VVTR	33	-	87.2	Y-phosphorylation clear, but first phosphorylation site impossible to accurately assign
	DDQVMSS**S**DL**T**QYVVTR	30	S:0.00 T:4.55	-	Not confirmed
LmxMPK4K59M	No confirmable phosphopeptides detected				
LmxMPK4K59M (LmxMKK5)	DDQ**M**SSSDLTQ**Y**VVTR	77	44.94	188.8	
	DDQVMSSSDLTQ**Y**VVTR	74	52.24	98.4	
	DDQV**M**SSSDL**T**QYVVTR	67	12.48	100.1	Confirmed by manual validation
	DDQVMSSSDL**T**QYVVTR	70	10.20	100.1	Confirmed by manual validation
	DDQV**M**SSSDL**T**Q**Y**VVTR	41	T:7.62 Y:25.85	66.5	Confirmed by manual validation
	DDQVMSSSDL**T**Q**Y**VVTR	55	T:18.12 Y:27.87	122.0	Confirmed by manual validation

Single phosphorylation of tyrosine 192 or threonine 190 was confirmed for both protein samples, as well as the phosphorylation of both residues. His-LmxMPK4 co-expressed with LmxMKK5 additionally displayed single phosphorylation of either serine 186 or 187. Serine phosphorylation in co-expressed His-LmxMPK4 also occurred on peptides which were additionally phosphorylated on tyrosine 192 or threonine 190. No serine

phosphorylation was observed in peptides of His-LmxMPK4K59M co-expressed with LmxMKK5 (Table 1).

4.1.1.5 Inhibition of the phosphotransferase activity of activated LmxMPK4 by three different kinase inhibitors

To assess the suitability of activated LmxMPK4 as a target for the development of drug screening assays it was determined whether the activated protein could be inhibited by small molecules. For this purpose purified recombinant His-LmxMPK4, co-expressed with LmxMKK5, was incubated in a kinase assay with the solvent DMSO and varying concentrations of the three different kinase inhibitors alsterpaullone, staurosporine and SB203580, respectively. About 1 µg of purified His-LmxMPK4 on beads was incubated rotating end-over-end for 1 h at 34°C in a kinase assay in kinase buffer with 1 mM ATP, containing 5 µCi [γ^{32}]ATP (6000 Ci/mmol), 5 µg MBP and 1 µl of DMSO or 1 µl of the respective kinase inhibitor in its appropriate dilution in DMSO. The kinase buffer used had previously been found optimal for LmxMPK4, containing 50 mM 3(N-morpholino)-propanesulfonic acid (MOPS), pH 7.0, 10 mM $MnCl_2$ and 0.1 M NaCl (Wang, Q. et al. 2005). Thirty µl of each reaction was separated by SDS-PAGE, the gel Coomassie-stained, dried and analysed by autoradiography.

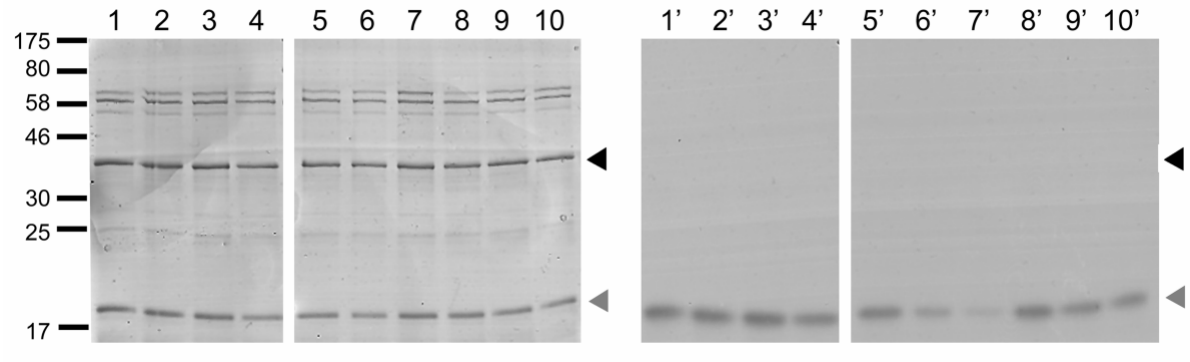

Figure 16. Kinase assay of activated His-LmxMPK4 with 3 different kinase inhibitors
left panel, Coomassie-stained gel; right panel, autoradiograph after 3 h exposure;
lanes 1, 1', addition of 1 µl DMSO; lanes 2-4, 2'-4', addition of alsterpaullone; lanes 5-7, 5'-7', addition of staurosporine; lanes 8-10, 8'-10', addition of SB203580; lanes 2, 2', 5, 5', 8,8', addition of 1 µM of the respective inhibitor; lanes 3, 3', 6, 6', 9, 9', addition of 10 µM of the respective inhibitor; lanes 4, 4', 7, 7', 10, 10', addition of 100 µM of the respective inhibitor; black arrowheads indicate His-LmxMPK4, grey arrowheads indicate MBP; molecular masses of standard proteins are indicated in kDa; all parts of the displayed autoradiographs originate from the same experiment.

The autoradiograph of the dried SDS-PA gels shows that neither alsterpaullone, nor SB203580 affect the phosphotransferase activity of co-expressed LmxMPK4 even at the high concentration of 100 µM (Fig. 16, lane 2'-4', 8'-10'). Staurosporine on the other hand inhibits LmxMPK4 activity in a dose-dependent manner with reduced MBP

phosphorylation at 10 µM and almost no MBP phosphorylation visible after the addition of 100 µM inhibitor (Fig. 16, lane 5'-7').

4.1.1.6 Activity of LmxMPK4 at different sodium concentrations

The sequence of the activation motif TQY of LmxMPK4 points to a possible connection with stress-activated protein kinases (SAPKs), as has been discussed in the introduction. It was therefore investigated whether different concentrations of NaCl in the buffer of a kinase assay would lead to significant changes in the activity of LmxMPK4. Singly expressed GST-LmxMPK4 and His-LmxMPK4 were compared in their activity under the influence of changing salt concentrations with His-LmxMPK4 that had been co-expressed with LmxMKK5. The plasmids pJCLinkerLmxMPK4, pJCLinkerLmxMPK4LmxPK5 and pGEX-KG-LmxMPK4 were transformed into *E. coli* BL21(DE3)[pAPlaclQ] or *E. coli* BL21(DE3), respectively. Expression was induced by 100 µM IPTG and proceeded over night at 18°C. His-LmxMPK4 was purified via its N-terminal hexahistidine tag on Co^{2+} sepharose and kept on beads for the subsequent assay, while GST-LmxMPK4 was purified on glutathione sepharose and eluted. The kinase assay was conducted for 1 hour at 34°C, with 1 µg kinase, 1 mM ATP, containing 5 µCi [γ^{32}]ATP (6000 Ci/mmol) and 5 µg MBP. Concentrations of 80 mM, 90 mM, 100 mM, 110 mM, 120 mM, 130 mM, 150 mM, 200 mM and 300 mM NaCl were used in the kinase buffer, which also contained 50 mM 3(N-morpholino)propanesulfonic acid (MOPS), pH 7.0 and 10 mM $MnCl_2$. The hitherto used buffer for kinase assays with LmxMPK4 contained a NaCl concentration of 100 mM. In general co-expressed LmxMPK4 has a far greater phosphotransferase activity towards MBP, which is already visible after 3 hours exposure time, than singly expressed LmxMPK4, regardless if purified by His-tag or GST-tag. While singly expressed His-LmxMPK4 shows no activity towards MBP and just a slight autophosphorylation activity (Fig. 17, B), GST-LmxMPK4 displays a stronger autophosphorylation activity and a weak activity towards MBP (Fig. 17, A). However, considering the long exposure time of 24 h, activity of GST-LmxMPK4 is very weak in comparison with co-expressed His-LmxMPK4. Varying NaCl concentrations seem to have no influence on autophosphorylation activity of GST-LmxMPK4, but MBP phosphorylation is strongest between 100 mM and 120 mM NaCl (Fig. 17, A, lane 3'-5'). Autophosphorylation of His-LmxMPK4 is affected just as little by varying NaCl concentrations (Fig. 17, B). The strong phosphotransferase activity of His-LmxMPK4, co-expressed with LmxMKK5, is not affected by the varying salt concentrations in the buffer (Fig. 17, C). The enzymatic activity remains stable and strong at all NaCl concentrations, ranging from 80 mM to 300 mM.

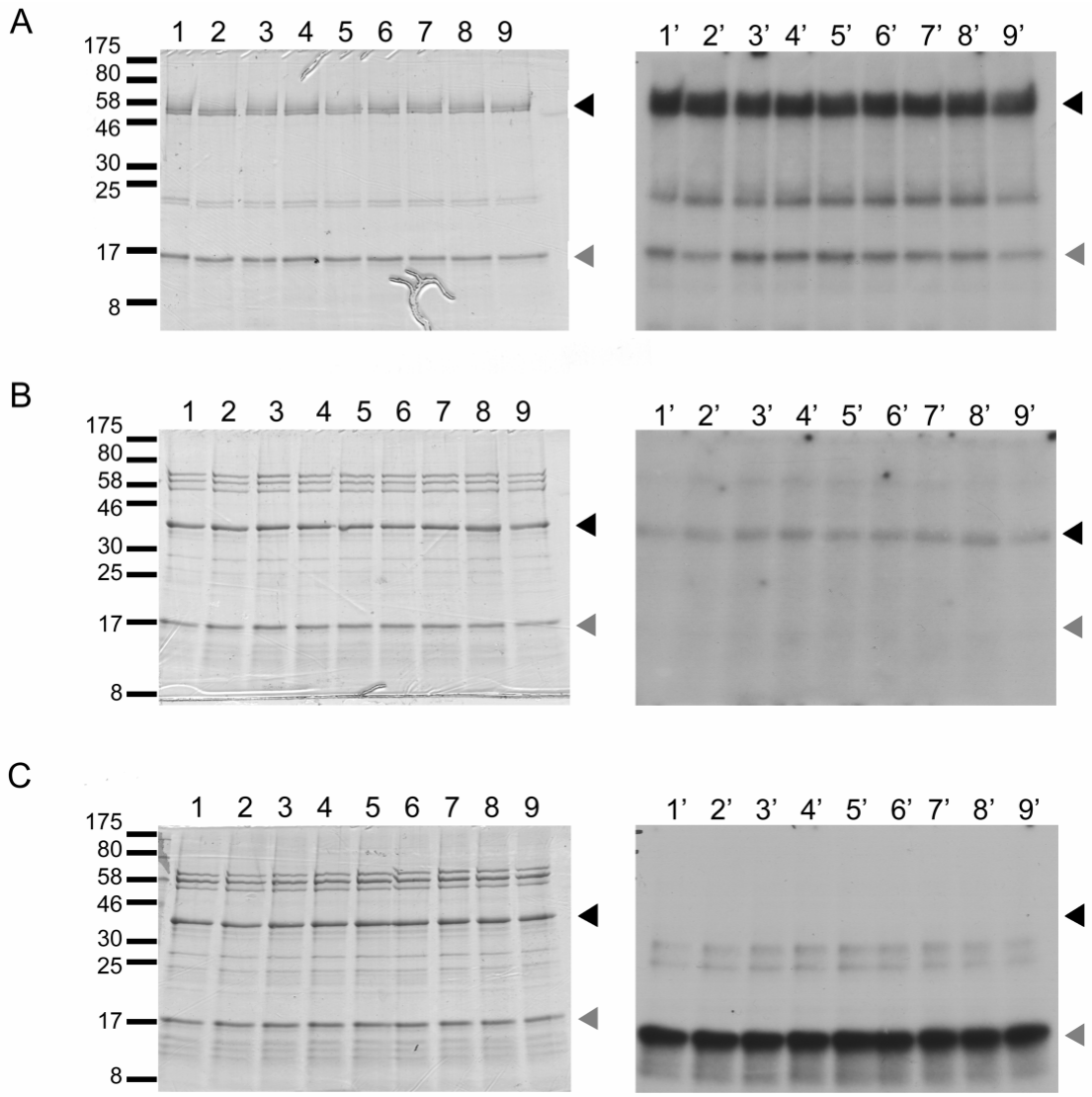

Figure 17. Kinase assays of different LmxMPK4 fusion proteins under varying NaCl concentrations
left panels, Coomassie-stained gels; right panels, kinase assays after 24 h exposure (A and B) and 3 h exposure (C), respectively;
A, assay with GST-LmxMPK4; B, assay with singly expressed His-LmxMPK4; C, assay with His-LmxMPK4, co-expressed with LmxMKK5;
lanes 1, 1', 80 mM NaCl; lanes 2, 2', 90 mM NaCl; lanes 3, 3', 100 mM NaCl; lanes 4, 4', 110 mM NaCl; lanes 5, 5', 120 mM NaCl; lanes 6, 6', 130 mM NaCl; lanes 7, 7', 150 mM NaCl; lanes 8, 8', 200 mM NaCl; lanes 9, 9', 300 mM NaCl; black arrowheads indicate LmxMPK4, grey arrowheads indicate MBP; molecular masses of standard proteins are indicated in kDa;

4.1.1.7 Substrate search for LmxMPK4

The availability of active recombinant LmxMPK4 does not only bring the development of inhibitor screenings with LmxMPK4 as a drug target within reach, but also facilitates the search for the *in vivo* substrate of LmxMPK4. As LmxMPK4 has been shown to play an important, although unknown, role in promastigotes and amastigotes (Wang, Q. et al. 2005) it was assumed that protein lysates of *L. mexicana* promastigotes or axenic amastigotes would contain the *in vivo* substrate of LmxMPK4 and that this substrate could be phosphorylated by recombinant active LmxMPK4. The plasmids pJCLinkerLmxMPK4-LmxPK5 and pJCLinkerLmxMPK4KMLmxPK5 were transformed into *E. coli* BL21 (DE3)

[pAPlacIQ] cells and the proteins expressed over night at 18℃. The His-tag fusion proteins LmxMPK4 and LmxMPK4K59M were purified on Co^{2+} sepharose and not eluted, but used in a radioactive kinase assay still bound to the resin. Parasite lysates were obtained by freeze-thaw-cycles (see 3.5.1). Twenty µg of *Leishmania* lysates were incubated in kinase assays with approximately 1 µg co-expressed His-LmxMPK4 and His-LmxMPK4K59M, as well as without the addition of protein. The assays were conducted in the presence of 1 mM ATP, containing 5 µCi [γ^{32}]ATP (6000 Ci/mmol), 10 mM of the phosphatase inhibitors Na-orthovanadate and sodium fluoride, respectively, and LmxMPK4 kinase buffer, containing 50 mM 3(N-morpholino)propanesulfonic acid (MOPS), pH 7.0, 10 mM $MnCl_2$ and 0.1 M NaCl (Wang, Q. et al. 2005). There is a possibility that the *in vivo* substrate of LmxMPK4 is contained in the *Leishmania* protein lysates in its activated, phosphorylated stage. If that was the case for all contained substrate molecules, activated LmxMPK4 could not phosphorylate them any further and no phosphorylation bands would be detected in the autoradiograph. To allow for this possibility one amastigote lysate was treated for 30 minutes at 30 ℃ with λ-phosphatase to achieve a dephosphorylation of most proteins contained in the lysate.

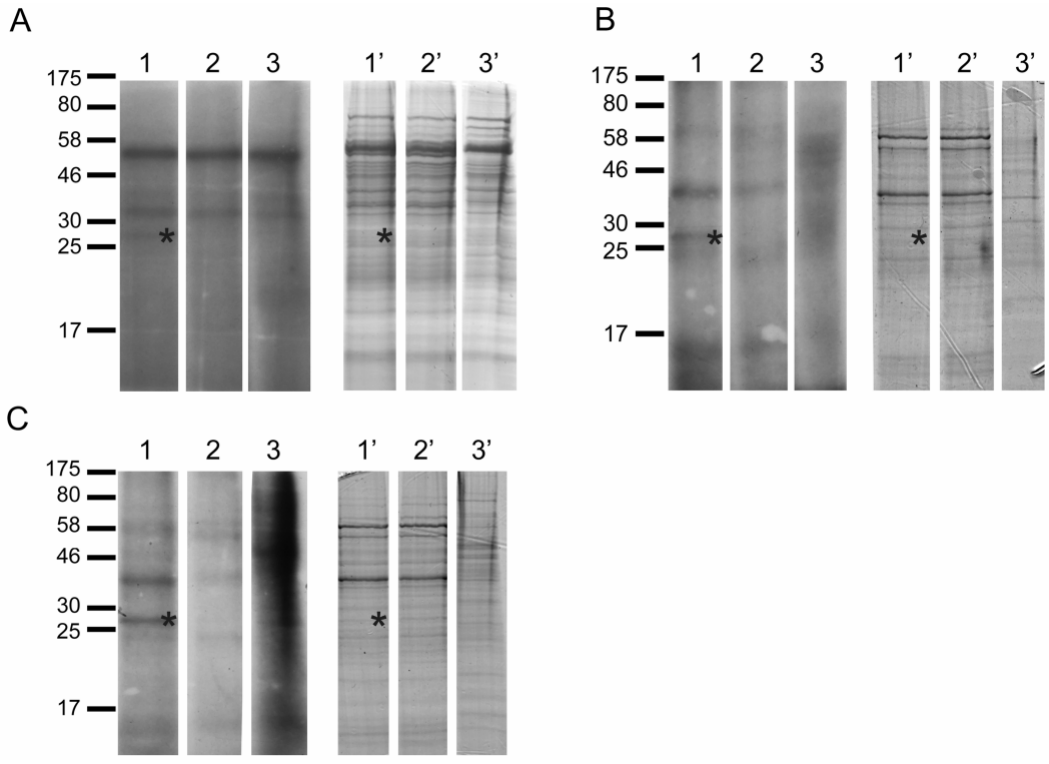

Figure 18. Kinase assays with co-expressed His-LmxMPK4 and *L. mexicana* lysates
left panels, autoradiographs of kinase assays after exposure time of 3 months (A) or 70 h (B and C), respectively; right panels, Coomassie-stained gels; A, dephosphorylated lysate of axenic amastigotes; B, untreated lysate of axenic amastigotes; C, promastigote lysate; lane 1, 1', assay in addition with His-LmxMPK4, co-expressed with LmxMKK5; lane 2, 2', assay in addition with His-LmxMPK4KM, co-expressed with LmxMKK5; lane 3, 3', assay without the addition of recombinant protein; * indicates phosphorylated protein bands in kinase assays and position of excised bands in the corresponding Coomassie-stained gels; masses of standard proteins are indicated in kDa.

The kinase assays in which *L. mexicana* protein lysates were incubated with recombinant His-LmxMPK4, resulted in autoradiographs showing a very blurred image per lane, instead of the expected clearly distinct multiple bands. Of the few distinct phosphorylation bands, however, one appeared only in the presence of active His-LmxMPK4 and not in the presence of the kinase-dead mutant His-LmxMPK4K59M or in the absence of any protein. This band at the size of about 27 kDa could be detected in both the dephosphorylated and untreated amastigote samples and also in the promastigote sample (Fig. 18). An approximately 2 mm high piece of the corresponding area of the Coomassie gel was carefully excised and sent to mass spectrometry (MS) analysis. Due to the lack of an appropriate *L. mexicana* protein database, the identified peptides were matched to a *L. major* protein database and allocated to proteins. As the phosphorylation detected in the autoradiograph (Fig. 18) occurred on a protein of the size of about 27 kDa, only proteins between 20 and 40 kDa were deemed expedient possible substrates of LmxMPK4. The rather broad range of size was chosen to allow for varying behaviour of proteins in SDS-PAGE according to their phosphorylation status or other modifications. Table 2 lists all proteins that were considered possible substrates of LmxMPK4. A full table of peptides detected by MS analysis is included in the appendix. All peptides detected by matching with the *L. major* protein database were manually compared with the respective *L. mexicana* protein homologous and are marked in Table 2. Sequence alignments of the homologous *L. major* and *L. mexicana* proteins from Table 2 are displayed in the appendix, including the highlighted identified peptides. Only a small number of proteins that were detected by MS analysis in the excised gel band matched the expected size range. Only peptides that equally matched the respective homologous protein in *L. mexicana* were considered relevant for substrate analysis. No protein could be identified in all three samples, but two proteins were independently identified in two different samples. The first protein, the γ-subunit of ATP synthase F1 of 34.42 kDa, was identified in the dephosphorylated lysate of axenic amastigotes, as well as in the sample incubated with promastigote protein lysate. The other protein identified in two different samples was glycosomal malate dehydrogenase with a size of 33.63 kDa. This protein was identified in the untreated amastigote sample as well as in the promastigote sample. Notably here is also that in the sample incubated with untreated amastigote lysate a set of four different peptides, two of which also matched the *L. mexicana* homologue, were additionally identified as belonging to the malate dehydrogenase LmjF34.0140 or LmxM33.0140, respectively. Two of these peptides also matched the mitochondrial malate dehydrogenase LmjF34.0160, but not the *L. mexicana* homologue LmxM33.0160. Three proteins were each identified in only one of the analysed samples. These were the hypothetical proteins LmjF34.3830 in untreated amastigote sample, the hypothetical protein LmjF36.2480 in the dephosphorylated amastigote sample and tryparedoxin peroxidase in the sample incubated with promastigote protein lysate. As the peptide

identified for LmjF36.2480 did not match the homologous *L. mexicana* sequence, this protein was not considered a potential LmxMPK4 substrate.

Table 2. Results of MS analysis of excised gel bands of possible LmxMPK4 *in vivo* substrate; all peptides that also match *L. mexicana* genes are underlined in bold with the respective gene displayed in brackets and underlined in bold in the identification column

Sample	Peptides	Identification of protein	Size of protein
Band A (dephosphorylated amastigotes)	**VIDSVASSR**	**ATP synthase F1 subunit gamma protein**, LmjF21.1770 (**LmxM21.1770**)	34.42 kDa
	TNGGELPR	**Hypothetical protein, conserved** LmjF36.2480	27.93 kDa
	LLEAFQFVEK	**tryparedoxin peroxidase**, LmjF15.1120 (**LmxM15.1160**)	22.12 kDa
Band B (amastigotes)	**LLGVSLLDGLR**	**glycosomal malate dehydrogenase**, LmjF19.0710 (**LmxM19.0710**)	33.63 kDa
	DDLFNTNASIVR AVENADVVVIPAGIPR **VAVLGAAGGIGQPLSLLLK** **AIVGIITNPVNSTVPVAAEALK**	**malate dehydrogenase**, LmjF34.0140 (**LmxM33.0140**)	33.36 kDa
	AIVGIITNPVNSTVPVAAEALK VAVLGAAGGIGQPLSLLLK	**Mitochondrial malate dehydrogenase**, LmjF34.0160 (**LmxM33.0160**)	34.15 kDa
	DAEAAARTSR	**hypothetical protein, conserved**, LmjF34.3830 (**LmxM33.3830**)	26.47 kDa
Band C (promastigotes)	**LLGVSLLDGLR**	**glycosomal malate dehydrogenase**, LmjF19.0710 (**LmxM19.0710**)	33.63 kDa
	VIDSVASSR	**ATP synthase F1 subunit gamma protein, putative**, LmjF21.1770 (**LmxM21.1770**)	34.42 kDa

4.1.2 Characterisation of an inhibitor-sensitised LmxMPK4 mutant

As the essential MAP kinase LmxMPK4 could not be analysed by the conventional method of a knock-out mutant, an inhibitor-sensitised version of the protein was generated. For this purpose a mutation was introduced, changing the gatekeeper residue methionine111 to glycine and introducing an additional *Bgl*II restriction site into the genome. The generation of the inhibitor-sensitised mutant LmxMPK4IS has been previously described (Puls, G., diploma thesis, 2005).

4.1.2.1 *In vitro* analysis

To verify the phosphotransferase activity of the mutated protein LmxMPK4IS and to demonstrate the general ability of the inhibitor 1-naphthyl-pyrazolo [3,4*d*] pyrimidine (1Na) to inhibit LmxMPK4IS, recombinant LmxMPK4IS was co-expressed with LmxMKK5 in *E. coli* and subjected to radiometric kinase assays.

4.1.2.1.1 Generation of co-expression constructs with LmxMKK5

A 355 bp fragment, inclosing the inhibitor-sensitising M111G mutation, was liberated from the plasmid pBusMPK4ISpol*Nco*IPacds (described under 4.1.3.2.1) by cleavage with *Bst*BI and *Sac*II and ligated into pJCLinkerLmxMPK4 and pJCLinkerLmxMPK4LmxPK5, which had both been cleaved by *Bst*BI and *Sac*II (see 8.3 for plasmid maps).

4.1.2.1.2 Recombinant co-expression of His-LmxMPK4IS with LmxMKK5 and affinity purification

The co-expression constructs pJCLinkerLmxMPK4IS and pJCLinkerLmxMPK4ISLmxPK5 were transformed into competent *E. coli* BL21(DE3)[pAPlaclQ] cells, which were used to express the proteins at 18°C over night in a shaking incubator. Cells were harvested, lysed by sonification and His-LmxMPK4IS was purified on Co^{2+} sepharose. Wild type His-LmxMPK4 was co-expressed with LmxMKK5 under the same conditions to be used as a control in the following assays. Purified recombinant protein was not eluted from the sepharose resin, but stored in washing buffer, in a volume equal to that of the resin. Ten µl of the buffer/resin mixture were separated by SDS-PAGE and stained with Coomassie to assess the general expression level and purification of the recombinant proteins. Protein quantification by Bradford analysis was not possible with the resin still present in the protein samples.

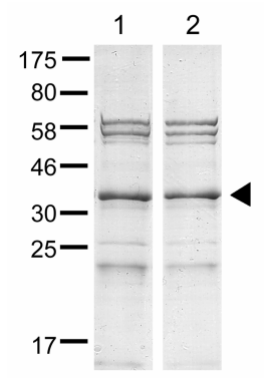

Figure 19. Coomassie-stained SDS-PA gel of purified co-expressed His-LmxMPK4 and His-LmxMPK4IS
lane 1, co-expressed His-LmxMPK4; lane 2, co-expressed His-LmxMPK4IS; black arrowhead indicates His-LmxMPK4/His-LmxMPK4IS; masses of standard proteins are indicated in kDa; both lanes originate from the same gel of one experiment.

Just as wild type His-LmxMPK4 (Fig. 19, lane 1), His-LmxMPK4IS is expressed in moderate abundance and cannot be completely purified (Fig. 19, lane 2). The His-LmxMPK4IS protein band at the expected molecular mass of 42.5 kDa does, however, constitute the most abundant protein in the mixture. There is no difference in the His-LmxMPK4IS abundance, compared to the wild type His-LmxMPK4.

4.1.2.1.3 Phosphotransferase activity of co-expressed His-LmxMPK4IS and inhibition by 1 Na

Kinase assays were performed to compare the phosphotransferase activity of co-expressed His-LmxMPK4IS and co-expressed wild type His-LmxMPK4. About 1 µg of purified protein on beads was incubated rotating end-over-end for 1 h at 34°C with 1 mM ATP, including 5 µCi [γ^{32}]ATP (6000 Ci/mmol) and 5 µg MBP in 50 µl kinase buffer, containing 50 mM 3(N-morpholino)propanesulfonic acid (MOPS), pH 7.0, 10 mM $MnCl_2$ and 0.1 M NaCl. Each sample, but one, was additionally supplemented with either 1 µl DMSO or 1 µl of an adequate dilution of 1Na in DMSO to measure the influence of 1Na on *in vitro* phosphotransferase activity. Thirty µl of each reaction was separated by SDS-PAGE, the gel Coomassie-stained, dried and analysed by autoradiography. After co-expression with LmxMKK5, the inhibitor-sensitised mutant His-LmxMPK4IS exhibited a rather weak phosphotransferase activity towards MBP (Fig. 20, B), when compared with the strong activity of co-expressed wild type His-LmxMPK4 (Fig. 20, A) (note the different exposure times of the autoradiographs). Due to the longer exposure time of 40 h, a slight autophosphorylation of co-expressed His-LmxMPK4IS is visible (Fig. 20, B), which co-expressed His-LmxMPK4 does not display after 16 h exposure (Fig. 20, A). Although co-expressed His-LmxMPK4IS was not activated by LmxMKK5 in an equivalent manner to the activation of wild type His-LmxMPK4, a slight activation could still be observed. The addition of DMSO or 1Na, respectively, did not affect the phosphotransferase activity of

co-expressed wild type His-LmxMPK4 (Fig. 20 A, lane 1-5). The phosphotransferase activity of co-expressed inhibitor-sensitised His-LmxMPK4IS was also not affected by the addition of DMSO alone (compare Fig. 20 B, lane 1 and 2). The inhibitor 1Na, however, negatively influenced His-LmxMPK4IS phosphotransferase activity at all added concentrations of 1 µM, 10 µM and 50 µM (Fig. 20, lane 3-5). Whereas an addition of 1 µM 1Na still led to a very slight activity of co-expressed His-LmxMPK4IS (Fig. 20, lane 3), phosphotransferase activity was fully inhibited after addition of 10 µM and 50 µM 1Na (Fig. 20, lane 4 and 5).

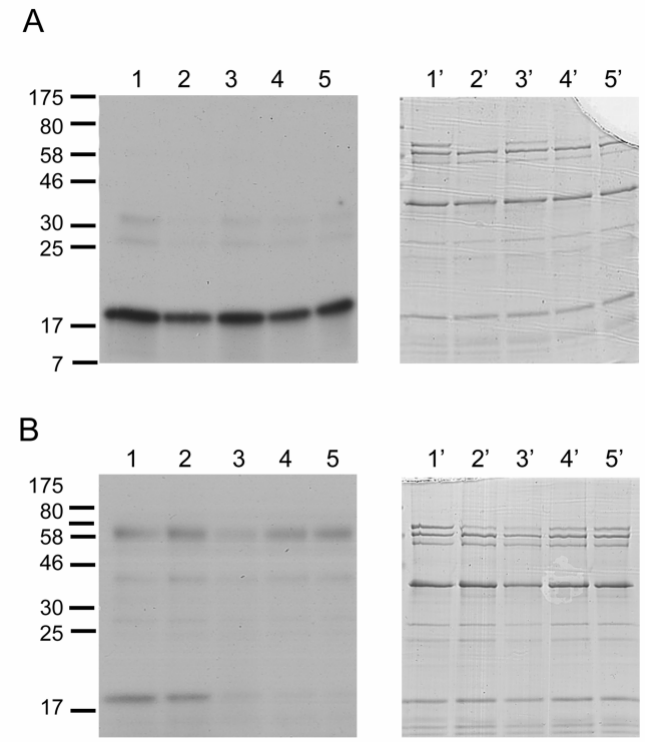

Figure 20. Kinase assay of co-expressed His-LmxMPK4 and His-LmxMPK4IS with different concentrations of inhibitor 1Na
A, wild type His-LmxMPK4, co-expressed with LmxMKK5; B, inhibitor-sensitised His-LmxMPK4IS, co-expressed with LmxMKK5; left panels, autoradiographs after 16 h (A) and 40 h (B) exposure, respectively; left panels, Coomassie-stained gels;
lanes 1, 1', no additive; lanes 2, 2', addition of 1µl DMSO; lanes 3, 3', addition of 1 µM 1Na; lanes 4, 4', addition of 10 µM 1Na; lanes 5, 5', addition of 50 µM 1Na; molecular masses of standard proteins are indicated in kDa; both kinase assays were conducted simultaneously under the same conditions to allow comparison.

4.1.2.2 *In vivo* analysis

As recombinant co-expressed His-LmxMPK4IS exhibited phosphotransferase activity *in vitro*, albeit low, analyses of the *in vivo* function of LmxMPK4 using the inhibitor-sensitised mutation were carried out. An impaired enzyme function will possibly play a less important role *in vivo* than *in vitro*, as the affinity of a kinase towards its natural substrate is expected to be much higher than the affinity to the general kinase substrate MBP. To investigate the function of LmxMPK4IS *in vivo*, promastigotes, expressing solely an extrachromosomal copy of LmxMPK4IS and no wild type LmxMPK4, were generated. The cloning of the

plasmid pXpolNeoMPK4IS and the generation of *Leishmania* promastigotes carrying this plasmid has been described previously (Puls, G., diploma thesis, 2005). The plasmid pXpolNeoMPK4IS had been transfected into cells which contained no genomic copy of *LmxMPK4* anymore, but only an extrachromosomal copy of the gene on the plasmid pXpolPacMPK4 (add-back mutants). Both genomic alleles of *LmxMPK4* had been replaced by selective marker genes conferring hygromycin B and phleomycin resistance, respectively. Cultivation of cells under continuous selection pressure for neomycin, led to the suspected loss of pXpolPacMPK4, which could not be confirmed anymore in the context of the described diploma thesis (Puls, G., diploma thesis, 2005). The existence and identity of pXpolNeoMPK4IS in the two resulting *L. mexicana* cell lines D12 and 3.2. was therefore confirmed as part of this thesis. Evidence was provided by verifying the loss of puromycin resistance, as well as by PCR on genomic mutant DNA with the oligonucleotides mapkin15_1.rev and mapkin150505_2.rev. The PCR generated a 340 bp fragment which contained the additional *Bgl*II restriction site that had been introduced alongside with the inhibitor-sensitising M111G mutation.

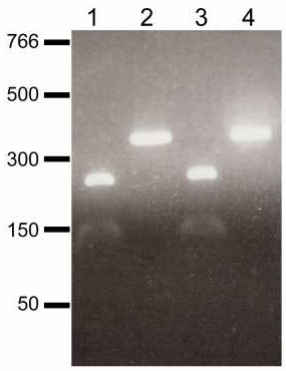

Figure 21. PCR analysis to confirm the existence of the inhibitor-sensitising mutation M111G in plasmids of *L. mexicana* mutants
lane 1, product of PCR on genomic DNA derived from mutant strain D12, cleaved with *Bgl*II; lane 2, untreated PCR product of D12; lane 3, product of PCR on genomic DNA derived from mutant strain 3.2., cleaved with *Bgl*II; lane 4, untreated PCR product of 3.2.; sizes of standard DNA fragments are indicated in bp.

Fig. 21 shows that the PCR products for the *L. mexicana* clones D12 and 3.2. were successfully cleaved by *Bgl*II restriction digest and therefore contained the M111G mutation, which conveyed the novel *Bgl*II restriction site. Complete sequencing of the LmxMPK4IS gene, amplified from total *Leishmania* DNA in a PCR reaction using the oligonucleotides 90 and 91, verified that the two clones 3.2. and D12 contained only the plasmid pXpolNeoMPK4IS and had lost all wild type *LmxMPK4* previously encoded on pXpolPacMPK4.

4.1.2.2.1 Generation of the construct for genomic integration of LmxMPK4IS

Fluctuating high plasmid numbers and uncontrolled extrachromosomal expression can lead to varying protein levels, which could negatively influence experimental results. To ensure consistent and reliable results of inhibition experiments, cells were therefore generated which contained *LmxMPK4IS* in the original genomic locus of *LmxMPK4.* The *LmxMPK4IS* gene was liberated from pCR9LmxMPK4IS (Puls, G., diploma thesis, 2005) by *Eco*RV and ligated into pX14polNcoIPac, linearised by *Eco*RV. The cassette of *LmxMPK4IS* and the resistance marker for puromycin, PAC, was extracted from pX-MPK4ISpolNcoIPac by cleavage with *Xba*I and *Nco*I and ligated into pB11mapkin150505-delphleo, from which the phleomycin resistance marker had been removed by *Avr*II and *Nco*I cleavage. Ligation was possible as *Xba*I and *Avr*II cleave DNA leaving compatible ends. The insertion cassette of MPK4ISpolNcoIPac, flanked by the 5'-UTR and 3'-UTR of *LmxMPK4* was liberated from pBusMPK4ISpol*Nco*IPacds using *Nru*I and *Cla*I and transfected into D12 (see 8.1 for plasmid maps). Positive clones were selected using puromycin as resistance marker. Continuous selection pressure by puromycin led to a newly emerging sensitivity to neomycin, indicating the loss of the plasmid pXpolNeoMPK4IS. The loss of the plasmid and the integration of *LmxMPK4IS* into the genome were confirmed by Southern blot analysis, providing the three positive clones AB6H2, BF11H4 and BF11E4 (Fig. 22).

Genomic *Leishmania* DNA was cleaved with *Hin*dIII and *Kpn*I, separated on an agarose gel, transferred to a nylon membrane and probed with a previously described DIG-labelled DNA probe, homologous to a fragment of the *LmxMPK4* open reading frame and generated with the oligonucleotides mapkin151505_2.for and mapkin150505_3.rev (Wang, Q. et al. 2005). The sequence corresponding to the probe is indicated in the *LmxMPK4* sequence shown in the appendix (8.1). The additional use of *Hin*dIII for cleavage was necessary to linearise pXpolNeoMPK4IS, as *Kpn*I cleaved only in the upstream and downstream region of *LmxMPK4* and not in the pXpolNeoMPK4IS plasmid. The expected band sizes of the Southern blot were about 4.4 kb for the genomic integration cassette of *LmxMPK4IS*polPac, around 2.4 kb for the wild type *LmxMPK4* gene and about 7.2 kb for the plasmid pXpolNeoMPK4IS. In Fig. 22 the lanes for the three positive clones AB6H2, BF11E4 and BF11H4 each depict solely one band around 4.4 kb, corresponding to the *LmxMPK4IS*polPac genomic integration cassette. The wild type control shows the band for genomic *LmxMPK4* at 2.4 kb, which is absent from all three isolated clones. The plasmid corresponding band at 7.2 kb was not visible in any of the samples, signifying the loss of the plasmid and the sole existence of *LmxMPK4IS*polPac in the genome of the isolated clones. The ability of the DIG-labelled DNA probe to detect

DNA derived from the plasmid pXpolNeoMPK4IS had been demonstrated previously (Wang, Q. et al.).

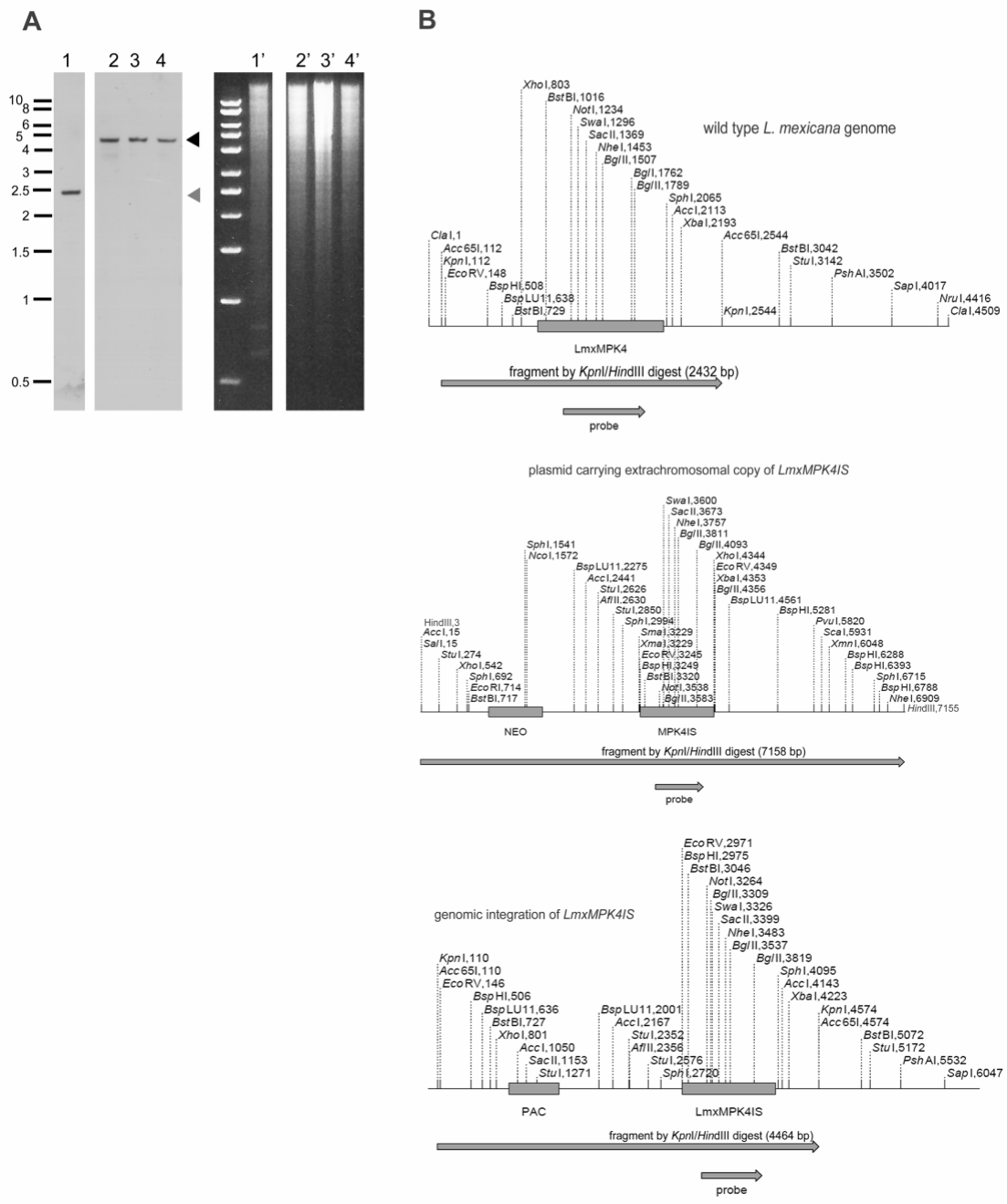

Figure 22. Southern blot analysis to verify the presence of *LmxMPK4IS* in the genome of newly generated *L. mexicana* cell lines AB6H2, BF11E4 and BF11H4
A, left panel, Southern blot, right panel, agarose gel, which separated the *Hin*dIII/*Kpn*I cleaved gDNA; the depicted lanes originate from the same Southern blot; lanes 1, 1', wild type *L. mexicana*; lanes 2, 2', inhibitor-sensitised cell line AB6H2; lanes 3, 3', inhibitor-sensitised cell line BF11E4; lanes 4, 4', inhibitor-sensitised cell line BF11H4; black arrowhead indicates detection of genomic *LmxMPK4IS*, grey arrowhead indicates genomic wild type *LmxMPK4*; sizes of standard DNA fragments are indicated in kb; fragments were detected by a DIG-labelled DNA probe corresponding to the *LmxMPK4* ORF and generated with the oligonucleotides mapkin150505_2.for and mapkin150505_3.rev (for a detailed display where the probe binds, see the sequence of *LmxMPK4* in appendix 8.1);
B, diagrammatic plan of the analysed DNA region, the utilised probe and the generated fragments;

4.1.2.2.2 Analysis of promastigote growth under inhibitor influence

The three affirmed clones, which all contained solely the inhibitor-sensitised mutant *LmxMPK4IS* in the original genomic locus of *LmxMPK4* were tested for any divergences in growth in comparison with wild type *L. mexicana* and under influence of different concentrations of 1Na. Cells were inoculated at 5×10^5 cells/ml in 1 ml SDM medium in 24 well plates and incubated for 4 days at 27°C. Samples for cell counting were taken each day at the same time to determine cell densities. Counted cell numbers of all conducted experiments with the same sample were normalised to a start density of 5×10^5 cells/ml and the mean value of all experiments, including the standard deviation, was plotted in a semi-logarithmic diagram (Fig. 23).

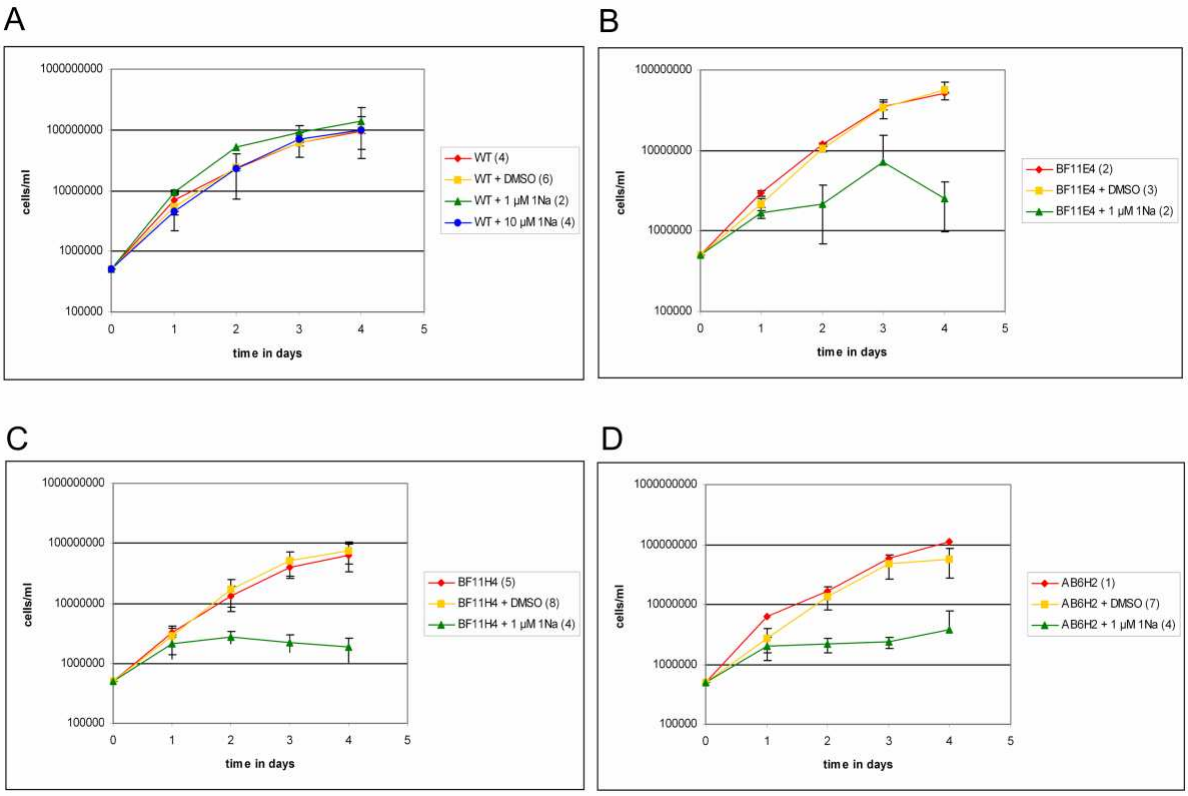

Figure 23. Growth of *L. mexicana* wild type (A) in comparison with the three different inhibitor-sensitised *L. mexicana* clones, BF11E4 (B), BF11H4 (C) and AB6H2 (D)
all cells were grown under the same conditions in 1 ml cultures in 24-well plates with a start cell number of 5×10^5 cells/ml, either with no additives (red curve) or under addition of 1 µl DMSO (yellow curve) or 1 µl inhibitor 1Na to a final concentration of 1 µM (dark green curves) or 10 µM (blue); the numbers of conducted experiments on which the graphs are based on, are shown in brackets behind the respective sample in the legend.

The diagrams show that the addition of the solvent DMSO alone does not noticeably influence the growth of any of the tested cell lines. Neither affects the addition of up to 10 µM 1Na the growth of wild type *L. mexicana* (Fig. 23, A). Growth of the inhibitor-sensitised mutants AB6H2, BF11H4 and BF11E4 on the other hand is considerably inhibited by the addition of 1Na (Fig. 23, B, C and D). The growth of BF11E4 spikes on day 3 after addition of 1µM inhibitor, before dropping to a low level of cells on day 4 again (Fig. 23,

B). The growth of BF11H4 after the addition of 1Na, reacts the most consistently, which is why this clone was chosen for all subsequent experiments.

The mere display of growth curves does not allow for statistical analyses of growth differences between separate clones or under varying conditions. For this purpose the growth rate k can be calculated and statistically evaluated. The growth rate k corresponds to the gradient of a culture during its log phase of logarithmic growth and can be assessed by the equation $f(t) = f(0) \times e^{kt}$, with f(t) being the number of cells at a specific time t and f(0) the number of cells at time 0 (Brody, S. 1927). Linear regression via application of a Microsoft Excel trend line of all time points in the log phase of the culture under consideration yields the above mentioned equation, off which the value of k can be read. Fig. 24 exemplifies this for the average growth curve of *L. mexicana* wild type without additives, which is also shown as part of Fig. 23, A.

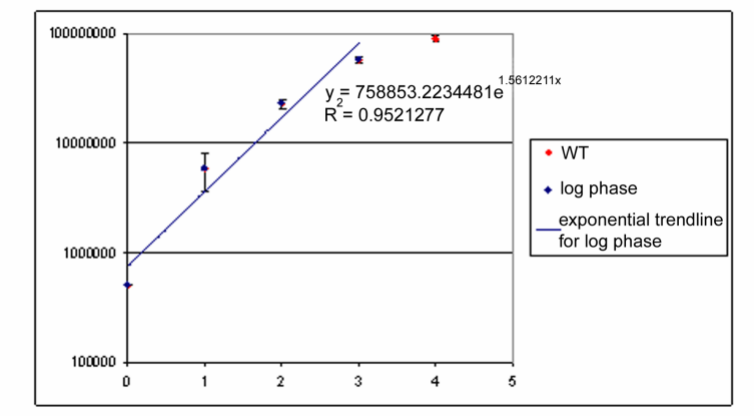

Figure 24. Exemplary calculation of growth rate k by linear regression of all time points in the logarithmic growth phase

To statistically compare growth rates, k was separately determined for each experiment per group by visual assessment of the number of time points which constitute the logarithmic growth phase of the growth curve in question, and linear regression of these. The mean value of all growth rates of one experimental group was calculated and plotted in a bar chart under consideration of the standard deviation. Two data sets were compared by an independent Student's T-test (Kirkman, T. W. 1996). Statistical significance was defined as the calculated p-value being below the threshold of 0.05. A Student's T-test requires each compared data set to consist of at least 3 data points. If any of the evaluated data sets contained only 2 time points, the mean of those was used as the calculated third time point. In the case of just one data point no Student's T-test was performed. The just described method was applied to compare the growth rates of the three clones expressing solely the inhibitor-sensitised mutant *LmxMPK4IS*, with the *L. mexicana* wild type (Fig. 25).

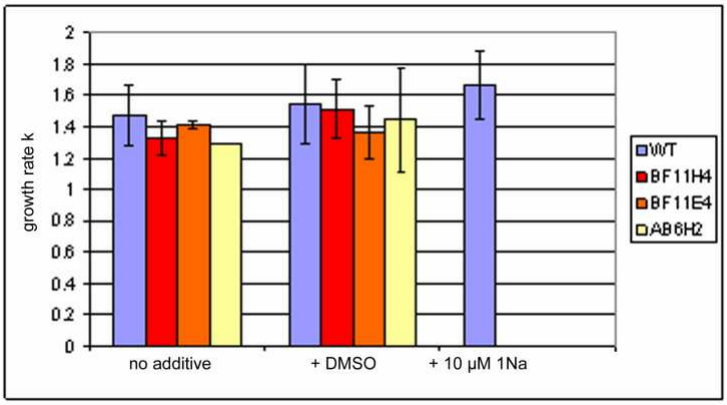

Figure 25. Comparison of the growth rates k of wild type *L. mexicana* with the inhibitor-sensitised clones BF11H4, BF11E4, and AB6H2

None of the differences in growth rate, shown in Fig. 25, were of statistical relevance, which means the uninhibited growth of the inhibitor-sensitised mutants can be regarded as essentially equal to the growth of *L. mexicana* wild type. The addition of DMSO to either the wild type or the inhibitor-sensitised clones did equally not lead to significantly impaired growth. Neither did the addition of 10 µM inhibitor 1Na have any significant effect on the growth rate of the wild type. The growth rate only sufficiently describes a growth curve during its logarithmic phase, which entails that inhibited growth of the mutant cell lines cannot be depicted by this method. Observation of the growth curves in Fig. 23 however already shows that inhibition by 1Na is considerable. Further experiments with the inhibitor-sensitised mutant cell line BF11H4 were conducted to investigate whether 1Na inhibits growth in promastigotes in a dose-dependent manner. To compare the rate of inhibition promastigote cells of the inhibitor-sensitised mutant BF11H4 were inoculated to a density of 5×10^5 cells/ml in 1 ml SDM medium in 24 well plates and incubated for 4 days at 27°C. Cultures were grown without any additives or with the addition of 1 µl DMSO or 1 µl of an adequate dilution of 1Na in DMSO, bringing the final concentration of 1Na in the culture to 0.05 µM, 0.1 µM, 0.2 µM, 0.5 µM, 1 µM or 10 µM, respectively. For all samples the average cell number reached on day 4, which was generally the last day of logarithmic growth, was plotted in a bar chart (Fig. 26) and a Student's t-test performed on the results.

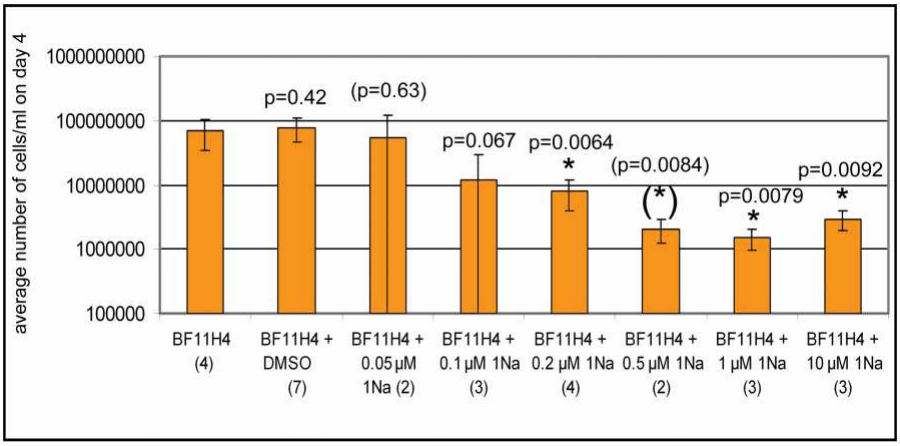

Figure 26. Differences in highest number of cells/ml reached on average on day 4 in BF11H4 after addition of various concentrations of inhibitor 1Na
* marks cell numbers which are significantly different from BF11H4 without additive; p-values are shown on top of the respective bars; p-values and (*) signify calculations which were made using an artificial third data point by calculating the mean of the two available data points; all statistical analysis shown refers to comparison of the respective data set with BF11H4 without additive.

Fig. 26 shows that cultures reached lower densities when incubated with higher amounts of inhibitor 1Na in a dose-dependent manner. The addition of 0.05 µM 1Na did not lead to a significant impairment of growth, but all concentrations higher than 0.1 µM 1Na led to significantly lower cell numbers on day 4. There was no statistically significant difference between the cell numbers reached on day 4 under the influence of 0.5 µM or 1 µM and 10 µM 1Na, respectively. Note the extremely high standard deviations in samples under influence of 0.05 µM and 0.1 µM 1Na.

Despite only reaching low densities, cells were still viable and moving on day 4, even after addition of 10 µM 1Na (as seen by visual examination). To follow up on this observation, experiments were conducted in which the inhibitor was removed after day 4 or day 5, respectively, by washing cells once in fresh SDM medium and resuspending them in fresh, inhibitor-free SDM medium.

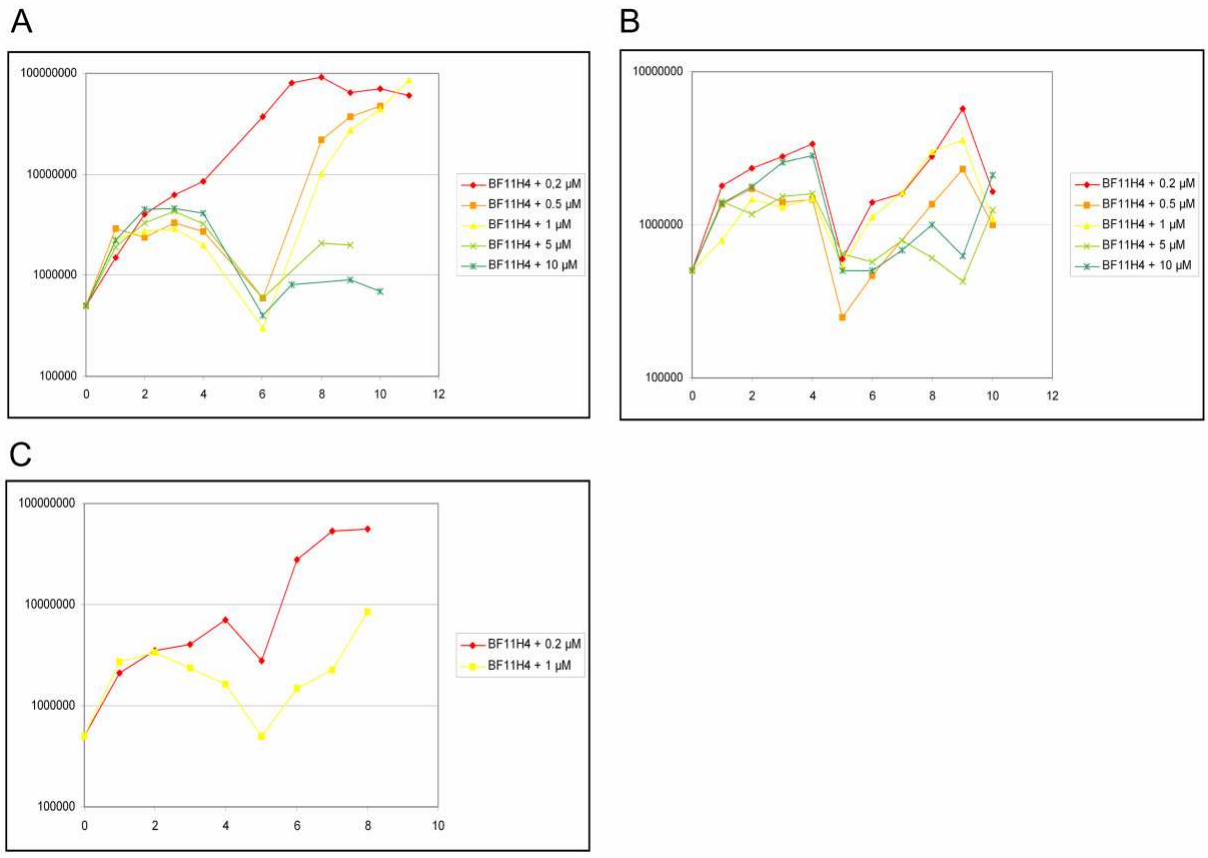

Figure 27. Growth curves of BF11H4 under influence of various concentrations of 1Na and after removal of the inhibitor
A, B and C show different experiments in which the inhibitor 1Na was removed by washing the cells in fresh SDM medium after 4 days (B and C) or 5 days (A), respectively

The growth curves all showed a clear decrease in cell numbers on day 5 (Fig. 27, B and C) or day 6 (Fig. 27, A), corresponding to loss of cells during the washing out of the inhibitor. After the inhibitor 1Na was removed by washing cells in fresh medium, all cultures resumed growth again apart from BF11H4 incubated with 10 µM 1Na in the experiment shown in Fig. 27, A. Here, the cell density remained extremely low. In all other cultures, including BF11H4 incubated with 10 µM 1Na in the experiment shown in Fig. 27, B, growth recurred. The resumption of growth was slower the higher the original inhibitor concentration had been. Cultures that had been incubated with 0.2 µM, 0.5 µM and 1 µM of inhibitor, respectively, reached higher cell numbers after the wash-out of inhibitor than were observed under influence of 1Na. Cultures that had been incubated with 5 µM 1Na resumed growth again, but did not exceed previous cell numbers. However, loss of cells during the wash-out procedure must be taken into consideration when regarding cell numbers. Cultures that had been incubated with 10 µM 1Na slowly resumed growth in the case of inhibitor removal after day 4 (Fig. 27, B), but did not resume growth again when cells were incubated with inhibitor for 5 days before the wash-out procedure. Instead of merging the different growth curves, resulting in an unclear, overfull graph, the growth

rates of cultures after the removal of inhibitor were determined as previously explained and depicted for comparison in a bar chart (Fig. 28).

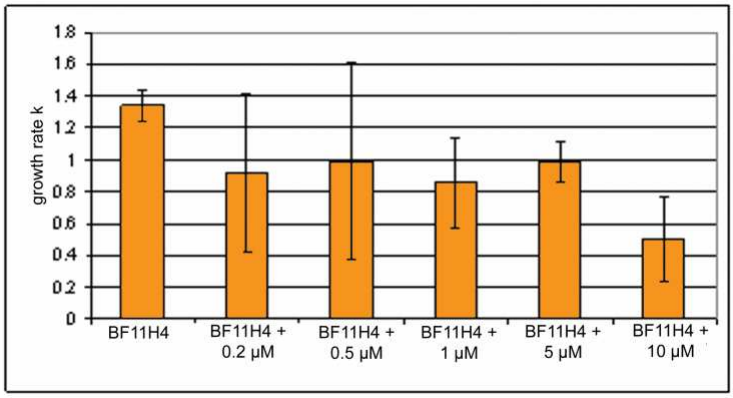

Figure 28. Growth rate reached by BF11H4 cultures after varying concentrations of inhibitor 1Na were removed by wash-out

Due to the strong variations in the different growth curves, the standard deviations for 0.2 µM, 0.5 µM and 10 µM 1Na in Fig. 28 are very high. The bar chart nevertheless shows the medial resumption of growth for all cultures that have been treated with 1Na concentrations of 5 µM and under, confirming that the inhibition of LmxMPK4 does not immediately have a cytotoxic effect on *L. mexicana* promastigotes, but is initially rather of cytostatic nature. The treatment with 10 µM 1Na for 5 days, however, seems to result in cell death.

4.1.2.2.3 Analysis of axenic amastigote growth under inhibitor influence

LmxMPK4 has previously been found to be essential in amastigotes (Wang, Q. et al. 2005). The *L. mexicana* mutant BF11H4, carrying solely the inhibitor-sensitised *LmxMPK4IS* gene, was analysed for its ability to differentiate from promastigotes into axenic amastigotes and proliferate as axenic amastigotes under the influence of inhibitor 1Na and compared to a *L. mexicana* wild type culture. Logarithmic promastigote cultures of the wild type and inhibitor-sensitised mutant strain BF11H4, cultivated without addition of antibiotics or inhibitor 1Na, were used to inoculate acidic Schneider's medium on day 0 to a density of 4×10^6 cells/ml. The cultures were incubated at 34°C and 5% CO_2 for 5 days. An appropriate dilution of inhibitor 1Na in DMSO, or a corresponding volume of DMSO, was added on day 2 after inoculation, to a final 1Na concentration of 1 µM, 2 µM or 5 µM, respectively. Samples were taken for cell counting at the same time every 24 h and the densities of cultures were plotted in a bar chart (Fig. 29).

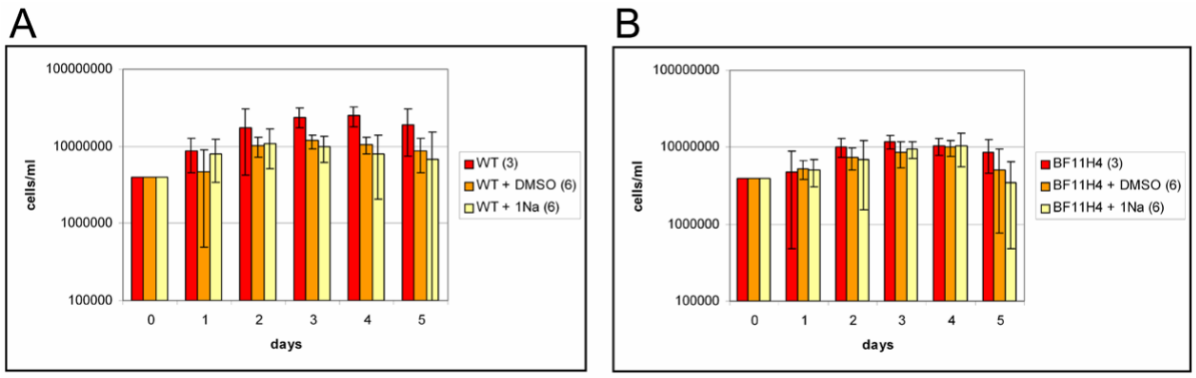

Figure 29. Growth of *L. mexicana* axenic amastigotes
days 0 -3: differentiation period; days 4 and 5: proliferation of axenic amastigotes; shown are average cell numbers of several experiments; the number of experiments conducted per strain are shown in parentheses behind the respective strain name.

In all experiments conducted, cell densities increased during the three day differentiation period (Fig. 29). No proliferation was observed after day 3 regardless of *L. mexicana* strain or the presence or absence of additives. Cells of the inhibitor-sensitised mutant strain BF11H4 were able to differentiate fully to amastigotes just like wild type *L. mexicana*. As growth was slow and minimal, the comparison of growth rates constitutes an imprecise method of comparison in this case. Instead the maximum average cell density reached by the observed cultures was compared in regard to the varying conditions (Fig. 30).

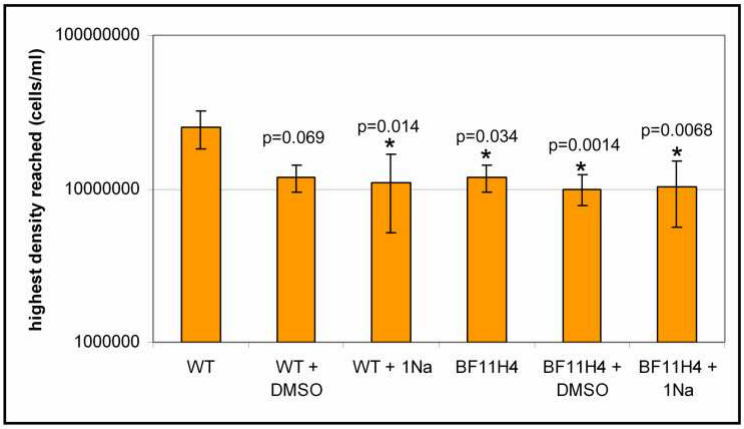

Figure 30. Maximum cell densities reached by WT and BF11H4 cultures while differentiating to axenic amastigotes under the influence of DMSO and 1Na
* marks cell densities which are significantly different to that of the wild type without additives ($p<0.05$); p-values of Student's t-test comparing the data set to the cell density of wild type without additives are shown above the column of each data set.

Fig. 30 shows that wild type *L. mexicana* cells reach higher cell numbers without additives than with. While the difference in obtained cell densities of wild type with or without the addition of DMSO is not statistically significant ($p = 0.069$), it is still pronounced. The maximum density of a wild type culture reached after the addition of 1Na on the other hand is significantly different from the one reached without additives ($p = 0.014$). Notably

there is no statistical difference between the cell densities reached by a wild type culture incubated with DMSO or 1Na, respectively (p = 0.56). The highest cell density reached by cells of the inhibitor-sensitised mutant BF11H4 was significantly lower than the maximum cell density reached by wild type cells, even without the influence of DMSO or 1Na (p = 0.034), indicating a negative influence of the inhibitor-sensitising mutation M111G of LmxMPK4IS on the differentiation process to axenic amastigotes. The addition of DMSO or 1Na showed no effect on the maximum cell density of BF11H4 cultures, but also led to a significantly lower maximal cell number than in a wild type culture without additives.

4.1.2.2.4 Mouse infection studies with *Leishmania*, carrying the inhibitor-sensitised LmxMPK4 mutant

The inhibitor-sensitising mutation M111G seems to impair the function of LmxMPK4IS during the differentiation process to axenic amastigotes. Footpad infection experiments were therefore conducted to demonstrate if the LmxMPK4IS expressing mutant strains of *L. mexicana* AB6H2, BF11H4 and BF11E4 could induce lesions corresponding to the wild type. For each strain five female Balb/c mice were injected in the left hind paw with 1×10^7 promastigotes from a culture in late logarithmic stage.

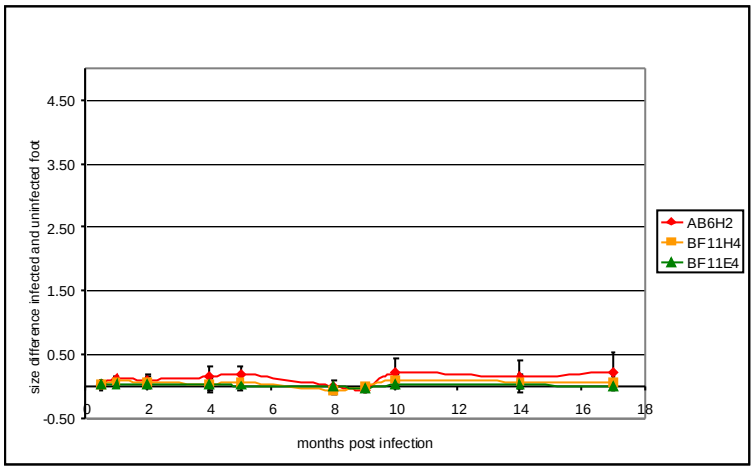

Figure 31. Footpad infections of Balb/c mice with the inhibitor-sensitised mutant strains
each graph is compiled of the data of 5 different mice

The diameter of both hind paws was monitored over time for each mouse and the difference between the infected left and the control right footpad was plotted in a graph (Fig. 31). All observed mice, infected with inhibitor-sensitised mutants developed none or only minor lesions during the observation period of 1.5 years. An infection with *L. mexicana* wild type promastigotes generally leads to the development of severe lesions of up to 4.5 mm within 8 months after infection (Wiese, M. 1998), hence the choice of scale for the y-axis of Fig. 31. Mouse 4, infected with BF11E4 had to be sacrificed before the final end of the experiment due to old age. All remaining mice were sacrificed after 17 months. Each left footpad was ground and incubated in SDM medium in an effort to

cultivate any parasites still present in the originally inoculated paw, despite the lack of lesion development. *L. mexicana* cells were successfully isolated from every footpad and promastigote cultures were established.

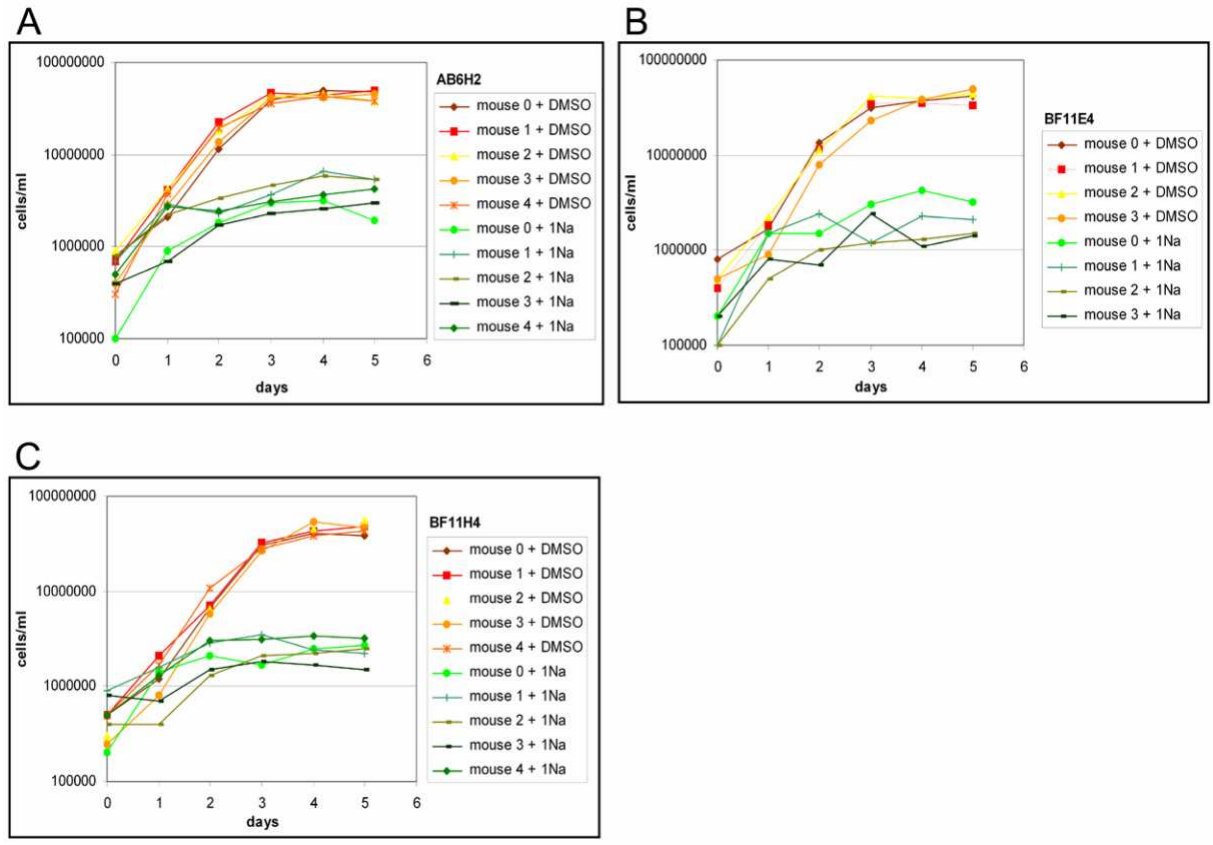

Figure 32. Growth and inhibition by 1Na of inhibitor-sensitised mutant promastigotes isolated after 1.5 years in the mouse
A: promastigotes isolated from mice infected with AB6H2; B: promastigotes isolated from mice infected with BF11E4; C: promastigotes isolated from mice infected with BF11H4.

In order to verify the persistence of the inhibitor-sensitising mutation M111G in LmxMPK4 expressed by these cells, the growth of all cultures was monitored after addition of 2 µM 1Na or a corresponding volume of the solvent DMSO.

Fig. 32 illustrates that all promastigote cultures differentiated from amastigotes, which had been isolated from infected mice, could indeed still be inhibited by 1Na in a dose-dependent manner. Consistent with the previously under chapter 4.1.3.2.2 shown results all promastigotes exhibited a certain level of growth even under the influence of 1Na. The depicted growth curves are based on a single experiment. The repetition of the experiment was deemed unnecessary due to the large number of different clones, all showing consistent growth and inhibition patterns. The results of Fig. 32 demonstrate that all promastigote cultures still contained the inhibitor-sensitised mutant LmxMPK4IS even 1.5 years after mice were initially infected with the parasites.

4.1.2.2.5 Analysis of the role of LmxMPK4 in cell cycle regulation

Experiments in which promastigotes resumed growth after the inhibitor 1Na was washed out demonstrated that the inhibition of LmxMPK4 has a cytostatic effect on *L. mexicana*. A possible cause for cytostasis would be a regulating role of LmxMPK4 in cell cycle progression, which would lead to an arrest in the respective phase of the cell cycle if LmxMPK4 was inhibited. *L. mexicana* samples were treated with the fluorescent dye propidium iodide, which is commonly used for cell cycle analysis as it intercalates into DNA and therefore allows a quantitative assessment of cellular DNA content. Fluorescence of cells was measured by flow cytrometry and results plotted in histograms, showing cell counts on the y-axis and fluorescence quantity detected by the forward scatter on the x-axis. The arising histograms allow the quantification of cells in the three phases, G1-, G2- and S-phase, which make up the interphase of the cell cycle. Each phase is represented by a typical peak in the histogram, as exemplified in Fig. 33.

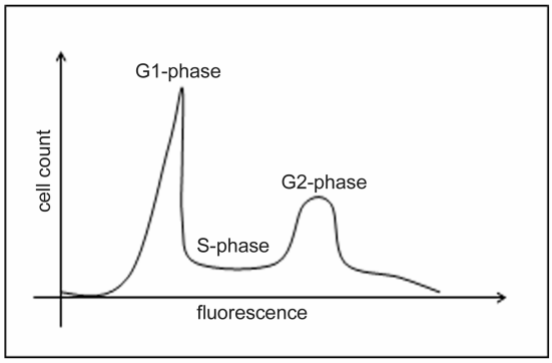

Figure 33. Illustration of the G1-, G2- and S-phase constituting the interphase of the cell cycle when visualised by flow cytrometry of propidium-iodide stained DNA

The G1-phase marks the start of the cell cycle. In this phase cells grow and synthesise enzymes needed for DNA replication. As cells contain only one copy of their genome during the G1-phase they all display roughly the same amount of fluorescence and cluster together as the peak with lowest fluorescence in the histograms. During the ensuing S-phase cells commence with the replication of DNA. Their varying DNA contents during this stage lead to a rather drawn-out, low peak over a wider area of fluorescence. Cells in the G2-phase all contain a duplicate set of their genome, therefore containing double the amount of intercalated propidium iodide than cells in the G1-phase. The G2-phase consequently appears in the histograms as a peak of cells at high fluorescence levels. The duration of the G1-phase is typically longer than the G2-phase, leading to a higher peak, as more cells stand in this phase. To analyse the cell cycle of inhibitor-sensitised *L. mexicana* mutants, cells of the clone AB6H2 were stained with propidium iodide after they had been grown under the addition of 5 µM of the inhibitor 1Na or a respective

volume of DMSO. *L. mexicana* wild type cells were treated with the same volume of DMSO to allow for the comparison with an unimpaired cell cycle. As a positive control for changes in the cell cycle, inhibitor-sensitised cells were treated with 2.5 µM Flavopiridol. This cyclin-dependent kinase inhibitor leads to an arrest in the G2-phase of the cell cycle (Hassan, P. et al. 2001). Samples were taken of all cultures at the beginning of the experiment and after one, three, seven, and ten hours, stained with 10 µg/ml propidium iodide and analysed by flow cytrometry.

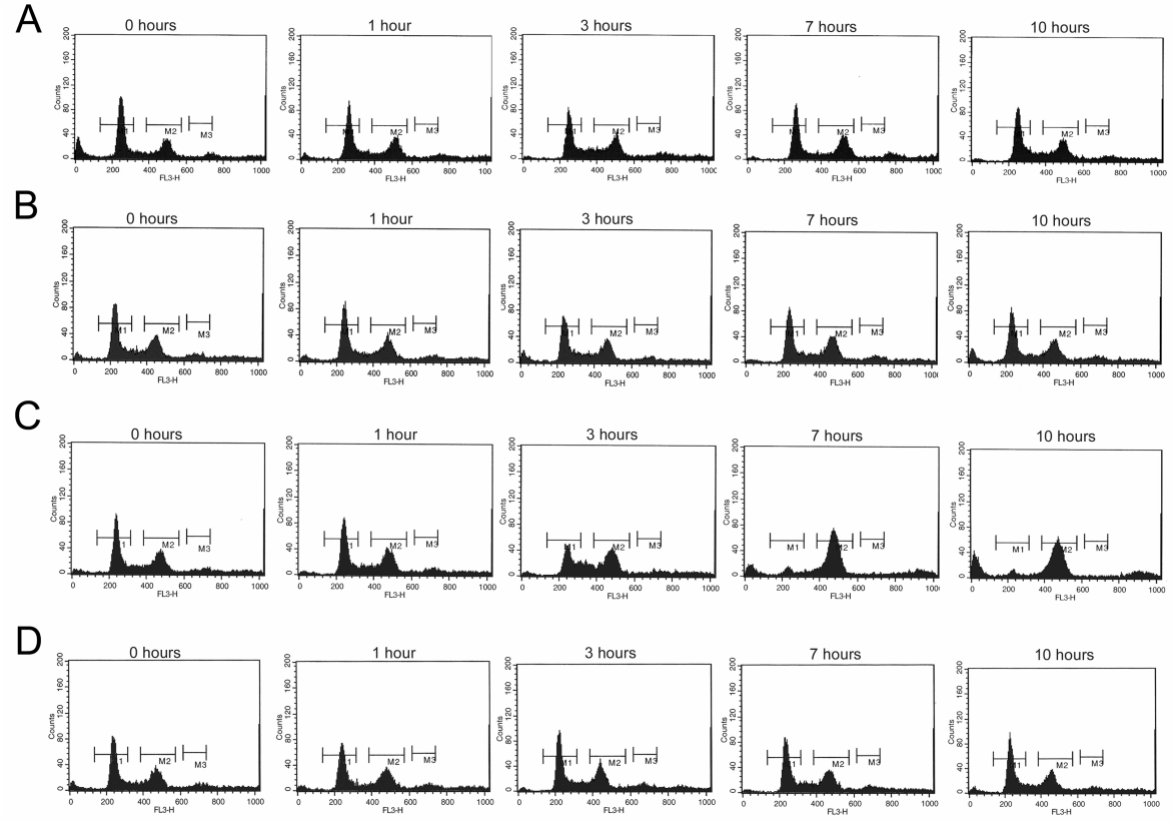

Figure 34. Flow cytrometry analysis of the cell cycle phases of wild type *L. mexicana* and inhibitor-sensitised clone AB6H2 under the influence of DMSO, 1Na and Flavopiridol
A, *L. mexicana* wild type, incubated with DMSO; B, *L. mexicana* AB6H2, treated with DMSO; C, *L. mexicana* AB6H2, treated with 5 µM 1Na; D, *L. mexicana* AB6H2, treated with 2.5 µM Flavopiridol. The first gate and second gate, shown in the diagrams were used to measure the number of cells in the G1- and G2-phase, respectively.

Treatment of cells expressing the inhibitor-sensitised mutant LmxMPK4IS with Flavopiridol led to the expected arrest in the G2-phase of the cell cycle (Fig. 34, C). The arrest was visible in the histogram as the corresponding G2-phase peak increased, and the peaks of the G1- and S-phase decreased and disappeared over time. There was no difference visible in the cell cycle progression of inhibitor-sensitised cells compared to those of *L. mexicana* wild type cells (Fig. 34, A), regardless if they had been treated with DMSO (Fig. 34, B) or the inhibitor 1Na (Fig. 34, D). The inhibition of LmxMPK4IS by 1Na does therefore not lead to a specific arrest of the cell cycle.

4.1.2.2.6 Analysis of the role of LmxMPK4 in metabolism regulation

The inhibition of LmxMPK4 has a cytostatic effect on *L. mexicana* cells that does not result from an arrest in one phase of the cell cycle. A possible explanation for the cytostasis other than a general arrest in the cell cycle would be a disturbance of metabolic processes, evoked by the inhibition of LmxMPK4IS. Metabolite profiling was therefore conducted to compare the metabolome of treated and untreated inhibitor-sensitised mutant cells with that of *L. mexicana* wild type cells and ultimately to ascertain if LmxMPK4 plays a role in the regulation of metabolic processes in the cells. Cultures of wild type *L. mexicana* and of the clone BF11H4, which expresses only the inhibitor-sensitised mutant LmxMPK4IS and no wild type LmxMPK4, were inoculated from logarithmic cultures to a density of 5×10^6 cells/ml. The promastigote cultures were each grown for 48 hours under the influence of 5 µM 1Na or an equivalent volume of DMSO, respectively, yielding the four data sets of BF11H4 incubated with DMSO ("4IS + DMSO"), BF11H4 incubated with 1Na ("4IS + 1Na"), wild type incubated with DMSO ("WT + DMSO") and wild type incubated with 1Na ("WT + 1Na"). Metabolites were extracted using hot Ethanol and analysed by high-resolution mass spectrometry on a Finnigan LTQ Orbitrap mass spectrometer fitted with a Surveyor HPLC pump. All samples were produced as biological triplicates and technical duplicates, providing sets of 6 data points for each of the four samples.

The entire experiment was repeated a second time completely independently from the first. However, the resulting data sets differed in quantifications and identifications of metabolites from the first experiment so that it was not possible to process both experiments together. The made observations can therefore not result in correct quantifications of metabolites but refer to trends of which metabolites are up- or downregulated in the respective data sets (T'Kindt, R., personal communication). All results shown in this thesis correspond to results of the first conducted experiment, but it is mentioned in the text if noted changes could be confirmed in the second experiment.

The first step of analysing the generated large amount of data involved unsupervised principal component analysis (PCA). This statistical procedure is widely used in multivariate data analysis to transform a large number of variables into a smaller amount of uncorrelated variables, which are called principal components. The separation on the first principal component describes the highest variability in the data, while the second principal component is a description of most of the remaining variability. PCA analysis applied to the data sets in our experiments revealed that the relative metabolite abundance profiles differ sufficiently to clearly and robustly separate the different sets of wild type and inhibitor-sensitised mutant samples (Fig. 35). Each data set, comprised of

biological and technical replicates of the same sample is correctly clustered together. Wild type and inhibitor-sensitive mutant BF11H4 are clearly separated on the first principal component, explaining 42.3% of the total variance, while the second principal component accounts for 26.4% of the total variance and separates the two different data sets of the inhibitor-sensitised mutant.

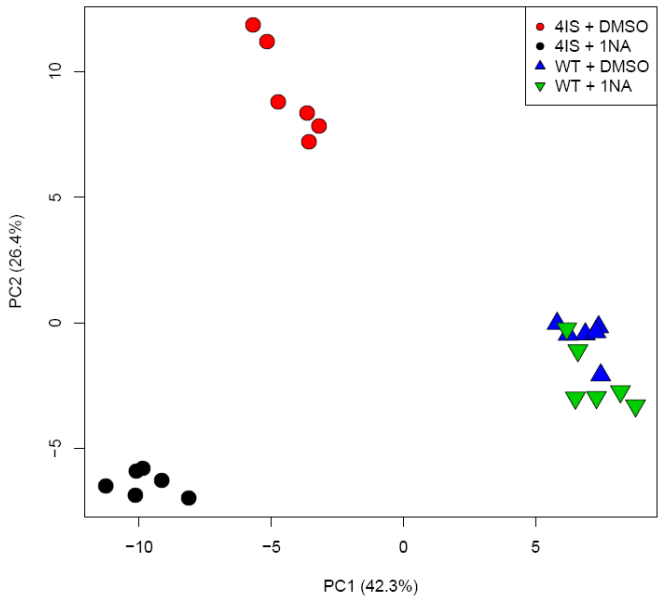

Figure 35. Principal component analysis of the four different sample sets, which were investigated by metabolic profiling
Each circle or arrowhead, respectively, corresponds to one set of data of the biological and technical replicates; red circles indicate LmxMPK4IS-expressing mutants BF11H4 which were grown under DMSO influence; black circles indicate LmxMPK4IS-expressing mutants BF11H4 which were grown under the influence of inhibitor 1Na; blue arrowheads indicate wild type *L. mexicana* which were grown under DMSO influence; green arrowheads indicate wild type *L. mexicana* which were grown under the influence of inhibitor 1Na.

The PCA analysis depicted in Fig. 35 revealed that there was only a minor variance between the wild type samples, regardless if they had been incubated with DMSO or 1Na. The metabolites analysed from cultures which expressed the inhibitor-sensitised mutant LmxMPK4IS and had been incubated with DMSO, on the other hand, differed profoundly from samples of BF11H4 mutant cultures that had been grown under the influence of the inhibitor 1Na for 48 hours. Both data sets also varied notably from wild type data sets, whereas the samples of BF11H4 grown with 1Na showed a higher variance from the wild type samples than samples of BF11H4 which had been incubated with DMSO.

A total of 134 different metabolites were identified in the four examined sample sets and their abundance compared, subject to the two different *Leishmania* cell lines and their respective growth treatment. 35.8 % of all identified metabolites showed a 2 fold or more change (Fig. 36) when the samples of the wild type culture treated with 1Na were compared with the samples of the clone BF11H4 in which the activity of LmxMPK4IS was

inhibited by the addition of 1Na. Most changes (24.63 %) were higher than two-fold but lower than five-fold. A considerable number of metabolites, however, showed changes between five-fold and ten-fold (8.21 %) and even higher than ten-fold (2.99 %). The highest change was observed for arginine, which was 179 times higher when LmxMPK4IS was inhibited by 1Na than in the wild type. Diagrams showing the identities of all the metabolites with more than twofold changes in BF11H4 + 1Na, in comparison to WT + 1Na, are shown in the appendix.

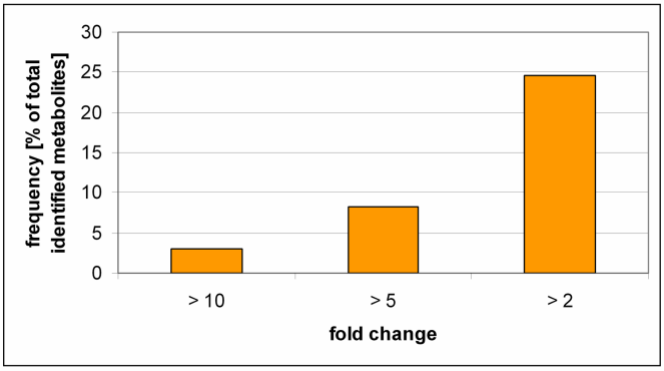

Figure 36. Frequency of fold changes of all identified metabolites in the comparison of the samples, wild type *L. mexicana* incubated with 1Na and inhibitor-sensitised mutant BF11H4 incubated with 1Na

Changes in metabolites are, however, not only observed between the samples of the 1Na treated cultures of inhibitor-sensitised mutant and wild type. There are already many changes observed in the inhibitor-sensitised mutant BF11H4 after it was grown under the influence of DMSO and without any addition of the inhibitor of LmxMPK4IS, 1Na, as can be seen in the clustering of the data set apart from the wild type data sets on the second principal component in the PCA analysis (Fig. 35). This was also obvious when the different samples were compared to each other in respect to the general pathways in which the observed changes occurred. Most of the observed changes were located on major pathways, mainly including amino acids and their derivatives, and lipids (Fig. 37).

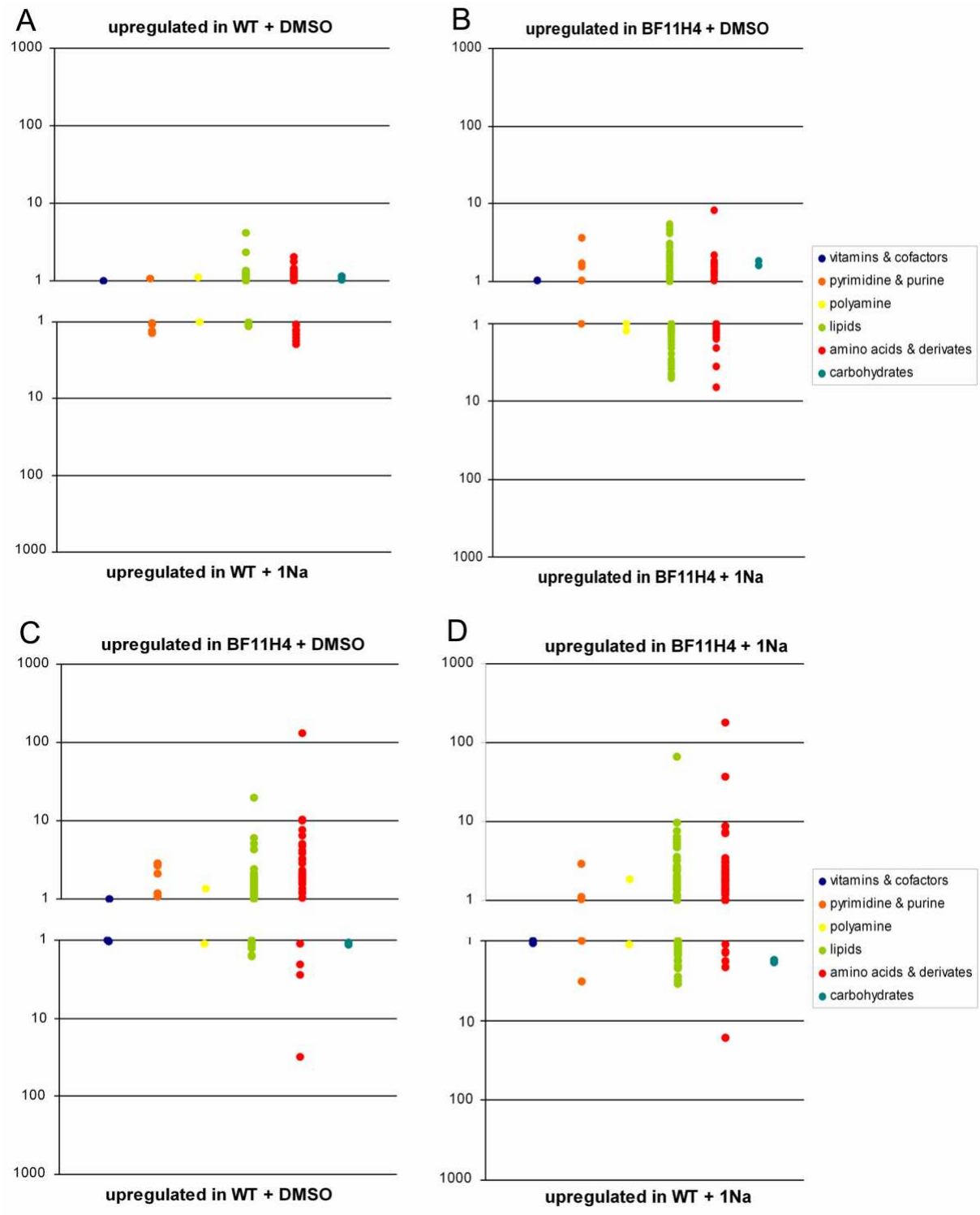

Figure 37. Distribution of all observed changes in metabolites to major metabolite classes
A, comparison of changes in wild type *L. mexicana* incubated with DMSO and 1Na, respectively; B, comparison of changes of inhibitor-sensitised mutant BF11H4 incubated with DMSO and 1Na, respectively; C, comparison of changes in wild type and BF11H4 cells, both incubated with DMSO; D, comparison of changes in wild type cells and BF11H4 cells, both incubated with 1Na; the y-axes show the fold of changes on a logarithmic scale; analysis conducted according to analyses in (Scheltema, R. A. et al. 2010).

The metabolism of wild type cells that were grown under the influence of DMSO or 1Na did not vary considerably from each other (Fig. 37, A). *L. mexicana* mutants BF11H4,

expressing the inhibitor-sensitised kinase LmxMPK4IS responded to the addition of the inhibitor 1Na with changes mainly in the amino acid and lipid metabolism (Fig. 37, B). BF11H4 metabolism differed from wild type metabolism even without the addition of 1Na (Fig. 37, C). Most changes were again observed in metabolites belonging to the classes of amino acids and lipids. The most dramatic changes, however, were observed when metabolites of the BF11H4 mutant cultures grown under 1Na influence were compared with metabolites of wild type cells grown under the influence of 1Na (Fig. 37, D and also compare PCA-analysis in Fig. 35). The most and the highest fold changes occurred again in the abundance of amino acids and lipids. Variations in metabolism of inhibitor-sensitised mutants were mainly due to upregulations of metabolites (Fig. 37, C and D, upper panels of diagrams), although downregulations did occur as well (Fig. 37, C and D, lower panels of diagrams).

The trend plots of all 134 identified metabolites are displayed in the appendix, but some of the more drastic changes in metabolites are shown in Fig. 38.

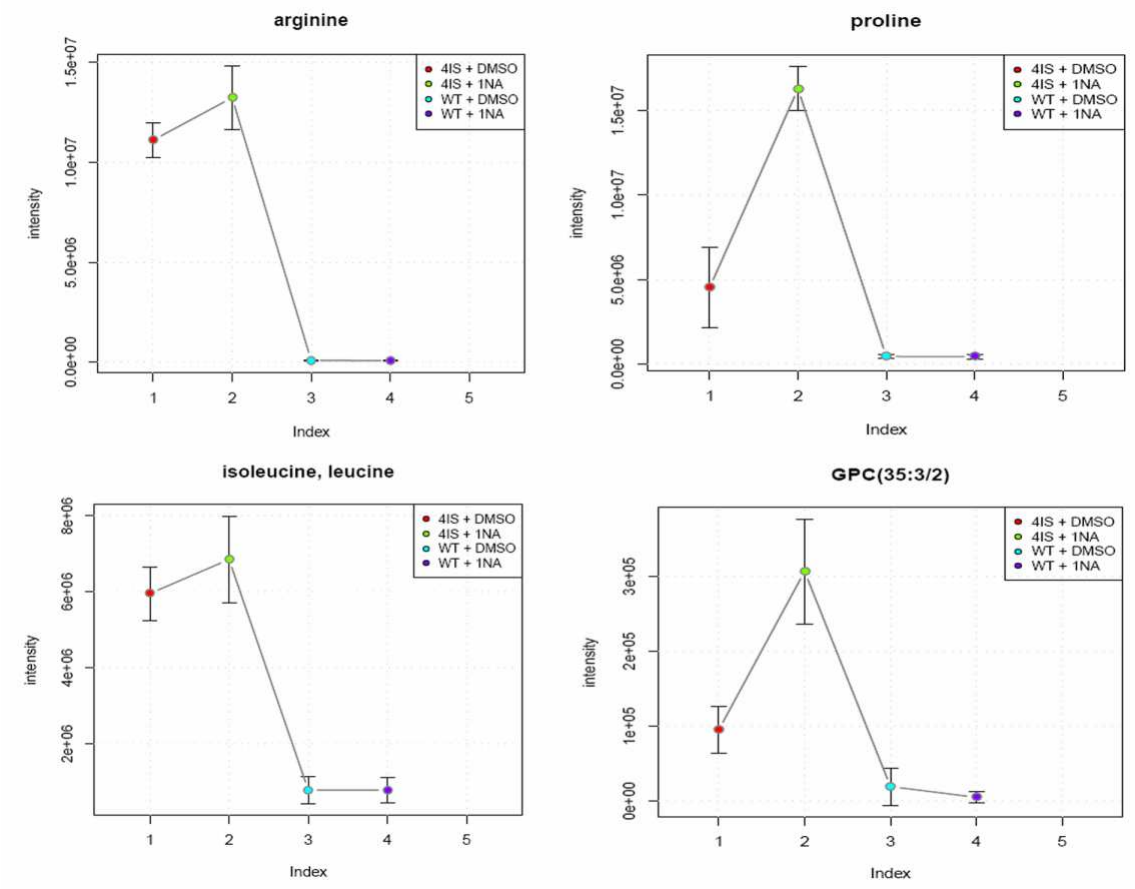

Figure 38. The four metabolites which displayed the highest fold changes between wild type + 1Na and BF11H4 + 1Na in the profiling analysis
arginine was 179 fold higher in BF11H4 + 1Na samples than in WT + 1Na samples; proline was 37.5 fold upregulated; isoleucine/leucine was 8.8 fold upregulated; the lipid GPC(35:3/2) was 66 fold upregulated.

In the case of arginine, proline, isoleucine/leucine and a glycerophosphocholine that contained side chains with a total of 35 carbons and 3 and 2 double bonds, respectively (GPC (35:3/2)), the metabolites were extremely upregulated in cells of the inhibitor-sensitised mutant cell line BF11H4 that had been incubated with the inhibitor 1Na. The incubation of BF11H4 with DMSO led to a somewhat intermediate stage of the metabolites, while both sample groups of wild type cells displayed a consistently low level of those metabolites. Citrulline, dimethylarginine, trypanothione, trypanothione-disulfide and glutathione levels were also severely changed in inhibitor-sensitised mutant cells after the addition of 1Na in comparison to the wild type (Fig. 39).

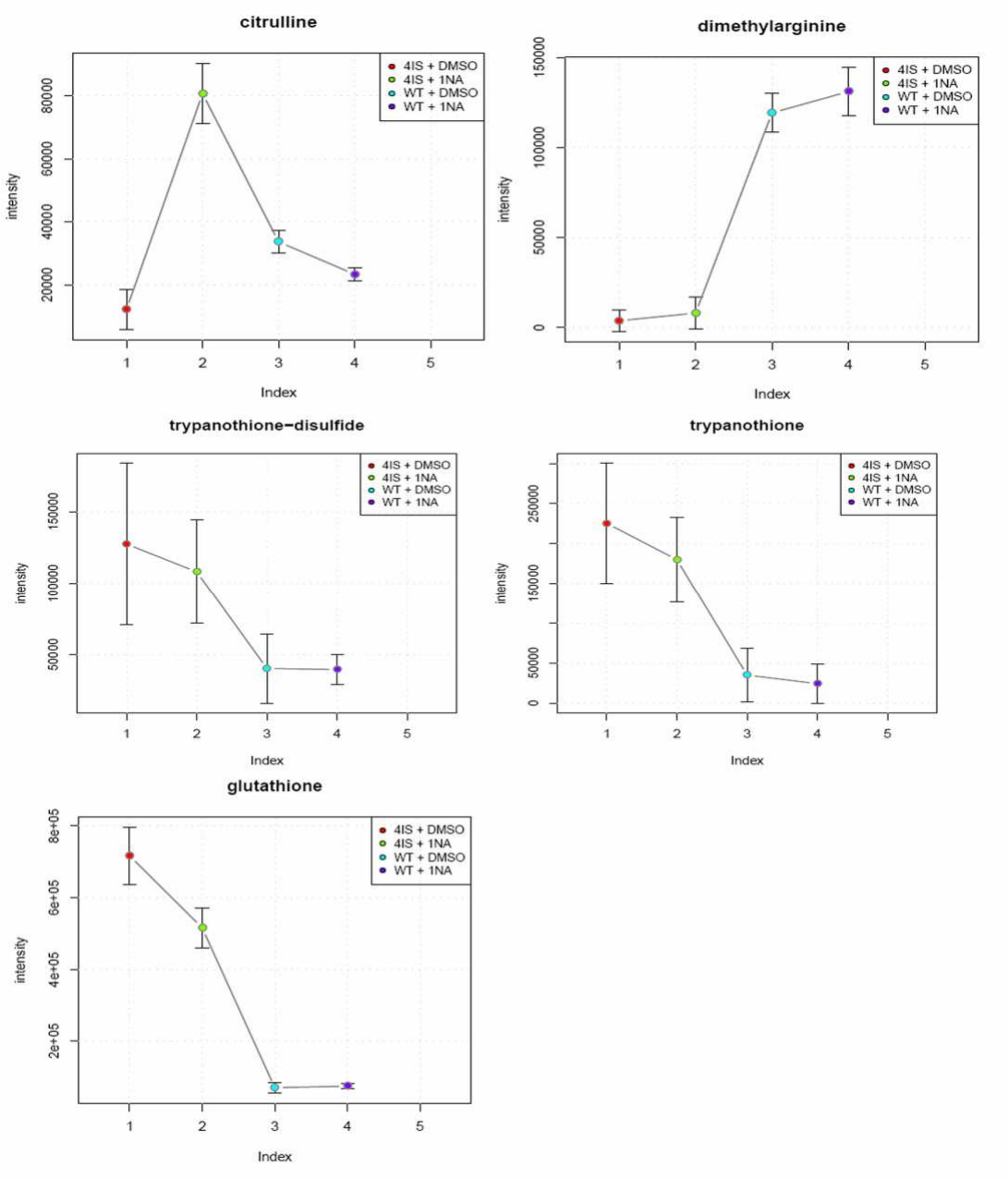

Figure 39. Metabolites which showed considerably different levels in wild type *L. mexicana* and inhibitor-sensitised cell line BF11H4

In the metabolites depicted in Fig. 39 the incubation of BF11H4 with DMSO did not lead to an intermediate level. In the case of citrulline the addition of DMSO to BF11H4 led to a slight downregulation in comparison to the wild type. Levels of dimethylarginine, trypanothione and trypanothione-disulfide did not considerably change in the inhibitor-sensitised mutant cell line BF11H4, regardless if the cells were grown under the influence of 1Na or DMSO. The metabolite levels did, however, differ considerably from the levels detected in wild type cells. The upregulation of glutathione on the other hand was even more pronounced in BF11H4 in the presence of DMSO than in the presence of 1Na.

All specified metabolites show the same trend of up- or downregulation in the independently conducted second experiment, although the fold differences vary. Hence the impossibility to process data sets together. In the comparison of BF11H4 + 1Na and WT + 1Na, arginine for example shows the still very high upregulation of 37-fold in the second experiment, while citrulline is upregulated 19-fold, as opposed to 3.5-fold in the first experiment whose data points are shown here. One notable factor is the detection of the polyamine spermidine, which was not identified in the data set of the first experiment, but showed an upregulation of 6-fold in the inhibitor-sensitised mutant under 1Na influence in comparison to the wild type grown with 1Na.

The metabolic profiling experiment showed in conclusion that the inhibition of LmxMPK4IS by 1Na led to a number of changes in the metabolome, which were mainly due to upregulations of amino acids and lipids.

4.1.2.2.7 Analysis of the role of LmxMPK4 in protein synthesis regulation

To investigate whether observed changes in amino acid abundances resulting from the inhibition of LmxMPK4IS were due to a general change in protein turnover, assays using protein labelling with radioactive [^{35}S]-methionine were conducted. Promastigote cultures were inoculated with cells in the logarithmic stage of the life cycle to a density of 5×10^6 cells/ml and incubated for 48 hours at 27°C, either without any additives or after addition of 5 µM 1Na or a respective volume of DMSO. To label all proteins that were produced during a specified period of time with [^{35}S]-methionine, cultures were harvested by centrifugation and the cells were washed and resuspended in SDM-medium containing no unlabelled methionine. The cultures were incubated for 1 hour at 27°C in the presence of [^{35}S]-methionine (5 µCi/ml), after which the reaction was quenched by the addition of 1 mM unlabelled methionine in PBS. Cells were harvested by centrifugation, lysed in lysis buffer and separated by SDS-PAGE with approximately 4×10^6 cells/lane. The Coomassie-stained gels were dried and subjected to autoradiography.

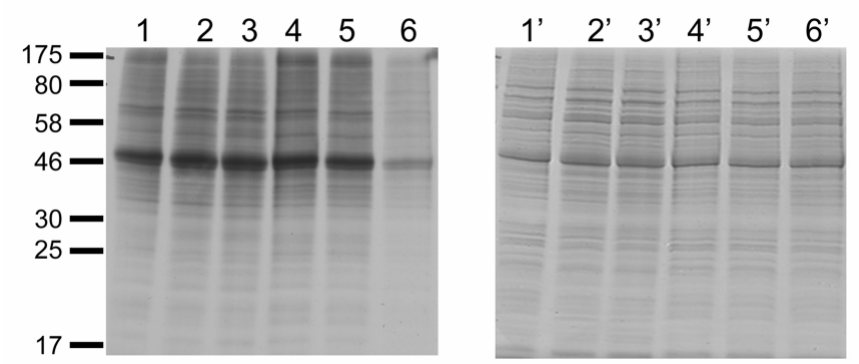

Figure 40. Analysis of protein turnover by incorporation of [^{35}S]-methionine depending on LmxMPK4IS inhibition
left panel, autoradiograph after 30 hours exposure; right panel, Coomassie-stained gel; lanes 1, 1', wild type cells without additive; lanes 2, 2', wild type cells grown under influence of DMSO; lanes 3, 3', wild type cells grown under influence of 5 µM 1Na; lanes 4, 4', inhibitor-sensitised mutant BF11H4, grown without additive; lanes 5, 5', inhibitor-sensitised mutant BF11H4, grown under influence of DMSO; lanes 6, 6', inhibitor-sensitised mutant BF11H4, grown under influence of 5 µM 1Na; molecular masses of standard proteins are indicated in kDa.

Fig. 40 shows that all lanes contained comparable amounts of proteins. All proteins visible in the lysates showed incorporation of [^{35}S]-methionine, with visibly less [^{35}S]-methionine incorporated into proteins of the inhibitor-sensitised mutant grown under the influence of 1Na. This indicates a downregulation of protein synthesis due to the inhibition of LmxMPK4IS by 1Na.

4.1.3 Generation and characterisation of a new inhibitor-sensitised mutant LmxMPK4ISMA

Previous results have pointed to a certain functional impairment of LmxMPK4IS *in vitro* and *in vivo*, in regard to the differentiation into axenic amastigotes and metabolism. It is possible that the mutation of the gatekeeper residue to alanine instead of glycine leads to a more stable confirmation of the mutated kinase, thus supporting the full functionality of the inhibitor-sensitised mutant. On grounds of this, a new inhibitor-sensitised mutant in which methionine111 was exchanged to alanine was generated and dubbed LmxMPK4ISMA.

4.1.3.1 Generation of LmxMPK4ISMA

The inhibitor-sensitising M111A mutation was introduced by a PCR reaction on the template pBuspolPacLmxMPK4ISds, using the primers MPK4IS-GA.for and MPK4IS-GA.rev. The primer MPK4IS-GA.rev hybridised to the gatekeeper region of *LmxMPK4* and introduced the mutation GGC, which removed the *Bgl*II restriction site of *LmxMPK4IS* and encodes alanine. MPK4IS-GA.rev also covered the existing *Swa*I restriction site, while MPK4IS-GA.rev, hybridised within the intergenic region of the polPac-cassette at the existing *Afl*II restriction site. The 989 bp long PCR product was integrated into the plasmid

pCR2.1TOPO via TA-cloning. The *LmxMPK4* fragment containing the new mutation was liberated from pCR2.1TOPO by cleavage with *Swa*I and *Afl*II and ligated into the equally digested plasmids pBuspolPACMPK4ISds and pJCLinkerLmxMPK4ISLmxPK5, respectively, thus exchanging the inhibitor-sensitising mutation M111G to M111A and generating the plasmids pBuspolPacMPK4ISMAds and pJCLinkerLmxMPK4ISMA-LmxPK5 (see 8.1 for plasmid maps). The identity of the new mutation was verified by the now absent *Bgl*II restriction site and sequencing.

4.1.3.2 Phosphotransferase activity of recombinant co-expressed LmxMPK4ISMA

As previously described in chapter 4.1.3.1.3, His-LmxMPK4IS could be activated by co-expression with LmxMKK5, but was significantly less active than co-expressed wild type His-LmxMPK4. His-LmxMPK4ISMA was subsequently co-expressed with LmxMKK5 to reveal whether the inhibitor-sensitising mutation M111A would lead to a higher activity. Recombinant expression proceeded from the plasmid pJCLinkerLmxMPK4ISMALmxPK5 in *E. coli* BL21(DE3)[pAPlacIQ] cells at 18°C over night. Lysis of cells via sonification was followed by affinity purification on Chelating Sepharose loaded with Co^{2+}. Wild type LmxMPK4 and the original inhibitor-sensitised mutant LmxMPK4IS, carrying the M111G mutation, were co-expressed with LmxMKK5 under the same conditions, to be used as controls. To control for innate activity LmxMPK4, LmxMPK4IS and LmxMPK4ISMA were expressed as His-tag fusion proteins without the presence of LmxMKK5 and purified under the same conditions.

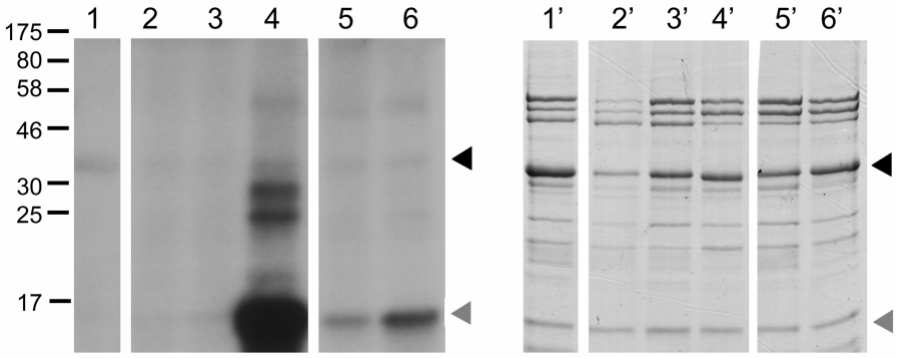

Figure 41. Kinase assay comparing the phosphotransferase activities of inhibitor-sensitised LmxMPK4 mutants with wild type LmxMPK4
left panel, autoradiograph, exposure time 24 hours, right panel, Coomassie stained-gel;
lanes 1, 1', singly expressed His-LmxMPK4; lanes 2, 2', singly expressed His-LmxMPK4IS;
lanes 3, 3', singly expressed His-LmxMPK4ISMA; lanes 4, 4', His-LmxMPK4, co-expressed with LmxMKK5; lanes 5, 5', His-LmxMPK4IS, co-expressed with LmxMKK5;
lanes 6, 6', His-LmxMPK4ISMA, co-expressed with LmxMKK5;
black arrowheads indicate His-LmxMPK4, grey arrowheads indicate MBP; masses of standard proteins are indicated in kDa.

The purified recombinant proteins were not eluted, but remained bound to the resin when they were employed in a radioactive kinase assay under standard conditions for LmxMPK4 and with MBP as substrate.

Fig. 41 illustrates that singly expressed His-LmxMPK4ISMA is just as inactive as singly expressed His-LmxMPK4 and His-LmxMPK4IS (lanes 1-3). Although phosphotransferase activity of co-expressed His-LmxMPK4ISMA is considerably higher than that of co-expressed His-LmxMPK4IS (compare Fig. 41, lanes 6 and 5) it is still significantly lower than the strong activity of wild type His-LmxMPK4 after co-expression with LmxMKK5 (Fig. 41, lane 4). No noteworthy autophosphorylation occurred in either of the samples.

The sensitivity of co-expressed LmxMPK4ISMA towards the inhibitor 1Na was equally tested with the help of a radioactive kinase assay. Approximately 1 µg of purified, resin-bound His-LmxMPK4ISMA, co-expressed with LmxMKK5, was incubated for 1 hour at 34°C with different concentrations of inhibitor 1Na or DMSO, 1 mM ATP, containing 5 µCi [γ^{32}]ATP (6000 Ci/mmol) and 5 µg MBP in 50 µl of LmxMPK4 kinase buffer, containing 50 mM 3(N-morpholino)propanesulfonic acid (MOPS), pH 7.0, 10 mM $MnCl_2$ and 0.1 M NaCl. The inhibitor was diluted in DMSO so that the addition of 1 µl to the kinase assay would lead to a final concentration of 1 µM, 10 µM or 50 µM, respectively. The samples were separated by SDS-PAGE and the autoradiograph of the dried, Coomassie-stained gel was used to compare the phosphotransferase activity of activated His-LmxMPK4ISMA under inhibitor influence with that of activated His-LmxMPK4ISMA alone or after addition of 1 µl DMSO, respectively.

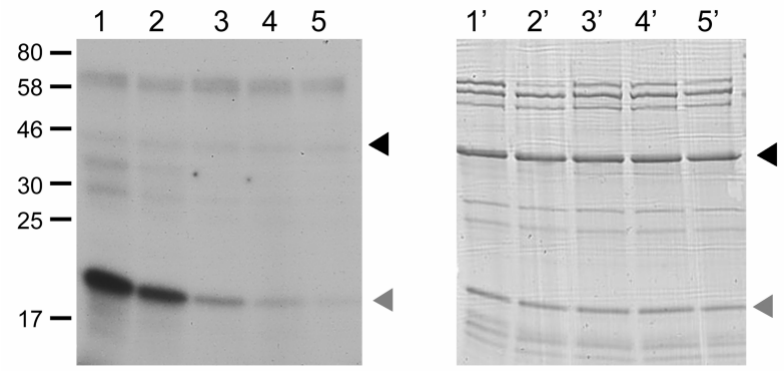

Figure 42. Kinase assay of His-LmxMPK4ISMA, co-expressed with LmxMKK5, with different concentrations of inhibitor 1Na
left panel, autoradiograph after 40 h exposure; right panel, Coomassie-stained gel;
lanes 1, 1', no additive; lanes 2, 2', addition of DMSO; lanes 3, 3', addition of 1 µM 1Na;
lanes 4, 4', addition of 10 µM 1Na; lanes 5, 5', addition of 50 µM 1Na;
black arrowheads indicate His-LmxMPK4ISMA, grey arrowheads indicate MBP; molecular masses of standard proteins are indicated in kDa.

The addition of 1 µl DMSO to co-expressed His-LmxMPK4ISMA has a slight inhibitory effect on its phosphotransferase activity as can be seen in comparison to the activity of His-LmxMPK4ISMA without additive (Fig. 42, lanes 1 and 2). The addition of 1Na to a final concentration of 1 µM results in a very slight phosphorylation of MBP (Fig. 42, lane 3), which is considerably less when 1Na is added to a final concentration of 10 µM (Fig. 42, lane 4) and all but negligible after the addition of 50 µM 1Na (Fig. 42, lane 5). The addition of 1Na therefore effectuates a dose-dependent inhibition of the phosphotransferase activity of His-LmxMPK4ISMA, co-expressed with LmxMKK5.

4.1.3.3 Generation of *L. mexicana* mutants containing LmxMPK4ISMA

L. mexicana mutants were generated which contained *LmxMPK4ISMA* in the original genomic locus of *LmxMPK4* and no wild type *LmxMPK4* anymore. The gene-cassette for homologous recombination was liberated from the plasmid pBuspolPacMPK4ISMAds by cleavage with *Cla*I and *Nru*I and transformed into wild type *L. mexicana* via electroporation. To remove the remaining *LmxMPK4* allele, the LmxMPK4 deletion cassette, that contained the phleomycin resistance marker flanked by the 5'- and 3'-UTRs of LmxMPK4, was liberated by cleavage with *Cla*I and *Nru*I from the previously generated plasmid pB11CΔLmxMPK4phleo (Wang, Q. et al. 2005). The fragment was transformed into cells that contained the cassette polPACLmxMPK4ISMA on one allele and the wild type gene *LmxMPK4* gene on the other. Clones were selected which were resistant to both puromycin and phleomycin and the correct genotype was confirmed by Southern blot analysis (Fig. 43).

One positive clone containing the *LmxMPK4ISMA* gene and lacking the wild type *LmxMPK4* gene was obtained and named A10 (Fig. 43, A, lane 4).

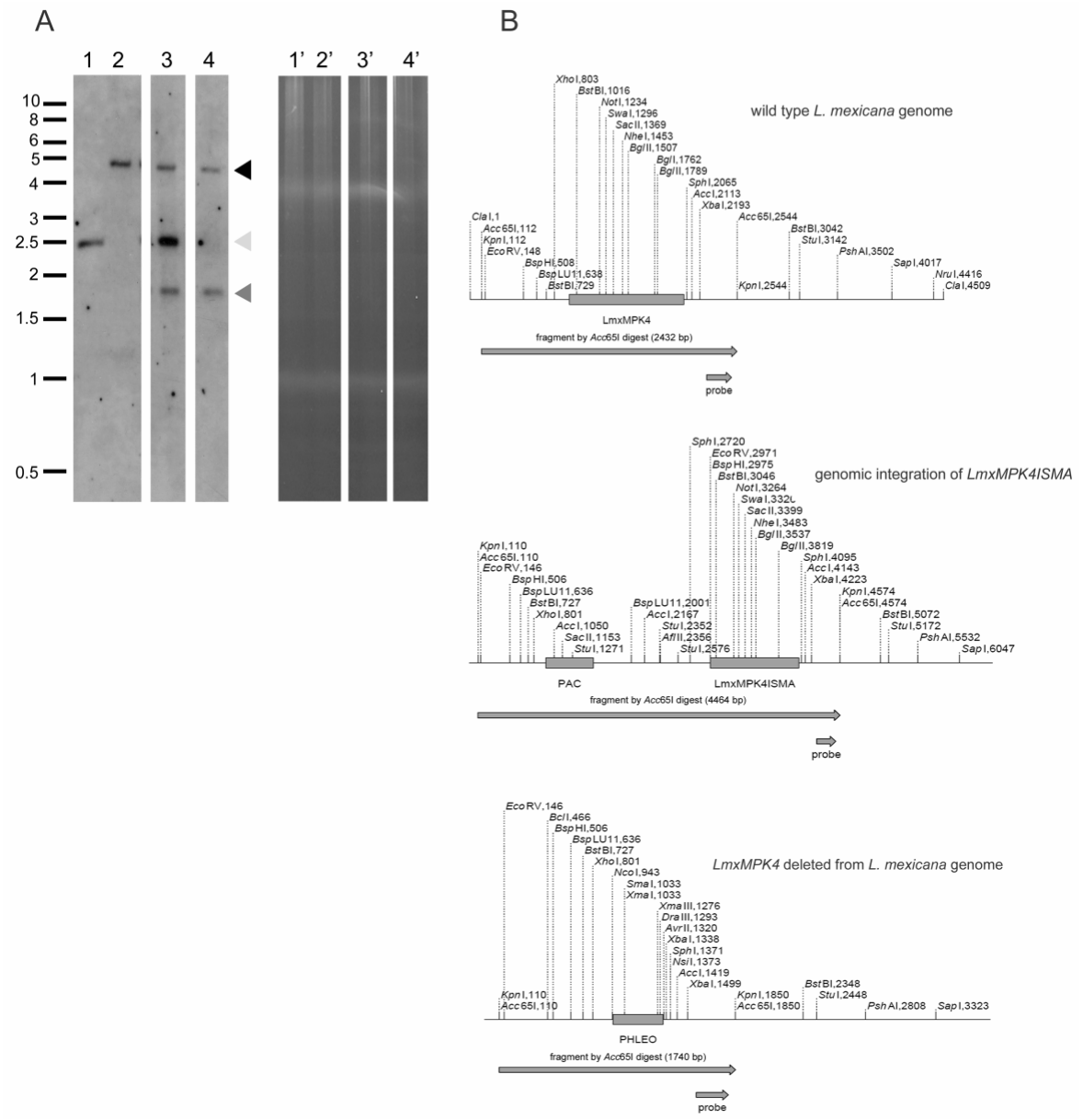

Figure 43. Southern blot analysis of mutants with genomic integration of *LmxMPK4ISMA*
A, left panel, Southern blot; right panel, corresponding agarose gel; genomic DNA was cleaved with *Acc*65I; lanes 1, 1', wild type; lanes 2, 2', *LmxMPK4ISMG* mutant BF11H4; lanes, 3, 3', potential *LmxMPK4ISMA* mutant A4 (false positive); lanes 4, 4', potential *LmxMPK4ISMA* mutant A10; black arrowheads indicate the LmxMPK4IS-pac integration cassette (4467 bp), light grey arrowheads indicate the wild type *LmxMPK4* gene (2432 bp), dark grey arrowheads indicate the phleomycin deletion cassette (1714 bp); fragments were detected by a DIG-labelled DNA probe corresponding to a downstream sequence of *LmxMPK4* and generated with the oligonucleotides mpk4_1.for and mpk4_6.for (for a detailed display where the probe binds, see the sequence of the *LmxMPK4* region in appendix 8.1); sizes of standard DNA fragments are indicated in kb; all depicted lanes result from the same blot in the same experiment;
B, diagrammatic plan of the analysed DNA region, the utilised probe and the generated fragments.

Promastigotes of the LmxMP4ISMA clone A10 were analysed for susceptibility to the inhibitor 1Na by counting cells over five days and generating a growth curve. Cells were cultivated in 1 ml cultures in 24 well plates in the presence of no additives, 1 µl DMSO or 1 µl of appropriate 1Na dilution, leading to the final inhibitor concentrations of 0.05 µM, 0.1 µM, 0.2 µM, 0.5 µM, 1 µM, 5 µM and 10 µM, respectively. *L. mexicana* wild type cells

were cultivated under the same conditions to serve as a control for the unimpaired growth of the inhibitor-sensitised mutant A10.

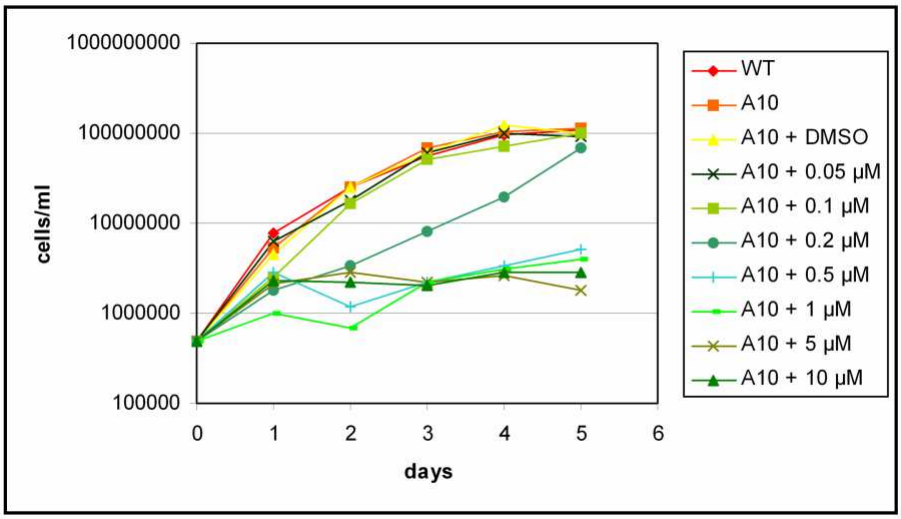

Figure 44, Growth curve of *L. mexicana* containing *LmxMPK4ISMA* in comparison with wild type *L. mexicana*

The growth curve in Fig. 44 shows that the growth of A10 promastigotes equals that of the wild type and was not impaired in the presence of DMSO, 0.05 µM 1Na or 0.1 µM 1Na, respectively. The addition of 0.2 µM 1Na led to considerably decelerated growth of promastigotes but did not result in a full cytostatic effect. An addition of 0.5 µM and higher on the other hand completely inhibited growth of A10 promastigotes. The presented data is based on one experiment only and must therefore be viewed as preliminary.

4.2 LmxMPK6

4.2.1 Biochemical characterisation of GST-LmxMPK6

LmxMPK6 was designed to be expressed as a recombinant GST-fusion protein with the help of the plasmid pGEX-KG. The GST-tag provided by this plasmid contains two SP-motifs, which are potential MAP-kinase phosphorylation sites. One SP-motif is contained within the GST-tag and can, should it be required, be removed with the GST-tag by thrombin cleavage. The other SP-motif is located directly C-terminal of the recombinant kinase at the end of the thrombin cleavage site so that it would still remain after removal of the GST-tag. As this motif could potentially be phosphorylated and thus be mistaken for autophosphorylation of the kinase, the sequence of the plasmid was altered by removing the CCC codon of proline. This was achieved by cleaving pGEX-KG with *Bam*HI and filling in the 5'-overhang with Klenow enzyme. The now blunt linearised plasmid was cleaved with *Pst*I, removing the fragment 3' of the original *Bam*HI restriction site, which was replaced by the corresponding fragment liberated with *Sma*I/*Pst*I from the original plasmid pGEX-KG. The newly generated plasmid, lacking the proline just after the thrombin cleavage site was called pGEX-KGS. When the work for this thesis started, LmxMPK6 had already been cloned into the expression construct pGEX-KG3-mapkin24-0505 (mapkin24-0505 being the old name for LmxMPK6) (Wiese, M. et al. 2003b). The *LmxMPK6* gene was liberated from this construct by *Xba*I/*Eco*RV cleavage and cloned into pGEX-KGS, which had been opened by *Xba*I/*Eco*RV.

4.2.1.1 Generation of kinase-dead mutant of LmxMPK6

The kinase-dead mutant LmxMPK6K33M was generated by PCR, using an N-terminal fragment of LmxMPK6 as template. The mutation of the lysine at this position generally leads to an inactive kinase, due to the inability to correctly bind and orientate ATP (Gibbs, C. S. et al. 1991). The fragment used as PCR template was liberated from pGEX-KG3-mapkin24-0505 by cleaving the *LmxMPK6* gene 502 bp after the start codon with *Sfo*I, and at the *Xba*I restriction site that was located 5' of *LmxMPK6* in the MCS of pGEX-KG. The plasmid was additionally digested with *Bsr*GI to cleave the other, undesired fragment to facilitate the separation of fragments. The *Sfo*I/*Xba*I fragment of the 5'-end of *LmxMPK6* and part of the pGEX-KG plasmid was ligated into pBluescript SKII(+) which had been treated with *Xba*I and *Eco*RV. As *Eco*RV and *Sfo*I both generate blunt end fragments a ligation was possible. The newly generated plasmid was used as template in two PCRs with the oligonucleotides ScaI.rev and MPK6KM.rev, as well as ScaI.for and MPK6KM.for, respectively. The oligonucleotides MPK6KM.for and MPK6KM.rev overlap and introduce the kinase-dead mutation of lysine33 to methionine33 as they contain the codon ATG instead of the endogenous codon AAG at this position. Both oligonucleotides

also introduce a restriction site for *Pme*I and destroy the *Afe*I restriction site 3' of the K33M mutation. The oligonucleotides ScaI.for and ScaI.rev anneal overlapping at the ampicillin resistance marker gene of pBluescript SKII(+). The two PCRs with the oligonucleotide pairs MPK6KM.rev/ScaI.rev and MPK6KM.for/ScaI.for led to the amplification of two fragments, which together constitute the entire template plasmid plus the newly introduced mutations. The amplified PCR products were purified and cleaved with *Sca*I and *Pme*I. The two blunt-ended fragments were joined together as the completed plasmid by ligation over night at 16°C and transformed into *E. coli* XL1-Blue cells. As the *Sca*I restriction site was located within the gene bestowing ampicillin resistance only cells which contained the correctly ligated plasmid could survive under the selection pressure of ampicillin. The identity and correct sequence of the newly generated *LmxMPK6K33M* 3'-fragment was confirmed by the absence of the *Afe*I restriction site and by sequencing. The fragment was liberated by cleavage with *Sph*I and *Xba*I and ligated into the equally treated pGEX-KG3-mapkin24-0505, generating pGEX-KG-MPK6KM. The *LmxMPK6K33M* gene was removed from pGEX-KG-MPK6KM by cleavage with *Xba*I/*Eco*RV and ligated into pGEX-KGS, which had been linearised using the same enzymes, creating pGEX-KGS-MPK6KM (see 8.1 for plasmid maps).

4.2.1.2 Recombinant expression and affinity purification of GST-LmxMPK6 and GST-LmxMPK6K33M

The plasmids pGEX-KGS-MPK6 and pGEX-KGS-MPK6KM were transformed into *E. coli* BL21 (DE3) cells and expressed over night at 18°C as GST-fusion proteins. Cells were lysed by sonification and recombinant proteins were subjected to affinity purification on glutathione sepharose. Recombinant proteins were eluted from the sepharose, quantified by Bradford analysis and separated on SDS-PAGE. The maximum volume of 20 µl was loaded on the SDS-PA gel as Bradford analysis indicated very low protein levels. The Coomassie-stained gel in Fig. 45 demonstrates the low expression rate and poor purity of recombinant GST-LmxMPK6 and GST-LmxMPK6K33M. The expression of GST-LmxMPK6K33M repeatedly led to more protein, but purification was still only moderately successful. Both proteins had the molecular mass of 144 kDa and were therefore expected to run slightly below the 175 kDa marker band. Although a band running directly below the 175 kDa marker appears in both samples, it is by no means the most abundant protein in the mixture.

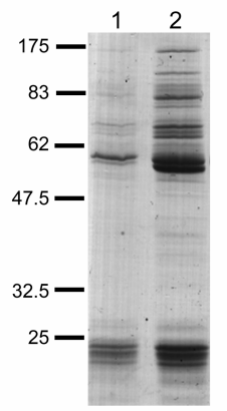

Figure 45. Coomassie-stained gel of purified, recombinant GST-LmxMPK6 and GST-LmxMPK6K33M
lane 1, GST-LmxMPK6; lane 2, GST-LmxMPK6K33M; molecular masses of standard proteins are indicated in kDa.

To determine which, if any, of the visible protein bands corresponded to LmxMPK6, *E. coli* cell extracts before and after induction of the expression of GST-LmxMPK6 and GST-LmxMPK6K33M were compared. The plasmids pGEX-KGS-MPK6 and pGEX-KGS-MPK6KM were transformed into *E. coli* afresh. When cultures reached an OD_{600} = 0.8 – 0.9 a sample was taken from each culture before recombinant expression was induced by the addition of 100 µM IPTG. After incubation of the cultures over night at 18°C another sample was taken from the cell suspensions. Ten µl from all samples were separated on SDS-PAGE.

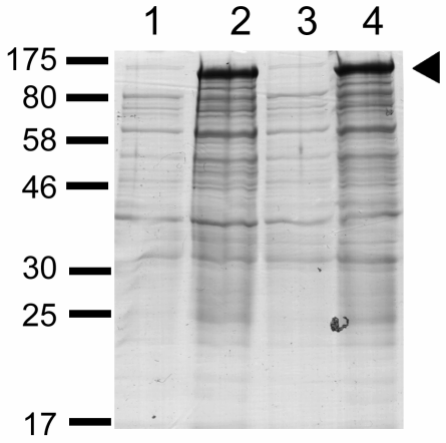

Figure 46. Comparison of *E. coli* lysates before and after induction of recombinant expression of GST-LmxMPK6 and GST-LmxMPK6K33M
lane 1, *E. coli* lysate before induction of GST-LmxMPK6 expression; lane 2, *E. coli* lysate after expression of GST-LmxMPK6 over night; lane 3, *E. coli* lysate before induction of GST-LmxMPK6K33M expression; lane 2, *E. coli* lysate after expression of GST-LmxMPK6K33M over night; black arrowhead indicates GST-LmxMPK6; molecular masses of standard proteins are indicated in kDa.

The comparison of *E. coli* lysates pre- and post-induction of the expression of GST-LmxMPK6 and GST-LmxMPK6K33M demonstrated the appearance of a strong protein

band just below the 175 kDa marker band after recombinant expression was induced (Fig. 46, lane 2 and 4). This band was considerably stronger than the other proteins and assumed to be GST-LmxMPK6 and GST-LmxMPK6K33M, respectively. Immunoblot analysis was used to further confirm this finding. For this, 20 µl of purified and eluted recombinant GST-LmxMPK6 and GST-LmxMPK6K33M were separated by SDS-PAGE and blotted on an Immobilon PVDF membrane. Blots were incubated over night at 4°C with antiserum against the carboxy-terminal peptide of LmxMPK6 and subsequently with a horseradish-peroxidase conjugated secondary antibody.

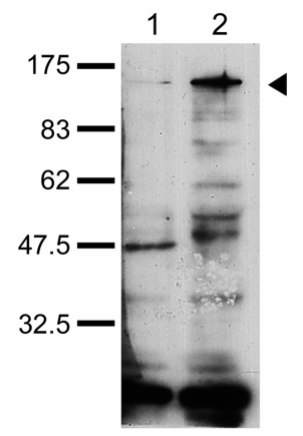

Figure 47. Immunoblot of purified recombinant GST-LmxMPK6 and GST-LmxMPK6K33M
lane 1, GST-LmxMPK6; lane 2, GST-LmxMPK6K33M; black arrowhead indicates GST-LmxMPK6; blot probed with antiserum against the carboxy-terminal peptide of LmxMPK6; exposure time 1 min; molecular masses of standard proteins are indicated in kDa.

Detection by chemiluminescence revealed several bands in both samples, the strongest appearing at just under 175 kDa in the GST-LmxMPK6K33M sample (Fig. 47, lane 2) and a lot weaker also in the sample containing GST-LmxMPK6 (Fig. 47, lane 1). In accordance with the results shown in Fig. 46 this protein band at just below 175 kDa was identified as LmxMPK6 (indicated by black arrowhead in Fig. 47).

4.2.1.3 Kinase assay with GST-LmxMPK6 and GST-LmxMPK6K33M

The purified recombinant GST-fusion proteins LmxMPK6 and LmxMPK6K33M were subjected to a radioactive kinase assay to investigate the *in vitro* activity of LmxMPK6. It was not possible to accurately ascertain the amount of LmxMPK6 contained in the purified samples due to the high number of contaminations. Instead of performing a Bradford assay the kinase assays were therefore conducted using the highest possible volume of eluted GST-LmxMPK6 and GST-LmxMPK6K33M. Proteins were incubated for 1 hour at 34°C with 1 mM ATP, containing 5 µCi [γ^{32}]ATP (6000 Ci/mmol) and 5 µg MBP in 50 µl of a standard kinase buffer, containing 50 mM 3(N-morpholino)propanesulfonic acid (MOPS), pH 7.2, 10 mM $MgCl_2$, 2 mM $MnCl_2$ and 0.1 M NaCl. The samples were

separated by SDS-PAGE and the SDS-PA gels were silver-stained, dried and exposed to autoradiography. The choice of silver-staining over the standard procedure Coomassie-staining was made to visualise the prospective low levels of recombinant GST-LmxMPK6 and GST-LmxMPK6K33M.

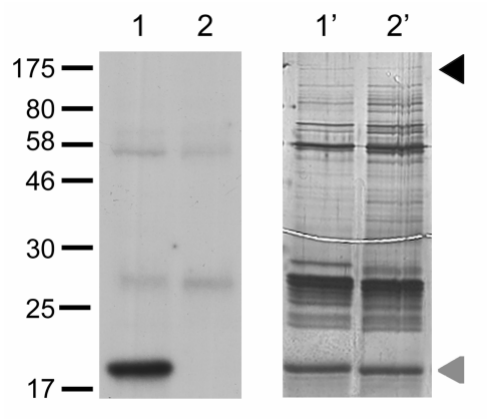

Figure 48. Kinase assay of recombinant GST-LmxMPK6 and GST-LmxMPK6K33M
left panel, autoradiograph, exposure time 26 h; right panel, silver-stained gel; 1,1', GST-LmxMPK6; 2, 2', GST-LmxMPK6K33M; black arrowhead indicates GST-LmxMPK6, grey arrowhead indicates MBP; molecular masses of standard proteins are indicated in kDa.

Regardless of its extremely low abundance in the sample (Fig. 48, lane 1'), GST-LmxMPK6 showed a considerable phosphotransferase activity towards MBP (Fig. 48, lane 1). As expected, GST-LmxMPK6K33M did not phosphorylate MBP (Fig. 48, lane 2). Neither of the recombinant proteins showed any autophosphorylation.

No data was available regarding the expression and importance of LmxMPK6 in the different *L. mexicana* life stages. It was therefore investigated whether the *in vitro* activity of GST-LmxMPK6 depended on incubation temperature. Kinase assays for *L. mexicana* proteins associated with the promastigote life stage are conducted at 27°C, the temperature of the sand fly host, whereas assays for proteins important in amastigotes take place at 34°C, which corresponds to the temperature in human skin. Recombinant GST-LmxMPK6 was subjected to a kinase assay at both temperatures and the resulting phosphotransferase activity was compared on the autoradiograph. The plasmid pGEX-KG3-mapkin24-0505 was used to recombinantly express GST-LmxMPK6, as this experiment was conducted before the cloning of pGEX-KGS.

The phosphotransferase activity of GST-LmxMPK6 towards MBP does not significantly change depending on the incubation temperature (Fig. 49). Although the signal for phosphorylated MBP seems to be stronger at 27°C in the depicted autoradiograph (Fig. 49, lane 1) it has to be taken into consideration that this sample also contains a higher total amount of MBP, as can be seen in the Coomassie-stained gel (Fig. 49, lane

1'). It was therefore concluded that GST-LmxMPK6 displays equal activity at both tested incubation temperatures. No autophosphorylation of GST-LmxMPK6 was visible at either temperature.

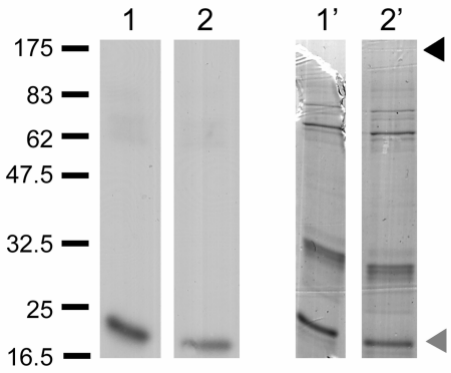

Figure 49. Kinase assay of GST-LmxMPK6 at different temperatures
left panel, autoradiograph, exposure 5 h; right panel, Coomassie-stained gel;
lanes 1, 1', GST-LmxMPK6 after a kinase assay at 27℃; lanes 2, 2', GST-LmxMPK6 after a kinase assay at 34℃; black arrowhead indicates GST-LmxMPK 6, grey arrowhead indicates MBP;
molecular masses of standard proteins are indicated in kDa; both depicted lanes result from the same gel.

GST-LmxMPK6 displayed a considerable phosphotransferase activity when incubated with the standard kinase assay buffer of 0.1 M NaCl, 10 mM $MgCl_2$, 2 mM $MnCl_2$ and 50 mM MOPS pH 7.2. To investigate whether the GST-LmxMPK6 activity could still be increased by a different pH in the sample, kinase assays were performed with a number of buffers differing in pH-value.

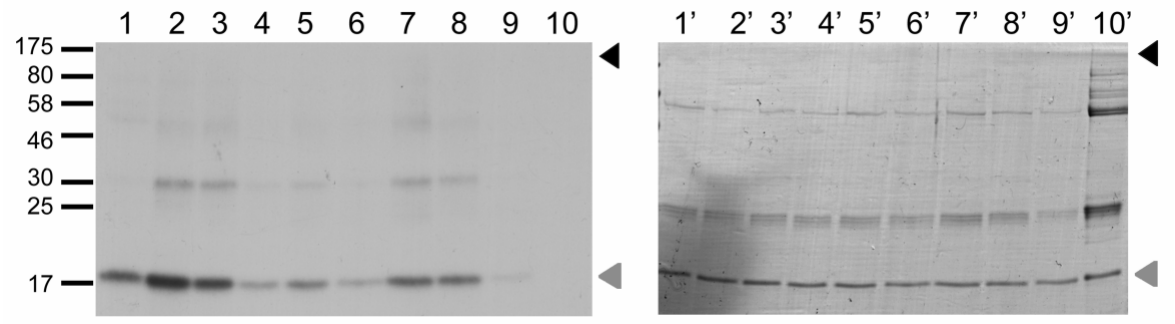

Figure 50. Kinase assay with LmxMPK6 at different pH-values
left panel, autoradiograph, 4h exposure; right panel, Coomassie-stained gel;
lanes 1,1', 50 mM MOPS, pH 7.0; lanes 2, 2', 50 mM MOPS, pH 7.2; lanes 3, 3', 50 mM MOPS, pH 7.5; lanes 4,4', 50 mM MOPS, pH 7.7; lanes 5, 5', 50 mM MOPS, pH 7.8; lanes 6, 6', 50 mM MOPS, pH 7.9; lanes 7, 7', 50 mM HEPES, pH 7.9; lanes 8, 8', 50 mM HEPES, pH 8.0;
lanes 9, 9', 50 mM HEPES, pH 8.2; lanes 1-9, 1'-9', GST-LmxMPK6; lanes 10, 10', GST-LmxMPK6K33M, 50 mM HEPES, pH 8.0; black arrowheads indicate GST-LmxMPK6, grey arrowheads indicate MBP; molecular masses of standard proteins are indicated in kDa.

GST-LmxMPK6 was recombinantly expressed from the plasmid pGEX-KGS-MPK6 in *E. coli* BL21 (DE3) cells, purified on glutathione sepharose, eluted and incubated for 1 h at

34°C with 1 mM ATP, containing 5 µCi [γ^{32}]ATP (6000 Ci/mmol) and 5 µg MBP in 50 µl of a kinase buffer, containing 10 mM $MgCl_2$, 2 mM $MnCl_2$ and 0.1 M NaCl and 50 mM MOPS with varying pH-values. MOPS is an excellent buffer at pH-values in the range of 6.5 – 7.9. pH-values above 7.9 were obtained by the addition of HEPES buffer. The kinase activity of GST-LmxMPK6 was slightly higher in the presence of HEPES than when using MOPS, as can be seen in lanes 6 and 7 of Fig. 50, which show assays conducted at the same pH of 7.9, but differing in the use of MOPS or HEPES. The activity of GST-LmxMPK6 at pH 7.2, however, was higher still. As a negative control, GST-LmxMPK6K33M was expressed using the plasmid pGEX-KGS-MPK6KM and subjected to a kinase assay at pH 8.0.

The autoradiograph in Fig. 50 shows clearly that the phosphotransferase activity of GST-LmxMPK6 is at its optimum at a pH-value of 7.2.

4.2.2 Analysis of the role of the C-terminus of LmxMPK6

LmxMPK6 contains an unusually long carboxy-terminus with unknown function. Different truncated mutants of LmxMPK6 were generated to shed light on the question if the carboxy-terminal peptide is required for activity of LmxMPK6. MAP kinases typically feature a stabilising α-helix after their kinase domain. No such helix was predicted for LmxMPK6, using the Advanced Protein Secondary Structure Prediction Server (APSSP) (http://imtech.res.in/raghava/apssp/). Despite that prediction two different truncated versions of LmxMPK6 were generated. One mutant, henceforth referred to as LmxMPK6short, was truncated directly after the kinase domain, whereas another mutant was called LmxMPK6short2 and additionally included a short sequence C-terminal of the kinase domain which generally contains the stabilising α-helix. The truncated mutant LmxMPK6short2 corresponded in length to the truncated version of TbECK1, which was used to investigate the function of the extended C-terminus of TbECK1, the *T. brucei* homologue of LmxMPK6 (Ellis, J. et al. 2004).

4.2.2.1 Generation of two truncated mutants of LmxMPK6

LmxMPK6short was cleaved from the plasmid pGEX-KG-MPK6 with *Msc*I and *Mlu*I. The plasmid was additionally digested with *Xho*I to prevent an inadvertent purification of another fragment of the same size as *LmxMPK6short*. The endonuclease *Msc*I produced blunt ends and the overhanging ends produced by the *Mlu*I digest were filled in with Klenow enzyme, generating a blunt fragment containing *LmxMPK6short* and a part of the GST-tag encoding sequence. The fragment was ligated with a pGEX-KG plasmid that had been cleaved with *Msc*I and *Xba*I and treated with Klenow enzyme. The resulting plasmid was termed pGEX-KG-MPK6short.

To generate LmxMPK6short2 a PCR was performed on the plasmid pB23mapkin24-0505 with the oligonucleotides MPK6short2.for and MPK6short2.rev. The oligonucleotide MPK6short2.for was designed to include a *Bam*HI and *Nco*I restriction site 5' of the start codon of LmxMPK6short2, whereas MPK6short2.rev included a *Pci*I and *Bgl*II restriction site before the stop codon of LmxMPK6short2 and a *Hind*III and *Eco*RV restriction site 3' of the stop codon. The PCR product was ligated into the plasmid pCR2.1 TOPO via TA-cloning and confirmed by sequencing. The gene for LmxMPK6short2 was subsequently liberated by cleavage with *Bam*HI and *Eco*RV and ligated into the *Bam*HI/*Sma*I treated plasmid pBluescript SKII(+), generating pBMPK6short2. It was intended to eventually express LmxMPK6short2 in *L. mexicana*, requiring the addition of a tag, in this case the TY epitope tag, to the truncated mutant protein. In this case the TY-epitope tag was added as a C-terminal tag to LmxMPK6short2 by excising LmxMPK6short2 with *Bam*HI/*Pci*I out of pBMPK6short2 and ligating it into the *Bam*HI/*Nco*I cleaved plasmid pGEX2TY-MPK7KM, which already contained the TY-tag. The fragment containing the *LmxMPK6short2* gene and at the 3'-end the sequence for the TY-tag was liberated by cleavage with *Sph*I and *Bgl*II. The restriction site for *Sph*I is contained in the wild type *LmxMPK6* gene. *Bgl*II is part of the pGEX-KG MCS and located directly after the sequence for the TY-tag in pGEX2TYMPK7KM. The *LmxMPK6short2-TY* fragment was ligated into pBMPK6short2 which had also been cleaved by *Sph*I and *Bgl*II, creating pBMPK6short2TY (see 8.1 for plasmid maps).

4.2.2.2 Recombinant expression and affinity purification of truncated LmxMPK6 mutants

To permit the recombinant expression of LmxMPK6short2TY the plasmid pGEX-KGS-MPK6short2TY was generated by *Hin*dIII cleavage of pBMPK6short2TY and pGEX-KGS-MPK6 and ligation. The *Hin*dIII restriction site was located within the 5'-end of *LmxMPK6* as well as in the MCS of pGEX-KGS, 3' of LmxMPK6, and directly after the stopcodon in pBMPK6short2TY. The plasmids pGEX-KG-MPK6short, pGEX-KGS-MPK6short2TY, pGEX-KGS-MPK6 and pGEX-KGS-MPK6KM were transformed into *E. coli* BL21(DE3) and expressed over night at 18℃. Cells were lysed by sonification and proteins were purified on glutathione sepharose and eluted with elution buffer. To compare expression levels 20 µl of each eluted protein sample was separated by SDS-PAGE. The Coomassie-stained gel is shown in Fig. 51.

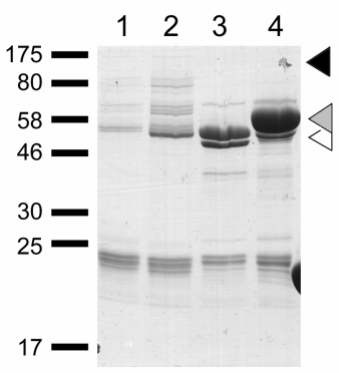

Figure 51. Recombinant expression of LmxMPK6 and its truncated mutants
Coomassie-stained gel; lane 1, GST-LmxMPK6; lane 2, GST-LmxMPK6K33M; lane 3, GST-LmxMPK6short; lane 4, GST-LmxMPK6short2TY; black arrowhead indicates GST-LmxMPK6, grey arrowhead indicates GST-LmxMPK6short2TY, white arrowhead indicates GST-LmxMPK6short; molecular masses of standard proteins are indicated in kDa.

The Coomassie-stained gel shows a strong double band just under 58 kDa in the sample containing LmxMPK6short and just above 58 kDa in the lane of LmxMPK6short2TY and only few other weak protein bands. The expected molecular masses were 59.5 kDa for recombinant GST-LmxMPK6short and 70 kDa for LmxMPK6short2TY and thus slightly larger than the observed strong protein bands. As these bands were the only strong protein bands observed in the samples it was nevertheless concluded that they presented the truncated versions LmxMPK6short and LmxMPK6short2TY, respectively. Thus GST-LmxMPK6short and GST-LmxMPK6short2TY were successfully expressed at much higher levels than GST-LmxMPK6 or GST-LmxMPK6K33M.

4.2.2.3 Kinase assay of truncated LmxMPK6 mutants

Kinase assays were conducted with the recombinant, eluted proteins GST-LmxMPK6, GST-LmxMPK6K33M, GST-LmxMPK6short and GST-LmxMPK6short2TY. The proteins were incubated at 34°C for 1 h with 1 mM ATP, containing 5 µCi [γ^{32}]ATP (6000 Ci/mmol) and 5 µg MBP in 50 µl of a standard kinase buffer, containing 50 mM 3(N-morpholino)propanesulfonic acid (MOPS), pH 7.2, 10 mM $MgCl_2$, 2 mM $MnCl_2$ and 0.1 M NaCl and subsequently separated by SDS-PAGE. The SDS-PA gels were stained with Coomassie, dried and subjected to autoradiography. Fig. 52 displays the autoradiographs and Coomassie-stained gels of two independently conducted assays, to demonstrate that phosphotransferase activity of MBP occurred in different quantities.

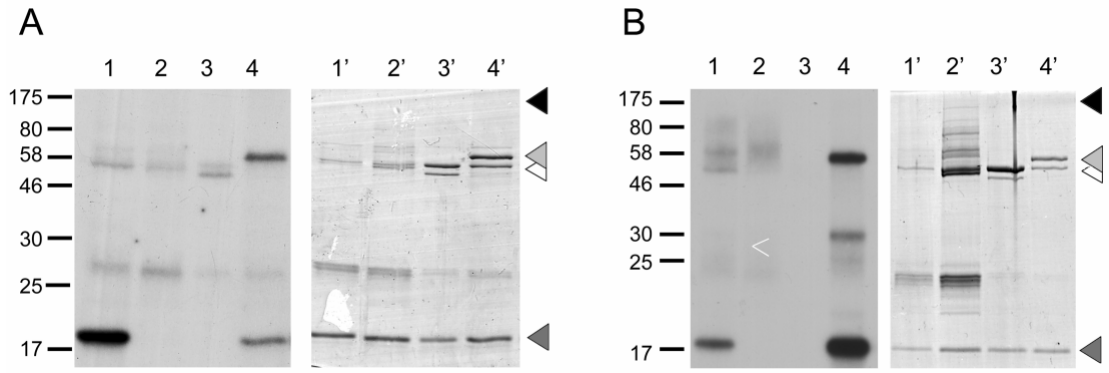

Figure 52. Kinase assay of LmxMPK6 truncated versions
A and B show the results of two independent experiments; left panel, autoradiograph, exposure times 26 h (A) and 14 h (B); right panel, Coomassie-stained gel; lanes 1,1', GST-LmxMPK6; lanes 2, 2', GST-LmxMPK6K33M; lanes 3, 3', GST-LmxMPK6short; lanes 4, 4', GST-LmxMPK6short2TY; black arrowheads indicate GST-LmxMPK6, light grey arrowheads indicate GST-LmxMPK6short2TY, white arrowheads indicate GST-LmxMPK6short, dark grey arrowheads indicate MBP; molecular masses of standard proteins are indicated in kDa.

In accordance with the previously shown results, GST-LmxMPK6 displayed no autophosphorylation, but a distinct kinase activity toward MBP despite its minimal abundance in the eluted protein mixture (Fig. 52, lanes 1 and 1'). GST-LmxMPK6short on the other hand did not phosphorylate MBP, but showed a very slight autophosphorylation, which was only visible after long exposure times as shown in Fig. 52, A. The autophosphorylation activity of GST-LmxMPK6short2TY (Fig. 52, lanes 4) was much stronger than for GST-LmxMPK6short (Fig. 52, lanes 3). GST-LmxMPK6short did not phosphorylate MBP, unlike GST-LmxMPK6short2TY which displayed a distinct kinase activity towards MBP (Fig. 52, lanes 4). Different assays, however, showed varying results concerning the intensity of kinase activity of GST-LmxMPK6short2TY in comparison to activity of the full-length GST-LmxMPK6. In experiment A GST-LmxMPK6 phosphorylated MBP to a higher extent, while GST-LmxMPK6short2TY was more active towards MBP in experiment B (compare lanes 1 and 4 of Fig. 52, A and B).

4.2.2.4 Extrachromosomal expression of the active truncated mutant of LmxMPK6 in *Leishmania*

To investigate whether the presence of LmxMPK6short2TY in *L. mexicana* would cause a visible phenotype, the plasmid pXpolPacMPK6short2TY was created and transformed into *L. mexicana* promastigotes. *LmxMPK6short2TY* was liberated from pBMPK6short2TY by *Bam*HI/*Eco*RV treatment and ligated into the equally cleaved plasmid pX63polPac (see 8.1 for plasmid maps). The plasmid pXpolPacMPK6short2TY was transformed into wild type *L. mexicana* promastigotes. Positive clones were selected based on puromycin resistance and confirmed by Southern blot analysis (Fig. 53).

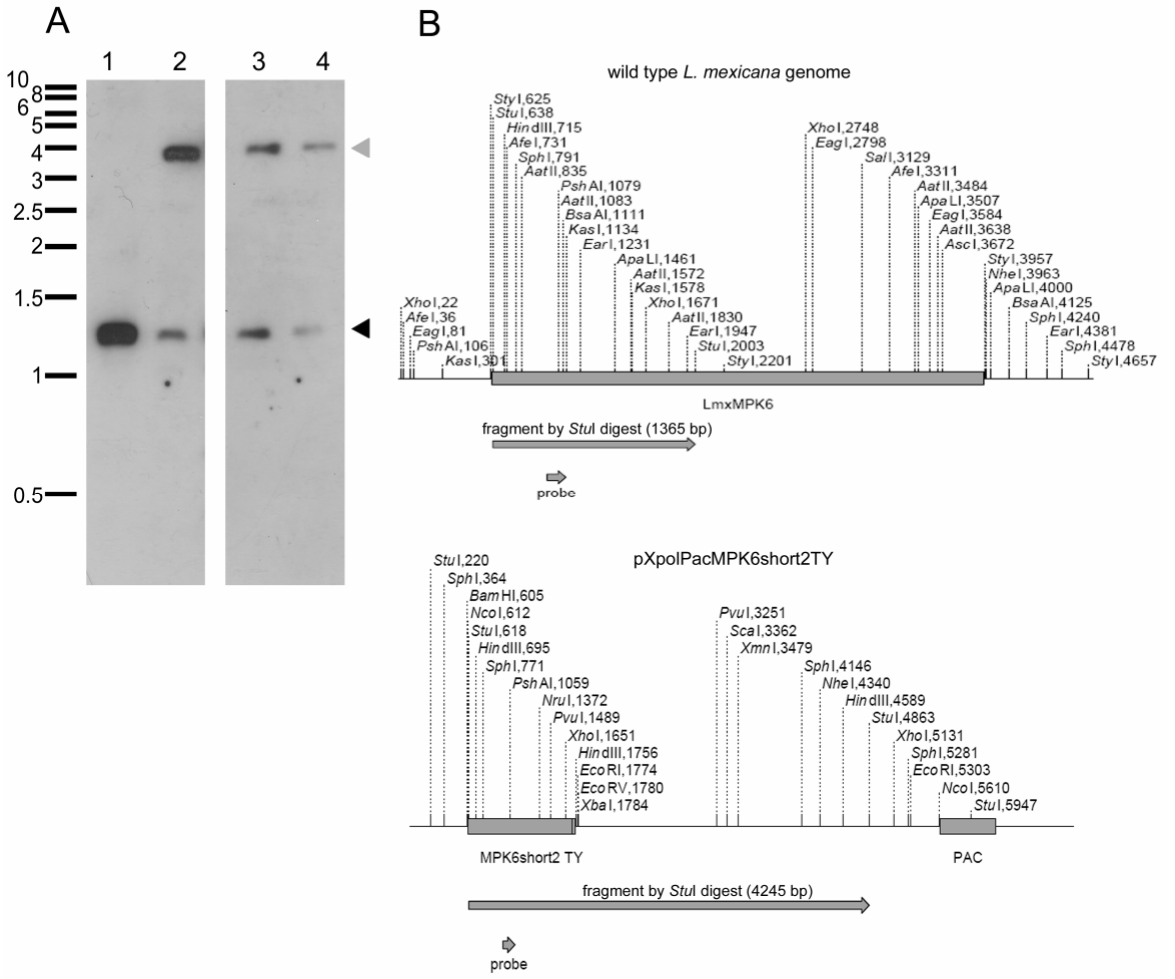

Figure 53, Southern blot analysis of *L. mexicana* mutants that carry the plasmid pXpolPacMPK6short2TY
A, Southern blot; lane 1, wild type; lane 2, Lmx + pXpolPacMPK6short2TY clone 1; lane 3, Lmx + pXpolPacMPK6short2TY clone 4; lane 4, Lmx + pXpolPacMPK6short2TY clone 5; all DNA was digested with *Stu*I; fragments were detected by a DIG-labelled DNA probe corresponding to a sequence in the ORF of *LmxMPK6* (for a detailed display where the probe binds, see the sequence of the *LmxMPK6* region in appendix 8.1); grey arrowhead indicates pXpolPacMPK6short2TY (4.2 kb); black arrowhead indicates genomic *LmxMPK6* (1.3 kb); sizes of standard DNA fragments are indicated in kb; all depicted lanes originate from one blot of the same experiment;
B, diagrammatic plan of the analysed DNA region, the utilised probe and the generated fragments

DAPI staining and fluorescence microscopy of one of the positive clones, in comparison with wild type *L. mexicana* showed no noticeable differences cell shape or in the number of kinetoplasts or nuclei (Fig. 54).

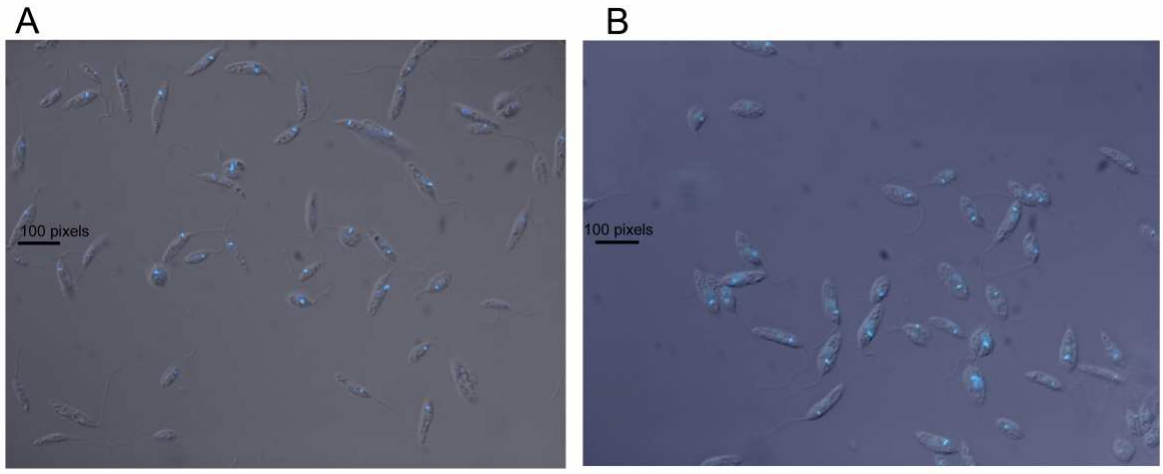

Figure 54. Fluorescence microscopy of DAPI-stained *L. mexicana* promastigotes
Overlay of DAPI and DIC2; A, wild type *L. mexicana* promastigotes; B, *L. mexicana* clone 3, containing pXpolPacMPK6short2TY

4.2.2.5 Generation of co-expression constructs for the expression of LmxMPK6 C-terminus and N-terminus

One of the theories to explain the role of the abnormally long C-terminus of LmxMPK6 assumes a regulatory function of the C-terminus towards the rest of the protein. Constructs were created to co-express the N-terminus and C-terminal end of LmxMPK6 in order to analyse if the C-terminus influences the activity of the N-terminus *in vitro*. The generated co-expression plasmid was based on the plasmid pJCLinker. The N-terminal peptide generated for co-expression corresponded in length to LmxMPK6short2. A PCR on the template pGEX-KGS-MPK6 with the oligonucleotides MPK6Nterm.for and MPK6Nterm.rev amplified the 1134 bp long N-terminal sequence of *LmxMPK6* with newly integrated restriction sites for *Bam*HI 5' of the gene and *Eco*RV 3' of the likewise inserted stop codon. The amplified fragment was sequenced, integrated into pCR2.1TOPO by TA-cloning, liberated from there by *Bam*HI/*Eco*RV digest and ligated into pJCLinker, which had been linearised using *Bam*HI and *Hpa*I. The resulting plasmid encoded for the N-terminal peptide of LmxMPK6 as a His-tag fusion protein and was named pJCLinkerMPK6Nterm. The C-terminal peptide that was generated for co-expression included a new start codon, which replaced the endogenous phenylalanine, located in the sequence directly after the end of LmxMPK6Nterm, with the equally hydrophobic methionine. A PCR on the template pGEX-KGS amplified the 2247 bp long C-terminal

fragment of *LmxMPK6*. The employed oligonucleotide MPK6Cterm.rev removed the endogenous stop codon and inserted the restriction sites for *Acc*65I at the 3' end of the sequence. The other oligonucleotide MPK6Cterm.for inserted the restriction site for *Nde*I 5' of the equally introduced start codon. TA-cloning created pCR2.1MPK6Cterm. The fragment in question was sequenced, liberated by *Nde*I/*Acc*65I cleavage and ligated into the equally treated pJCLinker, creating pJCLinkerMPK6Cterm. The co-expression plasmid pJCLinkerMPK6Cterm encoded the C-terminal peptide of LmxMPK6 as a fusion protein with a C-terminal S-tag. To co-express the two peptides, pJCLinkerMPK6Nterm-MPK6Cterm was created by cleaving *MPK6Nterm* from pCR2.1MPK6Nterm with *Bam*HI and *Eco*RV and ligating it into pJCLinkerMPK6Cterm, which had been linearised with *Bam*HI and *Hpa*I (see 8.1 for plasmid maps).

4.2.2.6 Recombinant co-expression and affinity purification of the LmxMPK6 C-terminus and N-terminus

The plasmids pJCLinker, pJCLinkerMPK6Nterm, pJCLinkerMPK6Cterm and pJCLinker-MPK6Nterm-MPK6Cterm were transformed into *E. coli* and proteins were expressed over night at 18°C. Cells were lysed by sonification and the lysates of cells which contained pJCLinker, pJCLinkerMPK6Nterm and pJCLinkerMPK6Nterm-MPK6Cterm were subjected to affinity purification on Co^{2+} sepharose. MPK6Cterm on the other hand was expressed as an S-tag fusion protein and therefore purified on agarose coupled with the ribonuclease S protein. As a control GST-LmxMPK6short2TY was expressed from pGEX-KGS-MPK6short2TY under the same conditions and purified on glutathione sepharose. Neither of the proteins, apart from GST-LmxMPK6short2TY, was eluted from its respective slurry, but used still coupled to it. To assess expression levels, 20 µl of each purified protein sample was separated by SDS-PAGE. The Coomassie-stained gel is depicted in Fig. 55.

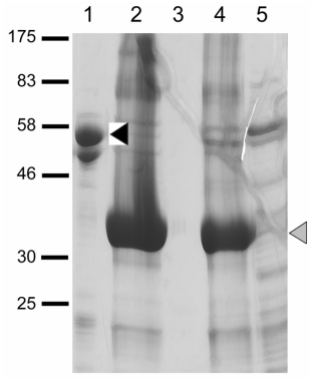

Figure 55. Coomassie-stained gel of purified, recombinant LmxMPK6 mutants
lane 1, GST-LmxMPK6short2TY; lane 2, His-LmxMPK6Nterm, expressed alone; lane 3, His-LmxMPK6Cterm, expressed alone; lane 4, His-LmxMPK6Nterm, co-expressed with LmxMPK6Cterm; lane 5, mock control, using the empty expression vector pJCLinker; black arrowhead indicates GST-LmxMPK6short2TY; grey arrowhead indicates His-LmxMPK6Nterm; molecular masses of standard proteins are indicated in kDa.

The expected sizes of the fusion proteins were 42.8 kDa for His-LmxMPK6Nterm and 79 kDa for S-LmxMPK6Cterm. The purification of S-LmxMPK6Cterm was not successful, as can be seen in Fig. 55, lane 3. For His-LmxMPK6Nterm on the other hand high amounts of recombinant proteins could be purified after expression alone and after co-expression with LmxMPK6Cterm (Fig. 55, lanes 2 and 4). The expression and purification of His-LmxMPK6Nterm yielded higher amounts of protein than that of GST-LmxMPK6short2TY (Fig. 55, compare lanes 1 and 2). The protein bands of highest abundance were assumed to be LmxMPK6Nterm, although they run in the Coomassie-stained gel slightly lower than would be expected from their size of 42.8 kDa. Their identity could additionally be confirmed by immunoblot analysis using the anti-serum against the N-terminal peptide of LmxMPK6. The immunoblot depicted in Fig. 56 shows the detection of a strong protein band equal to the protein bands seen with highest abundance in the Coomassie-stained gel of purified recombinant proteins (Fig. 55).

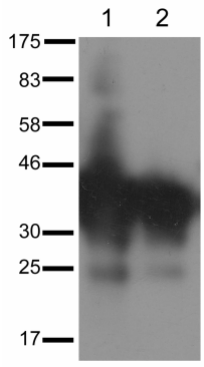

Figure 56. Immunoblot on recombinant His-LmxMPK6Nterm
lane 1, His-LmxMPK6Nterm, expressed alone; lane 2, His-LmxMPK6Nterm, co-expressed with LmxMPK6Cterm; detection with antiserum against the N-terminal peptide of LmxMPK6; molecular masses of standard proteins are indicated in kDa.

4.2.2.7 Kinase assays of LmxMPK6 C-terminus and N-terminus

The *in vitro* activity of His-LmxMPK6Nterm and His-LmxMPK6Nterm expressed alone and after co-expression with LmxMPK6Cterm was tested in a kinase assay and compared to the phosphotransferase activity of GST-LmxMPK6short2TY. Approximately 2 µg of eluted GST-LmxMPK6short2TY and 2 µl of slurry containing LmxMPK6Nterm singly expressed and co-expressed, respectively, as well as 15 µl of the empty expressed vector pJCLinker, functioning as the mock control, were used in a standard kinase assay at 34°C for 1 hour. The proteins were incubated rotating end-over-end with 1 mM ATP, containing 5 µCi [γ^{32}]ATP (6000 Ci/mmol) and 5 µg MBP in 50 µl of a standard kinase buffer, containing 50 mM 3(N-morpholino)propanesulfonic acid (MOPS), pH 7.2, 10 mM $MgCl_2$, 2 mM $MnCl_2$ and 0.1 M NaCl. The resulting samples were separated by SDS-PAGE and the SDS-PA gels were Coomassie-stained, dried and subjected to autoradiography.

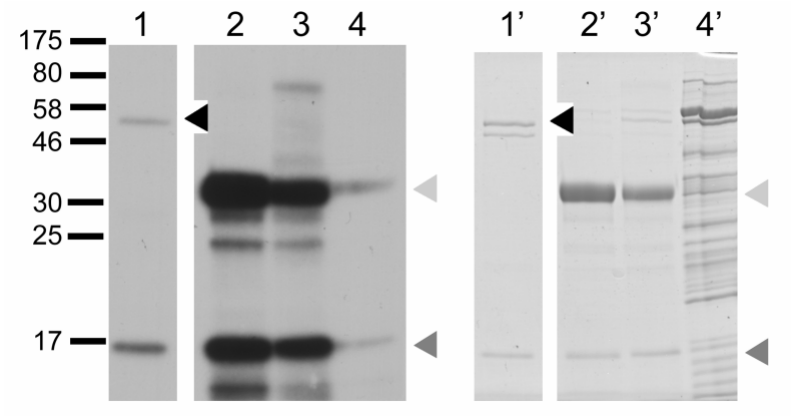

Figure 57. Kinase assay of co-expressed N-terminal peptide of LmxMPK6
left panel, autoradiograph, exposure time 3h; right panel, Coomassie-stained gel;
lanes 1, 1', GST-LmxMPK6short2TY; lanes 2, 2', His-LmxMPK6Nterm;
lanes 3, 3', His-LmxMPK6Nterm, co-expressed with LmxMPK6Cterm; lanes 4, 4', mock control using the empty expression vector pJCLinker; black arrowheads indicate GST-LmxMPK6short2TY, light grey arrowheads indicate His-LmxMPK6Nterm, dark grey arrowheads indicate MBP;
molecular masses of standard proteins are indicated in kDa; all depicted lanes result from one gel in the same experiment.

After the short exposure time of 3 hours co-expressed and singly expressed His-LmxMPK6Nterm showed strong phosphotransferase activity towards MBP and equally strong autophosphorylation (Fig. 57, lanes 2 and 3). There was a slight MBP phosphorylation and a phosphorylation at about 33 kDa visible in the mock control, containing the empty expressed vector pJCduet. The phosphotransferase activity of His-LmxMPK6Nterm was notably stronger than that of GST-LmxMPK6short2TY, which differs from singly expressed His-LmxMPK6Nterm only in respect of the GST- and TY-tag (Fig. 57, lane 1). His-LmxMPK6Nterm also appeared to have a slightly lower MBP and autophosphorylation activity after co-expression with S-LmxMPK6Cterm. However, it has to be taken into account that the amount of protein in the GST-LmxMPK6short2TY sample

was a lot lower than in the samples containing His-LmxMPK6Nterm (Fig. 57, lane 1', compare to lane 2' and 3') and that the sample of co-expressed His-LmxMPK6Nterm contained less protein than the singly expressed His-LmxMPK6Nterm (Fig. 57, compare lanes 2' and 3'). To evaluate if the perceived variations in phosphorylation activity were solely due to the dissimilar protein levels or indeed to differentially active proteins, the kinase assay was subjected to densitometric analysis using ImageJ. The density of the MBP autoradiograph bands was plotted and normalised against the plotted density of protein bands in the Coomassie-stained gel. The results were displayed in a bar chart (Fig. 58).

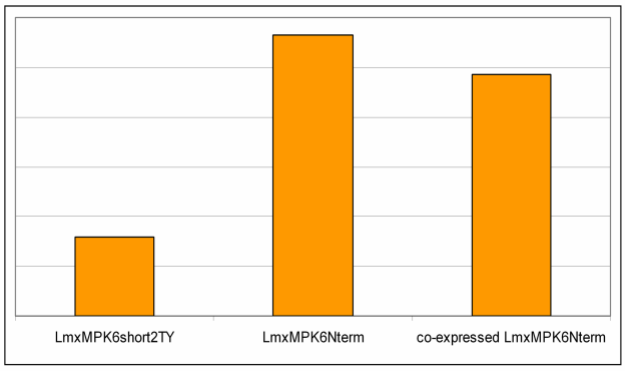

Figure 58. Densitometric plot comparing the normalised MBP phosphorylation by GST-LmxMPK6short2TY and His-LmxMPK6Nterm, expressed alone and after co-expression with S-LmxMPK6Cterm
ImageJ was used to plot the band densities of phosphorylated MBP in the autoradiograph normalised to the amount of protein in the Coomassie-stained gel; MBP phosphorylation was divided by protein amount and the result plotted as a bar chart

Densitometric analysis confirmed the observation that GST-LmxMPK6short2TY was considerably less active than His-LmxMPK6Nterm, expressed singly or after co-expression with LmxMPK6Cterm (Fig. 58). The difference in activity between singly expressed and co-expressed His-LmxMPK6Nterm was less pronounced.

4.2.3 Deletion of LmxMPK6 in *Leishmania*

It was attempted to delete the *LmxMPK6* gene in *L. mexicana* to ascertain whether LmxMPK6 is an essential protein for the parasite. Constructs for genomic integration of deletion cassettes by homologous recombination were created. The deletion cassettes consisted of resistance marker genes flanked by the upstream and downstream region of *LmxMPK6*. The upstream and downstream regions were amplified by PCR on the template pBE23mapkin24-0505P14 with the oligonucleotides LmxMPK6delup.for and MPK6NheAvrII.rev for the upstream flanking region and LmxMPK6delds.rev and MPK6NcoIAvrII.for for the downstream flanking region. A1 inserted a restriction site for *Eco*RV at the 5' and of the upstream region and restriction sites for *Nco*I and *Avr*II at the

3’ end. The amplified downstream region of *LmxMPK6* contained the newly inserted restriction sites for *Nhe*I at the 5’ end and *Eco*RV at the 3’ end. Both amplified fragments were ligated into pCR2.1TOPO via TA cloning, creating pCR2.1usMPK6 and pCR2.1dsMPK6, respectively. The fragment containing the downstream region of *LmxMPK6* was liberated from pCR2.1dsMPK6 by digest with *Avr*II and *Xho*I, which was located in the MCS of pCR2.1, and ligated into the equally cleaved pCR2.1usMPK6. The plasmid pCR2.1 contained a *Nco*I restriction site which made it impossible to integrate the restriction marker genes by *Nco*I/*Nhe*I cleavage and necessitated the generation of pBusLmxMPK6ds by ligating the *Eco*RV cleaved *usLMPK6ds* fragment from pCR2.1usMPK6ds into pBluescript SKII(+), linearised with *Eco*RV. The plasmid pBusMPK6ds was linearised by cleavage with *Nhe*I/*Nco*I and ligated with *Bsp*HI/*Nhe*I fragments containing the genes for hygromycin B phosphotransferase (*HYG*) and neomycin phosphotransferase (*NEO*) or the *Avr*II/*Nco*I fragment coding for the phleomycin binding protein (*PHLEO*), respectively (see 8.1 for plasmid maps). The deletion constructs were liberated from the resulting plasmids pBusMPK6dsHyg, pBusMPK6dsNeo and pBusMPK6dsPhleo by *Eco*RV, gel-purified and used for electroporation of *L. mexicana* promastigotes. Five separate rounds of electroporation yielded no single allele deletion mutants containing the restriction markers *PHLEO* or *NEO*, but several clones in which one *LmxMPK6* allele was substituted by the gene for hygromycin B phosphotransferase. In cultures which had been electroporated with the fragments usMPK6dsNeo or usMPK6dsPhleo either no cells grew under selective pressure or cells were revealed to be false positives by Southern blot analysis showing they did not contain the respective restriction marker gene (Fig. 59, D). Southern blot analysis was conducted on isolated genomic DNA which had been treated with *Xho*I and *Nco*I over night at 37°C. DNA samples were separated by agarose gel electrophoresis. The gels were plotted on a Biodyne A nylon membrane and samples were detected with the help of a probe hybridising to the 5’-UTR of *LmxMPK6*. The hybridisation probe was generated by PCR on the aforementioned PCR product usLmxMPK6 with the oligonucleotides mapkin_12.for and MPK6NcoIAvrII.for and DIG-labelled by using the DIG-labelling kit. Fig. 59, A, shows the Southern blot analysis of the three isolated potential ΔLmxMPK6 (+/-) Hyg clones AA12, AC5 and AE1.

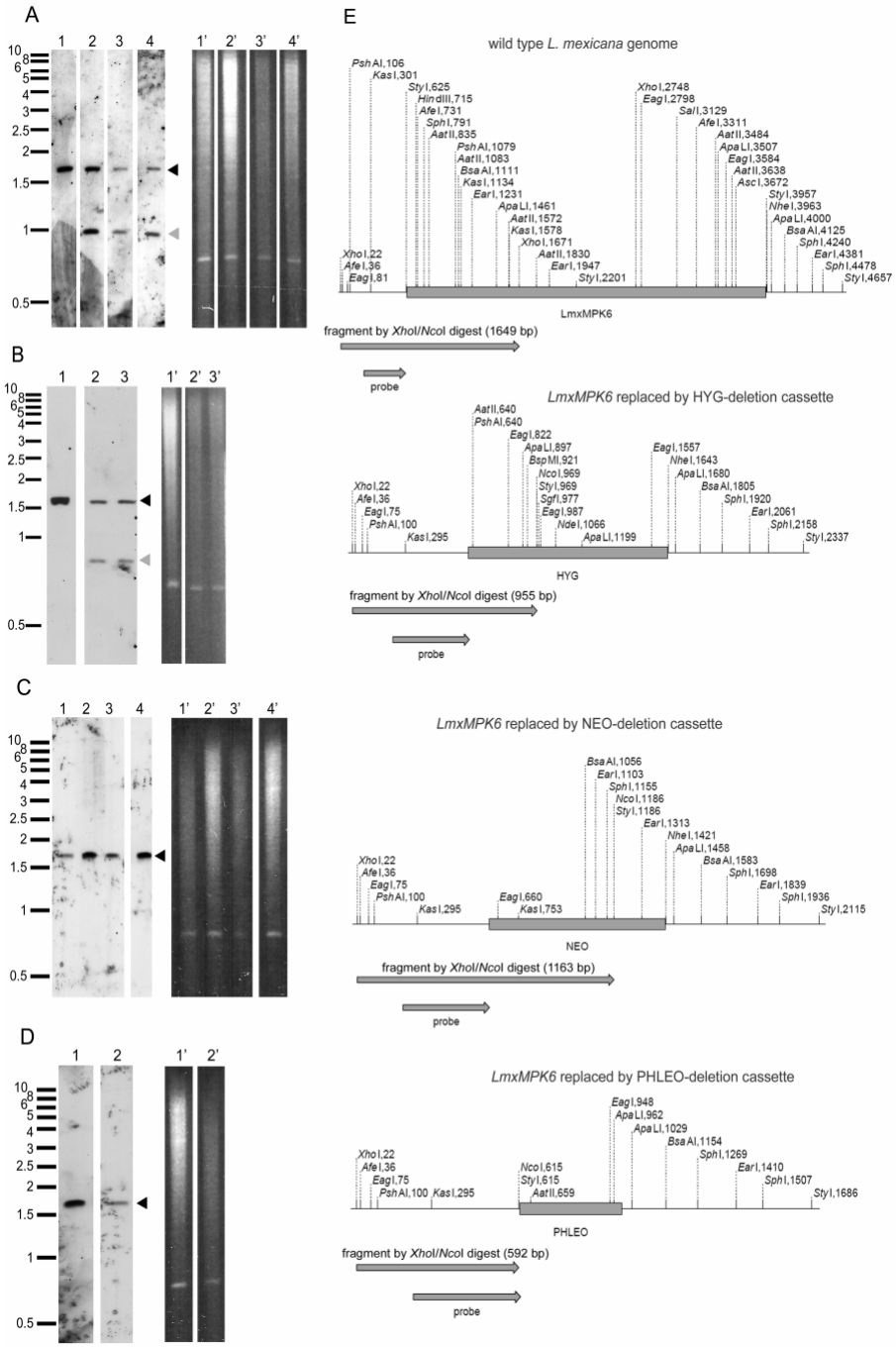

Figure 59. Southern blot analysis of several LmxMPK6 deletion clones
left panels Southern blots; right panels, corresponding 0.7% agarose gels;
A: lane 1, wild type; lane 2, potential ΔLmxMPK6 (+/-) Hyg clone AA12; lane 3, potential ΔLmxMPK6 (+/-) Hyg clone AC5; lane 4, potential ΔLmxMPK6 (+/-) Hyg clone AE1;
B: lane 1, wild type; lane 2 and 3, potential ΔLmxMPK6 (-/-) Hyg Neo clones;
C: lane 1, wild type; lane 2-4, potential ΔLmxMPK6 (-/-) Hyg Phleo clones;
D: lane 1, wild type; lane 2, potential ΔLmxMPK6 (+/-) Neo clone;
black arrowheads indicate *LmxMPK6* at 1.6 kb; grey arrowheads indicate *HYG* at 955 bp; expected size for *NEO* detection: 1.2 kb; expected size for *PHLEO* detection: 592 bp; fragments were generated by *Xho*I/*Nco*I digest and detected by a DIG-labelled DNA probe corresponding to the 5'-UTR of *LmxMPK6*, which was generated with the oligonucleotides mapkin24_12.for and MPK6NcoIAvrII.for (for a detailed display where the probe binds, see the sequence of the *LmxMPK6* region in appendix 8.1); sizes of standard DNA fragments are indicated in kb;
B, diagrammatic plan of the analysed DNA region, the utilised probe and the generated fragments

All three clones retain the *LmxMPK6* gene (band at 1.6 kb), but show an additional band just below 1 kb, corresponding to the *HYG* restriction marker gene digested with *Xho*I/*Nco*I (955 bp) (Fig. 59, A, lanes 2-4). In each sample both bands detected by the hybridisation probe are of equal density, indicating that the *LmxMPK6* and *HYG* gene exist with the same copy number. The positive Δ*LmxMPK6* (+/-) Hyg clones were used for electroporation with the fragments usMPK6dsNeo and usMPK6dsPhleo in four independent rounds. The few cells which grew under selective pressure after these electroporations were identified by Southern blot analysis as false positives, as can be seen in Fig. 59, B and C. Fig. 59, B, depicts the Southern blot analysis of the two potential ΔLmxMPK6 (-/-) Hyg Neo double deletion clones AV5 and D5. Although these clones were grown and selected in the presence of hygromycin and neomycin neither of them contained the *NEO* marker gene, which was expected to show at 1.2 kb in the Southern blot. The cells must have therefore acquired neomycin resistance by other means. Both clones still contained the wild type gene, which appears as a notably stronger band than the *HYG* marker in the Southern blot analysis, pointing to a possible multiplication of the *LmxMPK6* gene. Fig. 59, C, depicts the Southern blot analysis of the potential ΔLmxMPK6 (-/-) Hyg Phleo clones A6, A8 and D2 (lanes 2-4), which revealed that all clones had not only retained the wild type *LmxMPK6* gene but had also newly lost the *HYG* marker gene which had been present in the single allele knock-out mutant used to generate these clones. Fig. 59, D, shows an example of a potential ΔLmxMPK6 (+/-) Neo single allele deletion clone, which does not contain the *NEO* resistance marker gene (expected at 1.2 kb), despite displaying resistance against neomycin in the cell culture. Additionally to repeated rounds of electroporation it was also attempted to create double deletion mutants by the process known as loss of heterozygosity (LOH) (Gueiros-Filho, F. J. et al. 1996; Nascimento, M. et al. 2006). Two of the confirmed ΔLmxMPK6 (+/-) Hyg clones were cultivated in the presence of 200 µg/ml hygromycin (as opposed to the previously used 50 µg/ml). It was possible to isolate cells which survived the high amount of hygromycin but all still retained the wild type *LmxMPK6* gene as was shown by Southern blot analysis (Fig. 60).

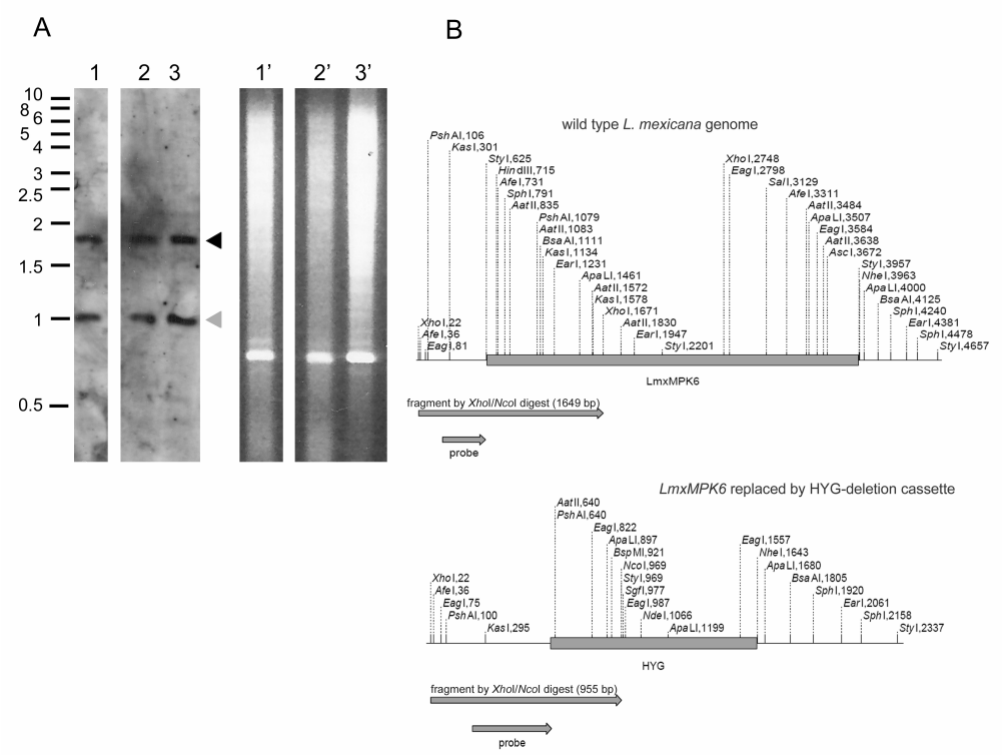

Figure 60, Southern blot analysis of potential LmxMPK6 double allele deletion mutants, generated by loss of heterozygosity
A, left panel, Southern blot; right panel, corresponding agarose gel; genomic DNA was cleaved with *Xho*I/*Nco*I; lanes 1-3, 1'-3', show ΔLmxMPK6 (+/-) Hyg mutants that retained the wild type *LmxMPK6* gene under high levels of hygromycin; black arrowhead indicates wild type *LmxMPK6* (1.6 kb); grey arrowhead indicates hygromycin deletion cassette (1kb); fragments were detected by a DIG-labelled DNA probe corresponding to the 5'-UTR of *LmxMPK6*, which was generated with the oligonucleotides mapkin24_12.for and MPK6NcoIAvrII.for (for a detailed display where the probe binds, see the sequence of the *LmxMPK6* region in appendix 8.1); sizes of standard DNA fragments are indicated in kb; all depicted lanes originate from one blot of the same experiment; B, diagrammatic plan of the analysed DNA region, the utilised probe and the generated fragments.

The routine approach if it is not possible to generate double allele deletion mutants of a gene is to introduce an extrachromosomal copy of the respective gene into the cells and then proceed to delete the genomic copies. To achieve this in the case of *LmxMPK6* the plasmid pXpolPacMPK6TY was generated. The TY-tag at the C-terminal end of the protein was included to allow for the immunodetection and purification of LmxMPK6. A PCR was performed on the template pGEX-KGS-MPK6 with the oligonucleotide primers abMPK6TY.for, which amplified 470 bp upstream of the stop codon of *LmxMPK6* and inserted the restriction sites for *Bam*HI and *Asi*SI into the 5'-UTR of the *LmxMPK6* gene, and abMPK6TY.rev. The primer abMPK6TY.rev included restriction sites for *Pci*I and *Bgl*II at the 3'-end of the gene directly before a newly introduced stop codon, followed by a *Hin*dIII and *Eco*RV restriction site. The amplified PCR product was ligated into pCR2.1TOPO by TA cloning and cloned into pBluescript SKII(+), using *Bam*HI and *Eco*RV, generating pBMPK6Cterm. To append the TY-tag to the gene the fragment was liberated from pBMPK6Cterm with *Bam*HI/*Pci*I and ligated into the *Bam*HI/*Nco*I digested plasmid pGEXTYMPK7KM. The fragment *LmxMPK6TY* was once again removed by

*Asi*SI/*Bgl*II cleavage and ligated into pBMPK6TYCterm, which had been digested accordingly. The central part of the *LmxMPK6* gene was isolated from the plasmid pGEX-KGS-MPK6 with *Asi*SI and *Asc*I and integrated into pBMPK6TYCterm, which had been linearised using the same enzymes. The complete C-terminal part of *LmxMPK6*, together with the TY-tag, was subsequently liberated by *Asi*SI and *Eco*RV and used to replace the truncated C-terminus of *LmxMPK6short2*TY in the plasmid pXpolPacMPK6short2TY, generating pXpolPacMPK6TY. The plasmid pXpolPacMPK6TY was transformed into wild type *L. mexicana* promastigotes and its presence confirmed by Southern blot analysis (Fig. 61).

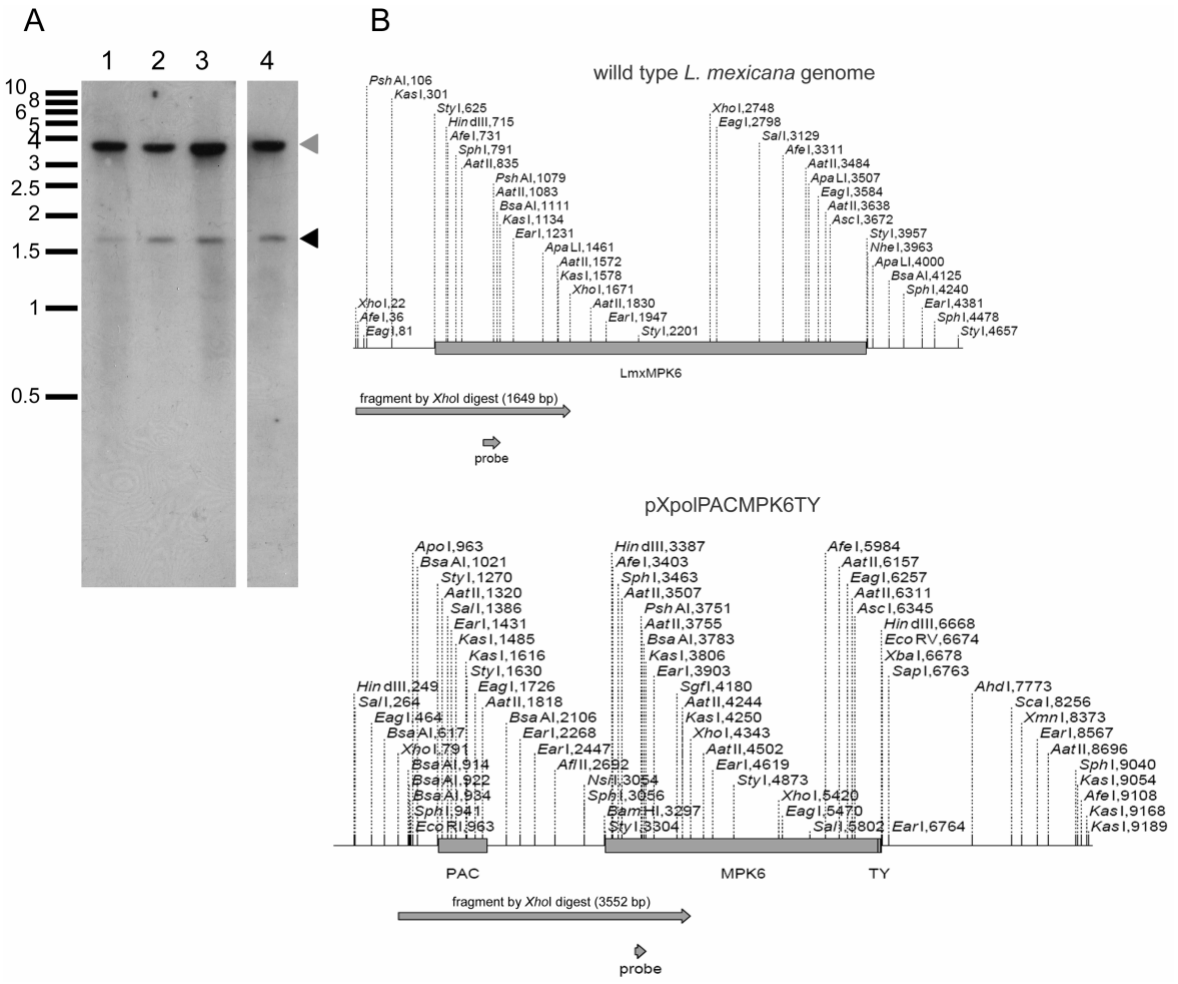

Figure 61. Southern blot analysis of wild type *L. mexicana*, containing the plasmid pXpolPacMPK6TY

A, Southern blot; genomic DNA was digested with *Xho*I, separated by agarose gelelectrophoresis, blotted on a Biodyne A nylon membrane and probed with DIG-labelled DNA corresponding to a sequence in the ORF of *LmxMPK6* (for a detailed display where the probe binds, see the sequence of the *LmxMPK6* region in appendix 8.1); lanes 1-4, clones A, B, C, H; black arrowhead indicates genomic copy of *LmxMPK6* (1.6 kb), grey arrowhead indicates extrachromosomal copy of *LmxMPK6* (3.5 kb); sizes of standard DNA fragments are indicated in kb; all depicted lanes originate from one blot of the same experiment.

B, diagrammatic plan of the analysed DNA region, the utilised probe and the generated fragments.

The total DNA of isolated clones was treated with *Xho*I at 37°C over night, separated by agarose gelelectrophoresis and blotted on a Biodyne A nylon membrane. The detection of genomic and extrachromosomal copies of *LmxMPK6* was accomplished with a DIG-labelled DNA probe which hybridises within the *LmxMPK6* gene (see appendix 8.1).

All clones depicted in Fig. 61 contain the plasmid pXpolPacMPK6TY in addition to the genomic copies of *LmxMPK6*. The high intensities of the bands detecting the extrachromosomal copy of *LmxMPK6* in comparison with the detection of genomic *LmxMPK6* indicate a high copy number of the plasmid pXpolPacMPK6TY within the cells. Based on these clones the deletion of the genomic alleles of LmxMPK6 will be realisable in the future.

5. Discussion

5.1 LmxMPK4

LmxMPK4 was found to be essential for amastigotes and for proliferation in promastigotes and consequently constitutes a possible drug target in the search of anti-leishmanial drugs. A prerequisite for the conduction of enzyme assay drug screenings is the availability of large amounts of pure and active protein. Previous analyses of the phosphotransferase activity of recombinant LmxMPK4 have used a GST-fusion protein, which was expressed and purified to reasonable amounts, but displayed only a marginal autophosphorylation, visible after an exposure time of several days, and no MBP phosphorylation (Wang, Q. et al. 2005). Another approach adopted by Morales et al. over-expressed GFP-LmaMPK4 in *L. major*, purified the protein via the GFP-tag and demonstrated MBP phosphotransferase activity of GFP-LmaMPK4 (Morales, M. A. et al. 2007). Yet this approach is laborious and leads only to small amounts of active protein, which is why the main objective of this thesis was to find a way of activating recombinant LmxMPK4.

5.1.1 Activation of LmxMPK4 by LmxMKK5

It was attempted to identify the *Leishmania* activator of LmxMPK4. Of all 7 *L. mexicana* MAP2K homologues LmxMKK5 appeared to be the most suitable and experimentally approachable candidate for activator of LmxMPK4 (see 4.1.2). On these grounds co-expression constructs of LmxMPK4 and LmxMPK4K59M with LmxMKK5 were generated. The use of pJCduet led to co-expression of LmxMKK5 with LmxMPK4 as a fusion protein with an N-terminal hexahistidine tag. Although the purification via His-tag was shown to result in lower amounts of recombinant protein than the purification via GST-tag, it was nevertheless used to initially evaluate the co-expression of LmxMPK4 with LmxMKK5. In the conducted kinase assays co-expressed LmxMPK4 clearly showed a very high phosphotransferase activity towards MBP (Fig. 13). Autophosphorylation of LmxMPK4, regardless if expressed alone or in co-expression with LmxMKK5, was weak and only discernible after high exposure times of the autoradiograph, like the 40 h depicted in Fig. 13. The kinase-dead mutant LmxMPK4K59M cannot correctly bind and orientate ATP, due to the mutation of lysine 59 to methionine, regardless of its phosphorylation state. MBP was not phosphorylated in kinase assays conducted with co-expressed LmxMPK4K59M or LmxMPK4 expressed alone, demonstrating that the responsible activity required the presence of functional LmxMPK4 and co-expression with LmxMKK5. The MBP phosphorylation was consequently due to the activation of LmxMPK4 by LmxMKK5 and not to the activity of co-purified LmxMKK5 or a bacterial kinase. LmxMKK5 has discernible autophosphorylation activity (Melzer, I. M., PhD thesis, 2007), which is

visible in the autoradiograph of co-expressed LmxMPK4K59M at 56 kDa after the long exposure time of 40 hours (Fig. 13). This indicates that a low amount of LmxMKK5 was co-purified with LmxMPK4 and explains the slight MBP phosphorylation which is visible in the sample of the co-expressed kinase-dead LmxMPK4K59M mutant (Fig. 13, lane 3''). LmxMPK4, activated by co-expression with LmxMKK5, however, displayed a phosphotransferase activity and affinity to ATP that was so much stronger than that of LmxMKK5 that no phosphorylated band at 56 kDa was visible in the sample containing co-expressed wild type LmxMPK4 after 40 hours exposure time (Fig. 13, lane 2'').

MAP2Ks activate MAP kinases *in vivo* by phosphorylating the threonine and tyrosine residues of the TXY-motif in the activation loop. Immunoblot and MS/MS analyses were used to investigate whether *in vitro* activation of LmxMPK4 by LmxMKK5 follows this pattern. Immunoblot analysis revealed a slight tyrosine autophosphorylation activity of singly expressed LmxMPK4, visible after a non-radioactive kinase assay, but not directly after purification from *E. coli* (Fig. 15). MS/MS analysis, however, detected LmxMPK4 phosphorylated on tyrosine 192 in the TXY-motif directly after purification from *E. coli* (Table 1), demonstrating the higher sensitivity of this technique. No phosphorylation of the kinase-dead mutant LmxMPK4K59M expressed alone could be detected by immunoblot or MS/MS analysis, which proves that the phosphorylation of singly expressed LmxMPK4 is due to its own activity and not to that of any other kinases. The findings are in accordance with the low innate autophosphorylation activity, which was reported for LmxMPK4 in previous experiments (Wang, Q. et al. 2005) and also appears in longer exposed autoradiographs of the conducted experiments (Fig. 13). Single threonine phosphorylation detected in co-expressed LmxMPK4 and LmxMPK4K59M by MS/MS analysis was not due to autophosphorylation but to the activity of LmxMKK5, as it occurred only in co-expressed samples regardless of the functionality of LmxMPK4 (Table 1). It can also be ruled out that LmxMKK5 acts as a scaffold protein, assisting in the complete autophosphorylation of LmxMPK4, as the functionally inactive mutant LmxMPK4K59M was equally phosphorylated on both residues of the TXY-motif after co-expression with LmxMKK5. Co-expressed LmxMPK4 and LmxMPK4K59M displayed high levels of tyrosine phosphorylation directly after purification from *E. coli*, which did not change after proteins were subjected to a non-radioactive kinase assay (Fig. 15). The already discussed low amount of co-purified LmxMKK5 in the co-expressed protein samples and the weak autophosphorylation activity of LmxMPK4 explain the invariant tyrosine phosphorylation level of the co-expressed proteins after a non-radioactive kinase assay and immunoblot analysis. Additional to tyrosine and threonine phosphorylation, MS/MS analysis also detected the presence of phosphorylated serine 186 or serine 187 exclusively in the sample of functional LmxMPK4 after co-expression with LmxMKK5 (Table 1). Serine phosphorylation only occurred in LmxMPK4 co-expressed with

LmxMKK5 either alone or in combination with phosphorylated tyrosine 192, indicating an inter-molecular phosphorylation by activated LmxMPK4. Further research would be necessary to reveal if this inter-molecular serine phosphorylation is of physiological importance. The discussed analyses demonstrated that LmxMKK5 phosphorylates LmxMPK4 in the typical manner of MAP2Ks on the threonine and tyrosine residue of the TXY-motif. The resulting activation of LmxMPK4 is most likely due to this double phosphorylation but it cannot be ruled out that single threonine phosphorylation activates the kinase, even though this would be unusual for a MAP kinase. Single tyrosine phosphorylation, however, did not activate the kinase. It has been reported that in ERK2 tyrosine phosphorylation occurs before threonine phosphorylation (Pearson, G. et al. 2001). This seems unlikely in the case of LmxMPK4 as co-expression with LmxMKK5 also results in peptides which are phosphorylated only on threonine 190. The fact that LmxMKK5 activates LmxMPK4 *in vitro* does not necessarily entail an *in vivo* interaction of the two kinases. Additional research would be required to conclusively show that LmxMKK5 also activates LmxMPK4 *in vivo*. To prove for instance that the MAP2K LmxMKK activates LmxMPK3 *in vivo* it was shown that the deletion of both genes in *Leishmania* led to similar phenotypes, and that no phosphorylated LmxMPK3 could be detected when *LmxMKK* had been deleted from the *L. mexicana* genome (Erdmann, M. et al. 2006). This experimental approach, however, is not feasible for LmxMPK4 and LmxMKK5, as the generation of a deletion mutant of LmxMPK4 is impossible due to its essentiality for both life stages. If LmxMKK5 is the *in vivo* activator of LmxMPK4 it should also not be possible to delete it from the *L. mexicana* genome, as it would be expected to be essential as well. Even if deletion experiments of LmxMKK5 were successful this would still not prove that it is not the *in vivo* activator of LmxMPK4, as another activator or compensation mechanisms could be present. One possible approach to establish LmxMKK5 as the *in vivo* activator of LmxMPK4 would be to generate an inhibitor-sensitised mutant of LmxMKK5 and to investigate whether the inhibition of LmxMKK5 leads to a change in the phosphorylation status of endogenous LmxMPK4. This could either be detected by immunoblot on enriched phosphopeptides from the parasites or by MS/MS analysis of tagged LmxMPK4, purified from *Leishmania*. Inhibiting LmxMKK5 should also result in the same changes in metabolism as are assigned to the function of LmxMPK4 (see 4.1.3.2.6 and discussion below). The immunoprecipitation of LmxMPK4 or LmxMKK5 could also provide additional evidence if it resulted in the respective co-precipitation of the other kinase. The discussed experiments exceeded the given time frame of this work and will have to be part of future projects. There are nevertheless some indications that the interaction of LmxMKK5 with LmxMPK4 could also be relevant *in vivo*. It has been shown for the dual-specificity kinases MEK and wee1, that the phosphorylation of tyrosine residues was very stringent and only occurred with their specific, physiological substrates (Crews, C. M. et al. 1992; Featherstone, C. et al. 1991).

Non-specific substrate tyrosine phosphorylation by dual-specificity kinases on the other hand does occur, but only relatively weak (Lindberg, R. A. et al. 1992; Menegay, H. J. et al. 2000). The correct phosphorylation of LmxMPK4 on tyrosine 192 by LmxMKK5 is therefore an indication that LmxMPK4 is the physiological substrate of the dual-specificity kinase LmxMKK5. LmxMKK5 was furthermore shown to be unable to activate LmxMPK1 (John von Freyend, S. et al. 2010; Melzer, I. M., PhD thesis, 2007). The activation of LmxMPK4 is consequently not simply due to circumstances of the co-expression system but is specific to some degree. LmxMKK5 also clusters on the same branch of the MAP2K phylogenetic tree with AtMKK6 from *A. thaliana* (Fig. 11), which has been shown to activate the MAP kinase AtMPK13 (Melikant, B. et al. 2004), the closest *A. thaliana* homologue of LmxMPK4. The same is true for the AtMKK6 homologue in *Nicotiana tabacum*, NtMEK1, whose substrate appears to be NRK1, the closest homologue of AtMPK13 (Andreasson, E. et al. 2010; Soyano, T. et al. 2003). It is therefore possible that this interaction is conserved within the homologous kinases of *L. mexicana*. Irrespective of the putative *in vivo* interaction of LmxMKK5 and LmxMPK4, the activation of recombinant LmxMPK4 by co-expression with LmxMKK5 now permits the development of drug screening assays against LmxMPK4 and expands the range of experimental procedures available for this kinase.

5.1.1.1 Inhibition of the phosphotransferase activity of activated LmxMPK4 by three different kinase inhibitors

The successful establishment of drug screenings using enzymes as targets does not only require the recombinant expression of high quantities of an active protein, but also the feasibility of enzyme inhibition by small molecules. It was consequently tested whether the universal protein kinase inhibitor staurosporine, the p38 inhibitor SB203580 and the CDK inhibitor alsterpaullone would affect the phosphotransferase activity of activated His-LmxMPK4. Staurosporine did indeed inhibit the activity of LmxMPK4 in a dose-dependent manner, albeit only at rather high concentrations with an estimated LC_{50} around 10 µM (Fig. 16). Although staurosporine is known as a broad kinase inhibitor effective at very low concentrations (Karaman, M. W. et al. 2008), other kinases like CK2 (IC_{50}=10 µM) and ERK1 (IC_{50}=1.5 µM) have been reported to be relatively insensitive to staurosporine (Meggio, F. et al. 1995). This poor receptiveness seems to be largely due to exchanges in the 7 amino acids which are mainly responsible for staurosporine binding (Meggio, F. et al. 1995) and which similarly differ in parts in LmxMPK4. The experiment nevertheless shows that activated LmxMPK4 can be generally inhibited by a small molecule. A specific inhibitor of LmxMPK4 would also be expected to be much more potent than staurosporine. SB203580 and alsterpaullone did not considerably influence the phosphotransferase activity of activated LmxMPK4. SB203580 is a specific ATP-

competitive inhibitor of the human MAP kinase p38 and binds mainly to threonine 106 in the active site of p38. The inhibitor looses its ability to inhibit p38 when threonine 106 is mutated to methionine (Wilson, K. P. et al. 1997) and inhibition can be achieved for the naturally insensitive kinases SAPK3 and SAPK4 when their natural methionine is exchanged to threonine (Eyers, P. A. et al. 1998). LmxMPK4 equally contains a methionine at the position in question, so that its insensitivity to SB203580 is consistent with the literature-based expectation. Alsterpaullone is a specific ATP-competitive inhibitor of CDKs and GSK3β and has been reported to poorly inhibit ERK1 (IC_{50}=22 µM) and ERK2 (IC_{50}=4.5 µM) (Leost, M. et al. 2000), similar to other purine-analogue inhibitors like roscovitin (Meijer, L. et al. 1997). The selectivity of paullones is mainly due to the forming of hydrogen bonds with leucine 83, leucine 134 and isoleucine 10 (amino acid positions for CDK2) (Zaharevitz, D. W. et al. 1999). The respective amino acid residues in LmxMPK4 are tyrosine, leucine and valine, which most likely play a role for the inability of alsterpaullone to inhibit LmxMPK4.

In conclusion, it was demonstrated that LmxMPK4, activated by co-expression with LmxMKK5, can be inhibited by small molecules in a dose-dependent manner but is by no means responsive to all inhibitors. The activated recombinant protein of LmxMPK4 is therefore a feasible target for the development of drug screenings. The only obstacle to the successful development of a screen is the relatively low expression level of His-LmxMPK4, as screening generally proceeds in several subsequent rounds and requires large amounts of protein. The expression and purification of LmxMPK4 as a GST-tag fusion protein led to much higher levels of recombinant protein than was the case for His-LmxMPK4 (Fig. 12). Current work in the Wiese laboratory is therefore concerned with the generation of a modified pJCLinker co-expression system to allow the co-expression of a GST-LmxMPK4 with LmxMKK5. The anticipated high levels of active recombinant LmxMPK4 will then be available for drug screens.

5.1.1.2 Activity of LmxMPK4 at different sodium concentrations

Many eukaryotic cells are sensitive to changes in osmolarity and respond by regulating cellular functions with the help of stress-activated protein kinases (SAPKs) (de, Nadal E. et al. 2002). The *Leishmania* kinome does not contain typical SAPKs, which usually display a glycine or proline as the variable amino acid in the TXY-motif of the activation loop (Kultz, D. 1998; Wiese, M. 2007). As two kinases from *A. aegyptii* and *C. elegans* have been identified as SAPKs and contain a glutamine residue just like LmxMPK4 in their TXY-motif, it has been argued that LmxMPK4 could potentially function as a SAPK in *L. mexicana* (Wiese, M. 2007). The previously discussed *Arabidopsis* homologue AtMKK6 of LmxMKK5 was shown to be involved in the activation of a promoter that is known to be

activated by NaCl and other stresses (Hua, Z. M. et al. 2006). The conducted *in vitro* kinase assay using activated His-LmxMPK4, however, showed no changes in protein activity in response to different levels of NaCl in the assay buffer (Fig. 17, C). The autophosphorylation of singly expressed His-LmxMPK4 and GST-LmxMPK4 are not affected by varying concentrations of NaCl (Fig. 17, A and B), whereas the weak substrate phosphorylation activity of GST-LmxMPK4 seems to be highest at innate NaCl concentrations of 100 mM – 120 mM (Fig. 17, A). Although this demonstrates that LmxMPK4 is not directly activated by high or low osmolarity it cannot be ruled out that other elements higher up in the signalling cascade involving LmxMPK4 are activated by high osmolarity or other stresses and that LmxMPK4 therefore does function as a SAPK in *L. mexicana*.

5.1.1.3 Substrate search using recombinant activated LmxMPK4

The activation of LmxMPK4 by co-expression with LmxMKK5 does not only facilitate the development of inhibitor screenings against LmxMPK4, but provides also the possibility to search for the natural substrate of LmxMPK4 in *L. mexicana*. As previous studies have shown LmxMPK4 to be important in promastigote and amastigote stages (Wang, Q. et al. 2005) it can be presumed that the *in vivo* substrate of LmxMPK4 is constitutively present in *Leishmania*. The addition of activated recombinant LmxMPK4 and radioactively labelled ATP to *Leishmania* lysates should therefore lead to the phosphorylation of the sought substrate and consequently to a detectable band in an autoradiograph corresponding to the protein band of the *in vivo* substrate of LmxMPK4. To ensure the phosphotransferase reaction would use radioactively labelled ATP, all endogenous ATP was removed from the lysates. One amastigote lysate was additionally treated with λ-phosphatase to remove any already present phosphorylations on the proteins, as not to interfere with substrate phosphorylation by LmxMPK4. The quality of the obtained autoradiographs was surprisingly low with hardly any separate protein bands visible in the blurred lane, despite the fact that the lysates displayed perfectly separated proteins without much degradation in the Coomassie-stained gel (Fig. 18, right panels). The blurred picture appeared regardless of the addition of recombinant co-expressed His-LmxMPK4, His-LmxMPK4K59M or no protein to the lysates. Nevertheless, a distinct band at about 27 kDa was detected in all three examined lysate samples after the addition of activated LmxMPK4, but not in the presence of the kinase-dead mutant LmxMPK4K59M or without addition of recombinant protein. It can therefore be concluded that the phosphorylation of the protein which constitutes the band at 27 kDa is solely due to the activity of LmxMPK4 and not any bacterial or *Leishmania* kinase that was present in the lysates. MS analysis of the excised protein band ascertained the masses of several contained peptides. Matching the masses with a *L. major* protein database led to the identification of several proteins as

potential natural substrates of LmxMPK4. Only peptides which also corresponded in mass to peptides in the respective *L. mexicana* homologues were considered relevant. It is likely that the excised protein band was made up of several distinct proteins, as parasite lysates contain a large number of proteins which will obviously overlap in size and as the analysed gel piece was deliberately chosen to be rather too broad than to risk missing out on putative substrates. None of the peptides identified by MS analysis contained any phosphorylations on serine, threonine or proline, which makes it impossible to definitely say which one, if any, of the detected proteins are the *in vivo* substrate of LmxMPK4. They do, however, provide us with a suggestion of possible interaction partners of LmxMPK4 in *L. mexicana*. Not one of the allocated proteins was detected in all three samples of promastigote, amastigote and dephosphorylated amastigote lysates. Proteins that were annotated by peptides found in only one analysed sample include the two hypothetical proteins LmjF36.2480 and LmjF34.3830 and tryparedoxin peroxidase (LmjF15.1120) all of which contain at least one potential MAP kinase phosphorylation site [S/T]-P (sequences including potential phosphorylation sites and annotated peptides shown in appendix). A regulatory MAP kinase phosphorylation site is expected to be conserved between *L. major* and *L. mexicana*, which is not the case for the SP-motif in tryparedoxin peroxidase that LmxM15.1160 misses. This makes it highly unlikely that tryparedoxin peroxidase is an *in vivo* substrate of LmxMPK4. The hypothetical protein LmxM36.2480 is equally out of the question, as the annotated *L. major* peptide does not correspond in mass to the homologous peptide sequence in *L. mexicana*. No statements can be made about the plausibility of the hypothetical protein LmjF34.3830/LmxM33.3830 being a LmxMPK4 substrate, apart from the fact that both proteins contain conserved SP-motifs. Two proteins were detected in two different samples, respectively. The γ-subunit of the ATP synthase F_1 was identified in promastigote lysate samples as well as in the sample containing the dephosphorylated lysate of axenic amastigotes. The F_1 enzyme is the cytoplasmic part of the F_1F_0-complex, which is responsible for the generation of energy by oxidative phosphorylation in most trypanosomatid life stages, apart from bloodstream trypanosomes where it hydrolyses ATP to generate the membrane potential (Schnaufer, A. et al. 2005). The ATP synthesis is driven by the proton electrochemical potential gradient and phosphorylations of subunits have so far not been linked with regulation of the enzyme-complex, which means that the γ-subunit of the ATP synthase F_1 is an unlikely *in vivo* substrate for LmxMPK4. Moreover, does the sequence of the γ-subunit not include any SP or TP motifs, the typical substrate phosphorylation sites of MAP kinases and was therefore not further considered as a potential substrate of LmxMPK4. The only other protein, which was identified in more than one sample, was the glycosomal malate dehydrogenase (MDH) (LmjF19.0710/LmxM19.0710) with a size of 33.63 kDa, annotated in the promastigote lysate and the non-phosphatase treated amastigote sample. Four peptides in the untreated amastigote sample were identified as

malate dehydrogenase (LmjF34.0140), two of which also matched the *L. mexicana* homologue LmxM33.0140. LmjF34.0140 and LmxM33.0140 are not annotated with a subcellular localisation in gene.db, but are predicted to be localised in the mitochondrion by the program TargetP1.1 (Emanuelsson, O. et al. 2000). An alignment of these two, as well as the mitochondrial MDH is enclosed in the appendix and contains markings of all annotated peptides. The two peptides matching the *L. major* mitochondrial MDH did not match the *L. mexicana* homologue LmxM33.0160, which is why this protein was dismissed as potential substrate. None of the identified MDHs contain the ideal MAP kinase substrate phosphorylation sequence P-X-[S/T]-P, but they do each contain at least one motif with the reduced consensus sequence [S/T]-P (Clark-Lewis, I. et al. 1991; Davis, R. J. 1993) that is conserved between *L. major* and *L. mexicana*. Unfortunately, none of the peptides identified by MS analysis contain any of the [S/T]-P motifs, so that there is no evidence on the phosphorylation status of these proteins in the *Leishmania* lysates after incubation with active LmxMPK4. Malate dehydrogenases play an important role in *Leishmania* metabolism, converting malate to oxaloacetate. *Leishmania* encodes MDHs with cytosolic, mitochondrial and glycosomal localisation. The mitochondrial MDH is part of the TCA cycle whose enzymes are mainly used for non-cyclic pathways in trypanosomatids. Mitochondrial MDH is therefore one of the enzymes involved in the generation of precursors for fatty acid biosynthesis and in the degradation of amino acids. Malate is also transported through membranes and is a precursor for the generation of phosphoenolpyruvate (PEP), the starting point of gluconeogenesis. It has so far not been reported that MDH activity is regulated by phosphorylation, but as many metabolic enzymes are regulated by kinases and the protein contains potential MAP kinase phosphorylation sites, MDH is potentially a substrate for LmxMPK4 *in vivo*. The fact that LmxMPK4 and its *T. brucei* homologue TbMAPK2 are essential in *Leishmania* promastigotes and amastigotes, as well as in procyclic *T. brucei* forms suggests that the kinase plays a central role in the parasites and the regulation of MDH would be consistent with that. Moreover, as TbMAPK2 is not essential in bloodstream forms of *T. brucei* it can be concluded that either TbMAPK2 and LmxMPK4 play different roles in the parasites or that their function is essential in promastigotes, amastigotes and procyclics, but not in bloodstream forms. As bloodstream form trypanosomes rely solely on glycolysis for their energy metabolism they only express cytosolic malate dehydrogenase (Aranda, A. et al. 2006), which could be a possible explanation for the relative unimportance of TbMAPK2 in bloodstream trypanosomes, if mitochondrial and glycosomal MDH were the natural substrates of the kinase. However, considering the poor quality of samples used for MS analysis, the potential for miss-matches due to the usage of a *L. major* protein database and the fact that no phosphorylated peptides were detected, MDH as a potential *in vivo* substrate for LmxMPK4 remains purely speculative. Further experimental approaches are required before a definite conclusion can be drawn.

5.1.2 Characterisation of an inhibitor-sensitised mutant of LmxMPK4

The gene encoding for LmxMPK4 cannot be deleted from promastigotes (Wang, Q. et al. 2005), which requisitioned a different experimental approach to investigate the function of LmxMPK4 in *L. mexicana*. Hence, the approach of an inhibitor-sensitised mutant of LmxMPK4 was used, which makes it possible to specifically inhibit LmxMPK4 at any given time point and directly analyse the effect on cells. The inhibitor-sensitising mutation changes the gatekeeper residue, a conserved large hydrophobic residue within the active site directly in contact with the N^6 group of ATP, to the small non polar amino acids glycine or alanine, thus creating a novel pocket in the ATP binding site, which is not found in any wild type kinase (Adams, J. et al. 2002; Bishop, A. et al. 2000; Bishop, A. C. et al. 2001). A class of synthetic pyrazolo[3,4-*d*]pyrimidine derivates, most notably 1-naphtyl-pyrazolo[3,4-*d*]pyrimidine (1Na), has been found to selectively bind to the pocket created by the inhibitor-sensitising mutation, thereby causing kinase inhibition (Bishop, A. C. et al. 2001). The gatekeeper residue of LmxMPK4 was identified as being methionine111 and the inhibitor-sensitised mutant LmxMPK4IS was engineered by mutating methionine111 to glycine.

5.1.2.1 The activity of recombinant co-expressed LmxMPK4IS *in vitro*

Kinase assays showed that the inhibitor 1Na had no effect on the phosphotransferase activity of activated wild type LmxMPK4, but inhibited the MBP phosphorylation and autophosphorylation of co-expressed inhibitor-sensitised LmxMPK4IS in a dose-dependent manner with full inhibition occurring between 1 µM and 10 µM 1Na (Fig. 20, B). The co-expressed inhibitor-sensitised mutant LmxMPK4IS displayed a notably reduced phosphotransferase activity towards MBP in comparison to activated wild type LmxMPK4 (Fig. 20). Although this is unfortunate, it is by no means unusual, as about 30% of all examined kinases show a severe loss in catalytic activity after the inhibitor-sensitising mutation of the gatekeeper residue (Zhang, C. et al. 2005). Zhang et al. have established a system of mutating a series of other amino acid residues in the kinase to try and rescue its full activity (Zhang, C. et al. 2005). This, however, was considered to be too time-consuming in the case of LmxMPK4 and it was also feared that additional mutations would impair the function of LmxMPK4 *in vivo*. As the natural substrate of LmxMPK4 is not known it is impossible to evaluate whether the additional mutations would affect substrate recognition *in vivo*. Moreover, it had been demonstrated for the cyclin-dependent kinase Cdc28 of budding yeast that, although the inhibitor-sensitising mutation led to a 10-fold reduction in ATP binding and to a 6-fold decrease in ATP turnover *in vitro*, the inhibitor-sensitised mutant was still able to assume the function of wild type Cdc28 *in*

vivo (Bishop, A. C. et al. 2000). Thus it was anticipated that despite the lower phosphotransferase activity of recombinant LmxMPK4IS *in vitro*, the recognition and phosphorylation of its endogenous substrate would not be affected and *in vivo* studies of LmxMPK4 function, using the inhibitor-sensitising mutant LmxMPK4IS were carried out.

5.1.2.2 The effect of LmxMPK4 inhibition on promastigote growth

In previous experiments add-back parasite cell lines where used, which contained no genomic copy of *LmxMPK4*, but only an extrachromosomal copy of the wild type gene on the plasmid pXpolPacMPK4. These cells were transfected with the plasmid pXpolNeoMPK4IS, carrying the gene for the inhibitor-sensitised mutant, and cultivated under continuous selection pressure for neomycin resistance. No puromycin was added to the cultures and those cells which were sensitive to puromycin, indicative for the loss of the plasmid pXpolPacMPK4, were selected. To confirm that these cells indeed contained the inhibitor-sensitised mutant LmxMPK4IS a PCR was conducted on total extracted DNA and the presence of the *Bgl*II restriction site, which had been introduced together with the M111G mutation, confirmed the identity of the gene as *LmxMPK4IS*. However, *Leishmania* plasmids typically vary greatly in numbers, which can lead to incoherent test results. To avoid this possibility and provide for a experimental set-up closer to the endogenous situation, cell lines were generated which contained the *LmxMPK4IS* gene in the original genomic locus of the wild type gene *LmxMPK4* and had lost the plasmid pXpolNeoMPK4IS. This was verified by the loss of neomycin resistance, as the genomic integration cassette used puromycin as resistance marker, and by Southern blot analysis (Fig. 22). LmxMPK4 is essential in *L. mexicana* promastigotes, as its gene could not be deleted from the genome. It was therefore expected that the specific inhibition of LmxMPK4IS would lead to the death of promastigotes. Initial investigations showed that neither DMSO nor 1Na have any effect on the growth of *L. mexicana* wild type promastigotes (Fig. 23, A). DMSO is the organic solvent in which 1Na is applied to cells and this shows that any putative effects by 1Na do not trace back to effects by DMSO. Yet, even the addition of the high inhibitor concentration of 10 µM did not affect wild type promastigotes, demonstrating that 1Na had no notable unspecific effects at the used concentrations. The engineered inhibitor-sensitive mutants on the other hand responded strongly to the addition of 1Na, but did not display reduced growth after the addition of DMSO. Low inhibitor concentrations led to a growth arrest in all three investigated independent LmxMPK4IS mutant clones (Fig. 23, B, C and D). The growth of mutant cell lines under influence of 1Na was extremely slow during the first one to two days of the experiment and then either stagnated (Fig. 23, D) or declined (Fig. 23, C). Only the mutant BF11E4 showed a spike of growth on day 3, followed by a sharp decline on day 4 back to the cell density of day 2. This spike is caused by outlying divergences in the conducted

experiments and is not due to a lower sensitivity of BF11E4 towards the inhibitor 1Na, as demonstrated by the particularly large standard deviations visible in the diagram (Fig. 23, B). Nevertheless, BF11H4 was chosen for all subsequent experiments as it demonstrated the most stable response to the addition of 1Na. The display of growth in line graphs as in Fig. 23 only allows the comparison of different cultures and conditions with the help of a disconcertingly high number of diagrams and furthermore statistical analyses of the results are not possible with this method. On this account the growth rate, which allegorises the gradient of the logarithmic growth of a culture, was calculated and statistically evaluated. The analyses showed that LmxMPK4IS mutant cell lines exhibited the same growth rate as wild type cells when grown without additives or after the addition of DMSO (Fig. 25). Although there were some fluctuations in growth rate, none of them were statistically significant. This demonstrates that LmxMPK4IS can indeed substitute the function of LmxMPK4 *in vivo*, despite its earlier discussed lower phosphotransferase activity *in vitro*. The inhibitor-sensitive cell lines did, however, in general not quite reach the same growth rate as wild type *L. mexicana* (Fig. 25). Although this effect was not statistically significant, it shows a certain trend and could be due to a slightly lower activity of LmxMPK4IS *in vivo* in comparison to wild type LmxMPK4. This observation was not further investigated at this point as it did not seem to be of great impact. The calculation of the growth rate is only applicable for cultures with logarithmic growth and can therefore not be used to describe and compare the inhibition of inhibitor-sensitive *L. mexicana* cell lines by 1Na. For this purpose the cell numbers on day 4 of the experiment were compared instead. This day was generally the last day of logarithmic growth in an uninhibited culture and consequently the day on which the culture reached its maximum cell number. The inhibitor-sensitive mutant strain BF11H4 was grown under varying concentrations of inhibitor, to investigate whether the growth defect would occur in a dose-dependent manner. The cell numbers reached on day 4 under the influence of 0.5 µM or 1 µM and 10 µM 1Na respectively, did not differ from each other in a statistically significant manner, indicating that a threshold of inhibition had been reached. The concentration of 0.2 µM 1Na was the lowest tested one to lead to a significantly different number of cells in comparison with the culture grown without additives (Fig. 26). The addition of 0.05 µM and 0.1 µM of 1Na led to a reduced number of cells, but the cell count here was not significantly different from BF11H4 grown without additives. However, a certain trend pointing to a dose-dependent inhibition can be observed. The two lowest 1Na concentrations notably resulted in highly fluctuating cell numbers, as can be seen in the extremely high standard deviations for those two sets of experiments (Fig. 26). All these results show that the effect of 1Na was a specific inhibition of LmxMPK4IS, which resulted in a severe growth arrest of the respective cells. The cells that were observed at the end of experiments after addition of more than 0.5 µM 1Na had a slightly abnormal appearance, looking rounder and grainier than the wild type cells or uninhibited

LmxMPK4IS mutant cell lines. Nevertheless, the inhibition of LmxMPK4IS did not lead to a quick lysis or apoptosis of all observed cells, as all experiments still contained viable, slowly moving cells at the end of the experiments. This observation was underlined by the resumed growth of cultures after the inhibitor was washed out with fresh medium at the end of a 4 or 5 day culture period under inhibitor influence (Fig. 27). The three conducted experiments were slightly heterogeneous, which is why they are not summed up in one diagram, but shown as separate experiments in Fig. 27. All three experiments show a distinct drop in cell numbers after the inhibitor was washed out, allegeable to the loss of cells during wash-out. All observed, previously arrested cultures resumed growth again after the inhibitor was removed, indicating either a reversible inhibition of LmxMPK4IS by 1Na or the rapid availability of new, uninhibited LmxMPK4IS. The resumption of growth was approximately dose-dependent, with cells recommencing proliferation the quicker the lower the previously added inhibitor concentration had been. None of the observed cultures, however, reached the full growth rate of BF11H4 without addition of inhibitor (Fig. 28). This is most likely due to experimental conditions as the cells that were used to inoculate the growth experiments were taken from logarithmic cultures and were therefore in ideal condition to start proliferating rapidly. Cells that had been incubated under the influence of 1Na on the other hand were of a non-proliferating stage. The experiment proves that viable cells were still present in cultures inhibited by 1Na. Cells that had been incubated with 5 µM and 10 µM 1Na in experiment A started to proliferate again but went quickly into a growth arrest, although the same conditions in experiment B resulted in the resumption of growth. The difference between the two experiments was the number of days after which the inhibitor was washed out. It is possible that unspecific effects at the high concentrations of 1Na come more into effect after incubation for 5 days, as in experiment A, as opposed to 4 days in experiment B. Equally could the implications of inhibited LmxMPK4IS be lethal for cells after a longer period of time, when potential procedures balancing out the effects start being ineffective. It can be concluded that the experiments with the inhibitor-sensitised mutant show that LmxMPK4 plays an important role for promastigote proliferation. Even though the inhibition of LmxMPK4 in promastigotes is not cytotoxic during the first 4 days of incubation, it has a strong cytostatic effect on *L. mexicana*. The deletion of the *T. brucei* homologue TbMAPK2 in bloodstream forms interestingly led to procyclic cells which were motile, but did not proliferate. A wash-out experiment could not be attempted in the case of genomic deletion, but it was shown that procyclics lacking TbMAPK2 equally survived for rather long periods in culture (Muller, I. B. et al. 2002), leading to the assumption that TbMAPK2 plays a similar role in *T. brucei* as LmxMPK4 in *L. mexicana*.

5.1.2.3 The effect of LmxMPK4 inhibition on amastigote growth

The same type of growth experiments that were conducted for *L. mexicana* promastigotes were also attempted with axenic amastigotes, to assess the importance of LmxMPK4 for the late stages of differentiation and for the proliferation of axenic amastigotes in culture. The inhibitor-sensitised *L. mexicana* mutant strain BF11H4 was incubated under conditions that trigger the differentiation to axenic amastigotes. Cells are generally considered to be fully differentiated on day three after the start of the experiment. The inhibitor 1Na was added at day 2 after the start of the experiments. All experiments showed an initial increase in cell numbers. This seems unexpected as *Leishmania* cells do not proliferate during differentiation to axenic amastigotes. However, as promastigote cultures are not synchronised when the experiments start, cells will finish their cell cycle first before starting to differentiate, leading to increasing cell numbers during the first three days. Neither the wild type strain, nor the inhibitor-sensitised mutant showed a high amount of proliferation as axenic amastigotes after day 3, regardless of the presence or absence of additives (Fig. 29), so that consequently only the differentiation period could be assessed. It is not clear why the cultures showed hardly any notable growth as axenic amastigotes, but it is likely that the high amount of agglomeration which the cultures displayed prevented proliferation and impeded the experimental evaluation. In regard to the differentiation of promastigotes to amastigotes it is nevertheless interesting to note that the inhibitor-sensitised mutant strain BF11H4 reached significantly lower cell numbers than wild type *L. mexicana* (Fig. 29). The impairment is highly likely due to the reduced activity of the inhibitor-sensitised LmxMPK4IS compared to wild type LmxMPK4, as this is the only feature in which the two strains differ. The observation could be due to several reasons, one being that promastigotes are impaired in growth by the inhibitor-sensitised mutation after all, but that the effect is slight and therefore not notable amidst the high cell numbers of the conducted promastigote experiments. It is also possible that promastigotes which proliferate under conditions promoting differentiation (high temperature and low pH) are more susceptible to slight changes in LmxMPK4 activity as they reside in a stress-inducing environment. The slightly impaired kinase function could equally lead to cell death during differentiation of axenic amastigotes, thus leading to lower maximal cell numbers. The last scenario would imply that *L. mexicana* are more susceptible to changes in the rate of LmxMPK4 activity during differentiation and as axenic amastigotes than as promastigotes, possibly lacking a compensation system, producing less protein or requiring a tighter regulation of activity. However, from the conducted experiment it is not possible to discern which of the mentioned theories is responsible for the significantly lower maximal cell numbers reached by uninhibited inhibitor-sensitised *L. mexicana* BF11H4. It is also doubtful if the system of an inhibitor-sensitised kinase is applicable in axenic amastigotes at all, as the addition of DMSO and

1Na already led to significantly lower maximal cell numbers in wild type *L. mexicana* (Fig. 30). The parasites seem to be more sensitive to the addition of DMSO during differentiation than as promastigotes. It is unlikely that the observation is due to unspecific effects of 1Na, as the maximal cell densities reached after addition of DMSO and 1Na were comparable. The addition of 1Na did not result in a notable effect on inhibitor-sensitised *L. mexicana* BF11H4 either, probably because the highest reached cell densities of BF11H4 were already rather low.

Differentiation of the cell line BF11H4, which did not contain wild type *LmxMPK4* but solely the inhibitor-sensitised mutant *LmxMPK4IS*, to axenic amastigotes suggested that amastigotes were more sensitive to changes in LmxMPK4 activity than promastigotes. Mouse infections studies were therefore conducted to investigate whether inhibitor-sensitised mutant strains would also show a different disease pattern than wild type *L. mexicana*. As a matter of fact all three of the investigated cell lines, which did not express LmxMPK4 but only LmxMPK4IS, induced no or only very small lesions in footpad infection experiments (Fig. 31). No inhibitor was included in this type of experiment, which signifies that the reduced infectivity of the *L. mexicana* mutant strains was exclusively due to the presence of LmxMPK4IS instead of LmxMPK4 and therefore most likely to the impaired functionality of LmxMPK4IS in comparison to LmxMPK4, as shown for the recombinant protein (Fig. 20). This result supports the theory that *L. mexicana* amastigotes are far more susceptible to changes in LmxMPK4 activity than promastigotes, implying that LmxMPK4 either plays different roles in promastigotes and amastigotes or that its function is more important for amastigotes or requires a more stringent regulation. Although the LmxMPK4IS mutant cell lines were not infective in mice this was not due to the death of cells or to an intensified susceptibility of the parasites to the mammalian immune system. The fact that viable *L. mexicana* were isolated from the footpads of infected mice after 1.5 years shows that they merely underwent a growth arrest due to the impaired function of LmxMPK4IS. Despite the failed investigation of growth in response to 1Na treatment in axenic amastigotes, this shows now that amastigotes are more sensitive to the inhibition of LmxMPK4 than promastigotes, but generally respond in a similar manner. The inhibition here is due to an impaired functionality as a result of the mutation and not the addition of inhibitor 1Na. The survival of parasites in the mice was not due to mutations of LmxMPK4IS which revoked the inhibitor-sensitising mutation. The isolated promastigotes from all test animals were still responsive to 1Na treatment, showing that the IS-mutation was still existent in all cultures (Fig. 32). It is to be expected that the full inhibition of LmxMPK4 in mice would lead to the eradication of *L. mexicana* amastigotes, seeing as the slight impairment in function already leads to a severe growth arrest and no lesion development.

5.1.2.4 Effect of LmxMPK4 inhibition on the promastigote cell cycle

The repeated observation of a cytostatic effect raised the question of a possible involvement of LmxMPK4 in cell cycle control. The *T. brucei* homologue TbMAPK2 had been proposed to be involved in a general regulation of cell cycle progression, as the deletion of the gene in bloodstream forms led to the differentiation into procyclics which displayed a non phase-specific cell cycle arrest (Muller, I. B. et al. 2002). The *L. mexicana* mutant AB6H2, which expressed only the inhibitor-sensitised LmxMPK4IS and no wild type LmxMPK4, was incubated with DMSO, Flavopiridol and 1Na for the duration of approximately one cell cycle and compared to wild type *L. mexicana* cells, incubated with DMSO. The cyclin-dependent kinase inhibitor Flavopiridol has been shown to arrest *L. mexicana* in the G2-phase of the cell cycle, presumably by inhibiting CRK3 (Hassan, P. et al. 2001) and was used in this experiment as positive control to demonstrate that an arrest in the cell cycle of inhibitor-sensitised mutants would be visible by flow cytometry. The demonstrated arrest of AB6H2 cells in the G2-phase of the cell cycle hence met the expectations (Fig. 34, D). Inhibitor-sensitised mutants did not differ in their progression through the cell cycle from wild type *L. mexicana* promastigotes (compare Fig. 34, A and B), which also matched the expectations, seeing that there is no difference in growth in wild type promastigotes and AB6H2 promastigotes (Fig. 23). The addition of 1Na to the inhibitor-sensitised mutant AB6H2 did not lead to an observable change in the distribution of cells in the various cell cycle phases (Fig. 34, C). The duration of one cell cycle of *Leishmania* promastigotes is approximately 8 hours, which means that after 10 hours there should be a considerable amount of cells which have undergone one full cell cycle. It was therefore expected that if the inhibition of LmxMPK4IS led to a specific block in the progression of the cell cycle this would be visible after 10 hours, as is the case for the block in the G2-phase induced by Flavopiridol. If LmxMPK4 plays a role in cell cycle control it is therefore a general function and not one that effectuates the progression from one specific phase of the cell cycle into another.

5.1.2.5 The effect of LmxMPK4IS inhibition on promastigote metabolism

The observed growth arrest of promastigotes, induced by the specific inhibition of LmxMPK4IS, can be an indicator for a metabolic arrest. This has been shown experimentally by the inhibition of the respiratory chain which has implicated the reduction of energy requiring processes like movement and proliferation as markers for metabolic arrest (van Hellemond, J. J. et al. 1997a; van Hellemond, J. J. et al. 1997b). The metabolism of wild type cells and mutants expressing the inhibiter-sensitive LmxMPK4IS was consequently compared in regard to the addition of DMSO or the inhibitor 1Na to the growing cultures. The preceding experiments have shown that 1Na specifically inhibits

LmxMPK4IS, so that all changes that would be observed in the metabolism of inhibitor-sensitised mutant (BF11H4) cultures, grown under the presence of 1Na, should at least indirectly result from the inhibition of LmxMPK4. Our experiments were not designed to give an extensive overview over the whole metabolome of *L. mexicana*, but were rather meant to highlight if the inhibition of LmxMPK4 led to a growth arrest due to changes in metabolism. It was also hoped that the metabolic profiling analyses would provide pointers to the natural function of LmxMPK4 in *L. mexicana*.

The metabolic profiling analysis was conducted in two independent experiments, each comparing biological triplicates and technical duplicates of wild type and inhibitor-sensitised mutant (BF11H4) cultures, grown for 48 hours under the influence of DMSO and the inhibitor 1Na, respectively. The experiments showed the same trends of up- and downregulations of metabolites but the detected quantities differed greatly and some metabolites were only identified in one of the experiments. This made it impossible to process the datasets of the two experiments together and only the first experiment, which showed the most drastic variations, was used for analysis. The variance in data is a common problem in metabolic profiling and one of the biggest challenges in this new research field. The levels of metabolites in organisms are generally highly fluctuating, which is why it is crucial to collect samples from cells which are in the same stage of growth (Scheltema, R. A. et al. 2010). It is not possible to completely synchronise *Leishmania* cultures and, although great care was taken to reproduce all conditions exactly in both experiments, it is very likely that small differences in age or density of inoculating cultures or growth conditions during the experiment could have resulted in changes of the identified metabolites. It is equally important to quench metabolism of cells rapidly and efficiently and to store samples only for a short period of time before the analysis, to minimise loss off metabolites by degradation and by steps such as centrifugation or washing of the cells. A certain degree of leakage of intracellular metabolites, however, is almost inevitable (Winder, C. L. et al. 2008) and can affect experimental outcomes strongly. The differences in metabolite levels between the two experiments were attributed to such changes. The overall objective of the metabolic profiling in our case was only to gain insight into metabolic trends associated with the activity of LmxMPK4. It was therefore possible to analyse the results of one experiment in depth and verify if observed trends also appeared in the second experiment. The metabolite quenching and extraction process, as well as the analysis itself led to very reproducible results within the groups composed of biological and technical replicates of the same sample. This was demonstrated by unsupervised principal component analysis (PCA) of the four sample groups, in which the datasets of all 6 replicates of each sample clustered closely together, indicating only few variations within each group (Fig. 35). This led to the assumption that differences between the two experiments were mainly due to

variations in the cultures which were used to inoculate the experiment, possibly based on differing numbers of cells in varying life stages, and not to a general methodical flaw. PCA also revealed that the two different wild type samples, one grown under influence of DMSO, the other with addition of the inhibitor 1Na, clustered closely together, meaning there were only few variations between the metabolites identified in these sample groups. This underlines that there are only few, if any, unspecific effects of the inhibitor 1Na. The highest amount of variance was observed between the samples of the inhibitor-sensitised mutant BF11H4, grown under influence of 1Na and the wild type samples, exhibited by the first principal component which explained 42.3 % of the total variance. This observation already indicates that the inhibition of LmxMPK4IS by 1Na leads to extensive changes in the metabolome of *L. mexicana*. The second highest amount of total variance (26.4 %), as described by the second principal component, separated the inhibitor-sensitive culture which had been incubated with 1Na, from BF11H4 grown under influence of DMSO. This met the expectations as any changes related to the inhibition of LmxMPK4IS should only emerge in the presence of the inhibitor 1Na and not of DMSO. Yet unanticipated was the observation that there was already an extensive variance between the wild type samples and the inhibitor-sensitised mutant BF11H4 incubated with DMSO, as demonstrated by the clustering of groups on the first principal component (Fig. 35). Instead it had been expected that the metabolome of BF11H4 without the addition of inhibitor would equate to that of the wild type samples, based on the fact that BF11H4 + DMSO displays the same growth phenotype as wild type cultures (Fig. 23). The changes cannot be due to any negative effects of DMSO as it was equally added to the wild type samples. It is most likely that any observed changes in metabolites extracted from an uninhibited culture BF11H4, in comparison with the wild type were due to the already discussed reduced activity of LmxMPK4IS caused by the inhibitor-sensitising mutation. This is consistent with the fact that, although the lower activity of LmxMPK4IS does not affect the growth phenotype of *L. mexicana* promastigotes, it leads to reduced lesion development in infection experiments and a slower differentiation to axenic amastigotes. As the reduced growth of promastigotes is insensible to a reduced activity of LmxMPK4IS, but not to the full inhibition of the enzyme, it can be speculated that the effect on growth is not immediately due to the function of LmxMPK4, but results from secondary, indirect effects.

A more in-depth analysis of the changes in the metabolome induced by LmxMPK4IS inhibition was conducted to provide further clues on the *in vivo* function of the kinase. A total of 134 separate metabolites were identified and compared with regard to their abundances in the four different sample sets. The most information on the effect of LmxMPK4 inhibition on the metabolism can be deduced from the comparison of the wild type sample and the mutant strain BF11H4 expressing LmxMPK4IS, both grown under

the influence of the inhibitor 1Na. Possible unspecific effects of 1Na should be minimal (see PCA), but would occur in both samples and therefore would not be detected as changes. All high variations in metabolite abundance between the two samples can therefore be assigned solely to the inhibition of LmxMPK4IS by 1Na. Low variations could also be due to metabolite loss causing fluctuations between the replicates, although the reproducibility of samples was shown to be high. For this reason only changes of or higher than 2-fold, which occurred in 35.8 % of all identified metabolites were considered relevant for analysis. A proportion of 11.2 % of metabolites displayed changed abundances of 5-fold or higher between the wild type sample and the BF11H4 sample, incubated with 1Na. This demonstrates that LmxMPK4 indeed plays a role in the metabolism of *L. mexicana* which additionally seems to be rather central, considering the high amount of metabolites which change in abundance in response to the inhibition of LmxMPK4IS.

Most of the observed changes between all compared samples affected substances of the amino acid or lipid metabolism (Fig. 37). This was especially obvious when samples derived from the inhibitor-sensitised mutant cell line BF11H4 were compared with samples of the wild type (Fig. 37, C and D). Changes in metabolite abundance between the two wild type samples, which are due either to methodical issues or unspecific effects of 1Na were only few and low (Fig. 37, A). The in-depth analysis of metabolite classes demonstrates once again that the changes observed in samples of the inhibitor-sensitised mutant BF11H4 grown under the influence of DMSO or 1Na, respectively, are not as many and as pronounced as originally expected, most likely due to the reduced activity of LmxMPK4IS even without the addition of the inhibitor 1Na (Fig 37, B). It is interesting to note that most, but by no means all, changes in amino acids and lipids resulting from the inhibition of LmxMPK4IS were upregulations of metabolites.

The highest upregulation of a metabolite was seen for arginine, which was 179-fold upregulated in the BF11H4 sample treated with the inhibitor 1Na, when compared to 1Na treated wild type cells. This upregulation already occurred 137-fold in cells which contained the less active mutant kinase LmxMPK4IS without the addition of 1Na (BF11H4 + DMSO compare to WT + DMSO) and could also be reproduced in the second independently conducted metabolic profiling experiment, although less drastically (37-fold upregulation). It is therefore safe to assume that the detected upregulation of arginine is due to the inhibition of LmxMPK4IS kinase activity. The same is true for the also gravely upregulated metabolites proline, isoleucine/leucine and the lipid GPC(35:3/2). A prominent downregulation, which displayed a downregulation of 3-fold was observed for hypoxanthine, a purine derivate. This downregulation, however, could not be reproduced in the second experiment, in which hypoxanthine displayed a 5-fold upregulation instead,

and was therefore not considered relevant for the analysis. Another prominent downregulation was that of dimethylarginine, an arginine derivative, which was not detected in the second conducted experiment. The regulation pattern of dimethylarginine showed that it was 16.4-fold downregulated in inhibitor-sensitised mutant samples, regardless of the presence of DMSO or 1Na, in comparison to wild type samples. This is a direct effect of the upregulation of arginine, as dimethylarginine inhibits NO-synthase which metabolises arginine and is therefore downregulated in the presence of high amounts of arginine. Trypanothione and trypanothione-disulfide, which are important for the defence against oxidative stress (Bocedi, A. et al. 2010), are both upregulated in inhibitor-sensitised mutants, in comparison to the wild type. The DMSO treated BF11H4 here does not represent an intermediate stage, but seems to be slightly higher than the 1Na treated BF11H4 sample. Considering the high standard deviations in both cases, however, it can be concluded that the upregulation of trypanothione and trypanothione-disulfide is on a similarly high level when the function of LmxMPK4 is impaired or inhibited. Whether this is due to a direct regulation by LmxMPK4, or rather to a general response against the stress, caused by the loss of LmxMPK4 activity, is impossible to deduct at this stage. Citrulline, a direct derivative of arginine, which is, just as arginine, a metabolite of the urea cycle is also upregulated in mutants expressing LmxMPK4IS and only in the presence of the inhibitor 1Na. The presence of DMSO in cultures of inhibitor-sensitised mutants results in roughly the same citrulline levels as in wild type cultures. The assumption that changes in BF11H4 cells treated with DMSO originated from the reduced activity of mutated LmxMPK4IS in comparison with wild type LmxMPK4 was supported by the finding that the abundance of metabolites of BF11H4 + DMSO in many cases presented an intermediate level between wild type samples and samples containing fully inhibited LmxMPK4IS (BF11H4 + 1Na) (Fig. 38 and appendix).

The effects on *L. mexicana* metabolism caused by the inhibition of LmxMPK4 are manifold and diverse, which makes it impossible to clearly ascertain the function of LmxMPK4. Nevertheless it can be concluded that LmxMPK4 plays a very central role in metabolic regulation in *Leishmania.* Observed changes could either result from an enhanced transport of metabolites into the cells, a block at a very central metabolic reaction which results in the accumulation of upstream substrates or an upregulation of metabolic processes. Many metabolic reactions require the activities of kinases which are themselves regulated by phosphorylations. It is therefore plausible to speculate that MAP kinases, as they do not act on transcription factors, act on metabolic enzymes instead, playing a major role in the regulation of metabolism.

Analysis of protein turnover rates by the incorporation of [^{35}S]-methionine into newly synthesised proteins demonstrated that the inhibition of LmxMPK4IS leads to a reduction

in protein synthesis (Fig. 40). This could be the cause of the upregulation of amino acid levels or it could be due to a general metabolic arrest in response to energy deficiency as a result of LmxMPK4IS inhibition. No definite function could be assigned to LmxMPK4, but the extremely high upregulation of the essential amino acid arginine, in response to LmxMPK4IS inhibition, led to the speculation that LmxMPK4 might be involved in the regulation of arginine transport. It has been shown that the activity of the specific arginine transporter LdAAP3 in *L. donovani* is most likely downregulated in the presence of high arginine levels in the cell (Darlyuk, I. et al. 2009). A negative regulatory effect of LmxMPK4 on LdAAP3, which indeed displays possible MAP kinase phosphorylation sites, would therefore explain why arginine levels increase drastically when LmxMPK4IS is inhibited. It does not, however, explain the abundance of changes in amino acid and lipid metabolic pathways, which are also observed. In *Leishmania,* arginine is the sole precursor for the synthesis of polyamines, which play an essential role in kinetoplastids, especially in regard to cell growth (see introduction). How increased arginine levels would negatively influence polyamine levels, however, is not clear. Additionally, *Leishmania* amastigotes have been shown not to depend on the synthesis of polyamines for survival and virulence, as they possess effective means of salvaging polyamines from host cells (Gaur, U. et al. 2007; Reguera, R. M. et al. 2009; Saunders, E. C. et al. 2010). No polyamines were directly identified in the displayed experiment, but the second independently conducted experiment identified a 6-fold increase in the levels of spermidine when LmxMPK4IS was inhibited. Both experiments also showed an increase in trypanothione, which is synthesised partly from spermidine. It was therefore considered unlikely that the cytostatic effect of LmxMPK4IS inhibition was due to a decrease in polyamines. It must also be considered that the *in vivo* role of LmxMPK4 is most likely involved in the regulation of metabolic processes which play an essential role in *Leishmania* promastigotes and amastigotes, as well as in *T. brucei* procyclics, but not in *T. brucei* bloodstream forms, as these are the only life stages in which the deletion of LmxMPK4 displayed no phenotype (Muller, I. B. et al. 2002; Wang, Q. et al. 2005). These observations rule out a regulatory role of LmxMPK4 in glycolysis, as the entire energy metabolism of *T. brucei* bloodstream forms relies solely on this metabolic process and glycolysis is not essential for procyclics (Hellemond, J. J. et al. 2005; van Weelden, S. W. et al. 2005). In consequence of their simple energy metabolism *T. brucei* bloodstream forms largely repress most functions of mitochondrial metabolism, apart from the electron transport chain, which nevertheless acts with a different function than in procyclics (Schnaufer, A. et al. 2005; Tielens, A. G. et al. 2009). The observed effects of impaired or inhibited LmxMPK4IS function in *L. mexicana* promastigotes and amastigotes and *T. brucei* procyclics, could therefore result from an impairment of mitochondrial metabolism. A key role in trypanosomatid mitochondrial metabolism is played by the enzymes of the TCA-cycle, which produce metabolites ultimately involved in amino acid

degradation, fatty acid biosynthesis and gluconeogenesis (Bringaud, F. et al. 2006; van Weelden, S. W. et al. 2005). Intriguingly one of the enzymes of the TCA-cycle, malate dehydrogenase, has been detected in a screening for possible substrates of LmxMPK4 (see 5.1.2.3). Malate dehydrogenase (MDH) does not only play a role in the TCA cycle, but also in the glyoxylate bypass, in amino acid biosynthesis and in gluconeogenesis and is expressed in three different isoforms in *Leishmania* (Aranda, A. et al. 2006; Musrati, R. A. et al. 1998). MDH has also been found to be the major binding partner of paullones in *L. mexicana*, which induce a growth arrest in promastigotes (Knockaert, M. et al. 2002). It was, however, not verified whether the growth arrest induced by paullones is truly due to the inhibition of MDH *in vivo*, but the findings demonstrate a possible connection between the central role of MDH in metabolism and a growth arrest in promastigotes. Catabolism of several amino acids provide precursors for the TCA-cycle, however, arginine is not one of those amino acids. It is therefore doubtful why a regulatory effect of LmxMPK4 on MDH would result in the observed drastic increase in arginine. The only connection between arginine and the TCA-cycle is in the enzyme arginino-succinate lyase, which produces arginine and fumarate from arginino-succinate as part of the urea cycle. Fumarate is subsequently turned into malate by fumarase. However, the genomes of *Leishmania* and *T. brucei* do not encode the enzyme arginino-succinate lyase (Opperdoes, F. R. et al. 2007). Although functional homologues of arginino-succinate lyase might exist in trypanosomatids it is still hard to explain the amount of upregulation observed in arginine levels when LmxMPK4 is inhibited. Yet it is possible and even likely that identified changes of metabolism are not all due to direct effects of the inhibition of LmxMPK4IS but could also arise from cells trying to compensate for the effect of LmxMPK4 inhibition (Raamsdonk, L. M. et al. 2001). Further experiments are needed to resolve the question what role LmxMPK4 plays in the regulation of metabolism. One possible future approach to identify the substrate of LmxMPK4 *in vivo* will be by labelling substrates with the help of ATP analogues. The inhibitor-sensitising mutation of engineered kinases confers the ability to uniquely bind ATP analogues which are not recognised by any other endogenous kinases (Liu, Y. et al. 1998; Shah, K. et al. 1997). Based on this, a method has been developed to use recombinant inhibitor-sensitised kinases to label putative substrates in protein lysates with a thiophosphate tag and subsequently purify them for MS/MS analysis (Blethrow, J. D. et al. 2008). The method does, however, require active recombinant LmxMPK4IS, which is not the case for LmxMPK4IS with the mutation M111G.

It can be noted in summary that, although the specific *in vivo* function of LmxMPK4 was not identified, it was possible to ascertain that LmxMPK4 plays a central role in metabolism regulation.

5.1.3 Generation and characterisation of a new inhibitor-sensitised mutant LmxMPK4ISMA

The approach using an inhibitor-sensitised mutant of LmxMPK4 proved a great method to identify changes in the parasites *in vivo* without having to apprehend the selection of mutants which compensate for the loss of the kinase, as it can happen in knock-out mutants. The experiments conducted with LmxMPK4IS showed that the inhibitor-sensitising mutation of methionine111 to glycine reduces the phosphotransferase activity of the kinase (as shown *in vitro* for recombinant protein) and affects the function of LmxMPK4IS *in vivo* (as shown by infection studies in mice and metabolic profiling experiments). To fully exclude the influence of any possible compensatory effects it was deemed necessary to generate an inhibitor-sensitised mutant that is not impaired in its kinase activity. Such an inhibitor-sensitised mutant could also be used for the identification of LmxMPK4 substrates by thiophosphate labelling, as discussed above. A number of second-site suppressor mutations have been identified, which can rescue an impaired kinase activity evoked by the mutation of the gatekeeper residue (Zhang, C. et al. 2005). Equally it has been reported that the mutation of the gatekeeper residue to alanine, instead of glycine, leads to a more stable conformation, thereby supporting activity of inhibitor-sensitised kinases (Bishop, A. et al. 2000; Zhang, C. et al. 2005). The identification of second-site suppressor mutations was based on sequence analysis of kinases of higher eukaryotes, which is not necessarily applicable for kinetoplastid kinases and also involves the laborious generation of several mutations. It was therefore rather attempted to generate a more active inhibitor-sensitised mutant of LmxMPK4IS by exchanging the gatekeeper residue methionine111 to alanine. The resulting inhibitor-sensitised mutant was termed LmxMPK4ISMA, to distinguish it from the previously investigated mutant LmxMPK4IS, which contained the gatekeeper mutation M111G. Kinase assays of recombinant LmxMPK4ISMA, co-expressed with LmxMKK5, showed that the inhibitor-sensitised mutant indeed displayed a higher phosphotransferase activity than co-expressed LmxMPK4IS (Fig. 41) and was inhibitable by 1Na in a dose-dependent manner (Fig. 42). Although the activation of LmxMPK4ISMA was still not comparable to the activation of wild type LmxMPK4 by LmxMKK5 (Fig. 41), the phosphotransferase activity present in LmxMPK4ISMA could be enough to use LmxMPK4ISMA in thiophosphate labelling experiments of possible substrates and to reduce possible compensatory effects *in vivo*. Therefore, the *L. mexicana* mutant A10, expressing only the LmxMPK4ISMA mutant and no wild type LmxMPK4 from the genomic locus of LmxMPK4, was generated. Preliminary experiments showed that 1Na inhibited the growth of the inhibitor-sensitised mutant A10 in a dose-dependent manner, with full growth arrest occurring when 1Na was added to the culture at a concentration of 0.5 µM or higher (Fig. 44). Future research will show if the changes in metabolism resulting from the

impaired activity of the inhibitor-sensitised LmxMPK4IS mutant are less pronounced in cells expressing the new LmxMPK4ISMA mutant. It will also be interesting to see whether thiophosphate labelling experiments yield possible substrates for LmxMPK4 and if these comply with any of the theories for LmxMPK4 function, proposed in this discussion.

Furthermore, a noteworthy observation was made in the Southern blot analysis conducted to verify the genomic integration of *LmxMPK4ISMA* and the deletion of the wild type *LmxMPK4* gene. The Southern blot used samples of genomic DNA and of the inhibitor-sensitised mutant BF11H4, solely expressing LmxMPK4IS, as positive controls. BF11H4 was generated by integrating the gene for *LmxMPK4IS* (M111G) into the original genomic locus of LmxMPK4 on one allele. Original experiments confirmed the integration of *LmxMPK4IS* and the presence of hygromycin resistance conferred by the LmxMPK4 deletion-cassette on the other allele. The Southern blot shown in Fig. 43, however, does not detect the presence of the LmxMPK4 hygromycin-resistance conferring deletion cassette. This observation was not apparent in earlier Southern blot analyses as they used a probe hybridising within the gene *LmxMPK4* to confirm *LmxMPK4IS* integration (Fig. 22). Growth experiments confirmed the emerged absence of hygromycin resistance in BF11H4 cells, supporting the notion that the inhibitor-sensitised mutant strain BF11H4 has duplicated the *LmxMPK4IS* gene and now contains it on both alleles. It is not possible to say when this event has happened, but as the metabolic profiling experiments were conducted shortly before the Southern Blot analysis shown in Fig. 43, it is likely that BF11H4 mutants already contained *LmxMPK4IS* on both alleles. This excludes the possibility that any observed metabolic changes in the inhibitor-sensitised mutant without the full inhibition of LmxMPK4IS by addition of 1Na, are simply due to effects caused by lower expression of LmxMPK4IS from one allele.

5.2 LmxMPK6

The *L. mexicana* MAP kinase homologue LmxMPK6, which also comprises attributes of cyclin-dependent protein kinases, contains a TDY-motif in its activation loop and was found to be upregulated in stationary phase promastigotes (Wiese, M. et al. 2003b). During the course of this thesis the kinase-dead mutant LmxMPK6K33M was generated and recombinantly expressed as a GST-tag fusion protein in *E. coli* alongside wild type LmxMPK6. The investigation of *E. coli* cell lysates before and after the induction of recombinant expression demonstrated the appearance of a protein band corresponding in size to the 144 kDa of GST-LmxMPK6, after expression was induced (Fig. 46). Immunoblot analysis using antiserum against the carboxy-terminal peptide of LmxMPK6 detected a band at the same size (Fig. 47), alongside several other proteins. This implies that the antiserum either cross-reacted with other proteins than GST-LmxMPK6 or a high

amount of degradation reduced the abundance of recombinant GST-LmxMPK6. Nevertheless, considering the detection of the same band corresponding in size to GST-LmxMPK6 after expression was induced and in immunoblot analysis, this band was justifiably assigned as GST-LmxMPK6. Although GST-LmxMPK6 did not appear in overly high amounts in *E. coli* lysates induced over night, it was still the highest abundant protein band in the lysate (Fig. 46). After affinity purification on glutathione-sepharose, however, GST-LmxMPK6 ceased to be of the highest abundance in the mixture of several co-purified proteins (Fig. 45). The poor recombinant expression and inadequate purification are very likely consequences of the large size of GST-LmxMPK6. The quantities of expressed GST-LmxMPK6 are already relatively low in cell lysates at the beginning of purification so that poor binding to the glutathione-sepharose results in an eluate which contains only marginal amounts of GST-LmxMPK6 alongside several other co-purified proteins of *E. coli* origin. It was unsuccessfully attempted to generate higher amounts of recombinant GST-LmxMPK6 by expression in BL21-CodonPlus (DE3)-RP cells, which supply a higher amount of additional G-C rich tRNAs that are normally rare in *E. coli* but might be limiting in the expression of *Leishmania* proteins. Despite the poor results from the recombinant expression and purification of GST-LmxMPK6, kinase assays were conducted with the eluted recombinant proteins and GST-LmxMPK6 was found to hold a distinct phosphotransferase activity towards MBP but no autophosphorylation activity (Fig. 48). This was the first experimental validation that LmxMPK6 indeed functions as a kinase. The displayed phosphorylation of MBP was proven to be caused by the activity of GST-LmxMPK6 and not by any co-purified bacterial kinases, as it did not occur in the presence of the kinase-dead mutant GST-LmxMPK6K33M. This result showed in addition that the generation of a kinase-dead mutant that did not possess the ability to correctly bind and align ATP after mutating lysine33 to methionine had been successful. Further analysis by kinase assays revealed that the phosphotransferase activity of GST-LmxMPK6 was not noticeably changed when the assay was conducted at 27°C or 34°C. This contradicts expectations to a certain extent, as LmxMPK6 had been found to be upregulated in stationary-phase promastigotes (Wiese, M. et al. 2003b), suggesting that LmxMPK6 might be more active at 27°C due to a more important role in promastigotes. However, the upregulation of mRNA levels does not necessarily imply that LmxMPK6 plays no role in amastigotes and even if LmxMPK6 were only active in promastigotes the regulation of its function could be caused by many other factors like protein degradation or mRNA stability instead of being differentially regulated by temperature. The kinase activity of GST-LmxMPK6 was apparent at a wide range of pH-levels with the highest activity present at pH 7.2. This is in accordance with the findings that *Leishmania* strictly control homeostasis to keep their pH balanced between 6.5 and 7.4, despite highly varying extracellular pH levels during their life cycle (Zilberstein, D. et al. 1994).

5.2.1 Analysis of the role of the C-terminus of LmxMPK6

LmxMPK6 is one of only two *L. mexicana* MAP kinase homologues with an extremely prolonged carboxy-terminus (Wiese, M. et al. 2003b). Within the C-terminus of LmxMPK6 four possible SH3-binding sites and two possible nuclear localisation signals have been identified (Wiese, M. et al. 2003b). SH3-motifs constitute binding sites for proline-rich peptides of, for instance, scaffold proteins or regulatory proteins (Engstrom, W. et al. 2010; Scott, J. D. et al. 2009). C-terminal extensions in other kinases have been found to play various roles. The C-terminus of ERK7 is required for kinase activity and for the subcellular localization of the MAP kinase (Abe, M. K. et al. 1999). The kinase activity of ERK5 on the other hand was greatly increased by the truncation of its C-terminal extension, but its nucleocytoplasmic shuttling was equally impaired (Buschbeck, M. et al. 2005). The prolonged C-terminus of TbECK1, the *T. brucei* homologue of LmxMPK6, has been suggested to have a negative autoregulatory function on the kinase as its absence leads to an aberrant activity of the truncated TbECK1 and consequently to abnormal phenotypes (Ellis, J. et al. 2004). To investigate the function of the C-terminal extension of LmxMPK6, two different truncated versions of the protein were created. The mutant LmxMPK6short was truncated directly after the kinase domain of LmxMPK6, while LmxMPK6short2TY additionally contained 78 amino acids of the C-terminus and thereby corresponded to the truncated mutant of TbECK1 used by Ellis et al. (Ellis, J. et al. 2004). The recombinant expression of both truncated mutants as GST-fusion proteins in *E. coli* yielded reasonable quantities of rather pure protein and was therefore drastically superior to the recombinant expression of the full-length GST-LmxMPK6. This confirms the notion that the poor recombinant expression of GST-LmxMPK6 and GST-LmxMPK6K33M is due to the large size of the proteins, as discussed earlier. GST-LmxMPK6short did not display any phosphotransferase activity towards MBP but a slight amount of autophosphorylation (Fig. 52, lanes 3, 3'). GST-LmxMPK6short2TY on the other hand phosphorylated MBP significantly and also displayed a prominent autophosphorylation (Fig. 52, lanes 4, 4'). This finding demonstrates that the additional 78 amino acids of the C-terminal extension which are present in LmxMPK6short2TY are essential for kinase activity. Despite the fact that the α-helix usually present in kinases C-terminal of the kinase domain had not been predicted for LmxMPK6, this region still played an indispensable role for the kinase activity of LmxMPK6 and likely does contain the α-helix. The phosphotransferase activity of GST-LmxMPK6short2TY towards MBP showed no consistent results in comparison with kinase activity levels of full-length GST-LmxMPK6. This is most likely at least partially due to the difficulty in judging protein levels of GST-LmxMPK6 contained in the kinase assays, owing to its extremely low abundance in protein eluates. No statement can therefore be made regarding the phosphotransferase activity of GST-LmxMPK6short2TY in comparison to the wild type protein GST-LmxMPK6 which contained the full C-terminal extension. It is

however striking that full-length GST-LmxMPK6 does not display any auto-phosphorylation, while both truncated mutants autophosphorylate. This can be viewed as an indicator for the enhanced activity of GST-LmxMPK6short2TY. The findings are in accordance with properties of ERK5. Truncated versions of ERK5 showed higher auto-phosphorylation than the wild type protein ERK5, but autophosphorylation decreased with increasing truncation of the protein (Buschbeck, M. et al. 2005). ERK5 was intriguingly also able to autophosphorylate within its C-terminus (Mody, N. et al. 2003).

To summarise, the truncation of LmxMPK6 at 78 amino acids after the end of its kinase domain led to the generation of LmxMPK6short2TY which could be recombinantly expressed to high quantities of pure protein and displayed a distinct phosphotransferase activity towards MBP as well as autophosphorylation activity. The 78 amino acids remaining of the C-terminus were required for the observed activity.

As LmxMPK6short2TY was constitutively active *in vitro* it was employed for *in vivo* investigations. The full-length protein TbECK1, the *T. brucei* homologue of LmxMPK6, was expressed from a tetracycline-inducible plasmid in *T. brucei* procyclics, which did not result in a distinct phenotype. When the truncated mutant of TbECK1 was extra-chromosomally expressed against an endogenous background expression of the full-length protein procyclic *T. brucei* cells displayed reduced growth and a high abundance of aberrant karyotypes. As the aberrant phenotype only emerged when the truncated mutant of TbECK1 was active, it was proposed that the C-terminus of TbECK1 has a negative autoregulatory function on the kinase (Ellis, J. et al. 2004). The extrachromosomal expression of LmxMPK6short2TY, the active truncated mutant of LmxMPK6, in the presence of genomic expression of endogenous full-length LmxMPK6 did not lead to any visible phenotype (Fig. 54). Neither did cells display delayed growth nor did they have a vast number of aberrant karyotypes. This indicates that the C-terminus in LmxMPK6 possibly does not play the same autoregulatory role as in its *T. brucei* homologue. However, it is also very likely that the observation of no phenotype results from the experimental approach used. Unlike for the TbECK1 analysis in *T. brucei,* the extra-chromosomal expression of LmxMPK6short2TY was not inducible by tetracycline. The transformation of promastigotes with pXpolPacMPK6short2TY and subsequent selection of positive clones could therefore select cells which are able to compensate the aberrant phenotypes induced by the presence of irregularly active LmxMPK6short2TY. Compensation could take place by suppression of plasmid numbers, by the inhibition of extrachromosomal expression or by degradation of the aberrantly active protein. The fact that attempts to detect extrachromosomal expression of LmxMPK6short2TY by immunoblot analysis using antiserum against the N-terminal end of LmxMPK6 (data not shown) failed, could be consistent with a lack of LmxMPK6short2TY in cells due to

compensation, but is by no means proof. Unfortunately, it was not possible within the scope of this thesis to investigate further, but future research would have to generate *L. mexicana* cell lines which allow tetracycline-inducible expression of proteins, as has been done for *L. chagasi* and *L. donovani* respectively (Yan, S. et al. 2002; Yao, C. et al. 2007).

As it was not possible to deduce any negative autoregulatory function of the C-terminal extension *in vivo* and the comparison of the *in vitro* kinase activity of full-length GST-LmxMPK6 with truncated GST-LmxMPK6short2TY was challenging, the effect of the C-terminus was investigated with the help of the pJCduet co-expression system. The poor expression and purification of full-length GST-LmxMPK6 were most likely arising from the large size of the protein. Therefore, the C-terminus and N-terminus of LmxMPK6 were cloned separately. With the help of the pJCduet co-expression system (John von Freyend, S. et al. 2010) it was possible to analyse the influence of the C-terminus on the kinase activity of the N-terminus. The recombinant expression and His-tag purification of His-LmxMPK6Nterm yielded high levels of pure, active recombinant protein (Fig. 57), which was considerably more active than GST-LmxMPK6short2TY (Fig. 57 and Fig. 58). The only difference between recombinant GST-LmxMPK6short2TY and His-LmxMPK6Nterm was in the choice of tags with which the proteins were expressed. This indicates that the GST-tag and possibly also the much smaller TY-tag have a negative impact on the expression levels and purification results of LmxMPKshort2, as well as on the phosphotransferase activity of LmxMPK6short2 to a certain extent. This finding is contrary to the enhanced expression of GST-LmxMPK4 in comparison to His-LmxMPK4 (4.1.2.2), which demonstrates that the choice of tag for recombinant expression must be validated independently for every protein. It can therefore be expected that the expression of full-length LmxMPK6 should also yield higher levels of protein after recombinant expression as a His-tag protein. It is nevertheless likely that the poor expression of LmxMPK6 is also due to the large size of the protein which can lead to premature abortion of translation and subsequent degradation of the protein. The co-expression of His-LmxMPK6Nterm with S-LmxMPK6Cterm had no definite effect on the kinase activity of His-LmxMPK6Nterm. A slight reduction in kinase activity was visible after the co-expression with S-LmxMPK6Cterm, but this could quite likely result from variations in the assay (Fig. 57). It is therefore unlikely that the C-terminus of LmxMPK6 has a negative autoregulatory function towards the kinase activity of LmxMPK6 *in vitro*, contrary to ERK5 in which the presence of the C-terminus has a negative effect on *in vitro* phosphotransferase activity (Buschbeck, M. et al. 2005). However, it can not be excluded that in *Leishmania* the C-terminus plays a role in regulation of LmxMPK6, as has been shown for the tyrosine kinases c-Src (Bjorge, J. D. et al. 2000), c-Abl (Pluk, H. et al. 2002), Bcr-Abl (Smith, K. M. et al. 2003) and the *T. brucei* homologue TbECK1 (Ellis, J. et al. 2004). The influence of

the C-terminus of TbECK1 on its *in vitro* kinase activity has not been investigated by Ellis et al., which is why it is still conceivable that TbECK1 and LmxMPK6 share the same regulatory mechanism. A regulatory influence of the C-terminus could be due to the binding of other proteins to the SH3-domains of the C-terminus changing its structure or to the translocation of the kinase into the nucleus. The translocation into the nucleus is somewhat unlikely as transcriptional control plays only a marginal role in kinetoplastids.

5.2.2 Deletion of LmxMPK6 in *Leishmania*

The transcript of TbECK1, the *T. brucei* homologue of LmxMPK6, could not be ablated in *T. brucei* through RNAi (Ellis, J. et al. 2004). This could be an indicator that the kinase is essential in trypanosomes as leaky dsRNA production would then lead to the selection of RNAi refractory cells (Ellis, J. et al. 2004). Deletion analyses of LmxMPK6 in *L. mexicana* promastigotes were carried out to show whether the protein was essential. Single allele knock-out mutants, which carried the wild type *LmxMPK6* gene on one allele and the deletion cassette conferring hygromycin resistance on the other, were generated repeatedly without problems. However, neither the generation of single allele knock-outs using the neomycin or phleomycin resistance marker, nor the generation of a double allele knock-out was successful. This could indeed indicate that LmxMPK6 is essential in *L. mexicana* promastigotes, but it is just as possible that the failure was due to properties of the neomycin and phleomycin resistance markers. The fact that no single allele knock-out mutants with these resistance markers could be obtained seems to point to the suggestion of the *LmxMPK6* gene locus being difficult to access. Yet why the locus would be accessible for the hygromycin resistance marker cassette but not for the ones carrying neomycin or phleomycin resistance is not clear. Another possible explanation would be that endogenous expression of the *LmxMPK6* locus is extremely low, impeding the establishment of resistance. Yet again it is unclear why this should affect neomycin and phleomycin resistance markers, but not hygromycin. However, if expression levels of the genomic locus of *LmxMPK6* were the issue then deletion cassettes including the gene for dihydrofolate reductase-thymidylate synthase (DHFR-TS) in addition to resistance markers should pose a solution, as the DHFR-TS gene confers high levels of expression. Deletion constructs carrying the DHFR-TS gene in addition to genes conferring hygromycin, phleomycin or puromycin resistance were generated during the work for this thesis. The generation of mutants and knock-out analyses, however, exceeded the given time frame. In addition plasmids carrying an extrachromosomal copy of wild type *LmxMPK6* were created and transformed into cells (Fig. 61). The deletion of the genomic copies of LmxMPK6 should be unproblematic in those cells carrying the gene extrachromosomally (add-back mutants). It will be revealed by future research if cells

subsequently retain copies of the plasmid carrying *LmxMPK6*, which would strongly indicate the essentiality of LmxMPK6.

If LmxMPK6 will indeed turn out to be essential a system to recombinantly express the highly active truncated version LmxMPK6Nterm in large quantities is already in place. Therefore, if LmxMPK6 will prove to be a drug target, His-LmxMPK6Nterm will be available to conduct drug screenings.

6. Summary

Kinetoplastid parasites of the genus *Leishmania* are responsible for a wide range of diseases known as leishmaniases, which affect 14 million people worldwide. Although treatment against the leishmaniases is available, it leaves much to be desired, as there are a number of adverse effects and existing resistances against drugs are growing, with new ones emerging. The search for and analysis of potential drug targets consequently constitutes an extremely important field of fundamental *Leishmania* research.

In all organisms signal transduction pathways play central roles in translating external stimuli into cellular responses, in particular by relaying phosphorylations with the help of kinases. Mitogen-activated protein (MAP) kinases, which constitute highly conserved pathways in all eukaryotes, represent a large portion of the kinetoplastid kinome and are therefore highly interesting research subjects. This thesis was concerned with the analysis of the two MAP kinase homologues, LmxMPK4 and LmxMPK6, of *Leishmania mexicana*. Previous investigations had already identified LmxMPK4 as a potential drug target as it was shown to be essential in amastigotes and promastigotes. The research presented in the thesis at hand successfully identified the MAP2K homologue LmxMKK5 as the *in vitro* activator of LmxMPK4. Recombinant co-expression of the two kinases in *E. coli* led to the purification of a highly active LmxMPK4, which could be inhibited by small molecules. LmxMKK5 was shown to phosphorylate LmxMPK4 in the typical pattern of MAP2Ks on the tyrosine and threonine residue of its TXY-motif in the activation loop, leading to an activation of recombinant LmxMPK4. The previously described weak autophosphorylation activity of recombinant LmxMPK4 was also confirmed and ascertained to be due to tyrosine phosphorylation of the TXY-motif. *In vivo* investigations revealed that *L. mexicana* promastigotes expressing solely the inhibitor-sensitised mutant LmxMPK4IS grow as well as wild type parasites, but undergo a growth arrest in response to the specific inhibition of LmxMPK4IS by the inhibitor 1-naphthyl-pyrazolo[3,4*d*]pyrimidine (1Na). The growth arrest was mostly reversible, resulting in the hypothesis that the inhibition of LmxMPK4IS in promastigotes leads to a metabolic arrest rather than apoptosis or cell lysis. This hypothesis was endorsed by metabolic profiling experiments which revealed a central role of LmxMPK4 in metabolic regulation, as the inhibition of LmxMPK4IS resulted in changes in the abundance of many metabolites, mainly lipids and amino acids. This was the first time that a MAP kinase was implicated in the control of metabolism in *Leishmania.* The importance of LmxMPK4 was further supported by the observation that a full inhibition of LmxMPK4IS was not even required to evoke strong changes in several metabolites. The impairment of LmxMPK4 activity that had been demonstrated in *in vitro* kinase assays to result from the inhibitor-sensitising mutation, already greatly impacted *L. mexicana* promastigote metabolism. This was shown in *L. mexicana* mutants expressing solely the

inhibitor-sensitised LmxMPK4IS that were grown without the addition of inhibitor. Therefore the role of LmxMPK4 in promastigotes is central and, as long exposures to the inhibitor had a cytotoxic effect instead of leading to a reversible growth arrest, very likely essential. The effects of the impaired activity of LmxMPK4IS in amastigotes, however, were even more pronounced. *L. mexicana* mutants expressing LmxMPK4IS showed a delayed differentiation into axenic amastigotes and did not induce the development of lesions, but persisted in mouse infection experiments without the addition of the inhibitor 1Na. In these experiments LmxMPK4IS was not fully inhibited by 1Na, but the impaired kinase activity, which was induced by the inhibitor-sensitising mutation, already led to the observed phenotypes. As LmxMPK4 leads to such drastic effects in amastigotes when its kinase activity is impaired it is to be expected that the full inhibition of LmxMPK4 would be cytotoxic and that LmxMPK4 is therefore indeed essential in amastigotes. This claim is consistent with previous studies, which had shown that mutant *L. mexicana* amastigotes expressing no genomic copy of *LmxMPK4*, but solely an extrachromosomal one, retain the plasmid during prolonged mouse infection experiments. Activated recombinant LmxMPK4, co-expressed with LmxMKK5, can therefore be used in screenings to search for specific inhibitors of the drug target LmxMPK4, potentially leading to the development of new anti-leishmanial drugs.

LmxMPK6 a previously unstudied *L. mexicana* MAP kinase with an unusually long C-terminus was demonstrated to be an active kinase, as the recombinant protein displayed *in vitro* phosphotransferase activity towards the exogenous substrate MBP. An inactive mutant, LmxMPK6K33M, was successfully generated and the role of the C-terminus was investigated with the help of truncated mutants. It was demonstrated that the kinase activity of LmxMPK6 was dependent on the presence of 78 amino acids after the end of the kinase domain, but not on the presence of the remaining C-terminus. The truncation directly after the kinase domain did not lead to an active protein, whereas the truncated mutant LmxMPK6short2 that was 78 amino acids longer displayed a distinct kinase and autophosphorylation activity. A negative autoregulatory function of the C-terminus, as it was proposed for the LmxMPK6 homologue in *Trypanosoma brucei,* TbECK1, could not be confirmed for LmxMPK6. Deletion experiments to determine whether LmxMPK6 is essential for *Leishmania* were conducted, but several successive rounds of electroporation did not produce a double allele knock-out mutant, suggesting that LmxMPK6 might be essential. Final proof of essentiality will be gained by the deletion of both *LmxMPK6* alleles in the generated *L. mexicana* mutants that additionally express LmxMPK6 from a plasmid. If those cells retain the extrachromosomal version of *LmxMPK6* without antibiotic selection pressure, the gene can be viewed as essential in promastigotes. If LmxMPK6 indeed proves to be a potential drug target in *Leishmania,* the highly active truncated version LmxMPK6Nterm, which can easily be expressed to high

amounts as a recombinant hexahistidine-tag fusion protein, will already be available to conduct drug screenings.

Reference List

Abe, M. K., Kuo, W. L., Hershenson, M. B., and Rosner, M. R. (1999) Extracellular signal-regulated kinase 7 (ERK7), a novel ERK with a C-terminal domain that regulates its activity, its cellular localization, and cell growth. Mol. Cell Biol. 19 (2): 1301

Adams, J., Huang, P., and Patrick, D. (2002) A strategy for the design of multiplex inhibitors for kinase-mediated signalling in angiogenesis. Curr. Opin. Chem. Biol. 6 (4): 486

Agron, P. G., Reed, S. L., and Engel, J. N. (2005) An essential, putative MEK kinase of *Leishmania major*. Mol. Biochem. Parasitol. 142 (1): 121

Akerman, M., Shaked-Mishan, P., Mazareb, S., Volpin, H., and Zilberstein, D. (2004) Novel motifs in amino acid permease genes from *Leishmania*. Biochem. Biophys. Res. Commun. 325 (1): 353

Akopyants, N. S., Kimblin, N., Secundino, N., Patrick, R., Peters, N., Lawyer, P., Dobson, D. E., Beverley, S. M., and Sacks, D. L. (2009) Demonstration of genetic exchange during cyclical development of *Leishmania* in the sand fly vector. Science 324 (5924): 265

Andreasson, E. and Ellis, B. (2010) Convergence and specificity in the *Arabidopsis* MAPK nexus. Trends Plant Sci. 15 (2): 106

Aranda, A., Maugeri, D., Uttaro, A. D., Opperdoes, F., Cazzulo, J. J., and Nowicki, C. (2006) The malate dehydrogenase isoforms from *Trypanosoma brucei*: subcellular localization and differential expression in bloodstream and procyclic forms. Int. J. Parasitol. 36 (3): 295

Bacchi, C. J., Nathan, H. C., Yarlett, N., Goldberg, B., McCann, P. P., Bitonti, A. J., and Sjoerdsma, A. (1992) Cure of murine *Trypanosoma brucei rhodesiense* infections with an S-adenosylmethionine decarboxylase inhibitor. Antimicrob. Agents Chemother. 36 (12): 2736

Bailey, H. and BISHOP, W. J. (1959) Leishman-Donovan bodies and donovaniasis; Sir William Boog Leishman, 1865-1926; Charles Donovan, 1863-1951. Br. J. Vener. Dis. 35 (1): 8

Bates, P. A. (2007) Transmission of *Leishmania* metacyclic promastigotes by phlebotomine sand flies. Int. J. Parasitol. 37 (10): 1097

Bates, P. A., Robertson, C. D., Tetley, L., and Coombs, G. H. (1992) Axenic cultivation and characterization of *Leishmania mexicana* amastigote-like forms. Parasitology 105 (Pt 2) : 193

Bates, P. A. and Rogers, M. E. (2004) New insights into the developmental biology and transmission mechanisms of *Leishmania*. Curr. Mol. Med. 4 (6): 601

Bee, A., Culley, F. J., Alkhalife, I. S., Bodman-Smith, K. B., Raynes, J. G., and Bates, P. A. (2001) Transformation of *Leishmania mexicana* metacyclic promastigotes to amastigote-like forms mediated by binding of human C-reactive protein. Parasitology 122 (Pt 5): 521

Bengs, F., Scholz, A., Kuhn, D., and Wiese, M. (2005) LmxMPK9, a mitogen-activated protein kinase homologue affects flagellar length in *Leishmania mexicana*. Mol. Microbiol. 55 (5): 1606

Berman, J. D., Gallalee, J. V., and Best, J. M. (1987) Sodium stibogluconate (Pentostam) inhibition of glucose catabolism via the glycolytic pathway, and fatty acid beta-oxidation in *Leishmania mexicana* amastigotes. Biochem. Pharmacol. 36 (2): 197

Bishop, A., Buzko, O., Heyeck-Dumas, S., Jung, I., Kraybill, B., Liu, Y., Shah, K., Ulrich, S., Witucki, L., Yang, F., Zhang, C., and Shokat, K. M. (2000) Unnatural ligands for engineered proteins: new tools for chemical genetics. Annu. Rev. Biophys. Biomol. Struct. 29 : 577

Bishop, A. C., Buzko, O., and Shokat, K. M. (2001) Magic bullets for protein kinases. Trends Cell Biol. 11 (4): 167

Bishop, A. C., Ubersax, J. A., Petsch, D. T., Matheos, D. P., Gray, N. S., Blethrow, J., Shimizu, E., Tsien, J. Z., Schultz, P. G., Rose, M. D., Wood, J. L., Morgan, D. O., and Shokat, K. M. (2000) A chemical switch for inhibitor-sensitive alleles of any protein kinase. Nature 407 (6802): 395

Bitonti, A. J., Byers, T. L., Bush, T. L., Casara, P. J., Bacchi, C. J., Clarkson, A. B., Jr., McCann, P. P., and Sjoerdsma, A. (1990) Cure of *Trypanosoma brucei brucei* and *Trypanosoma brucei rhodesiense* infections in mice with an irreversible inhibitor of S-adenosylmethionine decarboxylase. Antimicrob. Agents Chemother. 34 (8): 1485

Bjorge, J. D., Jakymiw, A., and Fujita, D. J. (2000) Selected glimpses into the activation and function of Src kinase. Oncogene 19 (49): 5620

Blethrow, J. D., Glavy, J. S., Morgan, D. O., and Shokat, K. M. (2008) Covalent capture of kinase-specific phosphopeptides reveals Cdk1-cyclin B substrates. Proc. Natl. Acad. Sci. U. S. A 105 (5): 1442

Bocedi, A., Dawood, K. F., Fabrini, R., Federici, G., Gradoni, L., Pedersen, J. Z., and Ricci, G. (2010) Trypanothione efficiently intercepts nitric oxide as a harmless iron complex in trypanosomatid parasites. FASEB J. 24 (4): 1035

Bogdan, C., Donhauser, N., Doring, R., Rollinghoff, M., Diefenbach, A., and Rittig, M. G. (2000) Fibroblasts as host cells in latent leishmaniosis. J. Exp. Med. 191 (12): 2121

Breitling, R., Pitt, A. R., and Barrett, M. P. (2006a) Precision mapping of the metabolome. Trends Biotechnol. 24 (12): 543

Breitling, R., Ritchie, S., Goodenowe, D., Stewart, M. L., and Barrett, M. P. (2006b) *Ab initio* prediction of metabolic networks using Fourier Transform Mass Spectrometry data. Metabolomics. 2 : 155

Bringaud, F., Riviere, L., and Coustou, V. (2006) Energy metabolism of trypanosomatids: adaptation to available carbon sources. Mol. Biochem. Parasitol. 149 (1): 1

Bringaud, F., Vedrenne, C., Cuvillier, A., Parzy, D., Baltz, D., Tetaud, E., Pays, E., Venegas, J., Merlin, G., and Baltz, T. (1998) Conserved organization of genes in trypanosomatids. Mol. Biochem. Parasitol. 94 (2): 249

Brody, S. (1927) TIME RELATIONS OF GROWTH : III. GROWTH CONSTANTS DURING THE SELF-ACCELERATING PHASE OF GROWTH. J. Gen. Physiol 10 (5): 637

Bruce-Chwatt, L. J. (1972) Blood transfusion and tropical disease. Trop. Dis. Bull. 69 (9): 825

Brun, R. and Jenni, L. (1977) A new semi-defined medium for *Trypanosoma brucei sspp*. Acta Trop. 34 (1): 21

Burchmore, R. J. and Barrett, M. P. (2001) Life in vacuoles--nutrient acquisition by *Leishmania* amastigotes. Int. J. Parasitol. 31 (12): 1311

Buschbeck, M. and Ullrich, A. (2005) The unique C-terminal tail of the mitogen-activated protein kinase ERK5 regulates its activation and nuclear shuttling. J. Biol. Chem. 280 (4): 2659

Cameron, M. M., Pessoa, F. A., Vasconcelos, A. W., and Ward, R. D. (1995) Sugar meal sources for the phlebotomine sandfly *Lutzomyia longipalpis* in Ceara State, Brazil. Med. Vet. Entomol. 9 (3): 263

Cerf, B. J., Jones, T. C., Badaro, R., Sampaio, D., Teixeira, R., and Johnson, W. D., Jr. (1987) Malnutrition as a risk factor for severe visceral leishmaniasis. J. Infect. Dis. 156 (6): 1030

Chang, L. and Karin, M. (2001) Mammalian MAP kinase signalling cascades. Nature 410 (6824): 37

Chavali, A. K., Whittemore, J. D., Eddy, J. A., Williams, K. T., and Papin, J. A. (2008) Systems analysis of metabolism in the pathogenic trypanosomatid *Leishmania major*. Mol. Syst. Biol. 4 : 177

Clark-Lewis, I., Sanghera, J. S., and Pelech, S. L. (1991) Definition of a consensus sequence for peptide substrate recognition by p44mpk, the meiosis-activated myelin basic protein kinase. J. Biol. Chem. 266 (23): 15180

Clayton, C. E. (2002) Life without transcriptional control? From fly to man and back again. EMBO J. 21 (8): 1881

Cohen, P. (2009) Targeting protein kinases for the development of anti-inflammatory drugs. Curr. Opin. Cell Biol. 21 (2): 317

Crews, C. M., Alessandrini, A., and Erikson, R. L. (1992) The primary structure of MEK, a protein kinase that phosphorylates the ERK gene product. Science 258 (5081): 478

Croft, S. L., Seifert, K., and Yardley, V. (2006) Current scenario of drug development for leishmaniasis. Indian J. Med. Res. 123 (3): 399

Cruz, A., Coburn, C. M., and Beverley, S. M. (1991) Double targeted gene replacement for creating null mutants. Proc. Natl. Acad. Sci. U. S. A 88 (16): 7170

Cruz, I., Nieto, J., Moreno, J., Canavate, C., Desjeux, P., and Alvar, J. (2006) *Leishmania*/HIV co-infections in the second decade. Indian J. Med. Res. 123 (3): 357

Culley, F. J., Harris, R. A., Kaye, P. M., McAdam, K. P., and Raynes, J. G. (1996) C-reactive protein binds to a novel ligand on *Leishmania donovani* and increases uptake into human macrophages. J. Immunol. 156 (12): 4691

Darlyuk, I., Goldman, A., Roberts, S. C., Ullman, B., Rentsch, D., and Zilberstein, D. (2009) Arginine homeostasis and transport in the human pathogen *Leishmania donovani*. J. Biol. Chem. 284 (30): 19800

Davidson, R. N., den, Boer M., and Ritmeijer, K. (2009) Paromomycin. Trans. R. Soc. Trop. Med. Hyg. 103 (7): 653

Davis, R. J. (1993) The mitogen-activated protein kinase signal transduction pathway. J. Biol. Chem. 268 (20): 14553

de, Nadal E., Alepuz, P. M., and Posas, F. (2002) Dealing with osmostress through MAP kinase activation. EMBO Rep. 3 (8): 735

Depledge, D. P., Evans, K. J., Ivens, A. C., Aziz, N., Maroof, A., Kaye, P. M., and Smith, D. F. (2009) Comparative expression profiling of *Leishmania*: modulation in gene expression between species and in different host genetic backgrounds. PLoS. Negl. Trop. Dis. 3 (7): e476

Desjeux, P. (2001) Worldwide increasing risk factors for leishmaniasis. Med. Microbiol. Immunol. 190 (1-2): 77

Desjeux, P. (2004) Leishmaniasis: current situation and new perspectives. Comp Immunol. Microbiol. Infect. Dis. 27 (5): 305

Docampo, R., de, Souza W., Miranda, K., Rohloff, P., and Moreno, S. N. (2005) Acidocalcisomes - conserved from bacteria to man. Nat. Rev. Microbiol. 3 (3): 251

Docampo, R. and Pignataro, O. P. (1991) The inositol phosphate/diacylglycerol signalling pathway in *Trypanosoma cruzi*. Biochem. J. 275 (Pt 2) : 407

Domenicali, Pfister D., Burkard, G., Morand, S., Renggli, C. K., Roditi, I., and Vassella, E. (2006) A Mitogen-activated protein kinase controls differentiation of bloodstream forms of *Trypanosoma brucei*. Eukaryot. Cell 5 (7): 1126

Donovan, C. (1903) Memoranda: On the possibility of the occurence of trypanomiasis in India. The British Medical Journal : 1252

Doyle, M. A., Macrae, J. I., DE Souza, D. P., Saunders, E. C., McConville, M. J., and Likic, V. A. (2009) LeishCyc: a biochemical pathways database for *Leishmania major*. BMC. Syst. Biol. 3 : 57

Dunn, W. B., Bailey, N. J., and Johnson, H. E. (2005) Measuring the metabolome: current analytical technologies. Analyst 130 (5): 606

Ellis, J., Sarkar, M., Hendriks, E., and Matthews, K. (2004) A novel ERK-like, CRK-like protein kinase that modulates growth in *Trypanosoma brucei* via an autoregulatory C-terminal extension. Mol. Microbiol. 53 (5): 1487

Eltoum, I. A., Zijlstra, E. E., Ali, M. S., Ghalib, H. W., Satti, M. M., Eltoum, B., and el-Hassan, A. M. (1992) Congenital kala-azar and leishmaniasis in the placenta. Am. J. Trop. Med. Hyg. 46 (1): 57

Emanuelsson, O., Nielsen, H., Brunak, S., and Von, Heijne G. (2000) Predicting subcellular localization of proteins based on their N-terminal amino acid sequence. J. Mol. Biol. 300 (4): 1005

Engstrom, W., Ward, A., and Moorwood, K. (2010) The role of scaffold proteins in JNK signalling. Cell Prolif. 43 (1): 56

Ephros, M., Bitnun, A., Shaked, P., Waldman, E., and Zilberstein, D. (1999) Stage-specific activity of pentavalent antimony against *Leishmania donovani* axenic amastigotes. Antimicrob. Agents Chemother. 43 (2): 278

Erdmann, M. (2009), PhD thesis, Bernhard Nocht Institute for Tropical Medicine / Department of Biology, University of Hamburg

Erdmann, M., Scholz, A., Melzer, I. M., Schmetz, C., and Wiese, M. (2006) Interacting protein kinases involved in the regulation of flagellar length. Mol. Biol. Cell 17 (4): 2035

Ersfeld, K., Barraclough, H., and Gull, K. (2005) Evolutionary relationships and protein domain architecture in an expanded calpain superfamily in kinetoplastid parasites. J. Mol. Evol. 61 (6): 742

Eyers, P. A., Craxton, M., Morrice, N., Cohen, P., and Goedert, M. (1998) Conversion of SB 203580-insensitive MAP kinase family members to drug-sensitive forms by a single amino-acid substitution. Chem. Biol. 5 (6): 321

Fahy, E., Subramaniam, S., Murphy, R. C., Nishijima, M., Raetz, C. R., Shimizu, T., Spener, F., van, Meer G., Wakelam, M. J., and Dennis, E. A. (2009) Update of the LIPID MAPS comprehensive classification system for lipids. J. Lipid Res. 50 Suppl : S9

Fahy, E., Sud, M., Cotter, D., and Subramaniam, S. (2007) LIPID MAPS online tools for lipid research. Nucleic Acids Res. 35 (Web Server issue): W606

Featherstone, C. and Russell, P. (1991) Fission yeast p107wee1 mitotic inhibitor is a tyrosine/serine kinase. Nature 349 (6312): 808

Fernie, A. R., Trethewey, R. N., Krotzky, A. J., and Willmitzer, L. (2004) Metabolite profiling: from diagnostics to systems biology. Nat. Rev. Mol. Cell Biol. 5 (9): 763

Folgueira, C. and Requena, J. M. (2007) A postgenomic view of the heat shock proteins in kinetoplastids. FEMS Microbiol. Rev. 31 (4): 359

Garofalo, J., Bacchi, C. J., McLaughlin, S. D., Mockenhaupt, D., Trueba, G., and Hutner, S. H. (1982) Ornithine decarboxylase in *Trypanosoma brucei brucei*: evidence for selective toxicity of difluoromethylornithine. J. Protozool. 29 (3): 389

Gaur, U., Roberts, S. C., Dalvi, R. P., Corraliza, I., Ullman, B., and Wilson, M. E. (2007) An effect of parasite-encoded arginase on the outcome of murine cutaneous leishmaniasis. J. Immunol. 179 (12): 8446

Gibbs, C. S. and Zoller, M. J. (1991) Rational scanning mutagenesis of a protein kinase identifies functional regions involved in catalysis and substrate interactions. J. Biol. Chem. 266 (14): 8923

Grewal, S., Molina, D. M., and Bardwell, L. (2006) Mitogen-activated protein kinase (MAPK)-docking sites in MAPK kinases function as tethers that are crucial for MAPK regulation in vivo. Cell Signal. 18 (1): 123

Guan, K. L. and Dixon, J. E. (1991) Eukaryotic proteins expressed in Escherichia coli: an improved thrombin cleavage and purification procedure of fusion proteins with glutathione S-transferase. Anal. Biochem. 192 (2): 262

Gueiros-Filho, F. J. and Beverley, S. M. (1996) Selection against the dihydrofolate reductase-thymidylate synthase (DHFR-TS) locus as a probe of genetic alterations in *Leishmania major*. Mol. Cell Biol. 16 (10): 5655

Haanstra, J. R., van, Tuijl A., Kessler, P., Reijnders, W., Michels, P. A., Westerhoff, H. V., Parsons, M., and Bakker, B. M. (2008) Compartmentation prevents a lethal turbo-explosion of glycolysis in trypanosomes. Proc. Natl. Acad. Sci. U. S. A 105 (46): 17718

Hammarton, T. C. (2007) Cell cycle regulation in *Trypanosoma brucei*. Mol. Biochem. Parasitol. 153 (1): 1

Hammarton, T. C., Clark, J., Douglas, F., Boshart, M., and Mottram, J. C. (2003) Stage-specific differences in cell cycle control in *Trypanosoma brucei* revealed by RNA interference of a mitotic cyclin. J. Biol. Chem. 278 (25): 22877

Hammarton, T. C., Engstler, M., and Mottram, J. C. (2004) The *Trypanosoma brucei* cyclin, CYC2, is required for cell cycle progression through G1 phase and for maintenance of procyclic form cell morphology. J. Biol. Chem. 279 (23): 24757

Han, J., Danell, R. M., Patel, J. R., Gumerov, D. R., Scarlett, C. O., Speir, J. P., Parker, C. E., Rusyn, I., Zeisel, S., and Borchers, C. H. (2008) Towards high-throughput metabolomics using ultrahigh-field Fourier transform ion cyclotron resonance mass spectrometry. Metabolomics. 4 (2): 128

Hanks, S. K. (2003) Genomic analysis of the eukaryotic protein kinase superfamily: a perspective. Genome Biol. 4 (5): 111

Hanks, S. K. and Hunter, T. (1995) Protein kinases 6. The eukaryotic protein kinase superfamily: kinase (catalytic) domain structure and classification. FASEB J. 9 (8): 576

Hart, D. T. and Coombs, G. H. (1982) *Leishmania mexicana*: energy metabolism of amastigotes and promastigotes. Exp. Parasitol. 54 (3): 397

Hassan, P., Fergusson, D., Grant, K. M., and Mottram, J. C. (2001) The CRK3 protein kinase is essential for cell cycle progression of *Leishmania mexicana*. Mol. Biochem. Parasitol. 113 (2): 189

Hellemond, J. J., Bakker, B. M., and Tielens, A. G. (2005) Energy metabolism and its compartmentation in *Trypanosoma brucei*. Adv. Microb. Physiol 50 : 199

Hermoso, T., Fishelson, Z., Becker, S. I., Hirschberg, K., and Jaffe, C. L. (1991) Leishmanial protein kinases phosphorylate components of the complement system. EMBO J. 10 (13): 4061

Holzer, T. R., McMaster, W. R., and Forney, J. D. (2006) Expression profiling by whole-genome interspecies microarray hybridization reveals differential gene expression in procyclic promastigotes, lesion-derived amastigotes, and axenic amastigotes in *Leishmania mexicana*. Mol. Biochem. Parasitol. 146 (2): 198

Hu, Q., Noll, R. J., Li, H., Makarov, A., Hardman, M., and Graham, Cooks R. (2005) The Orbitrap: a new mass spectrometer. J. Mass Spectrom. 40 (4): 430

Hua, S. B. and Wang, C. C. (1997) Interferon-gamma activation of a mitogen-activated protein kinase, KFR1, in the bloodstream form of *Trypanosoma brucei*. J. Biol. Chem. 272 (16): 10797

Hua, Z. M., Yang, X., and Fromm, M. E. (2006) Activation of the NaCl- and drought-induced RD29A and RD29B promoters by constitutively active *Arabidopsis* MAPKK or MAPK proteins. Plant Cell Environ. 29 (9): 1761

Huang, H., Weiss, L. M., Nagajyothi, F., Tanowitz, H. B., Wittner, M., Orr, G. A., and Bao, Y. (2006) Molecular cloning and characterization of the protein kinase A regulatory subunit of *Trypanosoma cruzi*. Mol. Biochem. Parasitol. 149 (2): 242

Hubbard, M. J. and Cohen, P. (1993) On target with a new mechanism for the regulation of protein phosphorylation. Trends Biochem. Sci. 18 (5): 172

Hunter, T. and Plowman, G. D. (1997) The protein kinases of budding yeast: six score and more. Trends Biochem. Sci. 22 (1): 18

Ivens, A. C., Peacock, C. S., Worthey, E. A., Murphy, L., Aggarwal, G., Berriman, M., Sisk, E., Rajandream, M. A., Adlem, E., Aert, R., Anupama, A., Apostolou, Z., Attipoe, P., Bason, N., Bauser, C., Beck, A., Beverley, S. M., Bianchettin, G., Borzym, K., Bothe, G., Bruschi, C. V., Collins, M., Cadag, E., Ciarloni, L., Clayton, C., Coulson, R. M., Cronin, A., Cruz, A. K., Davies, R. M., De, Gaudenzi J., Dobson, D. E., Duesterhoeft, A., Fazelina, G., Fosker, N., Frasch, A. C., Fraser, A., Fuchs, M., Gabel, C., Goble, A., Goffeau, A., Harris, D., Hertz-Fowler, C., Hilbert, H., Horn, D., Huang, Y., Klages, S., Knights, A., Kube, M., Larke, N., Litvin, L., Lord, A., Louie, T., Marra, M., Masuy, D., Matthews, K., Michaeli, S., Mottram, J. C., Muller-Auer, S., Munden, H., Nelson, S., Norbertczak, H., Oliver, K., O'neil, S., Pentony, M., Pohl, T. M., Price, C., Purnelle, B., Quail, M. A., Rabbinowitsch, E., Reinhardt, R., Rieger, M., Rinta, J., Robben, J., Robertson, L., Ruiz, J. C., Rutter, S., Saunders, D., Schafer, M., Schein, J., Schwartz, D. C., Seeger, K., Seyler, A., Sharp, S., Shin, H., Sivam, D., Squares, R., Squares, S., Tosato, V., Vogt, C., Volckaert, G., Wambutt, R., Warren, T., Wedler, H., Woodward, J., Zhou, S., Zimmermann, W., Smith, D. F., Blackwell, J. M., Stuart, K. D., Barrell, B., and Myler, P. J. (2005) The genome of the kinetoplastid parasite, *Leishmania major*. Science 309 (5733): 436

Jackson, A. P. (2007) Origins of amino acid transporter loci in trypanosomatid parasites. BMC. Evol. Biol. 7 : 26

John von Freyend, S., Rosenqvist, H., Fink, A., Melzer, I. M., Clos, J., Jensen, O. N., and Wiese, M. (2010) LmxMPK4, an essential mitogen-activated protein kinase of *Leishmania mexicana* is phosphorylated and activated by the STE7-like protein kinase LmxMKK5. Int. J. Parasitol.

Johnson, G. L. and Lapadat, R. (2002) Mitogen-activated protein kinase pathways mediated by ERK, JNK, and p38 protein kinases. Science 298 (5600): 1911

Johnson, L. N. and Lewis, R. J. (2001) Structural basis for control by phosphorylation. Chem. Rev. 101 (8): 2209

Kamhawi, S. (2006) Phlebotomine sand flies and *Leishmania* parasites: friends or foes? Trends Parasitol. 22 (9): 439

Kamhawi, S., Ramalho-Ortigao, M., Pham, V. M., Kumar, S., Lawyer, P. G., Turco, S. J., Barillas-Mury, C., Sacks, D. L., and Valenzuela, J. G. (2004) A role for insect galectins in parasite survival. Cell 119 (3): 329

Kanehisa, M. (2002) The KEGG database. Novartis. Found. Symp. 247 : 91

Karaman, M. W., Herrgard, S., Treiber, D. K., Gallant, P., Atteridge, C. E., Campbell, B. T., Chan, K. W., Ciceri, P., Davis, M. I., Edeen, P. T., Faraoni, R., Floyd, M., Hunt, J. P., Lockhart, D. J., Milanov, Z. V., Morrison, M. J., Pallares, G., Patel, H. K., Pritchard, S., Wodicka, L. M., and Zarrinkar, P. P. (2008) A quantitative analysis of kinase inhibitor selectivity. Nat. Biotechnol. 26 (1): 127

Killick-Kendrick, R. (1999) The biology and control of phlebotomine sand flies. Clin. Dermatol. 17 (3): 279

Kim, E. K. and Choi, E. J. (2010) Pathological roles of MAPK signaling pathways in human diseases. Biochim. Biophys. Acta 1802 (4): 396

Kima, P. E. (2007) The amastigote forms of *Leishmania* are experts at exploiting host cell processes to establish infection and persist. Int. J. Parasitol. 37 (10): 1087

Kirkman, T. W. (1996) Statistics to Use. http://www. physics. csbsju. edu/stats/ :

Knockaert, M., Wieking, K., Schmitt, S., Leost, M., Grant, K. M., Mottram, J. C., Kunick, C., and Meijer, L. (2002) Intracellular Targets of Paullones. Identification following affinity purification on immobilized inhibitor. J. Biol. Chem. 277 (28): 25493

Koumandou, V. L., Natesan, S. K., Sergeenko, T., and Field, M. C. (2008) The trypanosome transcriptome is remodelled during differentiation but displays limited responsiveness within life stages. BMC. Genomics 9 : 298

Krupa, A., Preethi, G., and Srinivasan, N. (2004) Structural modes of stabilization of permissive phosphorylation sites in protein kinases: distinct strategies in Ser/Thr and Tyr kinases. J. Mol. Biol. 339 (5): 1025

Kuhn, D. (2004), PhD thesis, Bernhard Nocht Institute for Tropical Medicine / Department of Chemistry, University of Hamburg

Kuhn, D. and Wiese, M. (2005) LmxPK4, a mitogen-activated protein kinase kinase homologue of *Leishmania mexicana* with a potential role in parasite differentiation. Mol. Microbiol. 56 (5): 1169

Kultz, D. (1998) Phylogenetic and functional classification of mitogen- and stress-activated protein kinases. J. Mol. Evol. 46 (5): 571

Kunz, S., Beavo, J. A., D'Angelo, M. A., Flawia, M. M., Francis, S. H., Johner, A., Laxman, S., Oberholzer, M., Rascon, A., Shakur, Y., Wentzinger, L., Zoraghi, R., and Seebeck, T. (2006) Cyclic nucleotide specific phosphodiesterases of the kinetoplastida: a unified nomenclature. Mol. Biochem. Parasitol. 145 (1): 133

Lainson, R. and Shaw, J. J. (1987) Evolution, classification and geographical distribution. The leishmaniases in Biology and Medicine 1 : 1

Lamour, N., Riviere, L., Coustou, V., Coombs, G. H., Barrett, M. P., and Bringaud, F. (2005) Proline metabolism in procyclic *Trypanosoma brucei* is down-regulated in the presence of glucose. J. Biol. Chem. 280 (12): 11902

Laxman, S. and Beavo, J. A. (2007) Cyclic nucleotide signaling mechanisms in trypanosomes: possible targets for therapeutic agents. Mol. Interv. 7 (4): 203

Le, Pape P. (2008) Development of new antileishmanial drugs--current knowledge and future prospects. J. Enzyme Inhib. Med. Chem. 23 (5): 708

Leifso, K., Cohen-Freue, G., Dogra, N., Murray, A., and McMaster, W. R. (2007b) Genomic and proteomic expression analysis of *Leishmania* promastigote and amastigote life stages: the *Leishmania* genome is constitutively expressed. Mol. Biochem. Parasitol. 152 (1): 35

Leifso, K., Cohen-Freue, G., Dogra, N., Murray, A., and McMaster, W. R. (2007a) Genomic and proteomic expression analysis of *Leishmania* promastigote and amastigote life stages: the *Leishmania* genome is constitutively expressed. Mol. Biochem. Parasitol. 152 (1): 35

Leishman, W. B. (1903) On the possibility of the occurence of trypanomiasis in India. The British Medical Journal : 1252

Leost, M., Schultz, C., Link, A., Wu, Y. Z., Biernat, J., Mandelkow, E. M., Bibb, J. A., Snyder, G. L., Greengard, P., Zaharevitz, D. W., Gussio, R., Senderowicz, A. M., Sausville, E. A., Kunick, C., and Meijer, L. (2000) Paullones are potent inhibitors of

glycogen synthase kinase-3beta and cyclin-dependent kinase 5/p25. Eur. J. Biochem. 267 (19): 5983

Li, S., Wilson, M. E., and Donelson, J. E. (1996) *Leishmania chagasi*: a gene encoding a protein kinase with a catalytic domain structurally related to MAP kinase kinase. Exp. Parasitol. 82 (2): 87

Liang, X. H., Haritan, A., Uliel, S., and Michaeli, S. (2003) trans and cis splicing in trypanosomatids: mechanism, factors, and regulation. Eukaryot. Cell 2 (5): 830

Lindberg, R. A., Quinn, A. M., and Hunter, T. (1992) Dual-specificity protein kinases: will any hydroxyl do? Trends Biochem. Sci. 17 (3): 114

Liu, Y., Shah, K., Yang, F., Witucki, L., and Shokat, K. M. (1998) Engineering Src family protein kinases with unnatural nucleotide specificity. Chem. Biol. 5 (2): 91

Lux, H., Hart, D. T., Parker, P. J., and Klenner, T. (1996) Ether lipid metabolism, GPI anchor biosynthesis, and signal transduction are putative targets for anti-leishmanial alkyl phospholipid analogues. Adv. Exp. Med. Biol. 416 : 201

Lux, H., Heise, N., Klenner, T., Hart, D., and Opperdoes, F. R. (2000) Ether--lipid (alkyl-phospholipid) metabolism and the mechanism of action of ether--lipid analogues in *Leishmania*. Mol. Biochem. Parasitol. 111 (1): 1

Maarouf, M., Adeline, M. T., Solignac, M., Vautrin, D., and Robert-Gero, M. (1998) Development and characterization of paromomycin-resistant *Leishmania donovani* promastigotes. Parasite 5 (2): 167

Maltezou, H. C. (2010) Drug resistance in visceral leishmaniasis. J. Biomed. Biotechnol. 2010 : 617521

Manning, G. (2005) Genomic overview of protein kinases. WormBook. 1

Manning, G., Plowman, G. D., Hunter, T., and Sudarsanam, S. (2002a) Evolution of protein kinase signaling from yeast to man. Trends Biochem. Sci. 27 (10): 514

Manning, G., Whyte, D. B., Martinez, R., Hunter, T., and Sudarsanam, S. (2002b) The protein kinase complement of the human genome. Science 298 (5600): 1912

Maugeri, D. A., Cazzulo, J. J., Burchmore, R. J., Barrett, M. P., and Ogbunude, P. O. (2003) Pentose phosphate metabolism in *Leishmania mexicana*. Mol. Biochem. Parasitol. 130 (2): 117

Mazareb, S., Fu, Z. Y., and Zilberstein, D. (1999) Developmental regulation of proline transport in *Leishmania donovani*. Exp. Parasitol. 91 (4): 341

McConville, M. J., de, Souza D., Saunders, E., Likic, V. A., and Naderer, T. (2007) Living in a phagolysosome; metabolism of *Leishmania* amastigotes. Trends Parasitol. 23 (8): 368

McKean, P. G. (2003) Coordination of cell cycle and cytokinesis in *Trypanosoma brucei*. Curr. Opin. Microbiol. 6 (6): 600

Meggio, F., Donella, Deana A., Ruzzene, M., Brunati, A. M., Cesaro, L., Guerra, B., Meyer, T., Mett, H., Fabbro, D., Furet, P., and . (1995) Different susceptibility of protein kinases to staurosporine inhibition. Kinetic studies and molecular bases for the resistance of protein kinase CK2. Eur. J. Biochem. 234 (1): 317

Meijer, L., Borgne, A., Mulner, O., Chong, J. P., Blow, J. J., Inagaki, N., Inagaki, M., Delcros, J. G., and Moulinoux, J. P. (1997) Biochemical and cellular effects of roscovitine, a potent and selective inhibitor of the cyclin-dependent kinases cdc2, cdk2 and cdk5. Eur. J. Biochem. 243 (1-2): 527

Melikant, B., Giuliani, C., Halbmayer-Watzina, S., Limmongkon, A., Heberle-Bors, E., and Wilson, C. (2004) The *Arabidopsis thaliana* MEK AtMKK6 activates the MAP kinase AtMPK13. FEBS Lett. 576 (1-2): 5

Melzer, I. M. (2007), PhD thesis, Bernhard Nocht Institute for Tropical Medicine / Department of Chemistry, University of Hamburg

Menegay, H. J., Myers, M. P., Moeslein, F. M., and Landreth, G. E. (2000) Biochemical characterization and localization of the dual specificity kinase CLK1. J. Cell Sci. 113 (Pt 18) : 3241

Miyata, Y. and Nishida, E. (1999) Distantly related cousins of MAP kinase: biochemical properties and possible physiological functions. Biochem. Biophys. Res. Commun. 266 (2): 291

Mody, N., Campbell, D. G., Morrice, N., Peggie, M., and Cohen, P. (2003) An analysis of the phosphorylation and activation of extracellular-signal-regulated protein kinase 5 (ERK5) by mitogen-activated protein kinase kinase 5 (MKK5) in vitro. Biochem. J. 372 (Pt 2): 567

Morales, M. A., Pescher, P., and Spath, G. F. (2010) *Leishmania major* MPK7 protein kinase activity inhibits intracellular growth of the pathogenic amastigote stage. Eukaryot. Cell 9 (1): 22

Morales, M. A., Renaud, O., Faigle, W., Shorte, S. L., and Spath, G. F. (2007) Over-expression of *Leishmania major* MAP kinases reveals stage-specific induction of phosphotransferase activity. Int. J. Parasitol. 37 (11): 1187

Mottram, J. C. (1994) cdc2-related protein kinases and cell cycle control in trypanosomatids. Parasitol. Today 10 (7): 253

Muller, I. B., Domenicali-Pfister, D., Roditi, I., and Vassella, E. (2002) Stage-specific requirement of a mitogen-activated protein kinase by *Trypanosoma brucei*. Mol. Biol. Cell 13 (11): 3787

Muller, S., Coombs, G. H., and Walter, R. D. (2001) Targeting polyamines of parasitic protozoa in chemotherapy. Trends Parasitol. 17 (5): 242

Murray, H. W., Berman, J. D., Davies, C. R., and Saravia, N. G. (2005) Advances in leishmaniasis. Lancet 366 (9496): 1561

Musrati, R. A., Kollarova, M., Mernik, N., and Mikulasova, D. (1998) Malate dehydrogenase: distribution, function and properties. Gen. Physiol Biophys. 17 (3): 193

Myler, P. J., Sisk, E., McDonagh, P. D., Martinez-Calvillo, S., Schnaufer, A., Sunkin, S. M., Yan, S., Madhubala, R., Ivens, A., and Stuart, K. (2000) Genomic organization and gene function in *Leishmania*. Biochem. Soc. Trans. 28 (5): 527

Myskova, J., Svobodova, M., Beverley, S. M., and Volf, P. (2007) A lipophosphoglycan-independent development of *Leishmania* in permissive sand flies. Microbes. Infect. 9 (3): 317

Nascimento, M., Zhang, W. W., Ghosh, A., Houston, D. R., Berghuis, A. M., Olivier, M., and Matlashewski, G. (2006) Identification and characterization of a protein-tyrosine phosphatase in *Leishmania*: Involvement in virulence. J. Biol. Chem. 281 (47): 36257

Naula, C., Parsons, M., and Mottram, J. C. (2005) Protein kinases as drug targets in trypanosomes and *Leishmania*. Biochim. Biophys. Acta 1754 (1-2): 151

Naula, C., Schaub, R., Leech, V., Melville, S., and Seebeck, T. (2001) Spontaneous dimerization and leucine-zipper induced activation of the recombinant catalytic domain of a new adenylyl cyclase of *Trypanosoma brucei*, GRESAG4.4B. Mol. Biochem. Parasitol. 112 (1): 19

Nozaki, T., Toh-e A, Fujii, M., Yagisawa, H., Nakazawa, M., and Takeuchi, T. (1999) Cloning and characterization of a gene encoding phosphatidyl inositol-specific phospholipase C from *Trypanosoma cruzi*. Mol. Biochem. Parasitol. 102 (2): 283

Oberholzer, M., Bregy, P., Marti, G., Minca, M., Peier, M., and Seebeck, T. (2007) Trypanosomes and mammalian sperm: one of a kind? Trends Parasitol. 23 (2): 71

Opperdoes, F. R. and Coombs, G. H. (2007) Metabolism of *Leishmania*: proven and predicted. Trends Parasitol. 23 (4): 149

Parsons, M. and Ruben, L. (2000) Pathways involved in environmental sensing in trypanosomatids. Parasitol. Today 16 (2): 56

Parsons, M., Worthey, E. A., Ward, P. N., and Mottram, J. C. (2005) Comparative analysis of the kinomes of three pathogenic trypanosomatids: *Leishmania major*, *Trypanosoma brucei* and *Trypanosoma cruzi*. BMC. Genomics 6 : 127

Peacock, C. S., Seeger, K., Harris, D., Murphy, L., Ruiz, J. C., Quail, M. A., Peters, N., Adlem, E., Tivey, A., Aslett, M., Kerhornou, A., Ivens, A., Fraser, A., Rajandream, M. A., Carver, T., Norbertczak, H., Chillingworth, T., Hance, Z., Jagels, K., Moule, S., Ormond, D., Rutter, S., Squares, R., Whitehead, S., Rabbinowitsch, E., Arrowsmith, C., White, B., Thurston, S., Bringaud, F., Baldauf, S. L., Faulconbridge, A., Jeffares, D., Depledge, D. P., Oyola, S. O., Hilley, J. D., Brito, L. O., Tosi, L. R., Barrell, B., Cruz, A. K., Mottram, J. C., Smith, D. F., and Berriman, M. (2007) Comparative genomic analysis of three *Leishmania* species that cause diverse human disease. Nat. Genet. 39 (7): 839

Pearson, G., Robinson, F., Beers, Gibson T., Xu, B. E., Karandikar, M., Berman, K., and Cobb, M. H. (2001) Mitogen-activated protein (MAP) kinase pathways: regulation and physiological functions. Endocr. Rev. 22 (2): 153

Pereira, C. A., Alonso, G. D., Paveto, M. C., Iribarren, A., Cabanas, M. L., Torres, H. N., and Flawia, M. M. (2000) *Trypanosoma cruzi* arginine kinase characterization and cloning. A novel energetic pathway in protozoan parasites. J. Biol. Chem. 275 (2): 1495

Pereira, C. A., Alonso, G. D., Torres, H. N., and Flawia, M. M. (2002) Arginine kinase: a common feature for management of energy reserves in African and American flagellated trypanosomatids. J. Eukaryot. Microbiol. 49 (1): 82

Persson, L., Jeppsson, A., and Nasizadeh, S. (2003) Turnover of trypanosomal ornithine decarboxylases. Biochem. Soc. Trans. 31 (2): 411

Pimenta, P. F., Modi, G. B., Pereira, S. T., Shahabuddin, M., and Sacks, D. L. (1997) A novel role for the peritrophic matrix in protecting *Leishmania* from the hydrolytic activities of the sand fly midgut. Parasitology 115 (Pt 4) : 359

Plowman, G. D., Sudarsanam, S., Bingham, J., Whyte, D., and Hunter, T. (1999) The protein kinases of *Caenorhabditis elegans*: a model for signal transduction in multicellular organisms. Proc. Natl. Acad. Sci. U. S. A 96 (24): 13603

Pluk, H., Dorey, K., and Superti-Furga, G. (2002) Autoinhibition of c-Abl. Cell 108 (2): 247

Puentes, S. M., Da Silva, R. P., Sacks, D. L., Hammer, C. H., and Joiner, K. A. (1990) Serum resistance of metacyclic stage *Leishmania major* promastigotes is due to release of C5b-9. J. Immunol. 145 (12): 4311

Puls, G. (2005), diploma thesis, Bernhard-Nocht Insitute for Tropical Medicine / TU Berlin, department III

Raamsdonk, L. M., Teusink, B., Broadhurst, D., Zhang, N., Hayes, A., Walsh, M. C., Berden, J. A., Brindle, K. M., Kell, D. B., Rowland, J. J., Westerhoff, H. V., van, Dam K., and Oliver, S. G. (2001) A functional genomics strategy that uses metabolome data to reveal the phenotype of silent mutations. Nat. Biotechnol. 19 (1): 45

Ralton, J. E., Naderer, T., Piraino, H. L., Bashtannyk, T. A., Callaghan, J. M., and McConville, M. J. (2003) Evidence that intracellular beta1-2 mannan is a virulence factor in *Leishmania* parasites. J. Biol. Chem. 278 (42): 40757

Reguera, R. M., Balana-Fouce, R., Showalter, M., Hickerson, S., and Beverley, S. M. (2009) *Leishmania major* lacking arginase (ARG) are auxotrophic for polyamines but retain infectivity to susceptible BALB/c mice. Mol. Biochem. Parasitol. 165 (1): 48

Reithinger, R. and Dujardin, J. C. (2007) Molecular diagnosis of leishmaniasis: current status and future applications. J. Clin. Microbiol. 45 (1): 21

Rijal, S., Chappuis, F., Singh, R., Bovier, P. A., Acharya, P., Karki, B. M., Das, M. L., Desjeux, P., Loutan, L., and Koirala, S. (2003) Treatment of visceral leishmaniasis in south-eastern Nepal: decreasing efficacy of sodium stibogluconate and need for a policy to limit further decline. Trans. R. Soc. Trop. Med. Hyg. 97 (3): 350

Rochette, A., Raymond, F., Corbeil, J., Ouellette, M., and Papadopoulou, B. (2009) Whole-genome comparative RNA expression profiling of axenic and intracellular amastigote forms of *Leishmania infantum*. Mol. Biochem. Parasitol. 165 (1): 32

Rogers, K. A., DeKrey, G. K., Mbow, M. L., Gillespie, R. D., Brodskyn, C. I., and Titus, R. G. (2002) Type 1 and type 2 responses to *Leishmania major*. FEMS Microbiol. Lett. 209 (1): 1

Rogers, M. E., Chance, M. L., and Bates, P. A. (2002) The role of promastigote secretory gel in the origin and transmission of the infective stage of *Leishmania mexicana* by the sandfly Lutzomyia longipalpis. Parasitology 124 (Pt 5): 495

Rogers, M. E., Hajmova, M., Joshi, M. B., Sadlova, J., Dwyer, D. M., Volf, P., and Bates, P. A. (2008) *Leishmania* chitinase facilitates colonization of sand fly vectors and enhances transmission to mice. Cell Microbiol. 10 (6): 1363

Rohousova, I. and Volf, P. (2006) Sand fly saliva: effects on host immune response and *Leishmania* transmission. Folia Parasitol. (Praha) 53 (3): 161

Sadlova, J. and Volf, P. (2009) Peritrophic matrix of *Phlebotomus duboscqi* and its kinetics during *Leishmania major* development. Cell Tissue Res. 337 (2): 313

Salotra, P., Ralhan, R., and Sreenivas, G. (2000) Heat-stress induced modulation of protein phosphorylation in virulent promastigotes of *Leishmania donovani*. Int. J. Biochem. Cell Biol. 32 (3): 309

Saunders, E. C., DE Souza, D. P., Naderer, T., Sernee, M. F., Ralton, J. E., Doyle, M. A., Macrae, J. I., Chambers, J. L., Heng, J., Nahid, A., Likic, V. A., and McConville, M. J. (2010) Central carbon metabolism of *Leishmania* parasites. Parasitology : 1

Scheltema, R. A., Decuypere, S., T'kindt, R., Dujardin, J. C., Coombs, G. H., and Breitling, R. (2010) The potential of metabolomics for *Leishmania* research in the post-genomics era. Parasitology : 1

Schlagenhauf, E., Etges, R., and Metcalf, P. (1998) The crystal structure of the *Leishmania major* surface proteinase leishmanolysin (gp63). Structure. 6 (8): 1035

Schnaufer, A., Clark-Walker, G. D., Steinberg, A. G., and Stuart, K. (2005) The F1-ATP synthase complex in bloodstream stage trypanosomes has an unusual and essential function. EMBO J. 24 (23): 4029

Scholz, A. (2008), PhD thesis, Bernhard Nocht Institute for Tropical Medicine / Departement of Chemistry, University of Hamburg

Scott, J. D. and Pawson, T. (2009) Cell signaling in space and time: where proteins come together and when they're apart. Science 326 (5957): 1220

Seebeck, T., Gong, K., Kunz, S., Schaub, R., Shalaby, T., and Zoraghi, R. (2001) cAMP signalling in *Trypanosoma brucei*. Int. J. Parasitol. 31 (5-6): 491

Seebeck, T., Schaub, R., and Johner, A. (2004) cAMP signalling in the kinetoplastid protozoa. Curr. Mol. Med. 4 (6): 585

Shah, K., Liu, Y., Deirmengian, C., and Shokat, K. M. (1997) Engineering unnatural nucleotide specificity for Rous sarcoma virus tyrosine kinase to uniquely label its direct substrates. Proc. Natl. Acad. Sci. U. S. A 94 (8): 3565

Shaked-Mishan, P., Suter-Grotemeyer, M., Yoel-Almagor, T., Holland, N., Zilberstein, D., and Rentsch, D. (2006) A novel high-affinity arginine transporter from the human parasitic protozoan *Leishmania donovani*. Mol. Microbiol. 60 (1): 30

Shao, L., Devenport, M., and Jacobs-Lorena, M. (2001) The peritrophic matrix of hematophagous insects. Arch. Insect Biochem. Physiol 47 (2): 119

Shiu, S. H., Karlowski, W. M., Pan, R., Tzeng, Y. H., Mayer, K. F., and Li, W. H. (2004) Comparative analysis of the receptor-like kinase family in *Arabidopsis* and rice. Plant Cell 16 (5): 1220

Simpson, A. G., Stevens, J. R., and Lukes, J. (2006) The evolution and diversity of kinetoplastid flagellates. Trends Parasitol. 22 (4): 168

Sindermann, H. and Engel, J. (2006) Development of miltefosine as an oral treatment for leishmaniasis. Trans. R. Soc. Trop. Med. Hyg. 100 Suppl 1 : S17

Smith, C. A., O'Maille, G., Want, E. J., Qin, C., Trauger, S. A., Brandon, T. R., Custodio, D. E., Abagyan, R., and Siuzdak, G. (2005) METLIN: a metabolite mass spectral database. Ther. Drug Monit. 27 (6): 747

Smith, K. M., Yacobi, R., and Van Etten, R. A. (2003) Autoinhibition of Bcr-Abl through its SH3 domain. Mol. Cell 12 (1): 27

Solbach, W. and Laskay, T. (2000) The host response to *Leishmania* infection. Adv. Immunol. 74 : 275

Souza, C. F., Carneiro, A. B., Silveira, A. B., Laranja, G. A., Silva-Neto, M. A., Costa, S. C., and Paes, M. C. (2009) Heme-induced *Trypanosoma cruzi* proliferation is mediated by CaM kinase II. Biochem. Biophys. Res. Commun. 390 (3): 541

Soyano, T., Nishihama, R., Morikiyo, K., Ishikawa, M., and Machida, Y. (2003) NQK1/NtMEK1 is a MAPKK that acts in the NPK1 MAPKKK-mediated MAPK cascade and is required for plant cytokinesis. Genes Dev. 17 (8): 1055

Sudhandiran, G. and Shaha, C. (2003) Antimonial-induced increase in intracellular Ca2+ through non-selective cation channels in the host and the parasite is responsible for apoptosis of intracellular *Leishmania donovani* amastigotes. J. Biol. Chem. 278 (27): 25120

Sundar, S., More, D. K., Singh, M. K., Singh, V. P., Sharma, S., Makharia, A., Kumar, P. C., and Murray, H. W. (2000) Failure of pentavalent antimony in visceral leishmaniasis in India: report from the center of the Indian epidemic. Clin. Infect. Dis. 31 (4): 1104

Swaminath, C. S., Shortt, H. E., and Anderson, L. A. P. (1942) Transmission of Indian kala-azar to man by the bites of *Phlebotomus argentipes*, Ann. and Brun. Indian J. Med. Res. 30 : 473

Symmers, W. S. (1960) Leishmaniasis acquired by contagion: a case of marital infection in Britain. Lancet 1 (7116): 127

Tabor, C. W. and Tabor, H. (1984) Polyamines. Annu. Rev. Biochem. 53 : 749

Tanoue, T. and Nishida, E. (2003) Molecular recognitions in the MAP kinase cascades. Cell Signal. 15 (5): 455

Tellam, R. L., Wijffels, G., and Willadsen, P. (1999) Peritrophic matrix proteins. Insect Biochem. Mol. Biol. 29 (2): 87

Tielens, A. G. and van Hellemond, J. J. (2009) Surprising variety in energy metabolism within Trypanosomatidae. Trends Parasitol. 25 (10): 482

Tu, X. and Wang, C. C. (2005) Pairwise knockdowns of cdc2-related kinases (CRKs) in *Trypanosoma brucei* identified the CRKs for G1/S and G2/M transitions and demonstrated distinctive cytokinetic regulations between two developmental stages of the organism. Eukaryot. Cell 4 (4): 755

Urano, J., Tabancay, A. P., Yang, W., and Tamanoi, F. (2000) The *Saccharomyces cerevisiae* Rheb G-protein is involved in regulating canavanine resistance and arginine uptake. J. Biol. Chem. 275 (15): 11198

van Hellemond, J. J. and Tielens, A. G. (1997a) Inhibition of the respiratory chain results in a reversible metabolic arrest in *Leishmania* promastigotes. Mol. Biochem. Parasitol. 85 (1): 135

van Hellemond, J. J., van der Meer, P., and Tielens, A. G. (1997b) *Leishmania infantum* promastigotes have a poor capacity for anaerobic functioning and depend mainly on respiration for their energy generation. Parasitology 114 : 351

van Weelden, S. W., van Hellemond, J. J., Opperdoes, F. R., and Tielens, A. G. (2005) New functions for parts of the Krebs cycle in procyclic *Trypanosoma brucei*, a cycle not operating as a cycle. J. Biol. Chem. 280 (13): 12451

van, Griensven J., Balasegaram, M., Meheus, F., Alvar, J., Lynen, L., and Boelaert, M. (2010) Combination therapy for visceral leishmaniasis. Lancet Infect. Dis. 10 (3): 184

van, Zandbergen G., Klinger, M., Mueller, A., Dannenberg, S., Gebert, A., Solbach, W., and Laskay, T. (2004) Cutting edge: neutrophil granulocyte serves as a vector for *Leishmania* entry into macrophages. J. Immunol. 173 (11): 6521

Wanders, P. (2004), MD thesis, University of Veterinary Medicine Hannover

Wang, Q., Melzer, I. M., Kruse, M., Sander-Juelch, C., and Wiese, M. (2005) LmxMPK4, a mitogen-activated protein (MAP) kinase homologue essential for promastigotes and amastigotes of *Leishmania mexicana*. Kinetoplastid. Biol. Dis. 4 : 6

Wang, Y., Xiao, J., Suzek, T. O., Zhang, J., Wang, J., and Bryant, S. H. (2009) PubChem: a public information system for analyzing bioactivities of small molecules. Nucleic Acids Res. 37 (Web Server issue): W623

Wiese, M. (1998) A mitogen-activated protein (MAP) kinase homologue of *Leishmania mexicana* is essential for parasite survival in the infected host. EMBO J. 17 (9): 2619

Wiese, M. (2007) *Leishmania* MAP kinases--familiar proteins in an unusual context. Int. J. Parasitol. 37 (10): 1053

Wiese, M., Kuhn, D., and Grunfelder, C. G. (2003a) Protein kinase involved in flagellar-length control. Eukaryot. Cell 2 (4): 769

Wiese, M., Wang, Q., and Gorcke, I. (2003b) Identification of mitogen-activated protein kinase homologues from *Leishmania mexicana*. Int. J. Parasitol. 33 (14): 1577

Wiesgigl, M. and Clos, J. (2001b) Heat shock protein 90 homeostasis controls stage differentiation in *Leishmania donovani*. Mol. Biol. Cell 12 (11): 3307

Wiesgigl, M. and Clos, J. (2001a) Heat shock protein 90 homeostasis controls stage differentiation in *Leishmania donovani*. Mol. Biol. Cell 12 (11): 3307

Wilson, K. P., McCaffrey, P. G., Hsiao, K., Pazhanisamy, S., Galullo, V., Bemis, G. W., Fitzgibbon, M. J., Caron, P. R., Murcko, M. A., and Su, M. S. (1997) The structural basis for the specificity of pyridinylimidazole inhibitors of p38 MAP kinase. Chem. Biol. 4 (6): 423

Windelberg, M. (2007), MD thesis, Bernhard Nocht Institute for Tropical Medicine / University Hamburg, Germany

Winder, C. L., Dunn, W. B., Schuler, S., Broadhurst, D., Jarvis, R., Stephens, G. M., and Goodacre, R. (2008) Global metabolic profiling of *Escherichia coli* cultures: an evaluation of methods for quenching and extraction of intracellular metabolites. Anal. Chem. 80 (8): 2939

Wishart, D. S., Tzur, D., Knox, C., Eisner, R., Guo, A. C., Young, N., Cheng, D., Jewell, K., Arndt, D., Sawhney, S., Fung, C., Nikolai, L., Lewis, M., Coutouly, M. A., Forsythe, I., Tang, P., Shrivastava, S., Jeroncic, K., Stothard, P., Amegbey, G., Block, D., Hau, D. D., Wagner, J., Miniaci, J., Clements, M., Gebremedhin, M., Guo, N., Zhang, Y., Duggan, G. E., Macinnis, G. D., Weljie, A. M., Dowlatabadi, R., Bamforth, F., Clive, D., Greiner, R., Li, L., Marrie, T., Sykes, B. D., Vogel, H. J., and Querengesser, L. (2007) HMDB: the Human Metabolome Database. Nucleic Acids Res. 35 (Database issue): D521

Wyllie, S., Cunningham, M. L., and Fairlamb, A. H. (2004) Dual action of antimonial drugs on thiol redox metabolism in the human pathogen *Leishmania donovani*. J. Biol. Chem. 279 (38): 39925

Yan, S., Martinez-Calvillo, S., Schnaufer, A., Sunkin, S., Myler, P. J., and Stuart, K. (2002) A low-background inducible promoter system in *Leishmania donovani*. Mol. Biochem. Parasitol. 119 (2): 217

Yao, C., Luo, J., Hsiao, C. H., Donelson, J. E., and Wilson, M. E. (2007) *Leishmania chagasi*: a tetracycline-inducible cell line driven by T7 RNA polymerase. Exp. Parasitol. 116 (3): 205

Zaharevitz, D. W., Gussio, R., Leost, M., Senderowicz, A. M., Lahusen, T., Kunick, C., Meijer, L., and Sausville, E. A. (1999) Discovery and initial characterization of the paullones, a novel class of small-molecule inhibitors of cyclin-dependent kinases. Cancer Res. 59 (11): 2566

Zhang, C., Kenski, D. M., Paulson, J. L., Bonshtien, A., Sessa, G., Cross, J. V., Templeton, D. J., and Shokat, K. M. (2005) A second-site suppressor strategy for chemical genetic analysis of diverse protein kinases. Nat. Methods 2 (6): 435

Zhou, C., Yang, Y., and Jong, A. Y. (1990) Mini-prep in ten minutes. Biotechniques 8 (2): 172

Zikova, A., Schnaufer, A., Dalley, R. A., Panigrahi, A. K., and Stuart, K. D. (2009) The F(0)F(1)-ATP synthase complex contains novel subunits and is essential for procyclic *Trypanosoma brucei*. PLoS. Pathog. 5 (5): e1000436

Zilberstein, D. (1993) Transport of nutrients and ions across membranes of trypanosomatid parasites. Adv. Parasitol. 32 : 261

Zilberstein, D. and Shapira, M. (1994) The role of pH and temperature in the development of *Leishmania* parasites. Annu. Rev. Microbiol. 48 : 449

7. Appendix

7.1 Nucleotide and amino acid sequences

LmxMPK4 ORF and flanking regions, LmxMPK4 translated sequence

The gatekeeper residue methionine111 and the lysine59 of the K59M mutation are underlined in bold; the sequences corresponding to probes used for Southern blot analyses are highlighted grey.

```
1       ATCGATAATCGAGCAGGCCGCTGGGCTGCTTCAGAGGAAGTCAAGTAGTT
51      CCGATTCTCGAAAGGACGAGCAAGACACCATTCCGGAGGCACTTAATTTA
101     CTGAAGGCACAGGTACCGGAGTGCAAACAACCGCTGATTCGTGAAGTGAT
151     ATCAACACCAGGGATCAAAAAAGGGTTTTTGGTGGACGGAAATGCACGAC
201     TCTACAGCCCTGAGGGGAGCAGTGAAGGTTCTGGCAAAGCACCAGACCCT
251     TTGGCACACATCCCAGAATCACTGCGGGAGAGGTGTCAAATTATTGACAC
301     ACGAAGGATGGAGGAGCTCACCGCTCCGCCTGCTAAAACACCCAAGTCCG
351     TCGATAAGACGCCAAGCCTGCACACTTCCGGCACGGTTGCTGCACCTACT
401     TCTGAGCCTAAAAGAAAAGACGAGGCTAACTGGACCCGCTTCTCCATAGA
451     GCGTACCGGGGAGAAGGTGATCATTAGATTTTTAGTGCCTGACAGTGTGG
501     GCTCACTTCATGACATTGATCTCTCTGCAACAAAAGACACACTGGAGATT
551     AATGGAAGCGTAACTCAGCTGCCAGTGCCTATCGTGACGGATGACGTGCG
601     GGCCAAATTTGTCAAAGCCACACGGATCTTGATCGTGACATGTCTGATTG
651     ATTTATCATAAAATAGTCAAGAAGAATTATTTTGTTACTCGACATCAGCA
701     ACCGACTAGCAGCAAATTCACTGCCCTGTTCGAAAACAAAGAGGATCTCT
751     CGCGGGGTATAAAGCGGAGTTTCGCACGACTTAACAAAATCTCTGCGCAC
801     TTCTCGAGTCAACTGCATGTGTTCAGGAAACTATCTATAAAATACTTCAA
851     ATTTACTCCCTTCACATCTCTGCCCACTACTGCTGCAAATGTTGGCTGTA
901     TGGCTGCTCACAGTCCAGAACATGACTGGAGGAGGCATAGAGAAGCATGA
                                                      M  T
951     CTCAGCTCGTCCCTTTAGCTGAACTTCCCAGCGGGAAAAAAATATATAGT
          Q  L  V  P  L  A  E  L  P  S  G  K  K  I  Y  S
1001    GTCCGGGGGCAGCGGTTCGAAGTGGACAGGCAATATGATCTGGTCAAGGT
        V  R  G  Q  R  F  E  V  D  R  Q  Y  D  L  V  K  V
1051    TGTTGGATTTGGTGCGTGTGGCACTGTTTGTTCAGCGGTCGTGAACGGGT
         V  G  F  G  A  C  G  T  V  C  S  A  V  V  N  G  S
1101    CAGGTGAGCGAGTGGCTATCAAGCGATTGTCGCGTGTCTTTGGTGATCTT
          G  E  R  V  A  I  K  R  L  S  R  V  F  G  D  L
1151    CGTGAAGGGAAACGAATTTTGCGGGAGATGGAGATAATGACGTCGCTGAA
        R  E  G  K  R  I  L  R  E  M  E  I  M  T  S  L  K
1201    GCACAATAATCTGATTCGCCTCCACCACTTCATGCGGCCGCAGTCAAAGG
         H  N  N  L  I  R  L  H  H  F  M  R  P  Q  S  K  E
1251    AGACGTTTGAGGACATTTACTTGGTGATGGATCTTTATGACACAGATTTA
          T  F  E  D  I  Y  L  V  M  D  L  Y  D  T  D  L
1301    AATCGTATTATACGAAGTCGGCAGAAACTCACTGATGAACATCTGCAGTA
        N  R  I  I  R  S  R  Q  K  L  T  D  E  H  L  Q  Y
1351    TTTTATGATTCAAGCATTCCGCGGATTGCATTACCTTCACTCTGCCAAGG
         F  M  I  Q  A  F  R  G  L  H  Y  L  H  S  A  K  V
1401    TGATGCATCGAGACCTGAAGCCGAGCAACTTGCTTGTAAATGCGGACTGC
          M  H  R  D  L  K  P  S  N  L  L  V  N  A  D  C
1451    GCGCTAGCAATCTGCGATTTTGGGCTGGCTCGTGATGATCAAGTGATGAG
        A  L  A  I  C  D  F  G  L  A  R  D  D  Q  V  M  S
1501    CTCGTCAGATCTCACACAGTACGTCGTAACACGGTGGTACAGACCCCCTG
         S  S  D  L  T  Q  Y  V  V  T  R  W  Y  R  P  P  E
```

```
1551  AGGTACTCGGGATGGGATCCAATCAGTACACGAGCGCGGTAGATGTCTGG
        V  L  G  M  G  S  N  Q  Y  T  S  A  V  D  V  W
1601  AGCCTTGGTCTAATCTTTGCGGAGCTGATGGTAGGGCGCGCTCTGCTTCC
      S  L  G  L  I  F  A  E  L  M  V  G  R  A  L  L  P
1651  AGGAACAGATTATATTGGACAGCTGGTAATGATTGTCAATCTATTAGGAT
       G  T  D  Y  I  G  Q  L  V  M  I  V  N  L  L  G  S
1701  CCCCGTCCATAGATGACATGGAGTTTCTGAGCTCAGAAGCAAAGGCATTT
        P  S  I  D  D  M  E  F  L  S  S  E  A  K  A  F
1751  ATTCTCTCTCAGCCGCATCGGCCGGCTCTCTCCTTCAGAGATCTTTTTCC
      I  L  S  Q  P  H  R  P  A  L  S  F  R  D  L  F  P
1801  AATGGCTACAGAAGAGGCAACTGACCTTCTGTCGAAGCTGCTCGTTTTCC
       M  A  T  E  E  A  T  D  L  L  S  K  L  L  V  F  H
1851  ATCCTGCAAGACGATTAACTGCGAAGCAAGTGATGGAGCATCCATATTTT
        P  A  R  R  L  T  A  K  Q  V  M  E  H  P  Y  F
1901  TCAAAGTACAGGGATGCCGCAGAAGAAGCTGACGCTCCTGATCCGTTTGT
      S  K  Y  R  D  A  A  E  E  A  D  A  P  D  P  F  V
1951  GTGGAATCACAGCCATATAGAAACCAAAGAGCAACTCCGTGAGGATTTGT
       W  N  H  S  H  I  E  T  K  E  Q  L  R  E  D  L  W
2001  GGCGCGTTGTCGAAGCCCATTCACAATTGAACGAATAGGAATCTGGTGCT
        R  V  V  E  A  H  S  Q  L  N  E  *
2051  CTCACTTTTTTTTTGCATGCATCACTCAAACCTCTTCTAATAAGAACACC
2101  CGCTTTTAAATCGTCTACTGACGGTGCACTGTGGCTATTGCTGAGCAGGG
2151  CAATACCCCATGTTTCTTCGCAAATCAAAATTCACTTTAATTTCTAGAGA
2201  TCGAAGATCCCTCGCTTCTGCACTGTCAAAAAAGGAAAAAAAATAAGAAA
2251  CTCCGATGAAGCGTAAACCAATCTTGTACGTGTTGCTGTCCACTCTATAC
2301  TTCCTCTTTTTTCCCCCACCTCTCAACAGTACATGGATACTTGGATCGTC
2351  TTTTTTTTCAAGGGATAATTATTCGACAATCGCCTTTGCATACACCGGTA
2401  AGTCGAGACGCATGAGACGTCCGCGTGAGCCAACCCCAGGGGAGTGCTGC
2451  GGAAGCGGCTGTACCCGCTGCGTATGGGATATTTACTACGATGAACTCGC
2501  TAGATTTGAGGAGTTTATAGCAGGCGGGGGAGTCGAAGAGGAGGGTACCC
2551  AATCCTCAGAGGAGGAAGAGGTTGCTAATTATATCGGTTCCGTTGTGGTG
2601  AAGTACATTGATCCACCGGCTTTGTCCACCACCGGCTCTCCAGGTGAATG
2651  GGAGAGAGCCGAAATGAAGGGGCGCGGTTTCTTTCCCATTGACAGAATCG
2701  AGCTAGTGAGGTGCAGCACATCCCTGTTTTCTCCAACTGATCCGGGAATC
2751  AGCGTCGTCAACCTCTTCACATCCGCAAAAGGCAGGGCAATGCTACCAGG
2801  CGATGTGGTAGAGGTTCTTGTGACTAACAGTCACGGTACTCAGGACGCCG
2851  ATGACGTTGAGAGGCTGTGCAAGGCGCTTCACCTGGATCCGTGTGCGTGG
2901  TGCGAGCTGCATCGCTCCCCGTTTGTGCCGGAAGACAACTTTCCCCCGTG
2951  GCTTCCGCTACAAAAGCCTCTGACGCTTGGGCAGCTTCTCTCTGCCTACG
3001  TCGATATAAGCAGTAGTAGCTACCTGTTGCATCAGAGCTTTTTCGAAAAT
3051  CTTTTTAGAATTTACAGCGACTCCAAACCTTCCTCGGCATCTTCGACTTC
3101  AACCACGCCGTCACCCGATCCAGAGAAGGTGCGGCTTCTTGAGGCCTGCG
3151  CGTCCTCTGAAACAGGTCCCCAGCTGCTGCGCTTGCTGTCCAAAAGCAGT
3201  GCGCCGCTTTGCTACCCTTCTCTTGTTGACGTACTTGAGGTCTTTTCCTT
3251  CGTCAATATTCCACTTGACCGTCTCCTTGAGGTCAGTGGACCGCTCCAGA
3301  CGCGCAGGTATAGTCTGGCAAACTGGCTTCCTGCAACGCTTCCGCCAAGT
3351  CCACTTCAGCTGTGCATGAGGGAGGTGTGCGCTCGACGCTCTGCAAATTT
3401  ACCTGCAGTTACCACAGTTGGCGCGGACGCTCAGCGCGTTGCAGACATGC
3451  TTAACAGAGTTTCTCAGGATGCCTCCAGGGACCACGGCGGCTTTTTCTTT
3501  GGACACACGTCCCACCCGTTGTGCTCTGCAGCGCGTTCTATGACGAGGAG
3551  TGCAGCTGGCGCAGGTCAGAGAGGCATGTACGTCAGTTTTTCTCTTTTTG
3601  GAAACTCTTCATTTGCCCAACAGCTTCAGGCTGGATGCACAGCTTTGTGC
3651  AGCCCTGGTCAAGCCAAGAGCTTGTGCAGTCAGCTTTTTCTTATCGGGTG
3701  TGGCACAGGGATTGCTCCTTTGATTGCGGCTGTCACGCAACTGATGCTTC
3751  GTCGCGCCTCCACAGCCGCCGGGAGTGCCCCATTTCCGTGCTGGGTGTTC
3801  TACGGAGCGCGCACAAAGGCGGAACTTTTGTATGATGAAACCCTCAAGGA
3851  AGCACTGAGGACCGGAGCAATTGCCAAGTACGAGTACGCGCTTTCCCGAG
3901  AGGAGGACAATGAGAAGCAAGGCAAGTATGTAACCGACCTTGTGAAGGGG
3951  AACCGGCTAATGGTCACGGATTCCCTGCAAAGCGAGGGTCAGCTATTTGT
```

```
4001   GTGTGGTCCGGCAAAGGCTCTTCTATCTGTTCGGGAGCTGGTCAAGTGCG
4051   ACCTGCTTGCCGAGTCAGACGATGATGACAGTGTGCAGGAGCAACGACTG
4101   TTGGTGCTAGAGAATCGAGGACGACTGAACTTCGATATATGGAGCACGGG
4151   AAACATATTTGAGTGATACACACGTTCCCATCGCTGTGTACGATGGATTA
4201   CATGAGTGGACGGGTAAAAAAAATACAGGCGCAGGAATGGGACTTTCAGTG
4251   AGTCAGTATTCCTCTGCATGGATCTTGCAGGGCTTTTCGGCGCGGCGCTT
4301   GGGATGTAAACTTCTAATTGAGTATGAGCCGCTAATGGATGCTTCGTTTT
4351   GTACATCACACACAGTCTCTTCACTGTTGACGTCGTGGCCTTATCGCTGA
4401   TACGGTGCACGTTCCTCGCGAGTGCGCCATCTCCATCTGTCGCGCTAGTA
4451   CAGCCACTGGTGTTCGTGAATCTGCATCATACATAGAAACCATTCAATGA
4501   TACAATTTATCGAT
```

LmxMPK6 ORF and flanking regions, LmxMPK6 translated sequence

The lysine33 of the K33M mutation is underlined in bold; the truncation sites of LmxMPK6short and LmxMPK6short2TY/LmxMPK6Nterm are marked in the amino acid sequence with **I** and **II** respectively; the sequences corresponding to probes used for Southern blot analyses are highlighted grey.

```
1      CGTAGCGCCGCGGGTACTCGTGTGGACGTGCTTGCGGGTCTTGTTGGCCGCTTGCTTGCT
61     CCTCCCCGCCCACATCGCCTCTCTGCAACCTCCCCTCGTCTCGCCCCCTTTCCTCAGCCA
121    ACGCTGTATACACTCGAGAGAGGAGGAGCGCTGGAAGACTCGGACACACACACACAGCGC
181    ATCCACGGCCGCTTATCTTCCTCTGCGCACGACGACGGTCCGCGTCTGCGTGTCTTCTGC
241    TCTGGAGCGGAACGAGGACCATAGAGGAGACCAAGAGAAATAAAAAAGGGAGGCACACAC
301    ACATACACACACGCGCAGACTGTGGGGTGGGGGCTAAGCTGCTGCGTTGTTGCGTGTTTT
361    GTACTTCTCTCGGTCGTTGTGTTTTTGGACCCGCGCTTCAAGAGAGGCGCCGTGCCCTCC
421    CGCCACCGCACACAACCAACAACGGTGCTGTATTTGGCTGGCACGTTGCCCCCTCCTCCC
481    TCCCTCCCTTTFCATCATCTTTCCTGTTGAAGTCTTTTCGTGTATTTGATTTAGTGTTGG
541    GGGACGGTATGTGCGTGTACATGGTTGGCTGCCGCACTCCTCTCAATACCTTTGGTTCTC
601    GCGCGCACGCTTGTGTGCTTGCGTCTTTCTTCTTCGTACCTCCCATGTGGGCCGGTGCTA
661    TTTTCTTGTCGTGCTACCCACGAGCCGAAGTCTCCATATCGCTGTACAAGCTGAGCCTTG
721    AAGTCGATGGAGGCCTACGAGACACTCGGCATCCTCGGCGAGGGCACCTACGGCGTGGTT
             M  E  A  Y  E  T  L  G  I  L  G  E  G  T  Y  G  V  V
781    GTCAAGGCCCGAAGCCGCGTAACGGGGAAGCTTGTCGCCATCAAGCGCTTTAAGCAGACA
       V  K  A  R  S  R  V  T  G  K  L  V  A  I  K  R  F  K  Q  T
841    GAGCAGGATGAGCACGTCCGCAAGACCTCCTCCCGCGAAGTGCGCATGCTGCAGCTGCTG
       E  Q  D  E  H  V  R  K  T  S  S  R  E  V  R  M  L  Q  L  L
901    CAGCACCCCAACGTGATCCGCTTAGAGGACGTCTTCCGCAGGGAGGGTAAGCTCTACCTC
       Q  H  P  N  V  I  R  L  E  D  V  F  R  R  E  G  K  L  Y  L
961    GTGTTTGAGTTCATTGATCACACGATCCTGCAGCTTCTGGAGAGCACCACGCGCGGTTTC
       V  F  E  F  I  D  H  T  I  L  Q  L  L  E  S  T  T  R  G  F
1021   CACCGCCACGAACTGCGCCGCTACACCTACCAACTGCTGCGCGGTATCGAGTTCTGCCAC
       H  R  H  E  L  R  R  Y  T  Y  Q  L  L  R  G  I  E  F  C  H
1081   AATCAAAACATCATACACCGCGACGTGAAGCCGGAAAATGTGCTCATCGACGAATCAGGA
       N  Q  N  I  I  H  R  D  V  K  P  E  N  V  L  I  D  E  S  G
1141   CTGCTGAAGCTCTGCGACTTTGGCTTTGCTCGACAGACGTCGGCCAAAGGCAAGTACACA
       L  L  K  L  C  D  F  G  F  A  R  Q  T  S  A  K  G  K  Y  T
1201   GACTACGTGGCAACGCGCTGGTATAGGGCGCCGGAGCTGCTCGTCGGAGACGTGGCCTAC
       D  Y  V  A  T  R  W  Y  R  A  P  E  L  L  V  G  D  V  A  Y
1261   GGCAAGCCGGTGGACGTGTGGGCGCTAGGGTGCATGTTTGCCGAGCTCTCCGATGGACAG
       G  K  P  V  D  V  W  A  L  G  C  M  F  A  E  L  S  D  G  Q
1321   CCACTCTTCCCCGGCGAGTCGGACCTAGACCAGCTATGCCTGATTATGCAGACCTGCGGG
       P  L  F  P  G  E  S  D  L  D  Q  L  C  L  I  M  Q  T  C  G
1381   CCAGTGCCGCAGCGCCTAGTTTTCATCTTCATGCACAACCCGCTGTACAACGGCATCAGC
       P  V  P  Q  R  L  V  F  I  F  M  H  N  P  L  Y  N  G  I  S
1441   TTTCCGCACACCGACATCCTGTACACGCTCAAGGATCGCTACCATCGCGAGTCGAACGAC
       F  P  H  T  D  I  L  Y  T  L  K  D  R  Y  H  R  E  S  N  D
```

```
1501    TGGATCGAGTTCCTCAGCTCTTGTCTCCACACGGACCCGGCGCAGCGGCTGACGTGCACG
        W  I  E  F  L  S  S  C  L  H  T  D  P  A  Q  R  L  T  C  T
1561    GAGCTTATGGAGCTCCCCTACTTCACGCGTGACGGCTTCCGCGATCGCTATGAGGCCGAG
        E  L  M  E  L  P  Y  F  T  R  I  D  G  F  R  D  R  Y  E  A  E
1621    CTGCGGGCTGCAACGGGCCTGCCTCAGCTGCGGTCCACTCCCACGACGTCGGCGCCTTCG
        L  R  A  A  T  G  L  P  Q  L  R  S  T  P  T  T  S  A  P  S
1681    ACACAGCGGCGTGCGCCGGATCAGGCAGCTGCTTTAGGAGGCGACATCAAGGCAGACGCC
        T  Q  R  R  A  P  D  Q  A  A  A  L  G  G  D  I  K  A  D  A
1741    GTCGTGCCTCCACACACGCGCCGCTCGAGTGAGAATATTTCACCGGCGCTGCAGGGACAA
        V  V  P  P  H  T  R  R  S  S  E  N  I  S  P  A  L  Q  G  Q
1801    CAACCGCCCACGGCCAAAAACAGCTTTAGCGAACCACACATCTCGAAGACGGCGCTCAAG
        Q  P  P  T  A  K  N  S  I  F  S  E  P  H  I  S  K  T  A  L  K
1861    CCTGCCGCGCACGACGCCAACCCCGGCAAGGGCAAAGGTGCAGGCGCACCAACGCTCAGG
        P  A  A  H  D  A  N  P  G  K  G  K  G  A  G  A  P  T  L  R
1921    TTGACGTCTCCACACAAGACGGCGTCTGAGCATCCCCTGCAGCTGCCGATGATCCTCAAC
        L  T  S  P  H  K  T  A  S  E  H  P  L  Q  L  P  M  I  L  N
1981    GTTAGCTCGGAGAGGGCCATCGCTGCGGCGCTGACGGACTACTTGAATCAGATGCCCACC
        V  S  S  E  R  A  I  A  A  A  L  T  D  Y  L  N  Q  M  P  T
2041    TCTTCGAGCACTGTGGTGTCGTCACCGGCACAGGCTACTCCAGCAGAGGTGGCCGAGGCC
        S  S  S  T  V  V  S  S  P  A  Q  A  T  P  A  E  V  A  E  A
2101    TTTACCAAAGCTGATCCGCTCTCCCGCTCGTGTGGGGCGGCACTGCCGCTGCAGACATCG
        F  T  K  A  D  P  L  S  R  S  C  G  A  A  L  P  L  Q  T  S
2161    CAGACCATCAACGCATCAACTACGCGAGATAAAAAGAAGAAGCGGAATAGCAGTTTAGCA
        Q  T  I  N  A  S  T  T  R  D  K  K  K  K  R  N  S  S  L  A
2221    GAGACCGAATTACACCGGCGCAGCAGCGCAAGCATCAGCAACGACACCGAGTACGCTGTG
        E  T  E  L  H  R  R  S  S  A  S  I  S  N  D  T  E  Y  A  V
2281    ACGACAGACGGCACCAAGGGTGAACCGGCCAGGCACATCAGCGACCATCCACGGGCATCG
        T  T  D  G  T  K  G  E  P  A  R  H  I  S  D  H  P  R  A  S
2341    GCCACACTTCCGCCCAACGGAGTTCGCGATGGCGGTGACTCTCACGAGCCGAGGCGCGAA
        A  T  L  P  P  N  G  V  R  D  G  G  D  S  H  E  P  R  R  E
2401    GGCGAAAAGACAAACGTGTCGCCACCGCTGCCGTCGCACGGAGTGGCAGAGAGTAACATG
        G  E  K  T  N  V  S  P  P  L  P  S  H  G  V  A  E  S  N  M
2461    CGGGCTCTCCTGACAACCGCAGCACCAGGAAAGGATGGTGGCGAGACGGCTGTGCTGAGC
        R  A  L  L  T  T  A  A  P  G  K  D  G  G  E  T  A  V  L  S
2521    CACCGAGCTTTGAAGCCGGCGTCAGCGGAGAAAGCCGCGGCAACGACGGCCACAGCTTTT
        H  R  A  L  K  P  A  S  A  E  K  A  A  A  T  T  A  T  A  F
2581    TCGCCGCCGCCGCTCACCGCCACCCACGGTGCTCCGCTGGCAGAGTGTCTGCAGGACCTC
        S  P  P  P  L  T  A  T  H  G  A  P  L  A  E  C  L  Q  D  L
2641    CCTGCCCTATCCCTGCACCTCCCGCGCCACTTACAGTCGGAACGGCAGACACCAGCGGCG
        P  A  L  S  L  H  L  P  R  H  L  Q  S  E  R  Q  T  P  A  A
2701    GAGCAGCCTCAGCCGCACACCTCACTCTCTGCCGAGACCTCGATGTCGTCCTTCCACGTC
        E  Q  P  Q  P  H  T  S  L  S  A  E  T  S  M  S  S  F  H  V
2761    CGCACGCGCAACCCACTCGCTGCAGCCTCGTCGGTGAACGATGGCGTTTCTCATGGCAAG
        R  T  R  N  P  L  A  A  A  S  S  V  N  D  G  V  S  H  G  K
2821    GCAAACATTGAGACGACTGGCTCGAGCGTCGCTAAGCCACGGCTCGGCCTCTCGAACTCA
        A  N  I  E  T  T  G  S  S  V  A  K  P  R  L  G  L  S  N  S
2881    AGTGTCTCAACGGCCGCCAGCGAAGTGAAGAAGCGCAAGTCCGCCAGGCACAAGAGTAAC
        S  V  S  T  A  A  S  E  V  K  K  R  K  S  A  R  H  K  S  N
2941    ACGAGCCGCCTGCAAGACAAGGCTGTGGGGCCCGTCAGCGGCAGCGCATCGCGTCGCCCT
        T  S  R  L  Q  D  K  A  V  G  P  V  S  G  S  A  S  R  R  P
3001    GTCCCAGGGAACGCGTCGGACGTAGTGGCTTACCGTGCGGGGTTCGCCTCGGTGGTGAAC
        V  P  G  N  A  S  D  V  V  A  Y  R  A  G  F  A  S  V  V  N
3061    TCTTTGAAGTCAACGGTGTCACAGTCGCTCTCTCATGTGCTGGGTCAGCAGCAACGGCAC
        S  L  K  S  T  V  S  Q  S  L  S  H  V  L  G  Q  Q  Q  R  H
3121    CGCTTGCTGTCCCCAGAGTCAGACGGAGTCCACACTGCCGAACCGCACCTGCACGGTGTT
        R  L  L  S  P  E  S  D  G  V  H  T  A  E  P  H  L  H  G  V
3181    GGTGCAGGCCCGAGCGCACCTGATTCCACCCGTAACCGAAACGTCGACGCAACCGGCCCA
        G  A  G  P  S  A  P  D  S  T  R  N  R  N  V  D  A  T  G  P
3241    CAGCCACGCAAGGAGCGGCGATGTAAACCGTTGGCTGCCTCAACACATGCTCTCCAGGGT
        Q  P  R  K  E  R  R  C  K  P  L  A  A  S  T  H  A  L  Q  G
3301    AGTGATCAGCGCCATCGCCAGCAGTCGCAGCCTCGACTGGACGGACCACTGCACCCTGAC
        S  D  Q  R  H  R  Q  Q  S  Q  P  R  L  D  G  P  L  H  P  D
3361    GGCGGTGCCTCTCAGCGAGCCACGGCTACCTTGATGGCTTTATCAGCGCTTCGCAACGTC
        G  G  A  S  Q  R  A  T  A  T  L  M  A  L  S  A  L  R  N  V
```

```
3421    TCCGGGCCGCCGCCGGCCAAGTCCGCCGGCGACGCGAACAAGAGCAGCTACGTCCACCAC
        S  G  P  P  P  A  K  S  A  G  D  A  N  K  S  S  Y  V  H  H
3481    ACACGCTCGCACACCAACAACAACGGAGGCGAGACCGTGATCCCGGTGGTTGGTGGGGAC
        T  R  S  H  T  N  N  N  G  G  E  T  V  I  P  V  V  G  G  D
3541    GGCAACGACACCAACACATGCGTTACAAGTCGCGCTCGACGTCCTATAGTTGCGTGCGCG
        G  N  D  T  N  T  C  V  T  S  R  A  R  R  P  I  V  A  C  A
3601    GTGCACGGCAACAACCGCGATAGTGACGAGCTGATGGCGACCCGCCGAGTGCAGAAGAAG
        V  H  G  N  N  R  D  S  D  E  L  M  A  T  R  R  V  Q  K  K
3661    AATGCCGTCGCGACACACGGCCGAACTGGCAACGGCGCTGTGGGTTCCATTGGCTGCACA
        N  A  V  A  T  H  G  R  T  G  N  G  A  V  G  S  I  G  C  T
3721    GATAGCTCCACGACGTCTTCCTATCAAGCAACCAGCATTATGTATGGCGCGCCGTACCAC
        D  S  S  T  T  S  S  Y  Q  A  T  S  I  M  Y  G  A  P  Y  H
3781    CCCTTTGCGAGGGCCTCAAAGGTGGACGGTGATGTGTGCGGGGCCCAGCAGCGGCAGACC
        P  F  A  R  A  S  K  V  D  G  D  V  C  G  A  Q  Q  R  Q  T
3841    CTACAGAGGCTCAAGAAGAAGATTGCCGACCACCGCGGCAGCGGCATCGCAAACACAACC
        L  Q  R  L  K  K  K  I  A  D  H  R  G  S  G  I  A  N  T  T
3901    AGCAGCATTGGCTCCCGTCACTCGCTGACGCCTGCGCGGCAGATACAGCACCAGCCGCAG
        S  S  I  G  S  R  H  S  L  T  P  A  R  Q  I  Q  H  Q  P  Q
3961    CTCGCGAAGGAGGATGGTGGCAGCGGCGACGGCAAAACGCCCCAGTTTAATGCCGCCACA
        L  A  K  E  D  G  G  S  G  D  G  K  T  P  Q  F  N  A  A  T
4021    GCTGCATCCCCCGATACTGGCATCTGACCAGCTTTGTGCCGTAAATCCAATGCACAGTAG
        A  A  S  P  D  T  G  I  *
4081    TGCACGGGCTTCTTTTTTCTGCTTTCTGTTGTCCTGTTGTTGTCCTCCGATGCACAGGAT
4141    GCCACATCCTCCCTTGCTCTCTCACGTCATTCGGGGGGGGGCAGGGGGTTGGGGGAGGGA
4201    GCGGCACGTGGGTGTGTTGGCTGGCTCGCTCCTCCCACTTCGCTCTGTTTTCGCTGTTCT
4261    GCGTTGTATGATTTCGTCGCTTCTCGTTCTCGTTCCTTCCTTGTCGTACGTTTGTGTGCG
4321    CATGCGTTGCGCGCGCTCTCCTGTTGTTGAGGGGGCCGGATGGAGGGTGGGAGGGGCGCG
4381    TACGAGTGCGCACACCGCACAAGGCAACGCCGCCGCTACCACAGTCTATCTTGTGCGCTA
4441    CTTTTCCATTTCGTCTCCGTCTCTTCCCGAGCCTCTTGAGTGTTCCTTTCGCTGTCACCT
4501    TCCTGCCGCGCTGTCGCCGGAGCTGACGTGGGTGAGATAGAGAGAGGCTGAGAAGGCGCA
4561    TGCTTTACTTCTCTCCTCACCCCGCACCACGGACACACGCACGCACACCCACCCACCCAC
4621    ACTGTATCAGGCGGTACAGTAACACTTTGTTTGTTTCTTCCTTTTTTCGGTGGTGTCGAT
4681    GGTAGTGGTGGTAGGGGGTGGAACAGACGAAACAACTCCGCCCCACCCCTACCTCTCCAA
4741    GGGAAAGGTGCGGGTATTGTGTGAT
```

Sequence of *LmxMPK6short*

```
1       GGATCCACCATGGAGGCCTACGAGACACTCGGCATCCTCGGCGAGGGCACCTACGGCGTG
                M  E  A  Y  E  T  L  G  I  L  G  E  G  T  Y  G  V
61      GTTGTCAAGGCCCGAAGCCGCGTAACGGGGAAGCTTGTCGCCATCAAGCGCTTTAAGCAG
        V  V  K  A  R  S  R  V  T  G  K  L  V  A  I  K  R  F  K  Q
121     ACAGAGCAGGATGAGCACGTCCGCAAGACCTCCTCCCGCGAAGTGCGCATGCTGCAGCTG
        T  E  Q  D  E  H  V  R  K  T  S  S  R  E  V  R  M  L  Q  L
181     CTGCAGCACCCCAACGTGATCCGCTTAGAGGACGTCTTCCGCAGGGAGGGTAAGCTCTAC
        L  Q  H  P  N  V  I  R  L  E  D  V  F  R  R  E  G  K  L  Y
241     CTCGTGTTTGAGTTCATTGATCACACGATCCTGCAGCTTCTGGAGAGCACCACGCGCGGT
        L  V  F  E  F  I  D  H  T  I  L  Q  L  L  E  S  T  T  R  G
301     TTCCACCGCCACGAACTGCGCCGCTACACCTACCAACTGCTGCGCGGTATCGAGTTCTGC
        F  H  R  H  E  L  R  R  Y  T  Y  Q  L  L  R  G  I  E  F  C
361     CACAATCAAAACATCATACACCGCGACGTGAAGCCGGAAAATGTGCTCATCGACGAATCA
        H  N  Q  N  I  I  H  R  D  V  K  P  E  N  V  L  I  D  E  S
421     GGACTGCTGAAGCTCTGCGACTTTGGCTTTGCTCGACAGACGTCGGCCAAAGGCAAGTAC
        G  L  L  K  L  C  D  F  G  F  A  R  Q  T  S  A  K  G  K  Y
481     ACAGACTACGTGGCAACGCGCTGGTATAGGGCGCCGGAGCTGCTCGTCGGAGACGTGGCC
        T  D  Y  V  A  T  R  W  Y  R  A  P  E  L  L  V  G  D  V  A
541     TACGGCAAGCCGGTGGACGTGTGGGCGCTAGGGTGCATGTTTGCCGAGCTCTCCGATGGA
        Y  G  K  P  V  D  V  W  A  L  G  C  M  F  A  E  L  S  D  G
601     CAGCCACTCTTCCCCGGCGAGTCGGACCTAGACCAGCTATGCCTGATTATGCAGACCTGC
        Q  P  L  F  P  G  E  S  D  L  D  Q  L  C  L  I  M  Q  T  C
661     GGGCCAGTGCCGCAGCGCCTAGTTTTCATCTTCATGCACAACCCGCTGTACAACGGCATC
        G  P  V  P  Q  R  L  V  F  I  F  M  H  N  P  L  Y  N  G  I
```

```
721     AGCTTTCCGCACACCGACATCCTGTACACGCTCAAGGATCGCTACCATCGCGAGTCGAAC
        S  F  P  H  T  D  I  L  Y  T  L  K  D  R  Y  H  R  E  S  N
781     GACTGGATCGAGTTCCTCAGCTCTTGTCTCCACACGGACCCGGCGCAGCGGCTGACGTGC
        D  W  I  E  F  L  S  S  C  L  H  T  D  P  A  Q  R  L  T  C
841     ACGGAGCTTATGGAGCTCCCCTACTTCACGCGTTGA
        T  E  L  M  E  L  P  Y  F  T  R  *
```

Sequence of *LmxMPK6short2TY*

The sequence corresponding to the TY-tag is underlined in grey;

```
1       GGATCCACCATGGAGGCCTACGAGACACTCGGCATCCTCGGCGAGGGCACCTACGGCGTG
                M  E  A  Y  E  T  L  G  I  L  G  E  G  T  Y  G  V
61      GTTGTCAAGGCCCGAAGCCGCGTAACGGGGAAGCTTGTCGCCATCAAGCGCTTTAAGCAG
        V  V  K  A  R  S  R  V  T  G  K  L  V  A  I  K  R  F  K  Q
121     ACAGAGCAGGATGAGCACGTCCGCAAGACCTCCTCCCGCGAAGTGCGCATGCTGCAGCTG
        T  E  Q  D  E  H  V  R  K  T  S  S  R  E  V  R  M  L  Q  L
181     CTGCAGCACCCCAACGTGATCCGCTTAGAGGACGTCTTCCGCAGGGAGGGTAAGCTCTAC
        L  Q  H  P  N  V  I  R  L  E  D  V  F  R  R  E  G  K  L  Y
241     CTCGTGTTTGAGTTCATTGATCACACGATCCTGCAGCTTCTGGAGAGCACCACGCGCGGT
        L  V  F  E  F  I  D  H  T  I  L  Q  L  L  E  S  T  T  R  G
301     TTCCACCGCCACGAACTGCGCCGCTACACCTACCAACTGCTGCGCGGTATCGAGTTCTGC
        F  H  R  H  E  L  R  R  Y  T  Y  Q  L  L  R  G  I  E  F  C
361     CACAATCAAAACATCATACACCGCGACGTGAAGCCGGAAAATGTGCTCATCGACGAATCA
        H  N  Q  N  I  I  H  R  D  V  K  P  E  N  V  L  I  D  E  S
421     GGACTGCTGAAGCTCTGCGACTTTGGCTTTGCTCGACAGACGTCGGCCAAAGGCAAGTAC
        G  L  L  K  L  C  D  F  G  F  A  R  Q  T  S  A  K  G  K  Y
481     ACAGACTACGTGGCAACGCGCTGGTATAGGGCGCCGGAGCTGCTCGTCGGAGACGTGGCC
        T  D  Y  V  A  T  R  W  Y  R  A  P  E  L  L  V  G  D  V  A
541     TACGGCAAGCCGGTGGACGTGTGGGCGCTAGGGTGCATGTTTGCCGAGCTCTCCGATGGA
        Y  G  K  P  V  D  V  W  A  L  G  C  M  F  A  E  L  S  D  G
601     CAGCCACTCTTCCCCGGCGAGTCGGACCTAGACCAGCTATGCCTGATTATGCAGACCTGC
        Q  P  L  F  P  G  E  S  D  L  D  Q  L  C  L  I  M  Q  T  C
661     GGGCCAGTGCCGCAGCGCCTAGTTTTCATCTTCATGCACAACCCGCTGTACAACGGCATC
        G  P  V  P  Q  R  L  V  F  I  F  M  H  N  P  L  Y  N  G  I
721     AGCTTTCCGCACACCGACATCCTGTACACGCTCAAGGATCGCTACCATCGCGAGTCGAAC
        S  F  P  H  T  D  I  L  Y  T  L  K  D  R  Y  H  R  E  S  N
781     GACTGGATCGAGTTCCTCAGCTCTTGTCTCCACACGGACCCGGCGCAGCGGCTGACGTGC
        D  W  I  E  F  L  S  S  C  L  H  T  D  P  A  Q  R  L  T  C
841     ACGGAGCTTATGGAGCTCCCCTACTTCACGCGTGACGGCTTCCGCGATCGCTATGAGGCC
        T  E  L  M  E  L  P  Y  F  T  R  D  G  F  R  D  R  Y  E  A
901     GAGCTGCGGGCTGCAACGGGCCTGCCTCAGCTGCGGTCCACTCCCACGACGTCGGCGCCT
        E  L  R  A  A  T  G  L  P  Q  L  R  S  T  P  T  T  S  A  P
961     TCGACACAGCGGCGTGCGCCGGATCAGGCAGCTGCTTTAGGAGGCGACATCAAGGCAGAC
        S  T  Q  R  R  A  P  D  Q  A  A  A  L  G  G  D  I  K  A  D
1021    GCCGTCGTGCCTCCACACACGCGCCGCTCGAGTGAGAATATTTCACCGGCGCTGCAGGGA
        A  V  V  P  P  H  T  R  R  S  S  E  N  I  S  P  A  L  Q  G
1081    CAACAACCGCCCACGGCCAAAAACAGCAACATGGAGGTGCACACGAACCAGGACCCGCTG
        Q  Q  P  P  T  A  K  N  S  N  M  E  V  H  T  N  Q  D  P  L
1141    GACAGATCTTGAAGCTTGATATC
        D  R  S  *
```

Sequence of LmxMPK6Nterm

```
1        GGATCCGATGGAGGCCTACGAGACACTCGGCATCCTCGGCGAGGGCACCTACGGCGTG
                M  E  A  Y  E  T  L  G  I  L  G  E  G  T  Y  G  V
61      GTTGTCAAGGCCCGAAGCCGCGTAACGGGGAAGCTTGTCGCCATCAAGCGCTTTAAGCAG
        V  V  K  A  R  S  R  V  T  G  K  L  V  A  I  K  R  F  K  Q
121     ACAGAGCAGGATGAGCACGTCCGCAAGACCTCCTCCCGCGAAGTGCGCATGCTGCAGCTG
        T  E  Q  D  E  H  V  R  K  T  S  S  R  E  V  R  M  L  Q  L
181     CTGCAGCACCCCAACGTGATCCGCTTAGAGGACGTCTTCCGCAGGGAGGGTAAGCTCTAC
        L  Q  H  P  N  V  I  R  L  E  D  V  F  R  R  E  G  K  L  Y
241     CTCGTGTTTGAGTTCATTGATCACACGATCCTGCAGCTTCTGGAGAGCACCACGCGCGGT
        L  V  F  E  F  I  D  H  T  I  L  Q  L  L  E  S  T  T  R  G
301     TTCCACCGCCACGAACTGCGCCGCTACACCTACCAACTGCTGCGCGGTATCGAGTTCTGC
        F  H  R  H  E  L  R  R  Y  T  Y  Q  L  L  R  G  I  E  F  C
361     CACAATCAAAACATCATACACCGCGACGTGAAGCCGGAAAATGTGCTCATCGACGAATCA
        H  N  Q  N  I  I  H  R  D  V  K  P  E  N  V  L  I  D  E  S
421     GGACTGCTGAAGCTCTGCGACTTTGGCTTTGCTCGACAGACGTCGGCCAAAGGCAAGTAC
        G  L  L  K  L  C  D  F  G  F  A  R  Q  T  S  A  K  G  K  Y
481     ACAGACTACGTGGCAACGCGCTGGTATAGGGCGCCGGAGCTGCTCGTCGGAGACGTGGCC
        T  D  Y  V  A  T  R  W  Y  R  A  P  E  L  L  V  G  D  V  A
541     TACGGCAAGCCGGTGGACGTGTGGGCGCTAGGGTGCATGTTTGCCGAGCTCTCCGATGGA
        Y  G  K  P  V  D  V  W  A  L  G  C  M  F  A  E  L  S  D  G
601     CAGCCACTCTTCCCCGGCGAGTCGGACCTAGACCAGCTATGCCTGATTATGCAGACCTGC
        Q  P  L  F  P  G  E  S  D  L  D  Q  L  C  L  I  M  Q  T  C
661     GGGCCAGTGCCGCAGCGCCTAGTTTTCATCTTCATGCACAACCCGCTGTACAACGGCATC
        G  P  V  P  Q  R  L  V  F  I  F  M  H  N  P  L  Y  N  G  I
721     AGCTTTCCGCACACCGACATCCTGTACACGCTCAAGGATCGCTACCATCGCGAGTCGAAC
        S  F  P  H  T  D  I  L  Y  T  L  K  D  R  Y  H  R  E  S  N
781     GACTGGATCGAGTTCCTCAGCTCTTGTCTCCACACGGACCCGGCGCAGCGGCTGACGTGC
        D  W  I  E  F  L  S  S  C  L  H  T  D  P  A  Q  R  L  T  C
841     ACGGAGCTTATGGAGCTCCCCTACTTCACGCGTGACGGCTTCCGCGATCGCTATGAGGCC
        T  E  L  M  E  L  P  Y  F  T  R  D  G  F  R  D  R  Y  E  A
901     GAGCTGCGGGCTGCAACGGGCCTGCCTCAGCTGCGGTCCACTCCCACGACGTCGGCGCCT
        E  L  R  A  A  T  G  L  P  Q  L  R  S  T  P  T  T  S  A  P
961     TCGACACAGCGGCGTGCGCCGGATCAGGCAGCTGCTTTAGGAGGCGACATCAAGGCAGAC
        S  T  Q  R  R  A  P  D  Q  A  A  A  L  G  G  D  I  K  A  D
1021    GCCGTCGTGCCTCCACACACGCGCCGCTCGAGTGAGAATATTTCACCGGCGCTGCAGGGA
        A  V  V  P  P  H  T  R  R  S  S  E  N  I  S  P  A  L  Q  G
1081    CAACAACCGCCCACGGCCAAAAACAGCTGATATC
        Q  Q  P  P  T  A  K  N  S  *
```

Alignment of LmxMPK6 and its closest homologues from other organisms

CLUSTAL 2.0.12 multiple sequence alignment; the reserved kinase domains of LmxMPK6 are underlined in grey; Lmx, *L. mexicana*; Lma, *L. major*; Lin, *L. infantum*; Lbr, *L. braziliensis*; Tb, *T. brucei*; Tc, *T. cruzi*; Smp, *Schistosoma mansoni*; Dd, *Dictyostelium discoideum*; Hs, *Homo sapiens*;

```
                          I                          II          III
LmxMPK6         MEAYETLGILGEGTYGVVVKARSRVTGKLVAIKRFKQTEQDEHVRKTSSREVRMLQLLQH 60
LmaMPK          MEAYETLGILGEGTYGVVVKARSRVTGKLVAIKRFKQTEQDEHVRKTSSREVRMLQLLQH 60
LinMPK          MEAYEILGILGEGTYGVVVKARSRVTGKLVAIKRFKQTEQDEHVRKTSSREVRMLQLLQH 60
LbrMPK          MESYETLGILGEGTYGVVVKARSRTTGKLVAIKRFKQTEQDEHVRKTSTREVRMLQLLRH 60
TbECK1          MDAYETLGMLGEGTYGVVVKARHRATSRIVAIKKYKQAEDDDHVRKTSLREVRVLKQLRH 60
TcMPK           MEGYETLGILGEGTYGVVVKARHRATGRIVAIKKYKQAEDDNHVRKTSLREVRVLKQLRH 60
SmpMPK          MEKYENLGLVGEGSYGMVIKCKNKESGRIVAIKKFIDSEDDKHVKKIALREIRMLKQLRH 60
DdMPK           MEKYSKIEKLGEGTYGIVYKAKNRETGEIVALKRIRLDSEDEGVPCTAIREISLLKELKH 60
HsCDKL2         MEKYENLGLVGEGSYGMVMKCRNKDTGRIVAIKKFLESDDDKMVKKIAMREIKLLKQLRH 60
                *: *. :  :***:**:* *.: : :..:**:*:    .:*. *   : **: :*: *:*

                   IV              V                        VIa
LmxMPK          PNVIRLEDVFRREGKLYLVFEFIDHTILQLLESTTRGFHRHELRRYTYQLLRGIEFCHNQ 120
LmaMPK          PNVIRLEDVFRREGKLYLVFEFIDQTILQLLESTTRGLHRRELRRYTYQLLRGIEFCHNH 120
LinMPK          PNVIRLEDVFRREGKLYLVFEFIDQTILQLLESTTRGLHRRELRRYTYQLLRGIEFCHNH 120
LbrMPK          PNVIRLEDVFRREGKLYLVFEFIDHTILQLLESTTRGLSRRELRRYAYQLLRGIEFCHKH 120
TbECK1          PNVIALLDVFRRDGKLYLVFEYVENTILQLIEEKKYGLSPDEVRRYTFQLLNGVSYCHAH 120
TcMPK           PNVISLLDVFRRDGKLFLVFEYVENTILQLIEEKRHGLPPDEVRRYTYQLLNGVDYCHAH 120
SmpMPK          DNLVNLLEVFRRKKRLYLVFEFVDNTILDDLEKNPNGIDELRTKRTLFQVIRGVEFCHLH 120
DdMPK           PNIVRLHDVIHTERKLTLVFEYLDQDLKKYLDECGGEISKPTIKSFMYQLLKGVAFCHDH 120
HsCDKL2         ENLVNLLEVCKKKKRWYLVFEFVDHTILDDLELFPNGLDYQVVQKYLFQIINGIGFCHSH 120
                 *:: * :* : . :  ****:::: : . ::     :     :   :*::.*: :** :

                    VIb               VII                VIII
LmxMPK          NIIHRDVKPENVLIDESGLLKLCDFGFARQTSA-KGKYTDYVATRWYRAPELLVGDVAYG 179
LmaMPK          NVIHRDVKPENVLIDESGLLKLCDFGFARQTSA-RGKYTDYVATRWYRAPELLVGDVAYG 179
LinMPK          NVIHRDVKPENVLIDESGLLKLCDFGFARQTSA-KGKYTDYVATRWYRAPELLVGDVAYG 179
LbrMPK          NVIHRDVKPENVLIDESGLLKLCDFGFARQMSA-KGKYTDYVATRWYRAPELLVGDVAYG 179
TbECK1          NIIHRDVKPENILVSRDGVLKLCDFGFARQLSC-RGNYTEYVATRWYRAPELLVGDVSYG 179
TcMPK           NIIHRDVKPENILVSKDGVLKLCDFGFARQLSS-KGKYTDYVATRWYRAPELLVGDVFYG 179
SmpMPK          NIVHRDIKPENILISRNGVVKLCDFGFARTLAAPGEVYTDYVATRWYRAPELLVGDTKYG 180
DdMPK           RVLHRDLKPQNLLINRKGELKLADFGLARAFGIPVRTYSHEVVTLWYRAPDVLMGSRKYS 180
HsCDKL2         NIIHRDIKPENILVSQSGVVKLCDFGFARTLAAPGEVYTDYVATRWYRAPELLVGDVKYG 180
                .::***:**:*:*:...* :**.***:**  .     *:. *.* *****::*:*.  *.

                      IX                          X
LmxMPK          KPVDVWALGCMFAELSDGQPLFPGESDLDQLCLIMQTCGPVPQRLVFIFMHNPLYNGISF 239
LmaMPK          KPVDVWALGCMFAELSDGQPLFPGESDLDQLCLIMQTCGPVPQRLVFIFMHNPLYNGISF 239
LinMPK          KPVDVWALGCMFAELSDGQPLFPGESDLDQLCLIMQTCGPVPQRLVFIFMHNPLYNGISF 239
LbrMPK          KPVDVWALGCMFAELSDGQPLFPGESDLDQLCLILQTCGPVPARMVFIFEHNPLYSGVSF 239
TbECK1          KAVDVWAIGCVFSELSDGQPLFPGDSDLDQLSLIMRACGPVPQQMVSTFEHNALYRRVTF 239
TcMPK           KAVDIWAIGCIFSELSDGQPLFPGDSDLDQLALIMRSCGPVPDRMVDIFERNALYRRVAF 239
SmpMPK          RPIDIWAIGCLASEMLTGDPLFPGDSDIDQLHRIVRCLGNLSEKYQNIFHRNPLFVGMRV 240
DdMPK           TPIDIWSAGCIFAEMASGRPLFPGSGTSDQLFRIFKILGTPNEESWPSITELPEYK-TDF 239
HsCDKL2         KAVDVWAIGCLVTEMFMGEPLFPGDSDIDQLYHIMMCLGNLIPRHQELFNKNPVFAGVRL 240
                 .:*:*: **: :*:  * *****..  ***  *.   *    .    : . . :    .

                                    XI
LmxMPK          PHTDILYTLKDRYHRESNDWIEFLSSCLHTDPAQRLTCTELMELPYFTRDGFRDRYEAEL 299
LmaMPK          PHTDILYTLKERYHRESNDWLEFLSSCLHTDPAQRLTCTELMELPYFTRDGFRDRYEAEL 299
LinMPK          PHTDILYTLKERYHRESNDWLEFLSSCLHTDPAQRLTCTELMELPYFTRDGFRDRYEAEL 299
LbrMPK          PKTGIIYTLKERYHRESDDWLDFLSSCLHTDPAQRLTCTELMELPYFTRDGFRDRYEAEL 299
TbECK1          PNVDVEETLQQRFPTAASPWLEFLTSCLRMDPVERPSCTALMSMAYFTENNFRATYELEL 299
TcMPK           PRTPMEETLQKRFKSCKASWLELLTSCLRTDPAERPSCAALMNMPYFTEDNFRVEYEAEL 299
SmpMPK          PFAKEIDPLDKRLAKVSKLTLGFIKTCLRIDANDRPTSSALLRSEYFTRENFASIFLEEL 300
DdMPK           P-VHPAHQLSSIVHGLDEKGLNLLSKMLQYDPNQRITAAAALKHPYFDG----------L 288
HsCDKL2         PEIKEREPLERRYPKLSEVVIDLAKKCLHIDPDKRPFCAELLHHDFFQMDGFAERFSQEL 300
                *       *.          : : .. *: *. .*  .:  :   :*           *
```

```
LmxMPK6         RAATGLPQLRSTPTTSAPSTQRRAPDQAAALGGDIKADAVVPPHTRRSSENISPALQGQQ 359
LmaMPK          QAAMGLPQLRSTPTTSAPSTQRRAPDQAAALGDDLKADTVVSPHKCRSSEIISPKLQGEQ 359
LinMPK          RAATGLPQLRSTPTTSAPSTQRRAPDQAVALGGDLKADTVVSPHERRSSEIISPKLQGEQ 359
LbrMPK          RAATGLPQLQSTPMTSTPSTQRRVPDHAAGVGDSLKADPVVSPSMPHSSEIISPKLQGQQ 359
TbECK1          RELFQHCQPPLVDVAPTSPDH--------NFSREQQHQQQTLGNDRVDAELTLPRLAAPS 351
TcMPK           RALFTQCQTPAVDASNSS-----------GLVAVQPKAPLFPGEPEETGEVFLPLLAMPP 348
SmpMPK          KTLIKNET--NINIPSSSTNITSDNSIVNNLNSNSNQIQVKNNQPCNANIMNVKNQNKDK 358
DdMPK           EPIN---------------------------------------------------------- 292
HsCDKL2         QLKVQKDAR-NVSLSKKSQNRK------------------------------KEKEKDD 328
                .

LmxMPK6         PPTAKNSFSEPHISKTALKPAAHDANPGKGKGAGAPTLRLTSPHKTASEHPLQLPMILNV 419
LmaMPK          PPTVKNSSSDTHISKTALRPAAHDANAGKGKGAGAPTFTLTSPHKAASEHPVQLPMILNS 419
LinMPK          PPTVKNSSSDTHISKTALKPAAHDANAGKGKGAGAPTFTLTSPHKAASEHPVQLPMILNS 419
LbrMPK          PLASNNNLSDTCLSKAPLEAVLHDANTAKGKAAGAPKSTLPPPHTPASDQSMQLPMILNG 419
TbECK1          LDAETTDKVDSAESKNTTMGVSSEVVGGVGGSV------------------------- 384
TcMPK           RVLESEDEWSLG-NKGTSRGGASLGNGCSG---------------------------- 377
SmpMPK          TTTPNRVDLSVTSQTGLHNSEIDEQNKSSNISTGFSSNTKPTQLEGNKIKSTMAEQVNLT 418
DdMPK           ---------------------------------------------------------- 
HsCDKL2         SLVEERKTLVVQDTN------ADPKIK----------DYKLFKIKGSKIDGEKAEKG--- 369


LmxMPK6         SSERAIAAALTDYLNQMPTSSSTVVSSPAQATPAEVAEAFTKADPLSRSCGAALPLQTSQ 479
LmaMPK          NSERAIAAALTDYLNQMPTSSSAVVPTPVQATPAEVAGGFTNTDLLSRSCGAVPPLQTSQ 479
LinMPK          NSERAVAAALTDYLNQMPASSSAVVSTPLQATPAEVAGGFTNADLLSRSCGAVPPPQTSQ 479
LbrMPK          NSERAIAASLTDYLHQEPTSSSVAASPPVGAAPTEVAEGLTNADLLAPSCEVVSALQASS 479
TbECK1          -----VVDSNSNSFHQLGALWSHYIGSTVGAT--------------------------- 411
TcMPK           ----------ASPFQQLGTLWSHYLGTAINGG--------------------------- 399
SmpMPK          YVASKSRVATKSQLYNEYLVHDENIDP------------------------------- 445
DdMPK           ---------------------------------------------------------- 
HsCDKL2         -----NRASNASCLHDSRTSHNKIVPS------------------------------- 391


LmxMPK6         TINASTTRDKKKKRNSSLAETELHRRSSASISNDTEYAVTTDGTKGEPARHISDHPRASA 539
LmaMPK          TINASNTRDKKKKRNVSLAETELHRPSSASVSGDTEYAVTTDGSKGEPAKHISGHPRASA 539
LinMPK          ITNPSTTRDKNRKRNVGLAETELHRPSSASISDDTEYAATIDSSKGEPAKHISDHPRASA 539
LbrMPK          ITNTLAMRDRKKKRCSSVAATELHRRSGVDKNSETDCAVSTGDNRGGLVKHISCHSPRST 539
TbECK1          ----------------------------------------------------MALSG 416
TcMPK           ----------------------------------------------------VNNSG 404
SmpMPK          ---------------------------------------------------------- 
DdMPK           ---------------------------------------------------------- 
HsCDKL2         ---------------------------------------------------------- 


LmxMPK6         TLPPNGVRDGGDSHEPRREGEKTNVSPPLPSHGVAESNMRALLTTAAPGKDGGETAVLSH 599
LmaMPK          TLPPNGALGGGDSHEPRREGEKTSASPPLPSHGVAESHVRLLLTTAAPGKDGGETAVLNR 599
LinMPK          TLPPNGVLGSGGSHEPTREGEKTNASPPLPSHGVAESSMRVLLTTAAPGKDDGETAVLSH 599
LbrMPK          TLPSSGVHGGGGCHGLGRESETMTVSPPSMSHGVADSNMRVVLTTAPPGKDGDETTVPTH 599
TbECK1          ELPN---------------------------IGPRQAHPYPSGLPPGVQVTK------ 441
TcMPK           ELPS---------------------------ISTRQMQTHHTMATPIFNGNK------ 429
SmpMPK          -------------------------------HHLLDTMKVSRKPHYGSDNVLNRNDDS 472
DdMPK           ---------------------------------------------------------- 
HsCDKL2         -------------------------------TSLKDCSNVS------VDHTRN----- 407


LmxMPK6         RALKPASAEKAAATTATAFSPPPLTATHGAPLAECLQDLPALSLHLPRHLQSERQTPAAE 659
LmaMPK          RVLKPASADKAAATTPTAFSSPTLVATHGAPLAECLQDLPALSPHLPHHVQQERQTPAAE 659
LinMPK          RPLKPASADKAAATAATAFSSPTLAATHGAPLAECLQGLPALSLHLPRHLQQERQTPAAE 659
LbrMPK          RASTPASADKLRTTATTILSSPSLAATHVAPLEACPQDLPALSRHLPHHLEQERQAAVVE 659
TbECK1          ----------------------------------------------------------P 442
TcMPK           ----------------------------------------------------------N 430
SmpMPK          DSKESFAVTEKMNDRLNEMPSIPQKSFGLLTTVKCKSPKPTNPISKPSILEDLREPLNDT 532
DdMPK           ---------------------------------------------------------- 
HsCDKL2         ---------------------------------------------------------- 
```

```
LmxMPK6         QPQPHTSLSAETSMSSFHVRTRNPLAAASSVNDGVSHGKANIETTGSSVAKPRLGLSNSS 719
LmaMPK          QPQSHTPLSAETSMSSFHVCTRNPLAAASSENDDVSHGKANIEPTGSSVAKPRRGLSNSS 719
LinMPK          QPQSHTPLSAETSISSFHVCRRNPLAAASTENDDVSRGKANIEPAGSSVANPRRGLSNSS 719
LbrMPK          QLQSRTPSSVETLMLSFRVRTRNPLASLSLENEGLSHSKANSEAAELSAAKTHGGISNSS 719
TbECK1          VPRSGTNSVGDKNYNGVQAMKVTGCLRLSAKNISRSPDVQRVKASAAQSG---------- 492
TcMPK           TSKPENKANREMLISSIQTLKMAGGSTQVPLNPPSTTSQQGSKVSGVPQG---------- 480
SmpMPK          DLSSASISISPLQVTNLTINEQSIINTTNQSPFNSSFVAKVTEVPNEQIDCTSTVIESSA 592
DdMPK           ------------------------------------------------------------
HsCDKL2         ----PSVAIPPLTHN--------------------------------------------- 418

LmxMPK6         ---VSTAASEVKKRKSARHKSNTSRLQDKAVGPVSGSASRRPVPGNASDVVAYRAGFASV 776
LmaMPK          ---VSTAASEVKKRKSARHKRDTSRLHDQAVGPVSGSASRRSVQGNASDMVAYRAGFGSM 776
LinMPK          ---VSTAASETKKRKSARHKRDTSRLHDQAVGPVSGSASRRSVPGNASDVVAYRAGFASV 776
LbrMPK          TYTTSHVASEAKKRKLSRHKRETSCVYDQLVASVKGSGSHCSVPGHAVDEDAYHTEIASV 779
TbECK1          --------PKVK-------QAKSEVKPEQKREWKSCSALGKSVK---------------- 521
TcMPK           --------TSTHSRKNWKNQGMASKKADPMGGWKLG-SLKKSIK---------------- 515
SmpMPK          SKYLDTKCGDSQPKEMTSNKRLPYLTLSQTSSYHFFPQQYRGVYQNS------------ 639
DdMPK           ------------------------------------------------------------
HsCDKL2         ------------------------------------------------------------

LmxMPK6         VNSLKSTVSQSLSHVLGQQQRHRLLSPESDGVHTAEPHLHGVGAGPSAPDSTRNRNVDAT 836
LmaMPK          VNSLKSTVSQSLSYTMGQQQRQPLLSPDSGGVHVADSHLHGVGAGPSAPDSTHNRNVDAA 836
LinMPK          VNSLKSTVSQSLSYILGQQQRQPLLSPDSRGVHAADPHLHGVGAGPSVPDSTHNRNADAA 836
LbrMPK          AGPSRPEASLLLANVPGKQQ-QHLLGSEPGGTHVTEQHLHCVGAGLSAPDFTHNRSVDAH 838
TbECK1          ------------------------------------PNY-LFPLLPNGTNNSGITSY 541
TcMPK           ------------------------------------LGYPMFPALPSGCSSPVSTAF 536
SmpMPK          ----------------------LKSDQTNTYNTGIVSSGTGLSSLSPLLTNSQTVSKH 675
DdMPK           ------------------------------------------------------------
HsCDKL2         ----------------------------------------LSAVAPSINSG------ 429

LmxMPK6         GPQPRKERRCKPLAASTHALQGSDQRHRQQSQPRLDGPLHPDGGASQRATATLMALSALR 896
LmaMPK          GPQLRKERRSKPLAASTHVLQGSDQRHRQQPQPRLDGPLLSDGGASQRATATLMALSALR 896
LinMPK          GPQLRKERRSKPLAASTHALQGSDQRHRQQSQPRLDGPLHPDGGASQRATATLMALSALR 896
LbrMPK          GPLQRKERRSKPLPGSTYALHNSDQRQRQQPHPRLDGSLQPDGGASQRATATLLALSALR 898
TbECK1          GP-------------------------------------------SGVAVGAGPAPQ 555
TcMPK           TTT-----------------------------------------SSVALNALSVLR 551
SmpMPK          ENH-------------------------------------------PTFQSINISA 688
DdMPK           ------------------------------------------------------------
HsCDKL2         ----------------------------------------------MG 431

LmxMPK6         NVSGPPPAKSAGDANKSSYVHHTRSHTNNNGGETVIPVVGGDGNDTNTCVTSRARRPIVA 956
LmaMPK          KVSLPPPTKSAGDADKSSYDHHTRSRTNRNGSESVSPVVGGDGNDTHTCIASRARRPVAV 956
LinMPK          NVSLPPPTKSAGDADKSSYGHHTRSHTNNNGGETVSPVVGGDGNGTQTCIASRARRPIAV 956
LbrMPK          NVSGPPPTKSTGDAGRCSYIHHIRSHINNNGGEAVGFVVGGDGKGPNTSTTGRARRSLGV 958
TbECK1          DACSPLVSKGLRPPSSNGIPGAG-LHSNGS--------------TTSFSAHKDEKMDLG 599
TcMPK           DANSNTVPKSMPKTHTNTVPTTTTTNTNTN--------------TNTTTPTTTVNASNG 596
SmpMPK          SPSIPLQTWTTQKNSSNTNNSSKDSKSRRY----------------YQPPNHHRKSTFS 731
DdMPK           ------------------------------------------------------------
HsCDKL2         TETIPIQGYRVDEKTKKCSIP------------------------FVKPNRH------ 459

LmxMPK6         CAVHGNNRDSDELMATRRVQKKNAVATHGRTGNGAVGSIGCTDSSTTSSYQATSIMYGAP 1016
LmaMPK          CTVHGNNRDSDELMATRRAQKKNAVVTHGRTGNGAVGSISCTDSSTTSSYQATSIMHGAP 1016
LinMPK          CAVHGNNRDSDELISTRRVQKKNAVATHGRTGNGAVGPISCTDSSTTSSYQATSIMYGAP 1016
LbrMPK          YALHGCSGNSDETEATRRVQKKNLFMAHGRTSNGAAGCISFPDKYTGPSCHAIGSLHGAP 1018
TbECK1          CGEQNNNG------SDHKQRKK----------------------------------- 615
TcMPK           DGVVNNN-------HPPKSKRK----------------------------------- 611
SmpMPK          LQFPMNISHSVCQPISTSLSNHYHNHNHHFSILQPIGIMPSPNIFDTNHDYLHPEQNESR 791
DdMPK           ------------------------------------------------------------
HsCDKL2         ------------------------------------------------------SP 461
```

```
LmxMPK6         YHPFARASKVDGDVCGAQQRQTLQRLKKKIADHRGSGIANTTSSIGSRHSLTPARQIQHQ 1076
LmaMPK          YHPFTRASKVDGEVSGAPQRQTLRRPKKKIADSRGSGIANTTSSIGPRHSLAPARQIQHQ 1076
LinMPK          YHPFTRASKMDGEVGGAPQRQTLRRPKKKIADSRGSGIANITSSIGPRHSLARARQIQHQ 1076
LbrMPK          YNSFAKASKVEGEVGGAQQRQSLRKPKKKIAGNRGSGIVNTSSIHSLRHSLTTGRQMQHQ 1078
TbECK1          ---HVKRTHDNGELEGPPRK--------------------VSDKPSSQHSVAGHRYSFRD 652
TcMPK           ---QSKRTPLPGGTPASPPR--------------------VSGNTTSRHNVNGQKCSLHD 648
SmpMPK          SYIGHVNFSTRSPLQSLSQQNIFKKSFTSNSTTGTSKQDNTYPLTGNQHSFSPQVLPAFT 851
DdMPK           ------------------------------------------------------------
HsCDKL2         SGIYNINVTTLVSGPPLSDD-----------------SGADLPQMEHQH----------- 493

LmxMPK6         PQLAKEDGGSGDGKTPQFNAATAASPDTGI---------- 1106
LmaMPK          PQLAKEDGGSGDGKTPQFNAATAASPYTGS---------- 1106
LinMPK          PQLAKEDGGSGDGKTPQFNAAAAASPYTSS---------- 1106
LbrMPK          QQLAKEEGGNGDGTARQFNAATAASPYTSN---------- 1108
TbECK1          GATKR----------------------------------- 657
TcMPK           VPSKR----------------------------------- 653
SmpMPK          CSSYSTNQYGTNTKSNHNNQFPINRLRNSDKFWLGSLPRR 891
DdMPK           ----------------------------------------
HsCDKL2         ----------------------------------------
```

CLUSTAL 2.0.12 multiple sequence alignment of the homologous malate dehydrogenases LmjF34.0140 and LmxM33.0140, homologous mitochondrial malate dehydrogenases LmjF34.0160 and LmxM33.0160 and homologous glycosomal malate dehydrogenases LmjF19.0710 and LmxM19.0710

Potential MAP kinase substrate phosphorylation sites with the consensus sequence [S/T]-P are boxed in, the peptides detected in MS/MS analysis are highlighted grey.
The peptides AIVGIITNPVNSTVPVAAEALK and AIIGIISNPVNSTVPVAAEALK match not by sequence, but by mass, which is the relevant factor in MS analyses.

```
LmjF34.0140     MRRSQGCFFRVAVLGAAGGIGQPLSLLLK-NNKYVKELKLYDVKGGPGVAADLSHICAPA 59
LmjF34.0160     MRSSATRLFRVAVLGAAGGIGQPLSLLLK-CSPLVTSLSLYDIRGGPGVAADLSHIPSPA 59
LmjF19.0710     -------MVNVCVVGAAGGIGQSLSLLLVRQLPYGSTLSLFDVVGAAGVAADLSHVDNAG 53
LmxM33.0140     MRRSQASFFRVAVLGAAGGIGQPLSLLLK-NNKYVKELKLYDIKGAPGVAADLSHIYTPA 59
LmxM33.0160     MRSSATRLFRVVVLGAAGGIGQPLSLLLK-CSPLVTSLSLYDIRGGPGVAADLSHITSPA 59
LmxM19.0710     -------MVNVCVVGAAGGIGQPLSLLLVRQLPHGSTLSLFDVVGAAGVAADLSHVDNAG 53
                      :..* *:********.*****       . *.*:*: *..********:  ..

LmjF34.0140     KVTGYTKD--------ELSRAVENADVVVIPAGIPRKPGMTRDDLFNTNASIVRDLAIAV 111
LmjF34.0160     EVIGFSSG--------ELEKAVKGADLVLVVAGIPRKPGMTRDDLLHTNASIVRDLAIAV 111
LmjF19.0710     VQVKFAEGKIGHKRDPALAELAKGVDVFVMVAGVPRKPGMTRDDLFKINAGIILDLVLTC 113
LmxM33.0140     KVFEYTKD--------ELSKAVEDADLVVIPAGVPRKPGMTRDDLFHTNASIVRDLSKAV 111
LmxM33.0160     EVSGFSSG--------ELEKAVKGADLALVVAGIPRKPGMTRDDLFHTNASIVRDLAIAV 111
LmxM19.0710     VQVKFAAGKIGQKRDPALAELAKGVDVFVMVAGVPRKPGMTRDDLFKINAGIVLDLVLTC 113
                    :: .         * . .:..*: :: **:***********:: **.*: **  :

LmjF34.0140     GTHAPKAIVGIITNPVNSTVPVAAEALKKVGVYDPARLFGVTTLDVVRARTFVAEALGAS 171
LmjF34.0160     GTHAPKAIVGIITNPVNSTVPVAAEALKKVGVYDPARLFGVTTLDVVRARTFVAEALGAS 171
LmjF19.0710     ASSSPKAVFCIVTNPVNSTVAIAAEALKSLGVYDRNRLLGVSLLDGLRATCFINEAR-KP 172
LmxM33.0140     GKASPKAIIGIISNPVNSTVPVAAEALKEF-AYDPARLFGVTTLDAVRARTFVAEALGAS 170
LmxM33.0160     GTHAPKAIVGIITNPVNSTVPVVAETLCKLGVYDPARLFGVTTLDAVRARTFVAEALGAS 171
LmxM19.0710     ASSSPKAVFCIVTNPVNSTVAIAAEALKSLGVYDRNRLLGVSLLDGLRATCFINEAR-KP 172
                .. :***:. *::*******.:.**:* .. .**  **:**: ** :**  *: **   .

LmjF34.0140     PYDVDVPVIGGHSGETIVPLLSGFPSLSEEQ--VRQLTHRIQFGGDEVVKAKDGAGSATL 229
LmjF34.0160     PYDVDVPVIGGHSGETIVPLLSGFPSLSEEQ--VRQLTHRIQFGGDEVVKAKDGAGSATL 229
LmjF19.0710     LVVSQVPVVGGHSDTTIVPLFYQLPGPLPEQATLDKIVKRVQVAGTEVVKAKAGRGSATL 232
LmxM33.0140     PYDVNVPVIGGHSGETIVPLLSGFPSLSEDQ--VRQLTHRIQFGGDEVVKAKEGAGSATL 228
LmxM33.0160     PYDVDVPVIGGHSGETIVPLLSGFPSLSEDQ--VRQLTHRIQFGGDEVVKAKEGAGSATL 229
LmxM19.0710     LVVRQVPVVGGHSDTTIVPLFHQLLGPLPEQAMLDKIIKRVQVAGTEVVKAKAGRGSATL 232
                    :***:****. *****:  : .   :*  : :: :*:*..* ****** * *****
```

```
LmjF34.0140      SMAFAGNEWTTAVLRALSGEKGVVVCTYVQS-TVEPSCAFFSSPVLLGNSGVEKIYPVPM 288
LmjF34.0160      SMAYAASEWSISMLKALRGDRGIVEYALVESDMQQPHSRFFGCAVELGTHGVERVLPMPK 289
LmjF19.0710      SMAEAGARFALKVVEGLTGTGNPLVYAYVDTDGQHE-TTFLAIPVVLGMNGIEKRLPIGP 291
LmxM33.0140      SMAYAGNEWTTAILRALNGEKGVVVCTYVQS-CVEPSCAFFSSPVLLGKRGVEKIYPVPT 287
LmxM33.0160      SMAYAASEWSISMLKALRGDKGIVEYALVENDTQKPHSRFFGCAVELGTHGVERVLPMPT 289
LmxM19.0710      SMAEAGARFVLKVVEGLTGTGKPLMYAYVDTDGQQE-TPFLAIPVVLGVNGIEKRLPIGP 291
                 *** *. .:   ::..* *    :  : *:.   .    *:. .* **  *:*:  *:

LmjF34.0140      LNAYEEKLMAKCLEGLQSNITKGIAFSNK------- 317
LmjF34.0160      LNAYEQQLLDACVPALSAEFRKGVDLAVKLHLSQDN 325
LmjF19.0710      LHSTEETLLKAALPVIKKNIVKGSEFARSHL----- 322
LmxM33.0140      LNIYEEKLMSKCLKVLPGDIKKGIELGNW------- 316
LmxM33.0160      LNAYEQQLLDACVPALSAELRKGVDFAVKSHLSQDS 325
LmxM19.0710      LHSTEEKLLKEALPVIKKNIAKGNEFARSN------ 321
                 *:  *: *:  .:  :  :: **  :.
```

CLUSTAL 2.0.12 sequence alignment of the homologous tryparedoxin peroxidases LmjF15.1120 and LmxM15.1160

Potential MAP kinase substrate phosphorylation sites with the consensus sequence [S/T]-P are boxed in, the peptides detected in MS/MS analysis are highlighted grey.

```
LmxM15.1160      MSCGDAKINCAAPAFEEMALMPNGSFKKISLSAYKGRWVVLFFYPLDFTFVCPTEIIQFS 60
LmjF15.1120      MSCGNAKINSPAPSFEEVALMPNGSFKKISLSSYKGKWVVLFFYPLDFSFVCPTEVIAFS 60
                 ****:****..**:***:**************:***:***********:******:* **

LmxM15.1160      DNVARFNELNCDVIACSMDSEYAHLQWTLQDRKKGGLGTMAIPMLADKTKSIARAYGVLA 120
LmjF15.1120      DSVSRFNELNCEVLACSIDSEYAHLQWTLQDRKKGGLGTMAIPMLADKTKSIARSYGVLE 120
                 *.*:*******:*:***:************************************:****

LmxM15.1160      EAQGVAYRGLFIIDPHGVLRQITVNDMPVGRNVEEVLRLLEAFQFVEKHGEVCPANWKKG 180
LmjF15.1120      ESQGVAYRGLFIIDPHGMLRQITVNDMPVGRSVEEVLRLLEAFQFVEKHGEVCPANWKKG 180
                 *:***************:*************.****************************

LmxM15.1160      DPTMKPEPKASIEGYFSKQ 199
LmjF15.1120      APTMKPEPNASVEGYFSKQ 199
                  *******:**:*******
```

CLUSTAL 2.0.12 sequence alignment of the homologous hypothetical proteins LmjF34.3830 and LmxM33.3830

Potential MAP kinase substrate phosphorylation sites with the consensus sequence [S/T]-P are boxed in, the peptides detected in MS/MS analysis are highlighted grey.

```
LmjF34.3830      MTVKPQVAQWQETVKQLAGLPHDVLRGMLRDVQAQLQEERRAFSQERKEFEHVQLRLAKL 60
LmxM33.3830      MIVRPRVAQRQEALWQLEGLPHDVLRCMLRDVQAQLQEERRAFAQERKELEHVQLRLAKL 60
                 * *:*:*** **:: ** ******** ****************:*****:**********

LmjF34.3830      TRDLESAQRQREQQRRHASKDAEAAARTSRLLRAARRRGQRYEEAIARTLDDIHQLRHGN 120
LmxM33.3830      KRDLEIAQRQREQQRQHASKDAEAAARTSRLLRAARRREQEYEEAIARTLDEIYQLRCGN 120
                 .**** *********:********************** *.**********:*:*** **

LmjF34.3830      RDTAASPTSVPAISVGMDVLSIDSPGRRHVDVHTEVSVPPTPARESSRAAAAVRAANEEQ 180
LmxM33.3830      RDGAASPTSVPVISAGVDVLSMNSPGPHRADVSTEARVPPTSARESSRAAAAARASNEEQ 180
                 ** ********.**.*:****::*** ::.** **. ****.**********.**:****

LmjF34.3830      RRSVLLHELAHRVARVERENRMLRSSIDVLSRGDASSVKLYCKLESLHPSRVV 233
LmxM33.3830      RRSVLLHKLAHCVARVERENRMLRSNIDVLSRGDASSVRLYHELESLRSSQVA 233
                 *******:*** ************.************:** :****:.*:*.
```

CLUSTAL 2.0.12 sequence alignment of the homologous hypothetical proteins LmjF36.2480 and LmxM36.2480

Potential MAP kinase substrate phosphorylation sites with the consensus sequence [S/T]-P are boxed in, the peptides detected in MS/MS analysis are highlighted grey.

```
LmjF36.2480       MDPSKRICLKNLPEGCTKREIAELVRNRTGTPIHSIDLGLGADGKTRRYAHFSCEGAKHV 60
LmxM36.2480       MDPSKRICLKNLPEGCTKRELAELVRNRTGTPIHSIDLGLDADGKTRRYAHFSCEGAKHV 60
                  ********************:******************.******************

LmjF36.2480       LEVLSAGVTLRDSTIYAHPAKSHYSFRYAEARRKREREEAEEKAQLEAFWAAARQRFLDR 120
LmxM36.2480       LEVLSTGVSLRDSTIYAHPAKTHYSFRYAEARRKRERAEAEEKEQLEAFWAASRQRFLDR 120
                  *****:**:************:*************** ***** ********:*******

LmjF36.2480       TNGGELPRNKIPKDFYAAKRKYARIAAEIAQVSRNAHAAAGGDAAYAEHPRGAAHAAPFF 180
LmxM36.2480       TNGGELPKNKIPKDFYASKRKYARIAAEIAQMSRNAHAAARGGAAYAEHPRGAAHAAPPF 180
                  *******:*********:*************:******** *.*************** *

LmjF36.2480       SGADCGTNSAPRATSKNHATSGG---------------GDANAAKKCASTLTAAKSKALA 225
LmxM36.2480       SGADCGTNSAYRAASKDHGTSGGGAAAACEPPRTTAGGGDANAAKKCASRLTAAKSQAPA 240
                  ********** **:**:*.****               *********** ******:* *

LmjF36.2480       AVPPPPPPPEPTKEERKLSGLQAKLAALKEKLKK 259
LmxM36.2480       VAPPPPPTPGPTKEERKLSGLQAKLAALKEKLKK 274
                  ..*****.* ************************
```

7.2 Results of mass spectrometry analyses

Peptides identified from LmxMPK4 by MS/MS analysis

Identified peptides are marked in bold in the displayed sequence of LmxMPK4
The table below lists the peptides together with the identification method and observed modifications. For peptides from the peptide mass fingerprint (PMF) analyses, the modifications listed are those suggested by MASCOT and have not been confirmed by MS/MS. For the peptides derived from LC-MS/MS analyses, the modifications have been validated, even if not all are present in the peptide at the same time.

Sequence Coverage: 62.5%

1 MTQLVPLAEL PSGKKIYSVR **GQRFEVDRQY DLVK**VVGFGA CGTVCSAVVN
51 GSGERVAIKR LSR**VFGDLRE GK**RILR**EMEI MTSLKHNNLI RLHHFMRPQS**
101 **KETFEDIYLV MDLYDTDLNR** IIRSR**QKLTD EHLQYFMIQA FRGLHYLHSA**
151 **K**VMHR**DLKPS NLLVNADCAL AICDFGLARD DQVMSSSDLT QYVVTR**WYRP
201 PEVLGMGSNQ YTSAVDVWSL GLIFAELMVG RALLPGTDYI GQLVMIVNLL
251 GSPSIDDMEF LSSEAK**AFIL SQPHRPALSF RDLFPMATEE ATDLLSKLLV**
301 **FHPARR**LTAK **QVMEHPYFSK YRDAAEEADA PDPFVWNHSH IETKEQLRED**
351 **LWRVVEAHSQ LNE**

Position	Sequence	MS-method	Modification(s)
21-34	GQRFEVDRQYDLVK	PMF, LC-MS/MS MSA	
64-72	VFGDLREGK	LC-MS/MS MSA	
77-85	EMEINTSLK	LC-MS/MS MSA	Oxidation (M)
86-91	HNNLIR	LC-MS/MS MSA	
92-120	LHHFMRPQSKETFEDIYLVMDLYDTDLNR	PMF	2 oxidation (M); phospho (Y)[a]
126-142	QKLTDEHLQYFMIQAFR	PMF, LC-MS/MS MSA	Oxidation (M)
143-151	GLHYLHSAK	LC-MS/MS MSA	
156-179	DLKPSNLLVNADCALAICDFGLAR	PMF	
180-196	DDQVMSSSDLTQYVVTR	LC-MS/MS MSA	Oxidation (M); phospho (S,T); phospho (Y)
267-281	AFILSQPHRPALSFR	PMF, LC-MS/MS MSA	
282-297	DLFPMATEEATDLLSK	LC-MS/MS MSA	Oxidation (M)
298-306	LLVFHPARR	PMF, LC-MS/MS MSA	
311-322	QVMEHPYFSKYR	PMF, LC-MS/MS MSA	Gln->pyro-Glu (N-term Q); oxidation (M)
323-344	DAAEEADAPDPFVWNHSHIETK	PMF	
345-353	EQLREDLWR	PMF, LC-MS/MS MSA	
354-363	VVEAHSQLNE	LC-MS/MS MSA	

[a] Suggested by MASCOT, but not confirmed by MS/MS.

MSA, multistage activation which simultaneously fragments the parent ion and the neutral loss product generated when peptide modifications are lost as uncharged chemical compounds, thus generating a hybrid spectrum that combines both MS/MS and MS/MS/MS fragment ion information.

MS/MS spectrum of doubly phosphorylated LmxMPK4 after co-expression with LmxMKK5

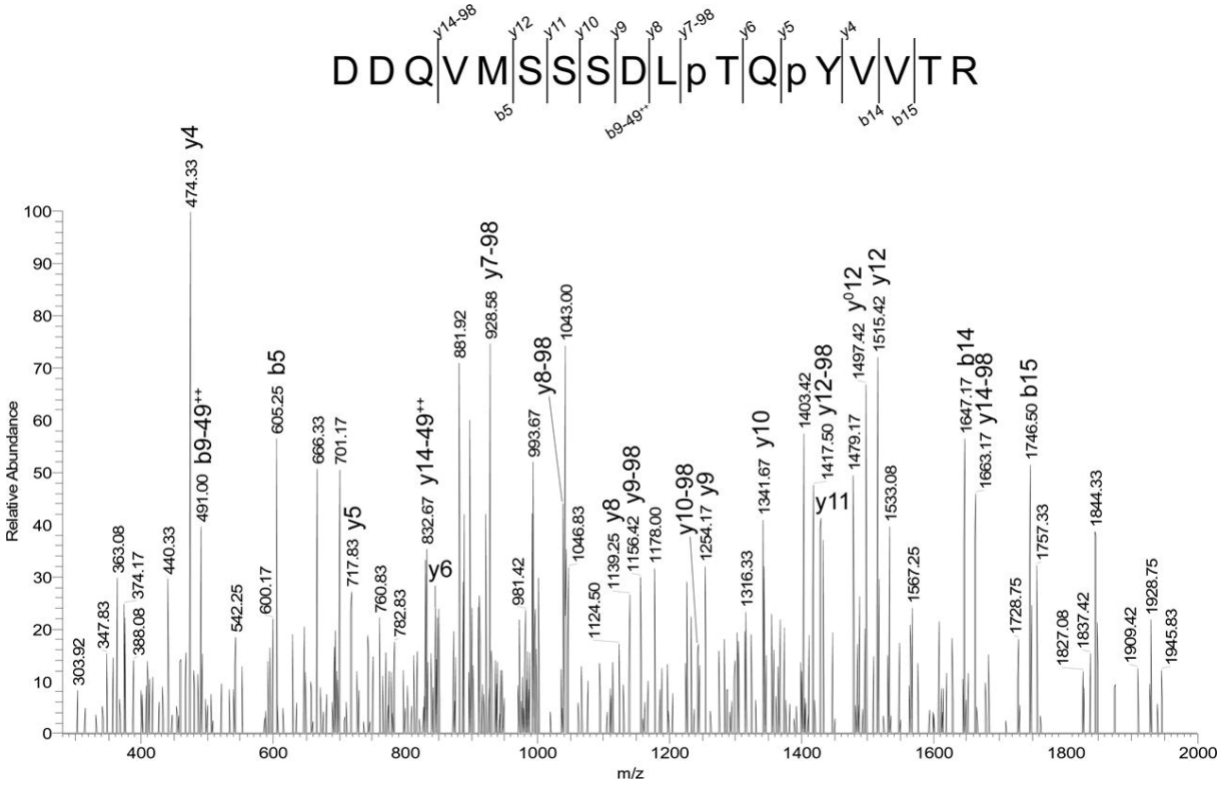

MS/MS spectrum of co-expressed LmxMPK4 phosphorylated on threonine

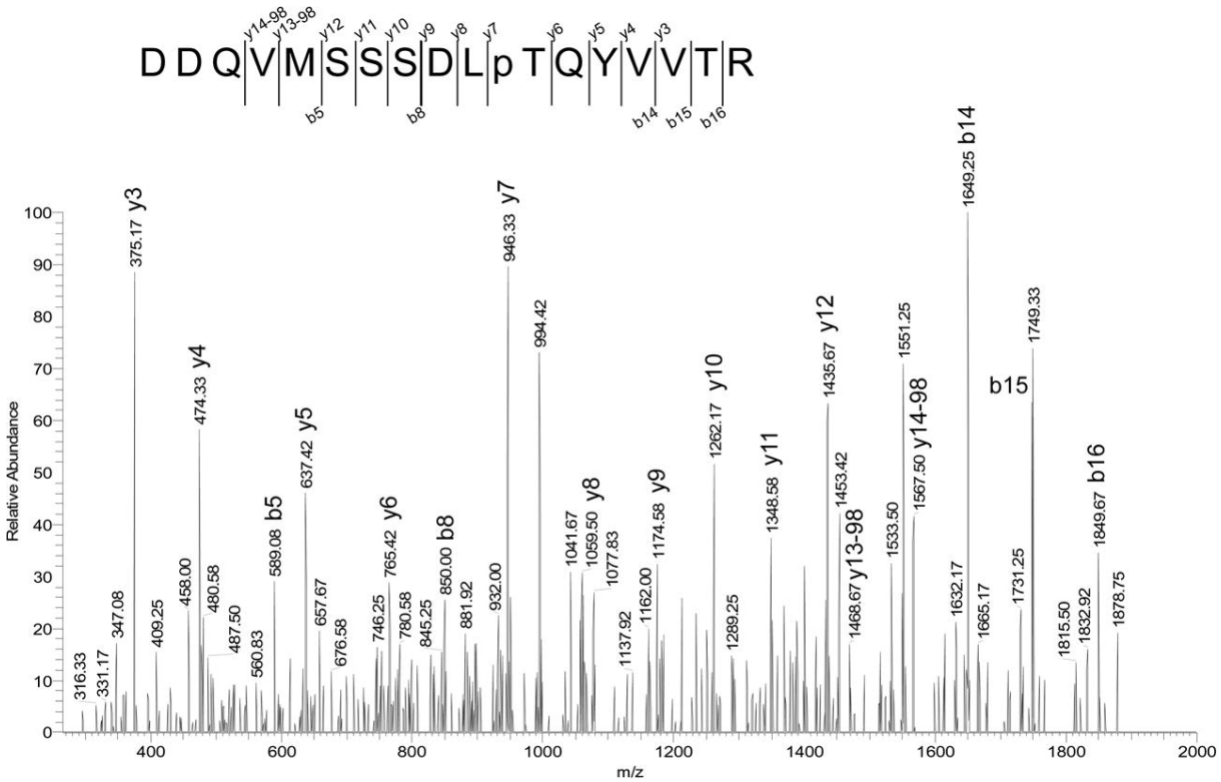

MS/MS spectrum of co-expressed LmxMPK4, phosphorylated on tyrosine

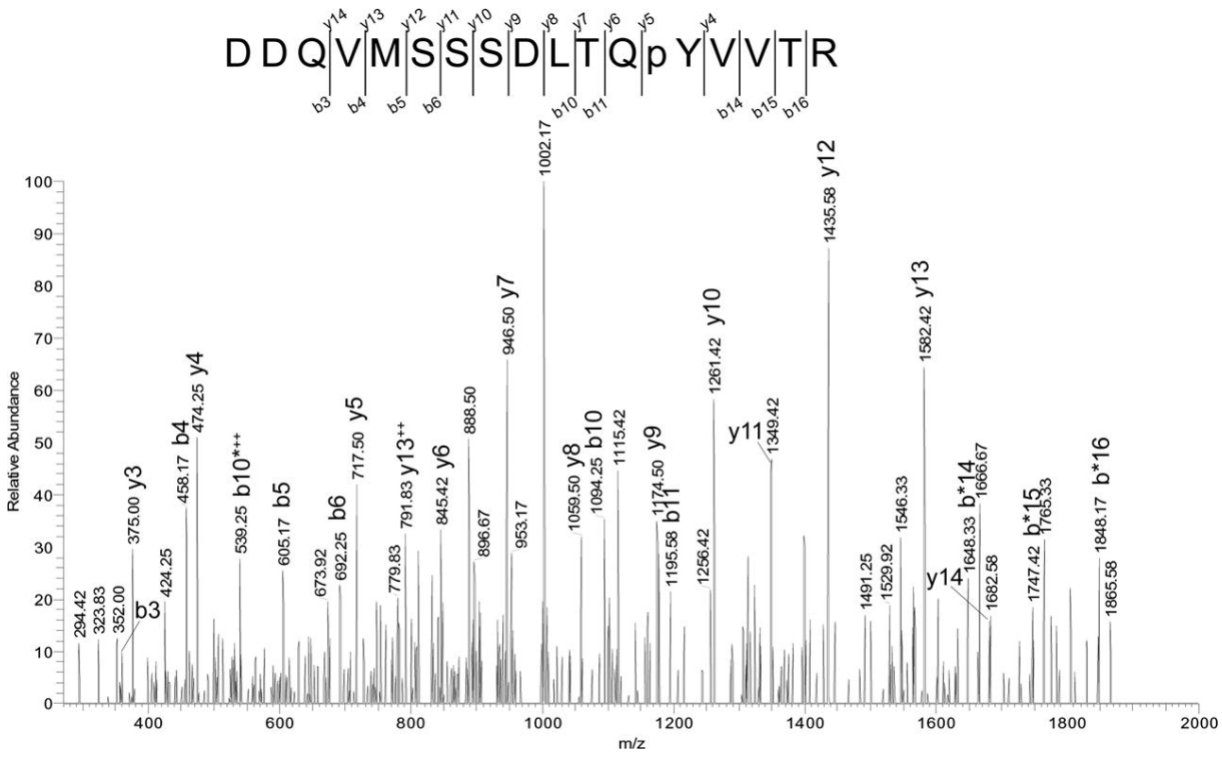

Table of all peptides annotated in MS analysis of a protein band from *L. mexicana* lysates, phosphorylated by activated LmxMPK4

Sample	Peptides	Identification of protein	Size of protein
Band A (dephosphorylated amastigotes)	LSKDEIER NQITITNDK VQSLVSDFFGGK	**Heat-shock protein hsp70**, LmjF28.2770	71.65 kDa
	QLFNPEQLVSGK EIVDLALDR LIGQVVSSLTASLR	**Alpha tubulin**, LmjF13.0280	49.76 kDa
	VIDSVASSR	**ATP synthase F1 subunit gamma protein**, LmjF21.1770	34.42 kDa
	LELSVEKR	**hypothetical protein** LmjF20.0160	87.6 kDa
	LASQLER	**glycosyltransferase family 28 protein**, LmjF30.0530	47.42 kDa
	TNGGELPR	**Hypothetical protein**, LmjF36.2480	27.93 kDa
	LLEAFQFVEK	**tryparedoxin peroxidase**, LmjF15.1120	22.12 kDa
Band B (amastigotes)	LLGVSLLDGLR	**glycosomal malate dehydrogenase**, LmjF19.0710	33.63 kDa
	DDLFNTNASIVR AVENADVVVIPAGIPR VAVLGAAGGIGQPLSLLLK AIVGIITNPVNSTVPVAAEALK	**malate dehydrogenase**, LmjF34.0140	33.36 kDa
	DAEAAARTSR	**hypothetical protein, conserved**, LmjF34.3830	26.47 kDa
Band C (promastigotes)	LREEYPDR LAVNLVPFPR FPGQLNSDLR GHYTEGAELIDSVLDVCR	**beta tubulin**, LmjF08.1230	49.71 kDa
	LIGRK NTTIPTKK LSKDEIER NQITITNDK VQSLVSDFFGGK	**heat-shock protein hsp70**, LmjF28.2770	71.65 kDa
	LPLQDVYK IGGIGTVPVGR	**elongation factor 1-alpha**, LmjF17.0080	49.12 kDa
	DVNAAIATIK EIVDLALDR QLFNPEQLVSGK TIQFVDWCPTGFK SLDIERPSYTNVNR SLDIERPSYTNVNR IHFVLTSYAPVVSAEK CIFLDLEPTVVDEVR FDGALNVDLTEFQTNLVPYPR AYHEQLSVADITNSVFEPAGMLTK	**alpha tubulin**, LmjF13.0280	49.76 kDa
	LLVFHPAR DDQVMSSSDLTQYVVTR DLKPSNLLVNADCALAICDFGLAR	**LmxMPK4**	
	LLGVSLLDGLR	**glycosomal malate dehydrogenase**, LmjF19.0710	33.63 kDa
	VIDSVASSR	**ATP synthase F1 γ-subunit** LmjF21.1770	34.42 kDa

7.3 Plasmid maps

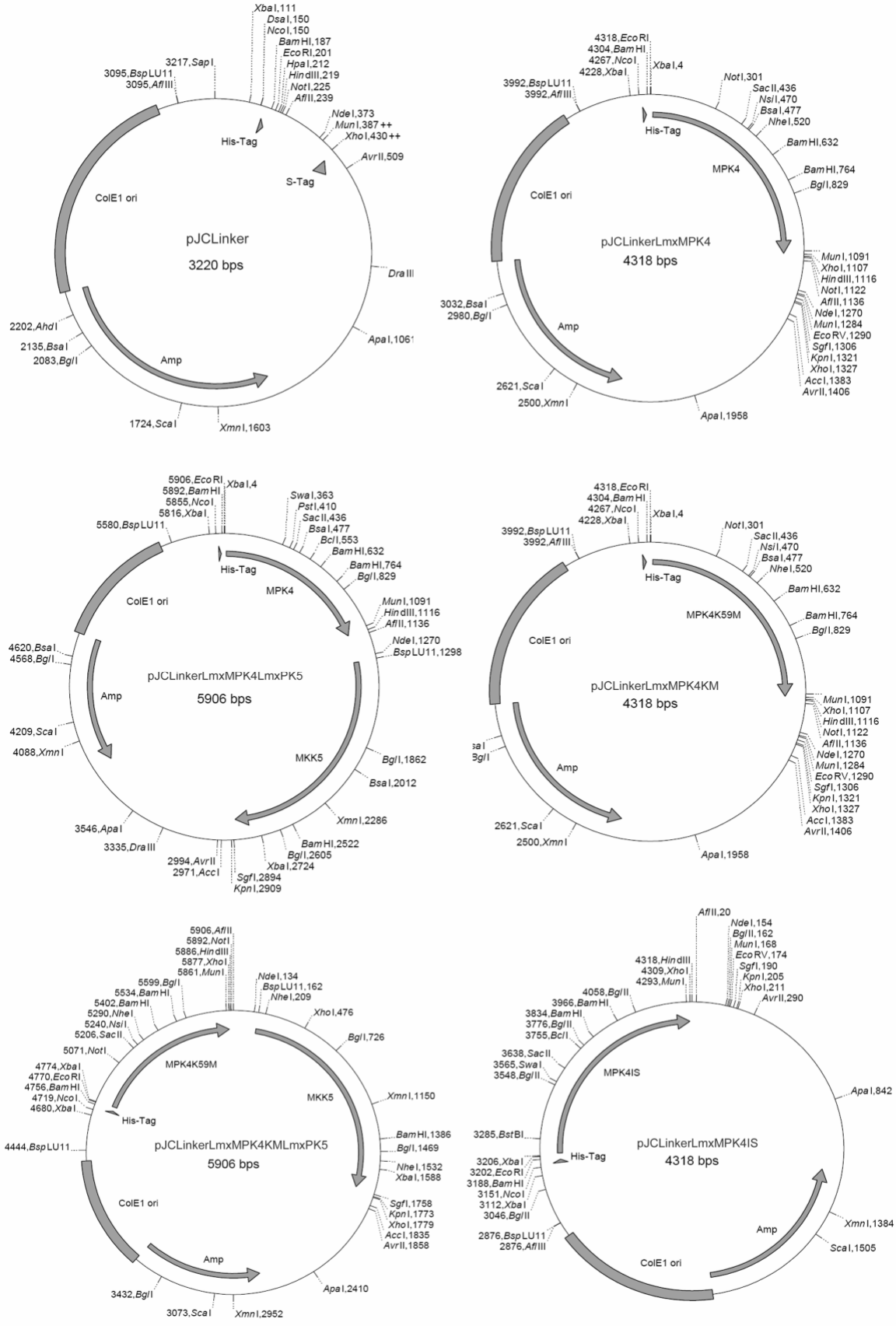

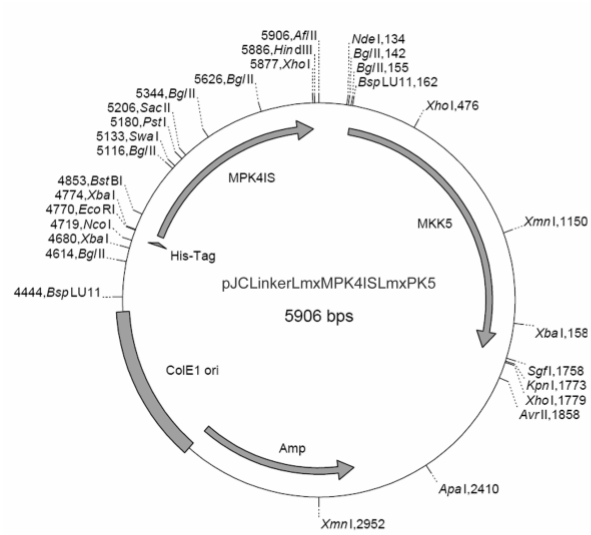
pJCLinkerLmxMPK4ISLmxPK5
5906 bps
MPK4IS
MKK5
His-Tag
ColE1 ori
Amp
5906,AflII
5886,HindIII
5877,XhoI
NdeI,134
BglII,142
BglII,155
BspLU11,162
XhoI,476
XmnI,1150
XbaI,158
SgfI,1758
KpnI,1773
XhoI,1779
AvrII,1858
ApaI,2410
XmnI,2952
4444,BspLU11
4853,BstBI
4774,XbaI
4770,EcoRI
4719,NcoI
4680,XbaI
4614,BglII
5626,BglII
5344,BglII
5206,SacII
5180,PstI
5133,SwaI
5116,BglII

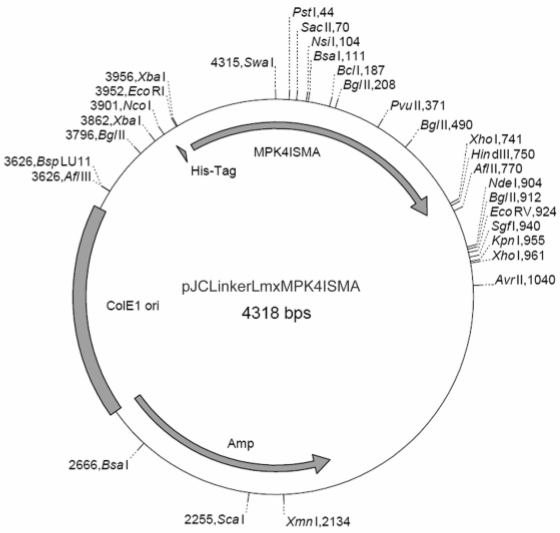
pJCLinkerLmxMPK4ISMA
4318 bps
MPK4ISMA
His-Tag
ColE1 ori
Amp
PstI,44
SacII,70
NsiI,104
BsaI,111
BclI,187
BglII,208
PvuII,371
BglII,490
XhoI,741
HindIII,750
AflII,770
NdeI,904
BglII,912
EcoRV,924
SgfI,940
KpnI,955
XhoI,961
AvrII,1040
4315,SwaI
3956,XbaI
3952,EcoRI
3901,NcoI
3862,XbaI
3796,BglII
3626,BspLU11
3626,AflIII
2666,BsaI
2255,ScaI
XmnI,2134

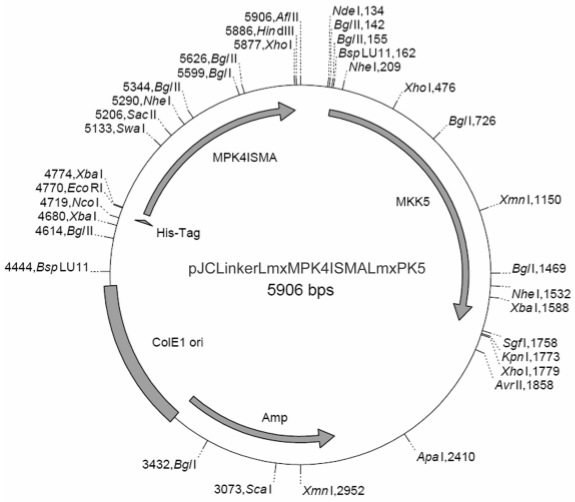
pJCLinkerLmxMPK4ISMALmxPK5
5906 bps
MPK4ISMA
MKK5
His-Tag
ColE1 ori
Amp
5906,AflII
5886,HindIII
5877,XhoI
NdeI,134
BglII,142
BglII,155
BspLU11,162
NheI,209
XhoI,476
BglI,726
XmnI,1150
BglI,1469
NheI,1532
XbaI,1588
SgfI,1758
KpnI,1773
XhoI,1779
AvrII,1858
ApaI,2410
XmnI,2952
4444,BspLU11
4774,XbaI
4770,EcoRI
4719,NcoI
4680,XbaI
4614,BglII
5626,BglII
5599,BglI
5344,BglII
5290,NheI
5206,SacII
5133,SwaI
3432,BglI
3073,ScaI

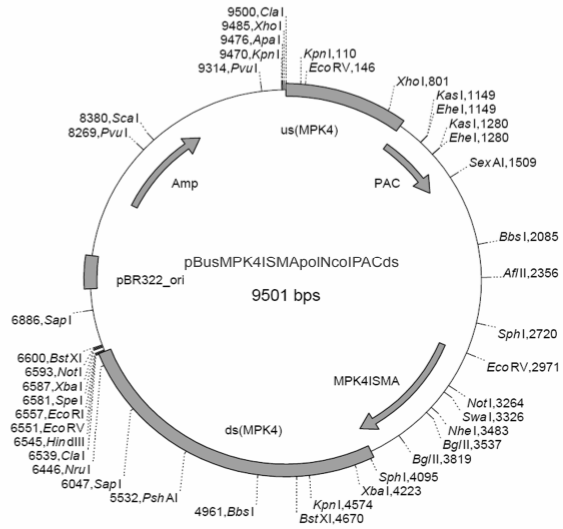
pBusMPK4ISMApolNcoIPACds
9501 bps
us(MPK4)
PAC
Amp
pBR322_ori
MPK4ISMA
ds(MPK4)
9500,ClaI
9485,XhoI
9476,ApaI
9470,KpnI
9314,PvuI
KpnI,110
EcoRV,146
XhoI,801
KasI,1149
EheI,1149
KasI,1280
EheI,1280
SexAI,1509
BbsI,2085
AflII,2356
SphI,2720
EcoRV,2971
NotI,3264
SwaI,3326
NheI,3483
BglII,3537
BglII,3819
SphI,4095
XbaI,4223
KpnI,4574
BstXI,4670
4961,BbsI
5532,PshAI
6047,SapI
6446,NruI
6539,ClaI
6545,HindIII
6551,EcoRV
6557,EcoRI
6581,SpeI
6587,XbaI
6593,NotI
6600,BstXI
6886,SapI
8380,ScaI
8269,PvuI

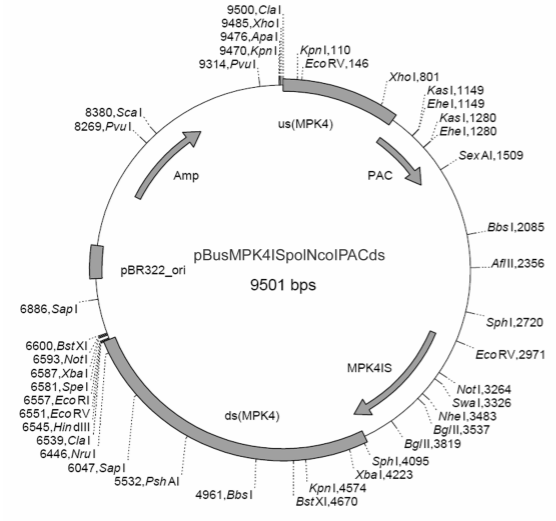
pBusMPK4ISpolNcoIPACds
9501 bps
us(MPK4)
PAC
Amp
pBR322_ori
MPK4IS
ds(MPK4)
9500,ClaI
9485,XhoI
9476,ApaI
9470,KpnI
9314,PvuI
KpnI,110
EcoRV,146
XhoI,801
KasI,1149
EheI,1149
KasI,1280
EheI,1280
SexAI,1509
BbsI,2085
AflII,2356
SphI,2720
EcoRV,2971
NotI,3264
SwaI,3326
NheI,3483
BglII,3537
BglII,3819
SphI,4095
XbaI,4223
KpnI,4574
BstXI,4670
4961,BbsI
5532,PshAI
6047,SapI
6446,NruI
6539,ClaI
6545,HindIII
6551,EcoRV
6557,EcoRI
6581,SpeI
6587,XbaI
6593,NotI
6600,BstXI
6886,SapI
8380,ScaI
8269,PvuI

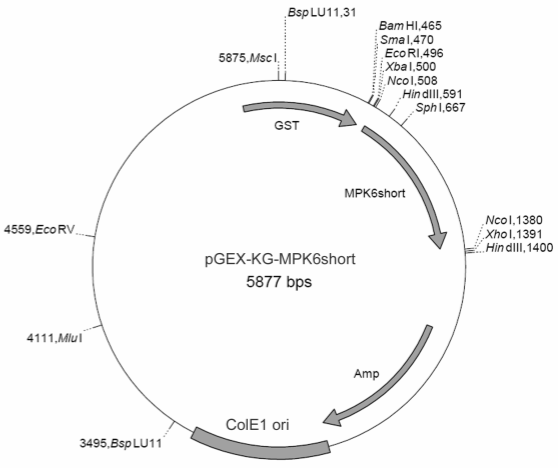
pGEX-KG-MPK6short
5877 bps
GST
MPK6short
ColE1 ori
Amp
BspLU11,31
BamHI,465
SmaI,470
EcoRI,496
XbaI,500
NcoI,508
HindIII,591
SphI,667
NcoI,1380
XhoI,1391
HindIII,1400
5875,MscI
4559,EcoRV
4111,MluI
3495,BspLU11

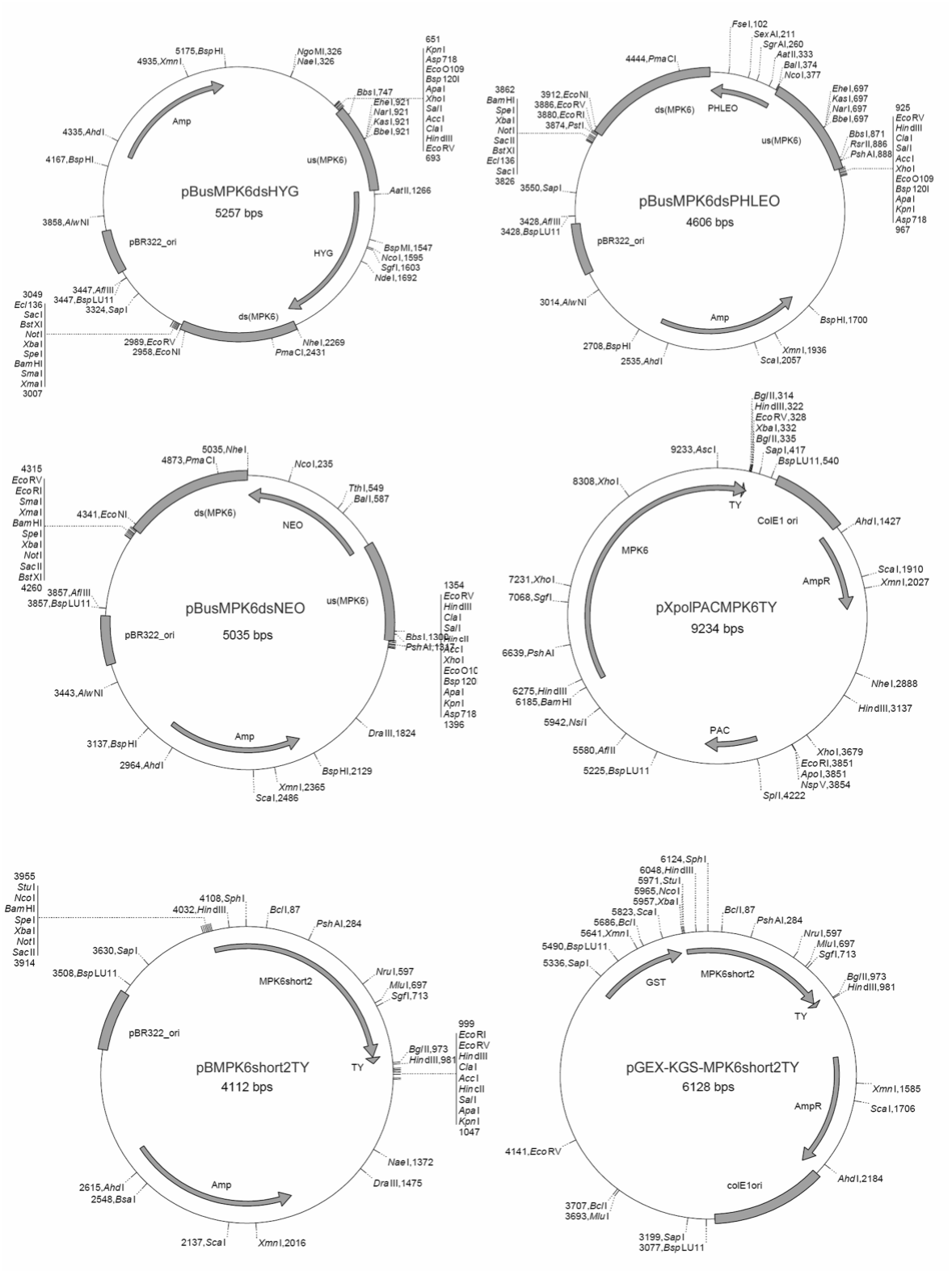
pBusMPK6dsHYG
5257 bps
pBusMPK6dsPHLEO
4606 bps
pBusMPK6dsNEO
5035 bps
pXpolPACMPK6TY
9234 bps
pBMPK6short2TY
4112 bps
pGEX-KGS-MPK6short2TY
6128 bps

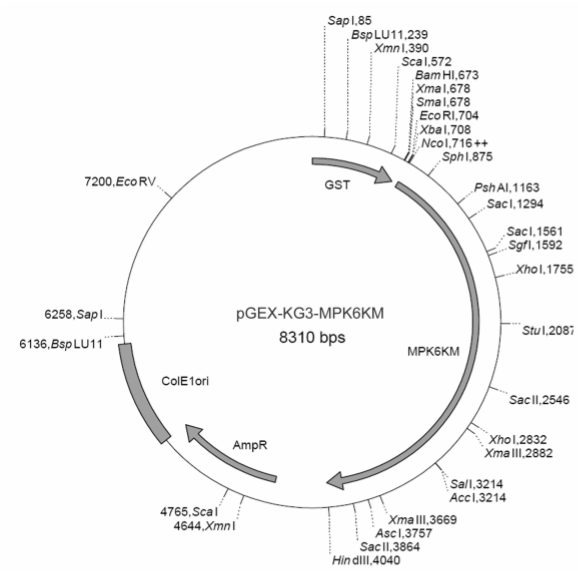
pGEX-KG3-MPK6KM
8310 bps
GST
MPK6KM
ColE1ori
AmpR
SapI,85
BspLU11,239
XmnI,390
ScaI,572
BamHI,673
XmaI,678
SmaI,678
EcoRI,704
XbaI,708
NcoI,716++
SphI,875
PshAI,1163
SacI,1294
SacI,1561
SgfI,1592
XhoI,1755
StuI,2087
SacII,2546
XhoI,2832
XmaIII,2882
SalI,3214
AccI,3214
XmaIII,3669
AscI,3757
SacII,3864
HindIII,4040
4765,ScaI
4644,XmnI
6258,SapI
6136,BspLU11
7200,EcoRV

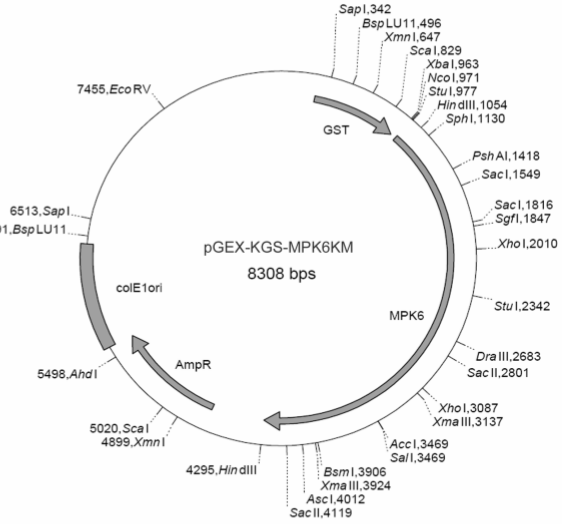
pGEX-KGS-MPK6KM
8308 bps
GST
MPK6
colE1ori
AmpR
SapI,342
BspLU11,496
XmnI,647
ScaI,829
XbaI,963
NcoI,971
StuI,977
HindIII,1054
SphI,1130
PshAI,1418
SacI,1549
SacI,1816
SgfI,1847
XhoI,2010
StuI,2342
DraIII,2683
SacII,2801
XhoI,3087
XmaIII,3137
AccI,3469
SalI,3469
BsmI,3906
XmaIII,3924
AscI,4012
SacII,4119
4295,HindIII
5020,ScaI
4899,XmnI
5498,AhdI
6513,SapI
6391,BspLU11
7455,EcoRV

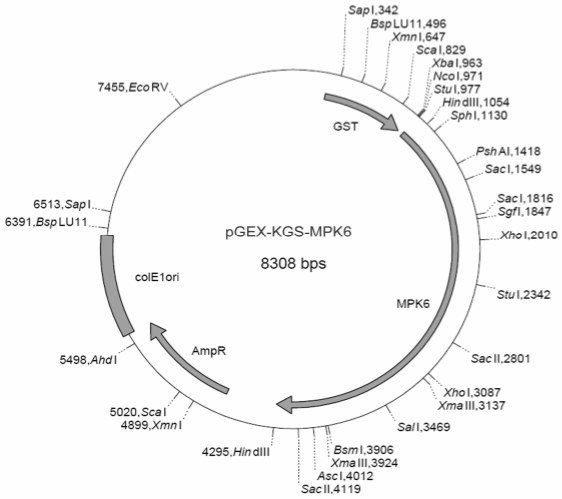
pGEX-KGS-MPK6
8308 bps
GST
MPK6
colE1ori
AmpR
SapI,342
BspLU11,496
XmnI,647
ScaI,829
XbaI,963
NcoI,971
StuI,977
HindIII,1054
SphI,1130
PshAI,1418
SacI,1549
SacI,1816
SgfI,1847
XhoI,2010
StuI,2342
SacII,2801
XhoI,3087
XmaIII,3137
SalI,3469
BsmI,3906
XmaIII,3924
AscI,4012
SacII,4119
4295,HindIII
5020,ScaI
4899,XmnI
5498,AhdI
6513,SapI
6391,BspLU11
7455,EcoRV

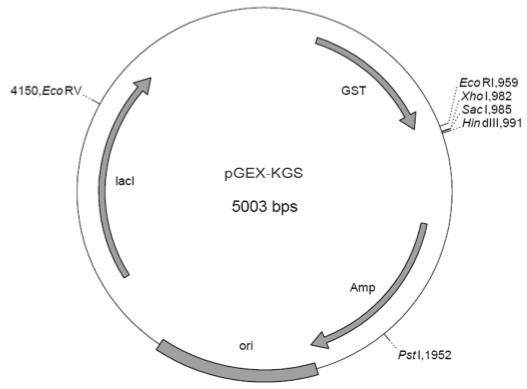
pGEX-KGS
5003 bps
GST
lacI
Amp
ori
EcoRI,959
XhoI,982
SacI,985
HindIII,991
PstI,1952
4150,EcoRV

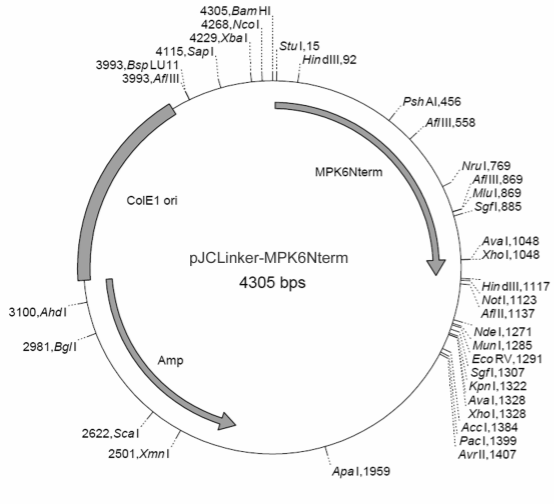
pJCLinker-MPK6Nterm
4305 bps
MPK6Nterm
ColE1 ori
Amp
PshAI,456
AflIII,558
NruI,769
AflIII,869
MluI,869
SgfI,885
AvaI,1048
XhoI,1048
HindIII,1117
NotI,1123
AflII,1137
NdeI,1271
MunI,1285
EcoRV,1291
SgfI,1307
KpnI,1322
AvaI,1328
XhoI,1328
AccI,1384
PacI,1399
AvrII,1407
ApaI,1959
4305,BamHI
4268,NcoI
4229,XbaI
4115,SapI
3993,BspLU11
3993,AflIII
StuI,15
HindIII,92
3100,AhdI
2981,BglI
2622,ScaI
2501,XmnI

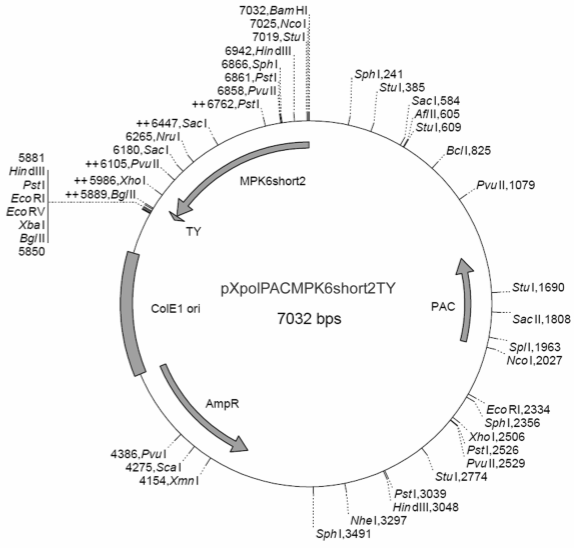
pXpolPACMPK6short2TY
7032 bps
MPK6short2
TY
ColE1 ori
PAC
AmpR
7032,BamHI
7025,NcoI
7019,StuI
6942,HindIII
6866,SphI
6861,PstI
6858,PvuII
++6762,PstI
++6447,SacI
6265,NruI
6180,SacI
++6105,PvuII
++5986,XhoI
++5889,BglII
5881
HindIII
PstI
EcoRI
EcoRV
XbaI
BglII
5850
SphI,241
StuI,385
SacI,584
AflII,605
StuI,609
BclI,825
PvuII,1079
StuI,1690
SacII,1808
SpeI,1963
NcoI,2027
EcoRI,2334
SphI,2356
XhoI,2506
PstI,2526
PvuII,2529
StuI,2774
PstI,3039
HindIII,3048
NheI,3297
SphI,3491
4386,PvuI
4275,ScaI
4154,XmnI

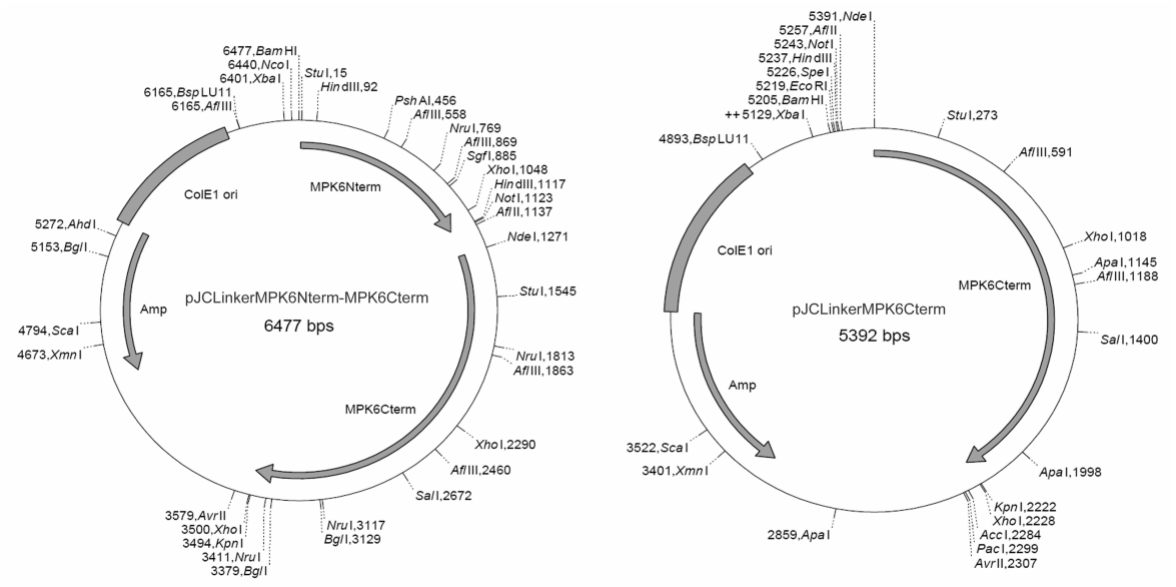
pJCLinkerMPK6Nterm-MPK6Cterm
6477 bps
ColE1 ori
Amp
MPK6Nterm
MPK6Cterm
6477,BamHI
6440,NcoI
6401,XbaI
StuI,15
HindIII,92
6165,BspLU11
6165,AflIII
PshAI,456
AflIII,558
NruI,769
AflIII,869
SgfI,885
XhoI,1048
HindIII,1117
NotI,1123
AflII,1137
NdeI,1271
StuI,1545
NruI,1813
AflIII,1863
XhoI,2290
AflIII,2460
SalI,2672
NruI,3117
BglI,3129
3579,AvrII
3500,XhoI
3494,KpnI
3411,NruI
3379,BglI
5272,AhdI
5153,BglI
4794,ScaI
4673,XmnI
pJCLinkerMPK6Cterm
5392 bps
ColE1 ori
Amp
MPK6Cterm
5391,NdeI
5257,AflII
5243,NotI
5237,HindIII
5226,SpeI
5219,EcoRI
5205,BamHI
++5129,XbaI
4893,BspLU11
StuI,273
AflIII,591
XhoI,1018
ApaI,1145
AflIII,1188
SalI,1400
ApaI,1998
KpnI,2222
XhoI,2228
AccI,2284
PacI,2299
AvrII,2307
2859,ApaI
3522,ScaI
3401,XmnI

7.4 Results of metabolic profiling analyses

All metabolites (apart from lipids) whose quantities are up- or downregulated more than 2-fold in BF11H4+1Na, in comparison to WT+1Na

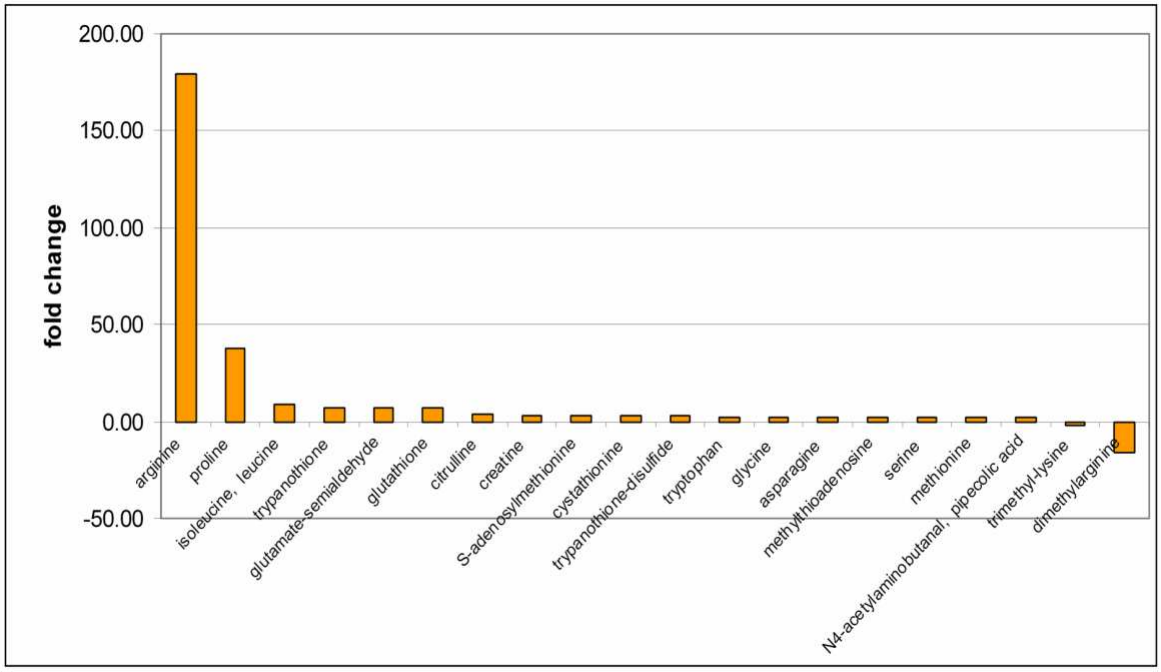

All lipids whose quantities are up- or downregulated more than 2-fold in BF11H4+1Na, in comparison to WT+1Na

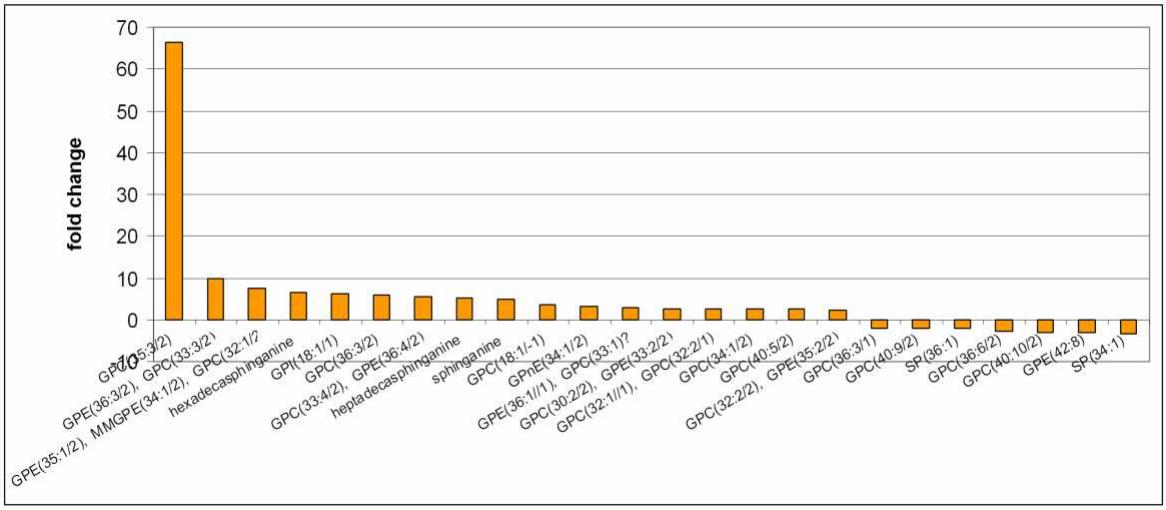

Trendplots of all identified metabolites

The naming of identified lipids was performed according to the LIPID MAPS comprehensive classification system for lipids (Fahy, E. et al. 2009).

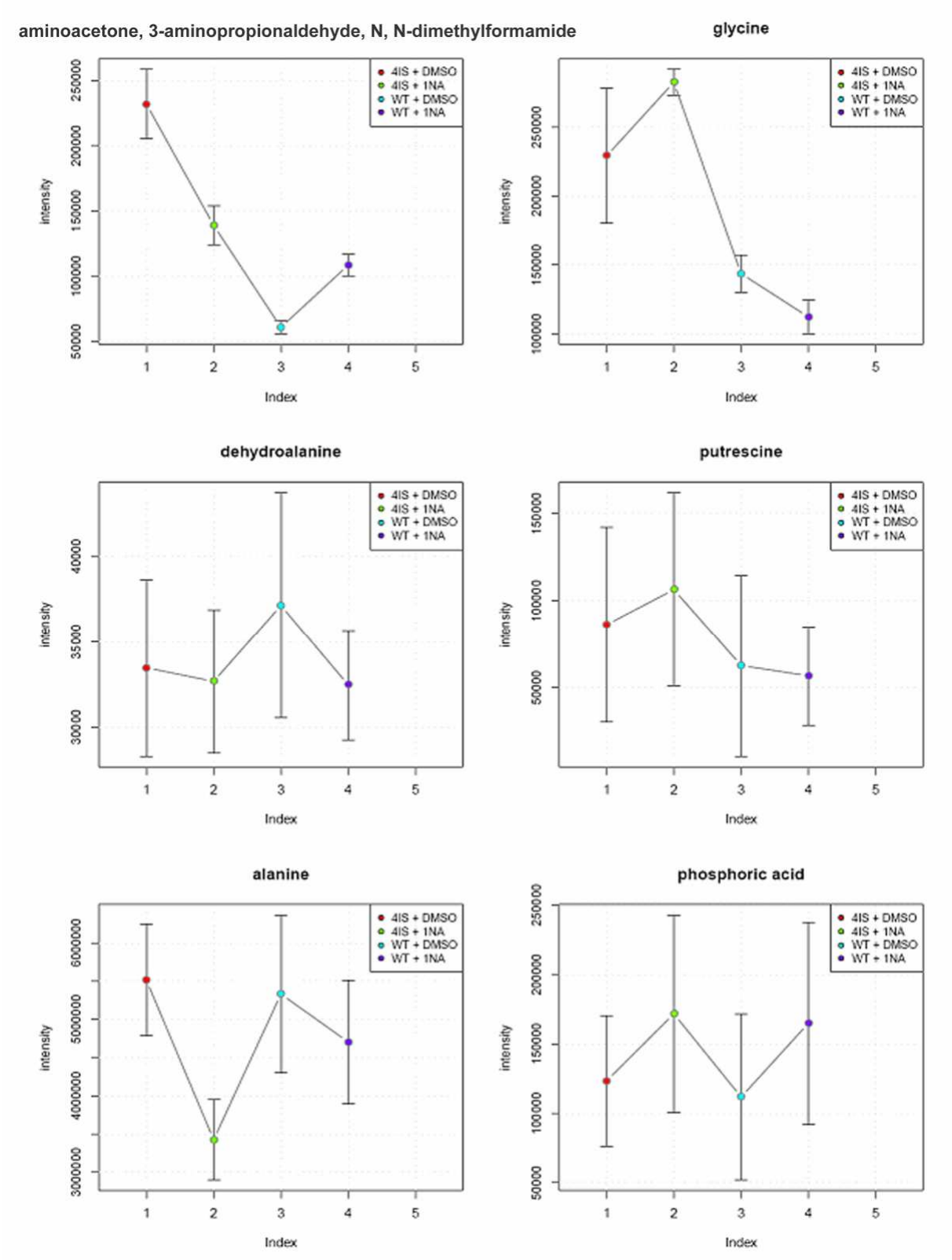

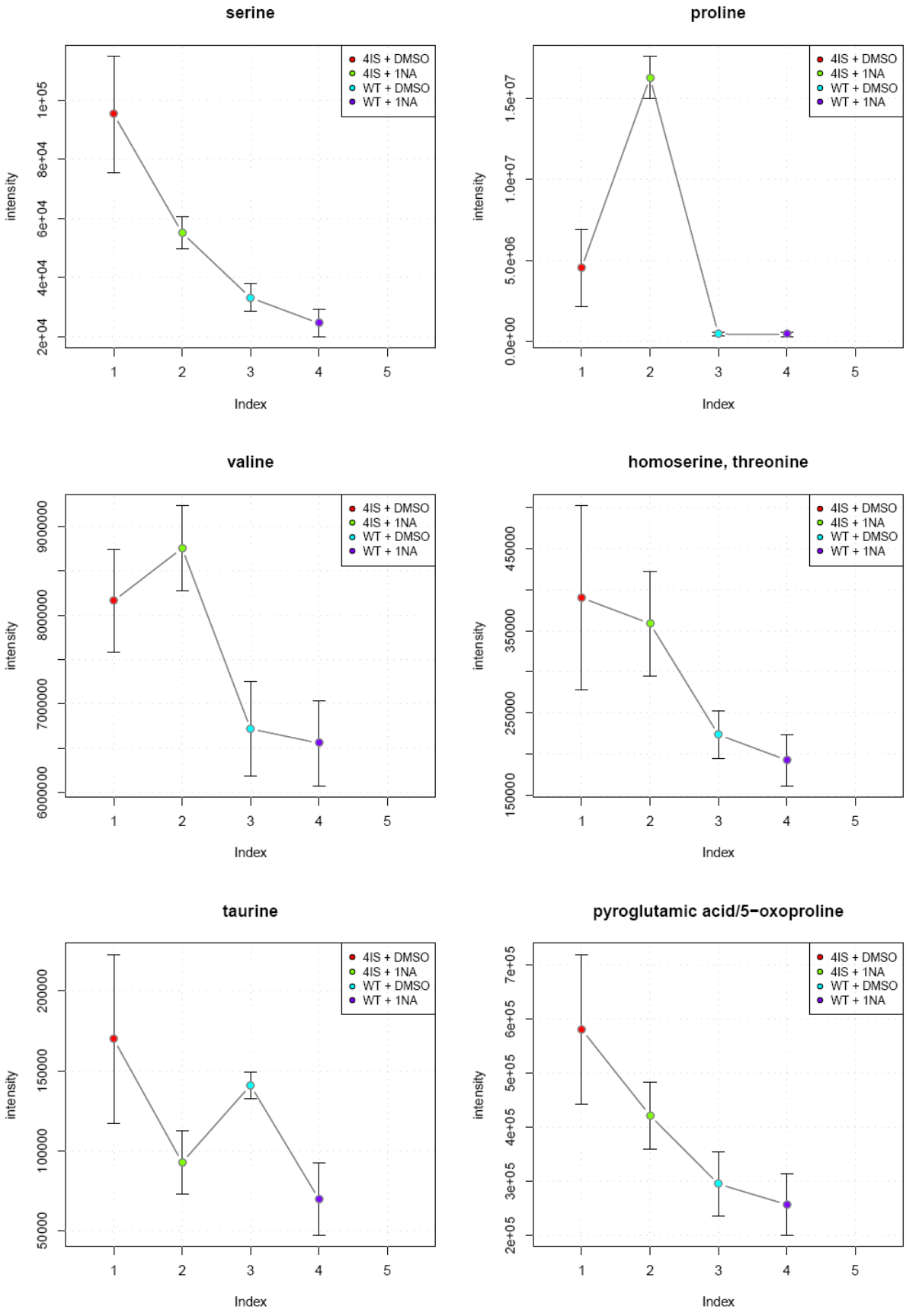
serine
proline
valine
homoserine, threonine
taurine
pyroglutamic acid/5−oxoproline
4IS + DMSO
4IS + 1NA
WT + DMSO
WT + 1NA
intensity
Index

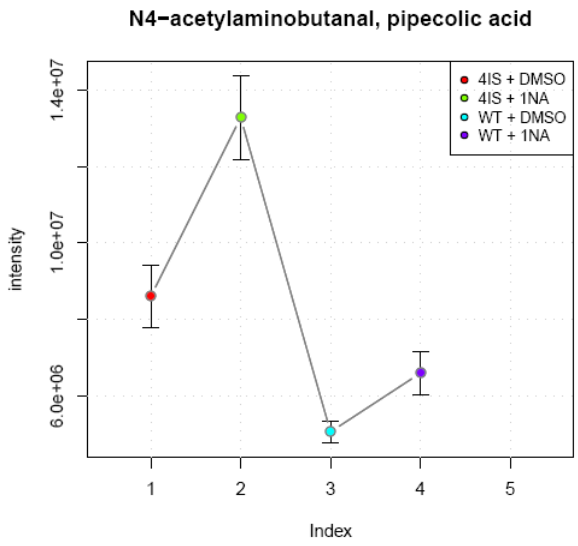
N4−acetylaminobutanal, pipecolic acid
intensity
Index
4IS + DMSO
4IS + 1NA
WT + DMSO
WT + 1NA

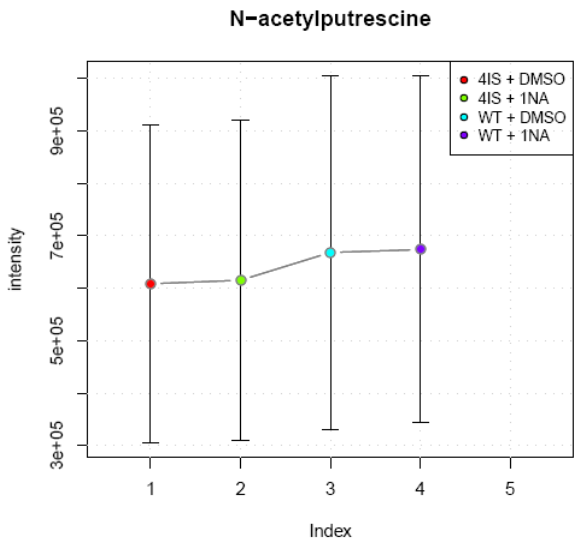
N−acetylputrescine
intensity
Index
4IS + DMSO
4IS + 1NA
WT + DMSO
WT + 1NA

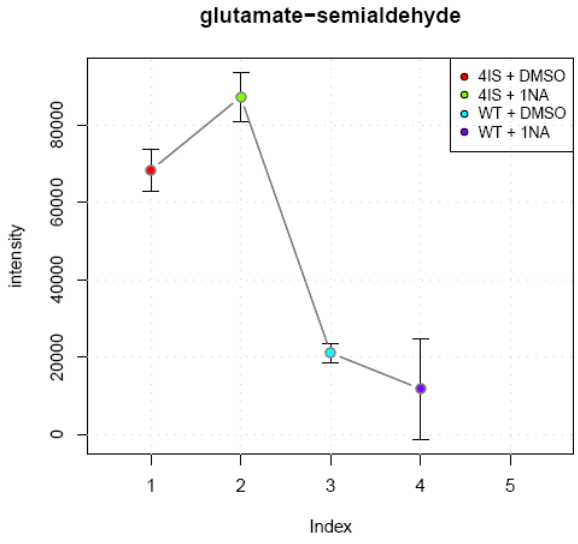
glutamate−semialdehyde
intensity
Index
4IS + DMSO
4IS + 1NA
WT + DMSO
WT + 1NA

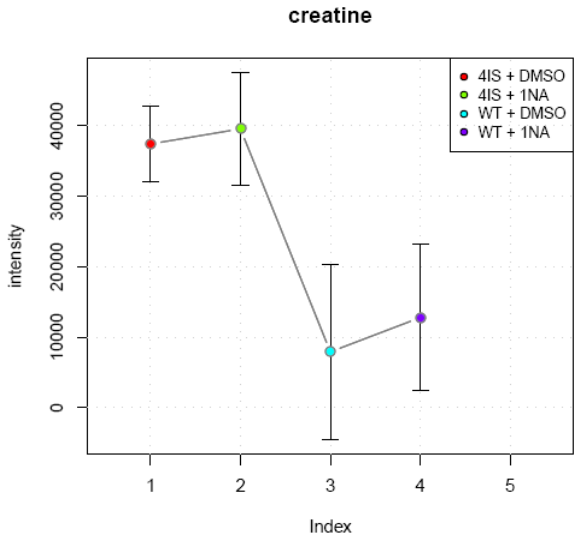
creatine
intensity
Index
4IS + DMSO
4IS + 1NA
WT + DMSO
WT + 1NA

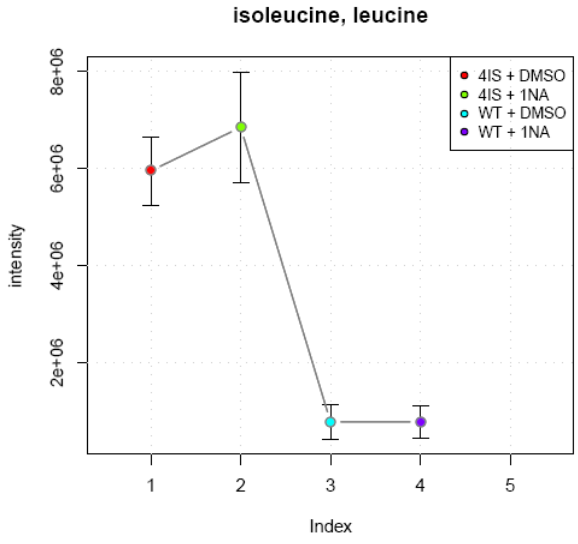
isoleucine, leucine
intensity
Index
4IS + DMSO
4IS + 1NA
WT + DMSO
WT + 1NA

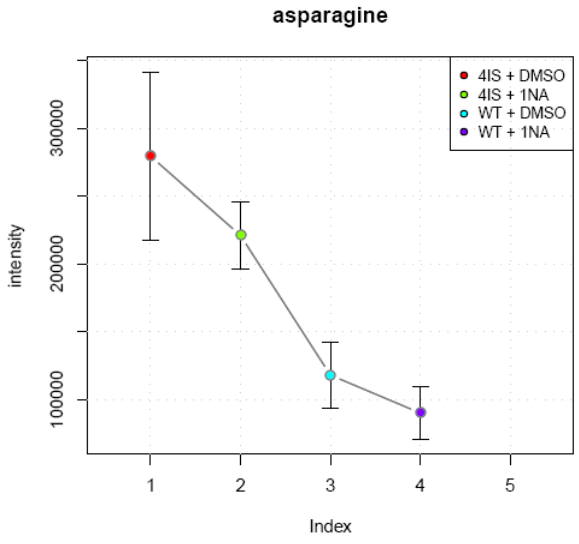
asparagine
intensity
Index
4IS + DMSO
4IS + 1NA
WT + DMSO
WT + 1NA

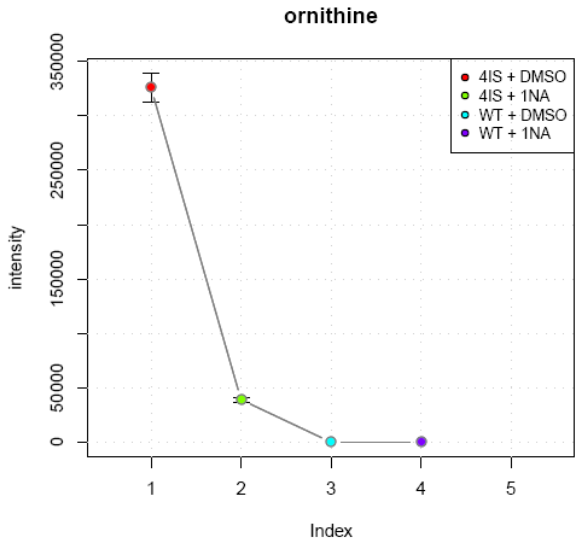
ornithine
intensity
0
50000
150000
250000
350000
1
2
3
4
5
Index
4IS + DMSO
4IS + 1NA
WT + DMSO
WT + 1NA

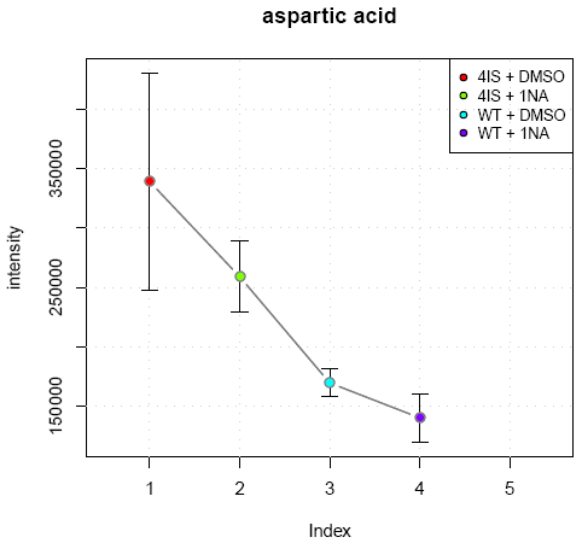
aspartic acid
intensity
150000
250000
350000
1
2
3
4
5
Index
4IS + DMSO
4IS + 1NA
WT + DMSO
WT + 1NA

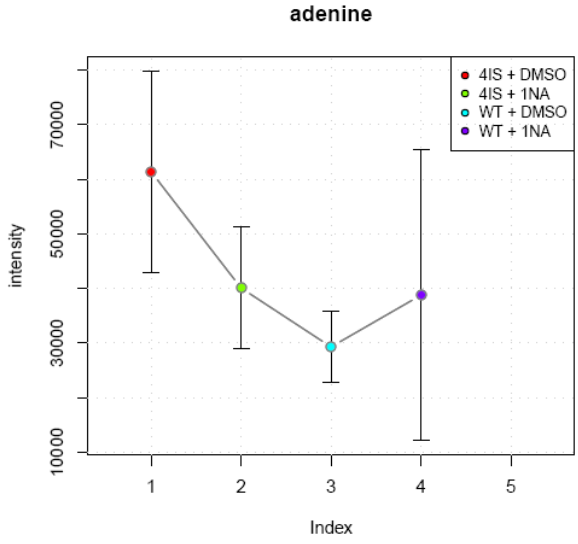
adenine
intensity
10000
30000
50000
70000
1
2
3
4
5
Index
4IS + DMSO
4IS + 1NA
WT + DMSO
WT + 1NA

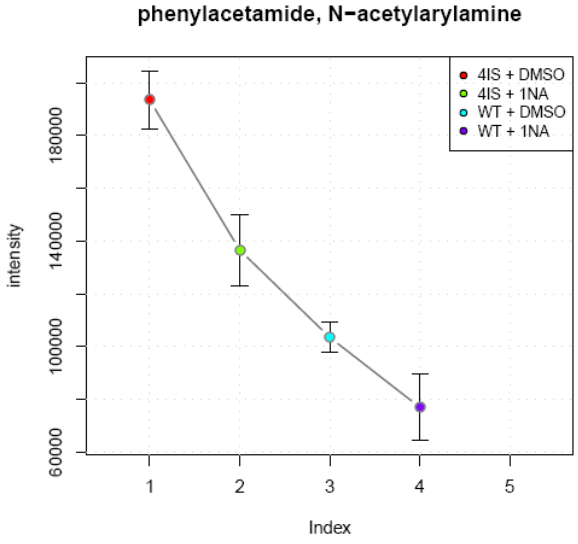
phenylacetamide, N−acetylarylamine
intensity
60000
100000
140000
180000
1
2
3
4
5
Index
4IS + DMSO
4IS + 1NA
WT + DMSO
WT + 1NA

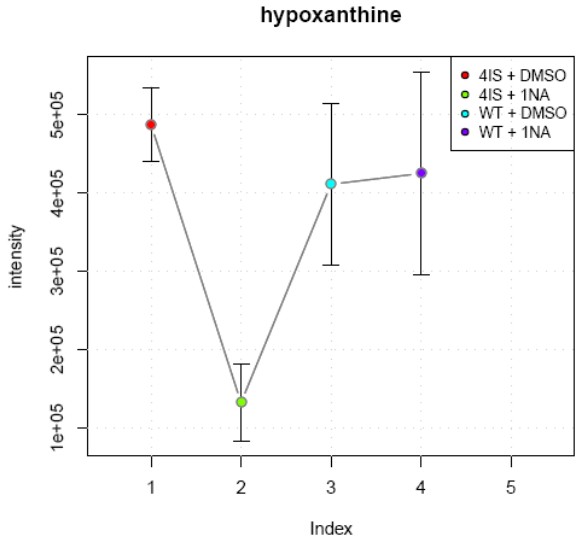
hypoxanthine
intensity
1e+05
2e+05
3e+05
4e+05
5e+05
1
2
3
4
5
Index
4IS + DMSO
4IS + 1NA
WT + DMSO
WT + 1NA

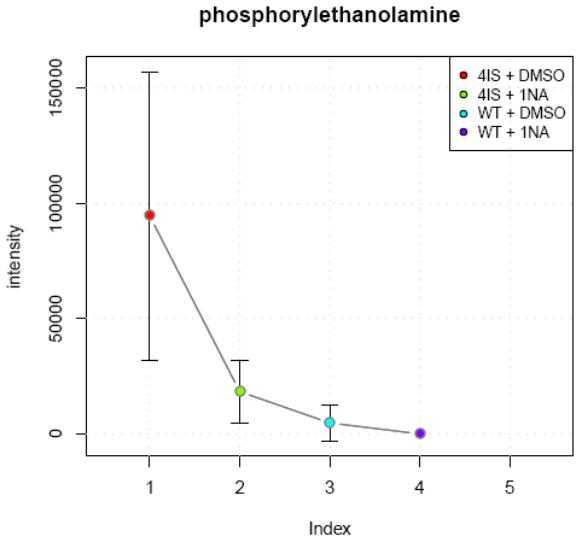
phosphorylethanolamine
intensity
0
50000
100000
150000
1
2
3
4
5
Index
4IS + DMSO
4IS + 1NA
WT + DMSO
WT + 1NA

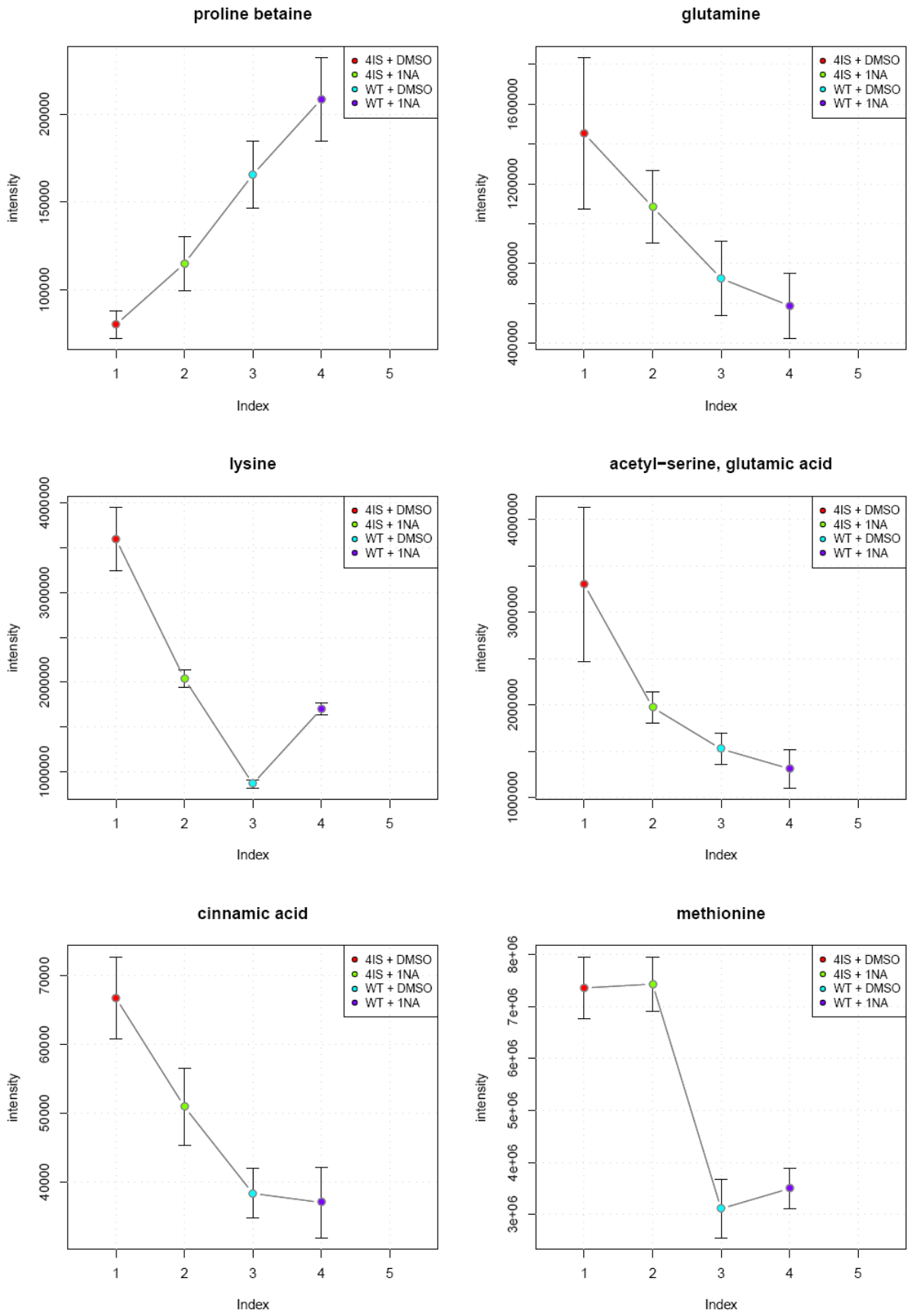
proline betaine
glutamine
lysine
acetyl−serine, glutamic acid
cinnamic acid
methionine
4IS + DMSO
4IS + 1NA
WT + DMSO
WT + 1NA
intensity
Index

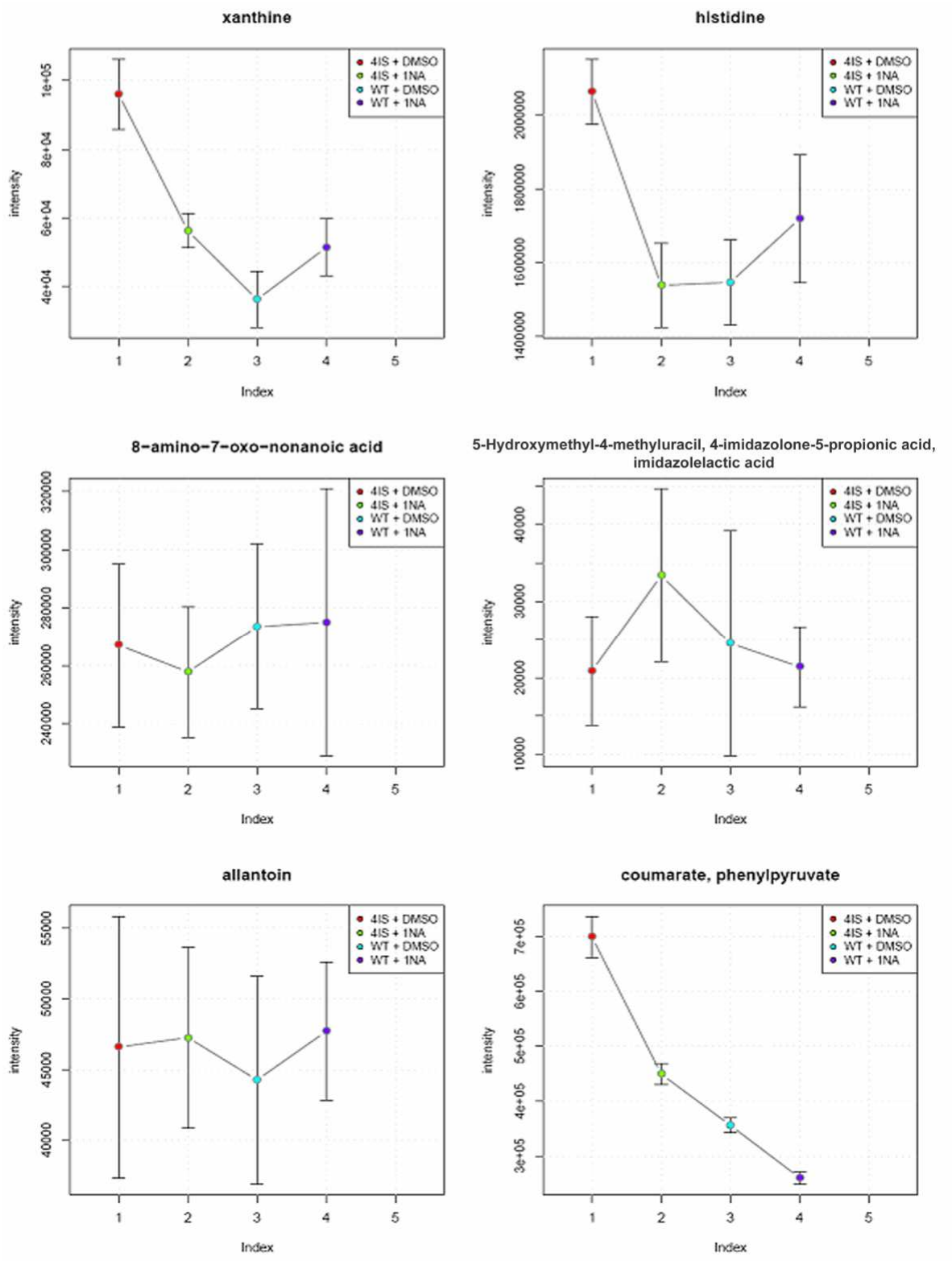
xanthine
histidine
8-amino-7-oxo-nonanoic acid
5-Hydroxymethyl-4-methyluracil, 4-imidazolone-5-propionic acid, imidazolelactic acid
allantoin
coumarate, phenylpyruvate
4IS + DMSO
4IS + 1NA
WT + DMSO
WT + 1NA
intensity
Index

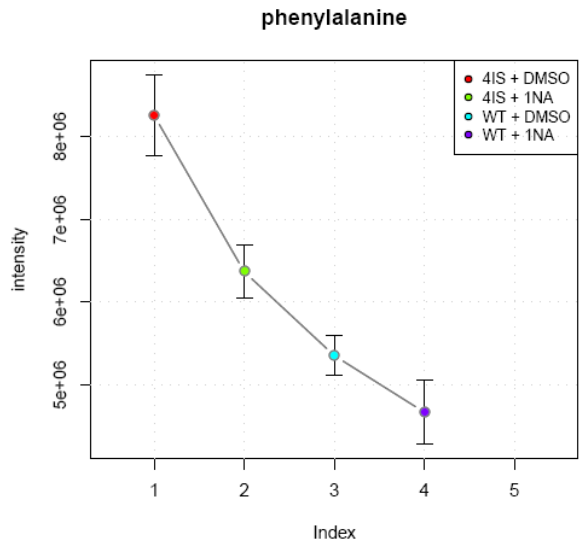
phenylalanine
4IS + DMSO
4IS + 1NA
WT + DMSO
WT + 1NA
intensity
5e+06
6e+06
7e+06
8e+06
1
2
3
4
5
Index

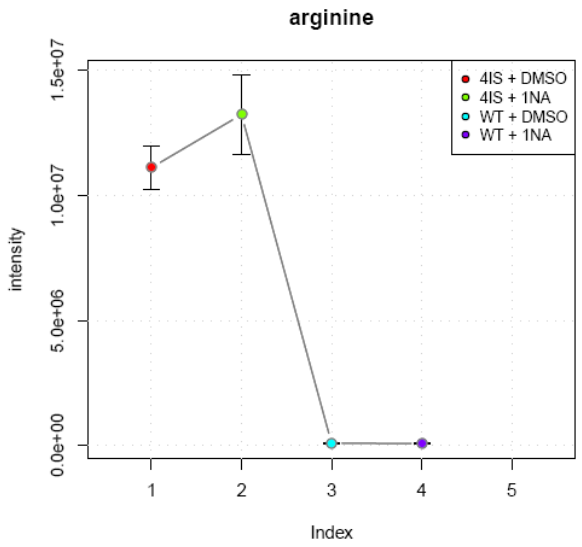
arginine
4IS + DMSO
4IS + 1NA
WT + DMSO
WT + 1NA
intensity
0.0e+00
5.0e+06
1.0e+07
1.5e+07
1
2
3
4
5
Index

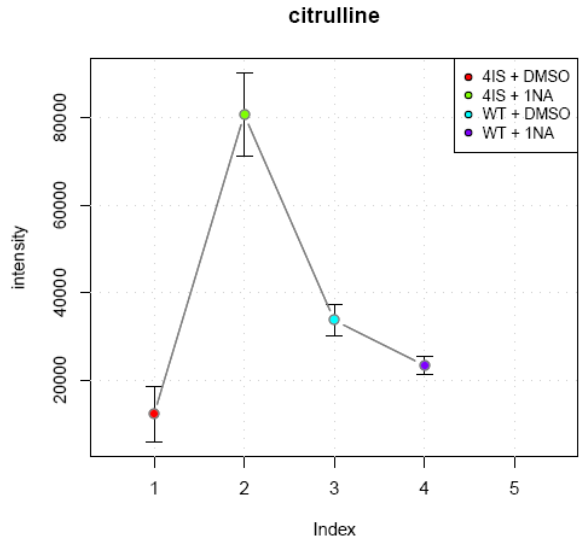
citrulline
4IS + DMSO
4IS + 1NA
WT + DMSO
WT + 1NA
intensity
20000
40000
60000
80000
1
2
3
4
5
Index

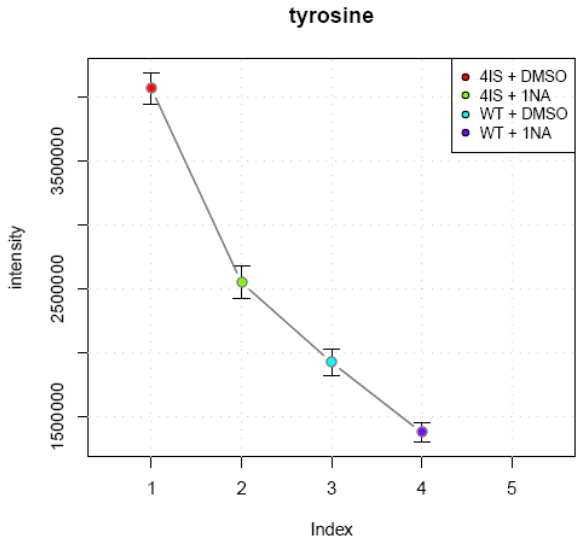
tyrosine
4IS + DMSO
4IS + 1NA
WT + DMSO
WT + 1NA
intensity
1500000
2500000
3500000
1
2
3
4
5
Index

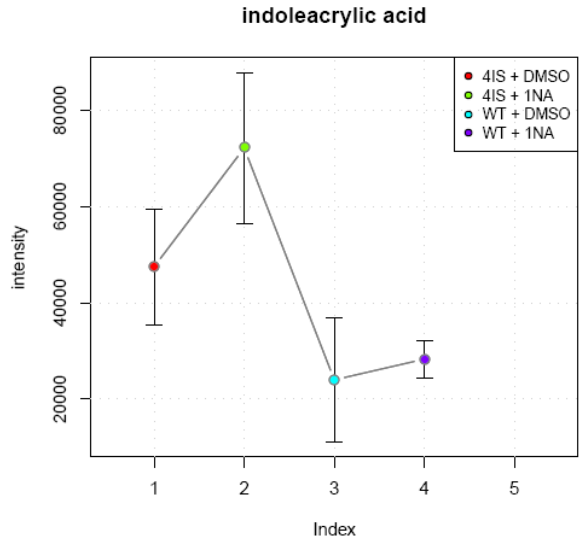
indoleacrylic acid
4IS + DMSO
4IS + 1NA
WT + DMSO
WT + 1NA
intensity
20000
40000
60000
80000
1
2
3
4
5
Index

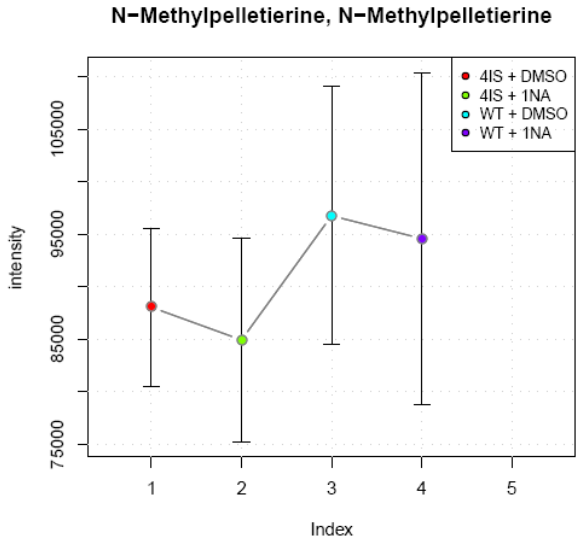
N−Methylpelletierine, N−Methylpelletierine
4IS + DMSO
4IS + 1NA
WT + DMSO
WT + 1NA
intensity
75000
85000
95000
105000
1
2
3
4
5
Index

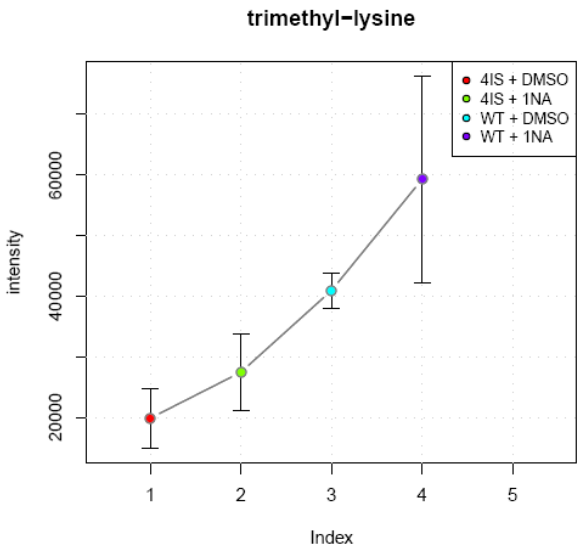
trimethyl−lysine
4IS + DMSO
4IS + 1NA
WT + DMSO
WT + 1NA
intensity
20000
40000
60000
1
2
3
4
5
Index

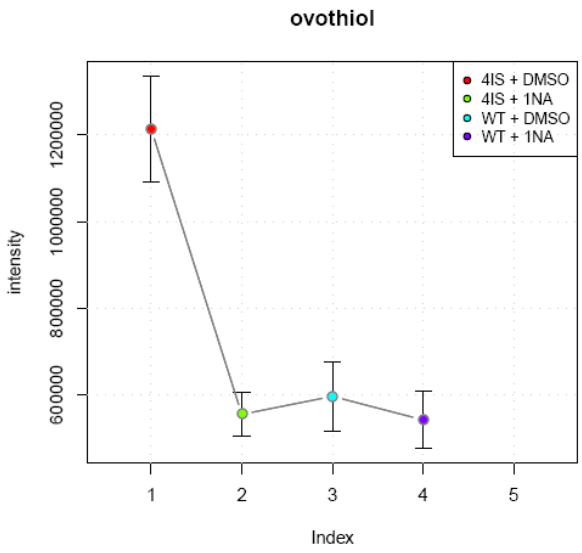
ovothiol
4IS + DMSO
4IS + 1NA
WT + DMSO
WT + 1NA
intensity
600000
800000
1000000
1200000
1
2
3
4
5
Index

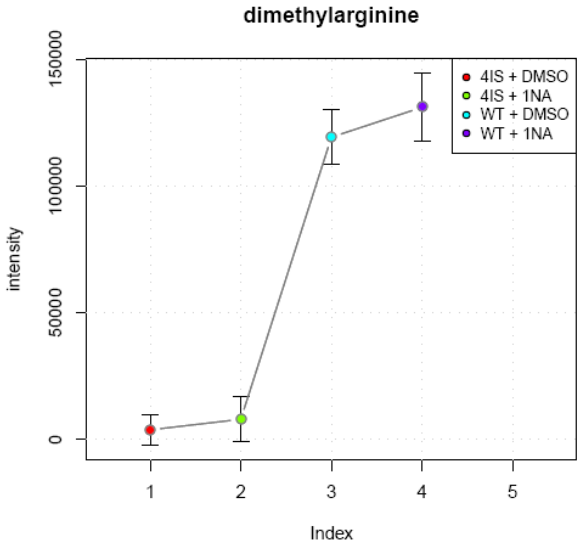
dimethylarginine
4IS + DMSO
4IS + 1NA
WT + DMSO
WT + 1NA
intensity
0
50000
100000
150000
1
2
3
4
5
Index

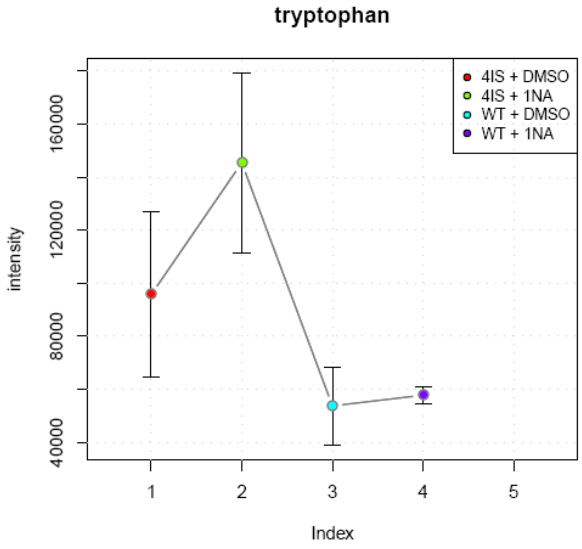
tryptophan
4IS + DMSO
4IS + 1NA
WT + DMSO
WT + 1NA
intensity
40000
80000
120000
160000
1
2
3
4
5
Index

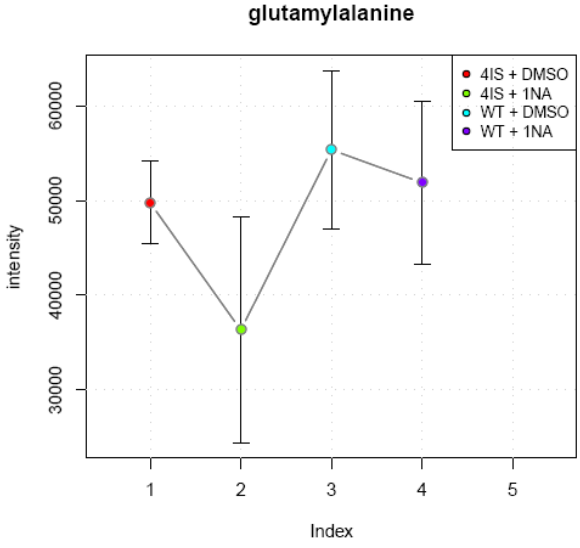
glutamylalanine
4IS + DMSO
4IS + 1NA
WT + DMSO
WT + 1NA
intensity
30000
40000
50000
60000
1
2
3
4
5
Index

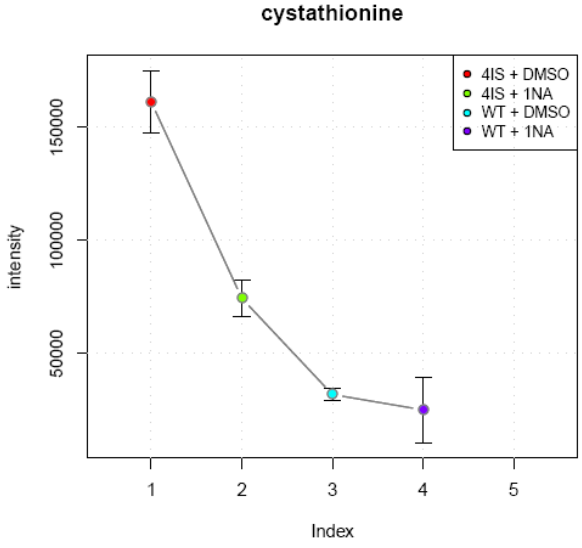
cystathionine
4IS + DMSO
4IS + 1NA
WT + DMSO
WT + 1NA
intensity
50000
100000
150000
1
2
3
4
5
Index

1−deoxy−tetradecasphing−13−enine

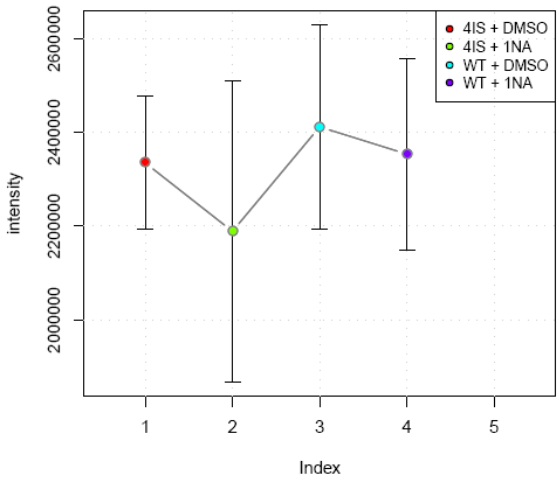

dihydrobiopterin

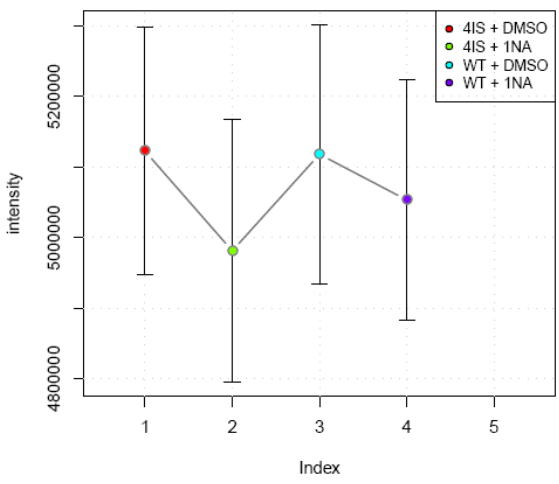

palmitic amide

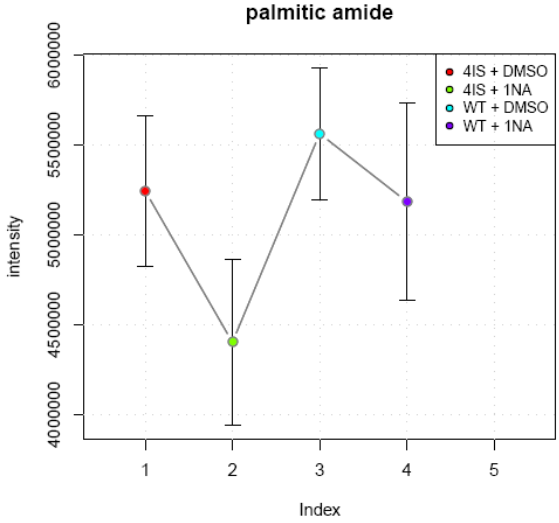

glycerophosphocholine

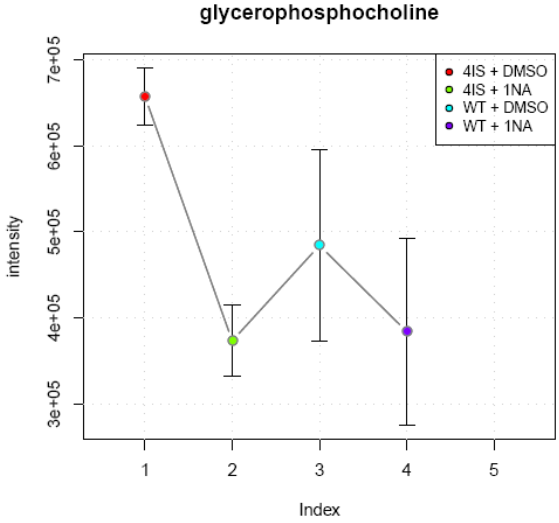

hexose phosphate

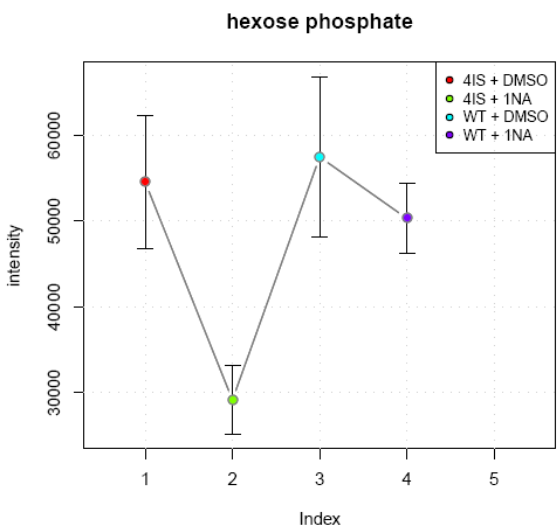

9,12,15−octadecatrienal, 6−[3]−ladderane−1−hexanol

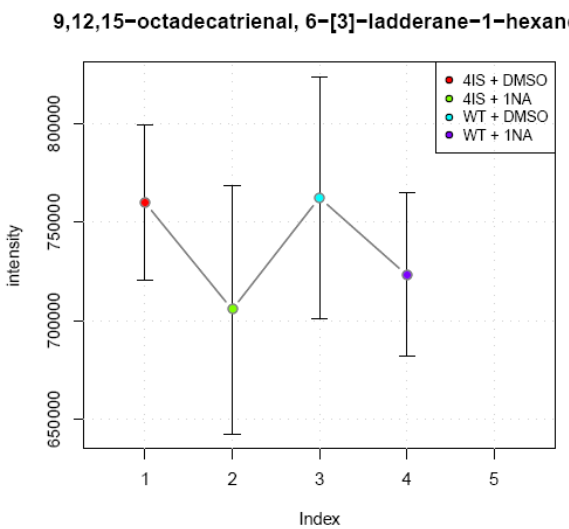

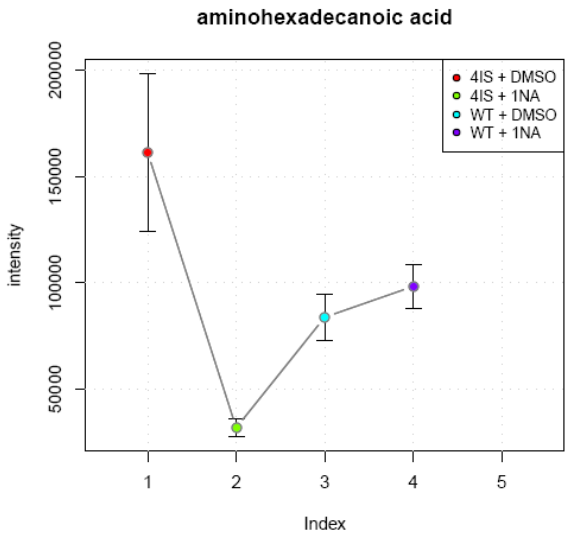
aminohexadecanoic acid
intensity
Index
4IS + DMSO
4IS + 1NA
WT + DMSO
WT + 1NA

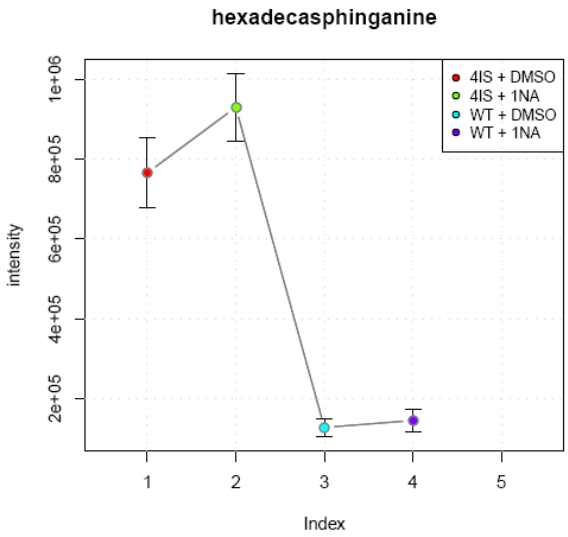
hexadecasphinganine
intensity
Index
4IS + DMSO
4IS + 1NA
WT + DMSO
WT + 1NA

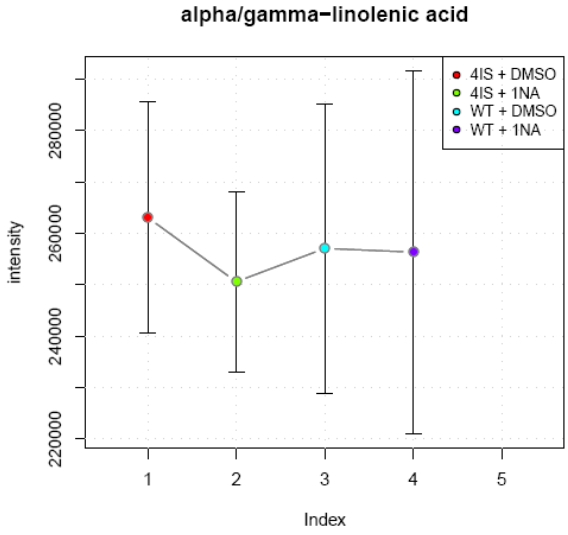
alpha/gamma−linolenic acid
intensity
Index
4IS + DMSO
4IS + 1NA
WT + DMSO
WT + 1NA

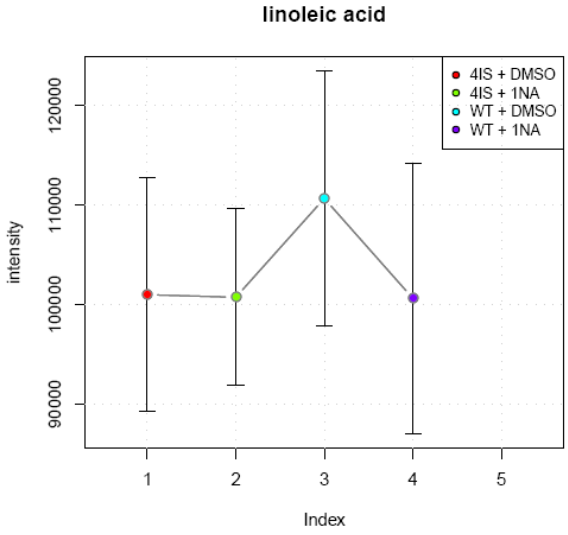
linoleic acid
intensity
Index
4IS + DMSO
4IS + 1NA
WT + DMSO
WT + 1NA

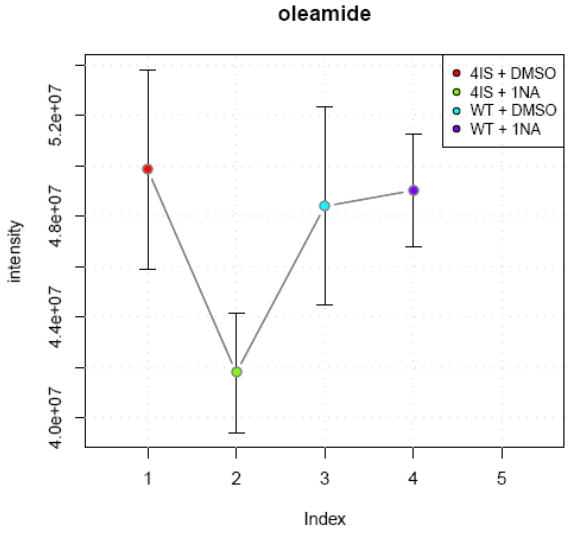
oleamide
intensity
Index
4IS + DMSO
4IS + 1NA
WT + DMSO
WT + 1NA

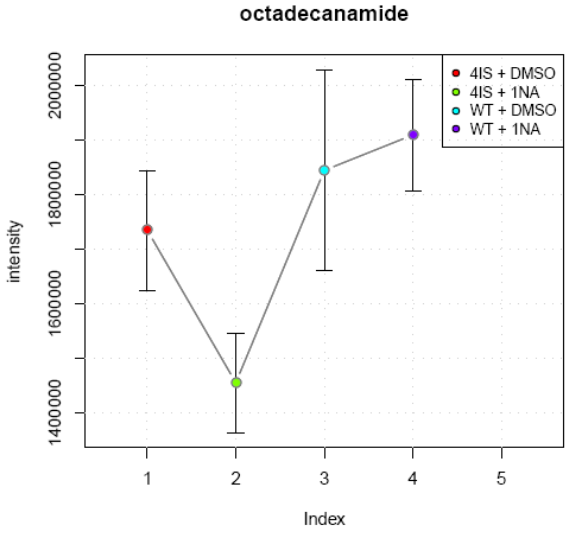
octadecanamide
intensity
Index
4IS + DMSO
4IS + 1NA
WT + DMSO
WT + 1NA

1−deoxy−sphinganine

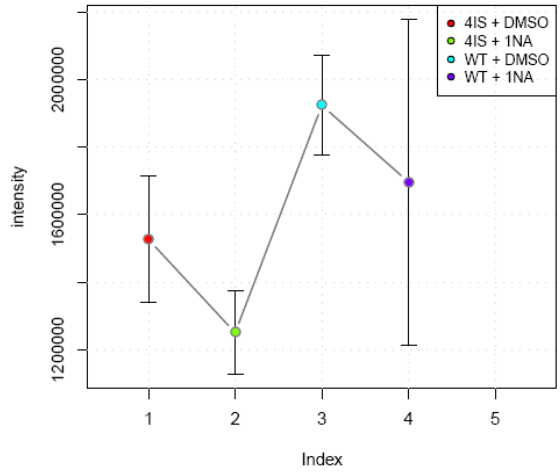

hydroxy−oxo−hexadecanoic acid, hexadecanedioic acid

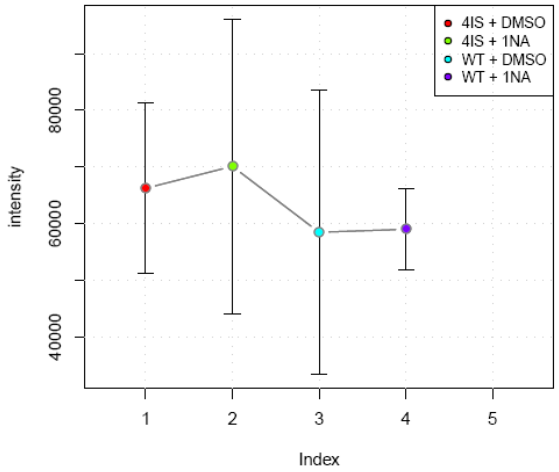

heptadecasphinganine

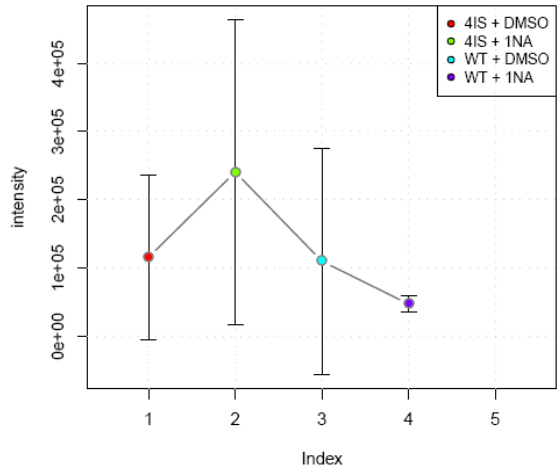

sphinga−4E,8E,10E−trienine

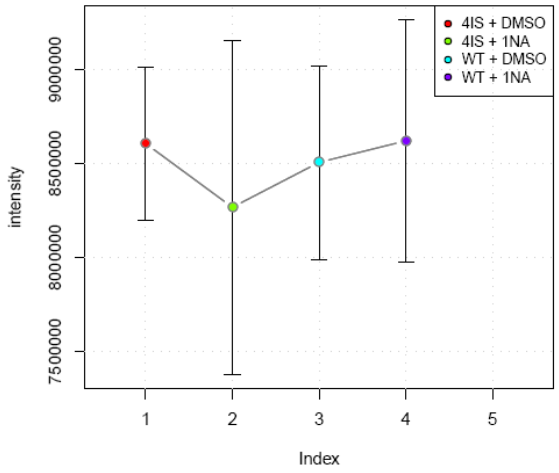

methylthioadenosine

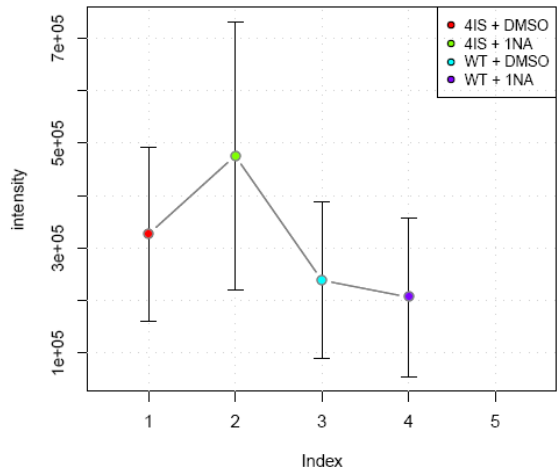

dehydrosphinganine, dehydrosphinganine

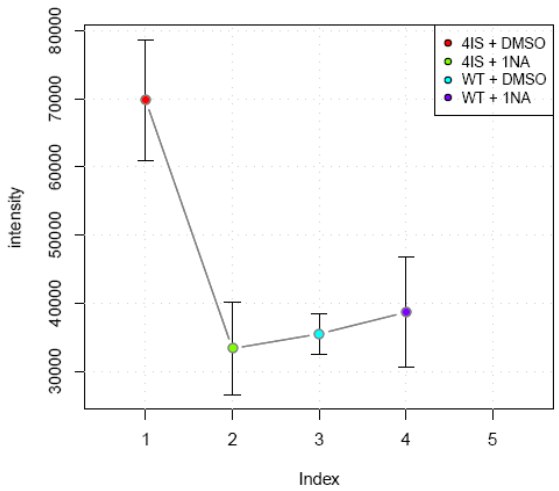

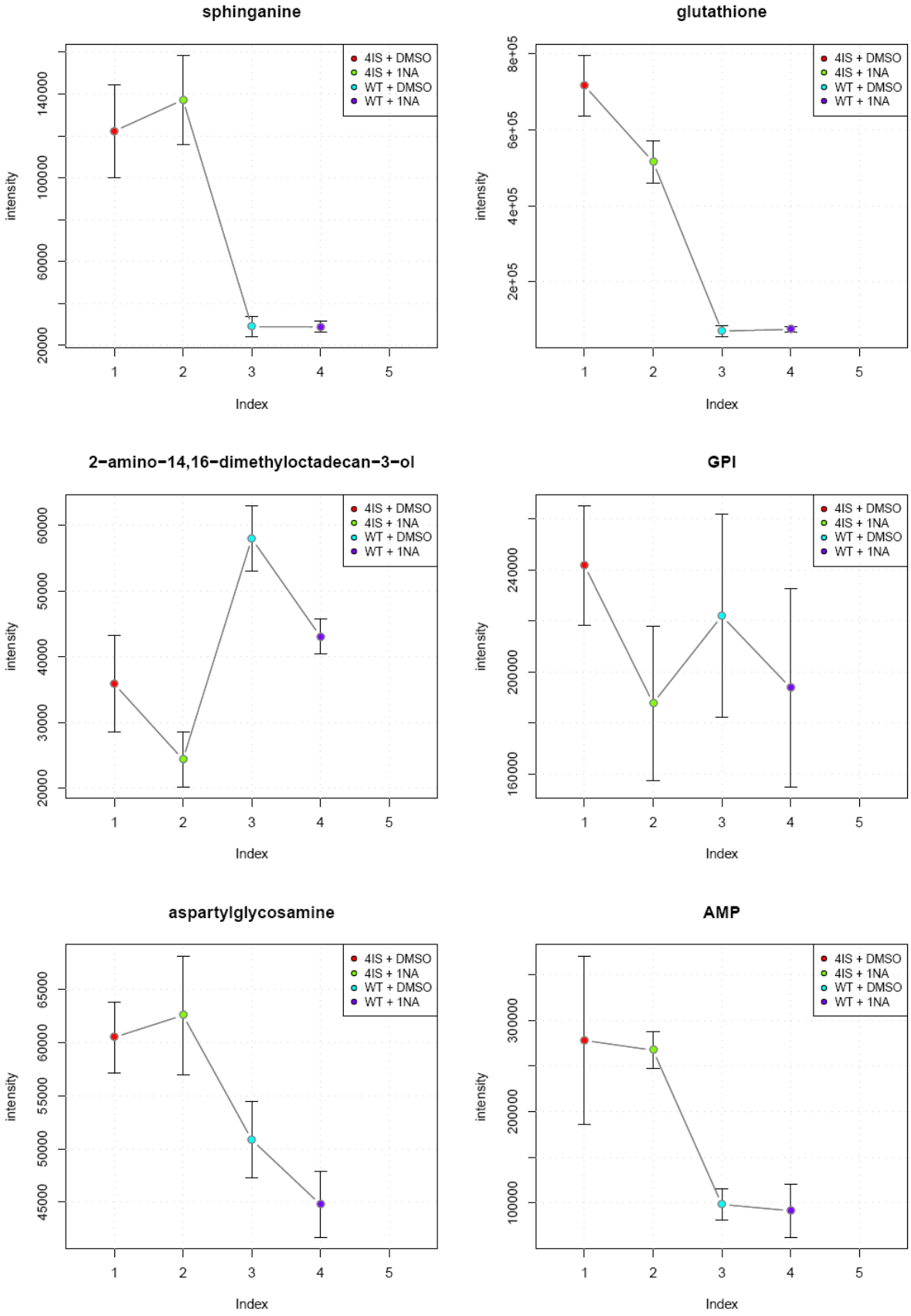
sphinganine
glutathione
2−amino−14,16−dimethyloctadecan−3−ol
GPI
aspartylglycosamine
AMP
4IS + DMSO
4IS + 1NA
WT + DMSO
WT + 1NA
intensity
Index

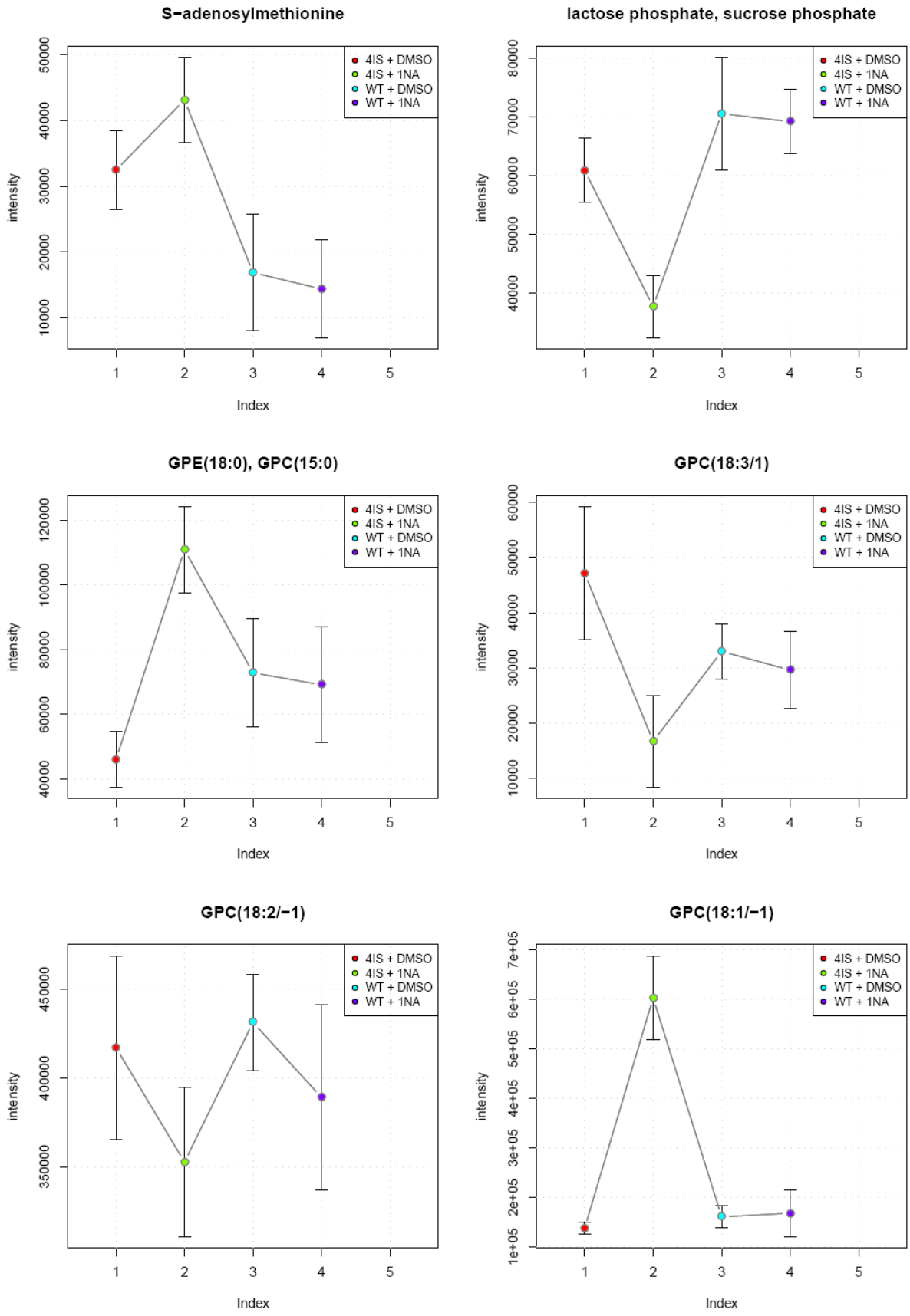
S−adenosylmethionine
lactose phosphate, sucrose phosphate
GPE(18:0), GPC(15:0)
GPC(18:3/1)
GPC(18:2/−1)
GPC(18:1/−1)
4IS + DMSO
4IS + 1NA
WT + DMSO
WT + 1NA
intensity
Index

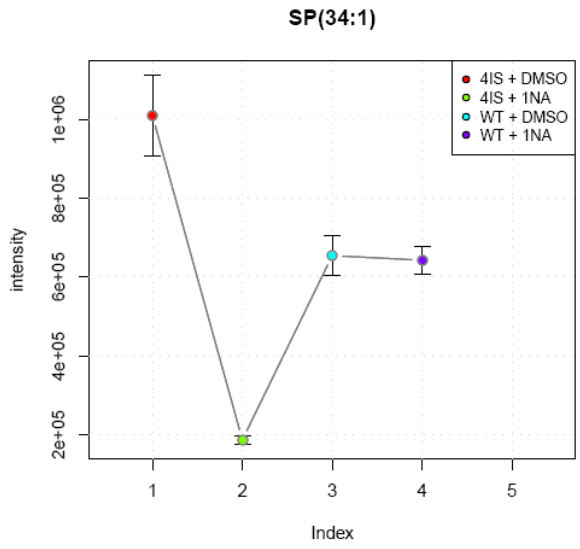
SP(34:1)
4IS + DMSO
4IS + 1NA
WT + DMSO
WT + 1NA
intensity
2e+05
4e+05
6e+05
8e+05
1e+06
1
2
3
4
5
Index

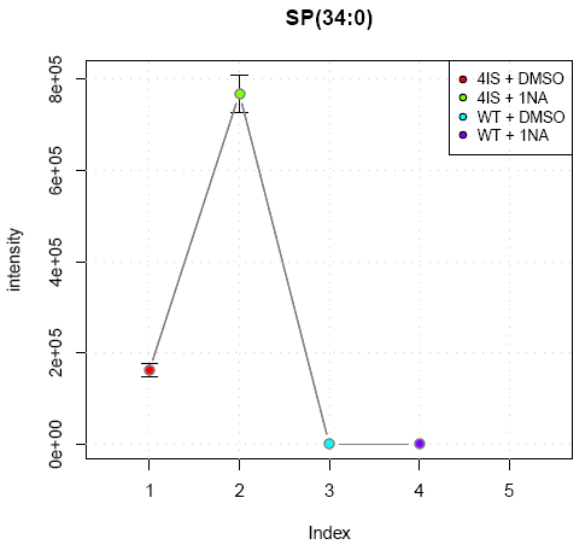
SP(34:0)
4IS + DMSO
4IS + 1NA
WT + DMSO
WT + 1NA
intensity
0e+00
2e+05
4e+05
6e+05
8e+05
1
2
3
4
5
Index

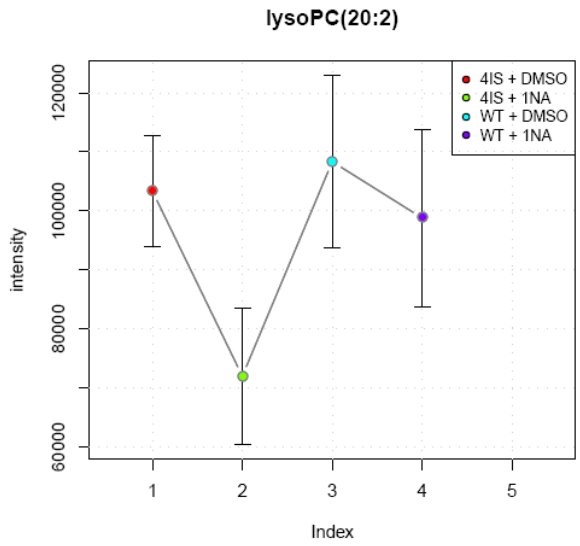
lysoPC(20:2)
4IS + DMSO
4IS + 1NA
WT + DMSO
WT + 1NA
intensity
60000
80000
100000
120000
1
2
3
4
5
Index

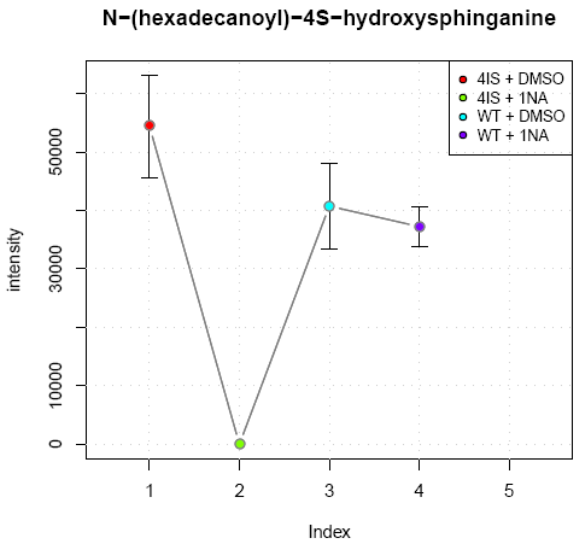
N−(hexadecanoyl)−4S−hydroxysphinganine
4IS + DMSO
4IS + 1NA
WT + DMSO
WT + 1NA
intensity
0
10000
30000
50000
1
2
3
4
5
Index

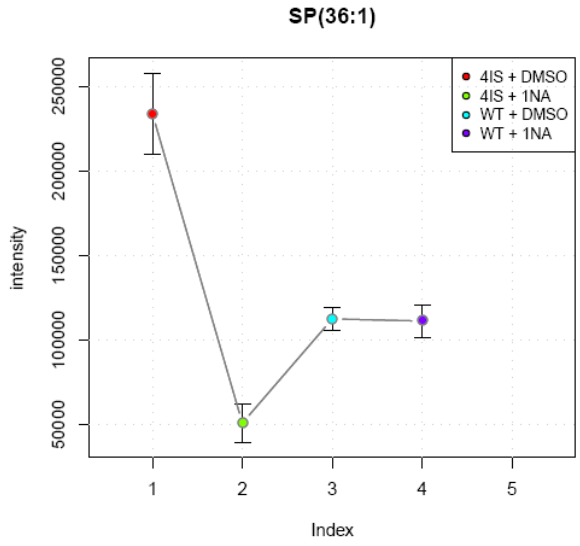
SP(36:1)
4IS + DMSO
4IS + 1NA
WT + DMSO
WT + 1NA
intensity
50000
100000
150000
200000
250000
1
2
3
4
5
Index

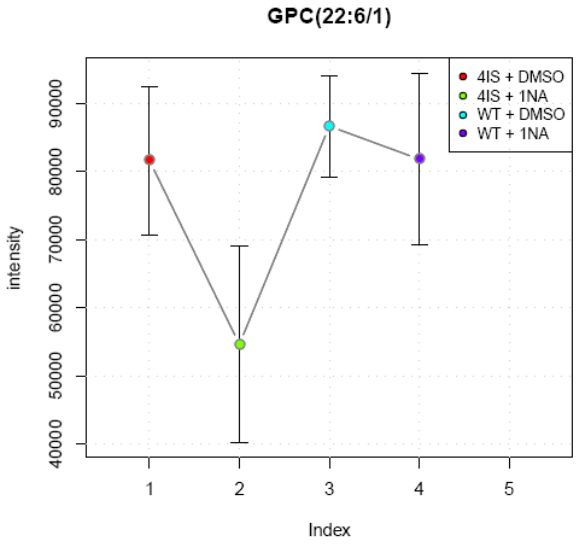
GPC(22:6/1)
4IS + DMSO
4IS + 1NA
WT + DMSO
WT + 1NA
intensity
40000
50000
60000
70000
80000
90000
1
2
3
4
5
Index

SP(36:0)

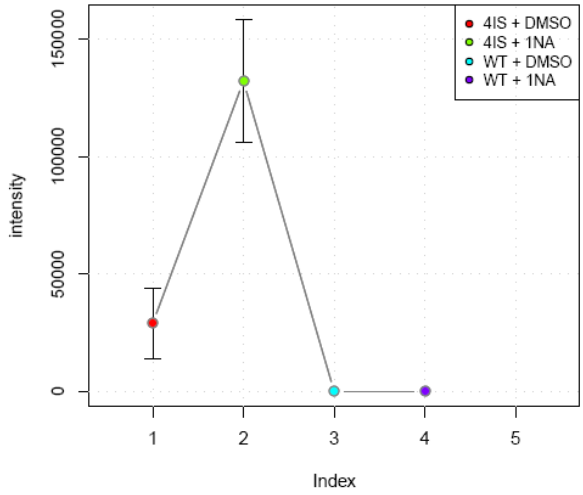

GPC(22:5/1)

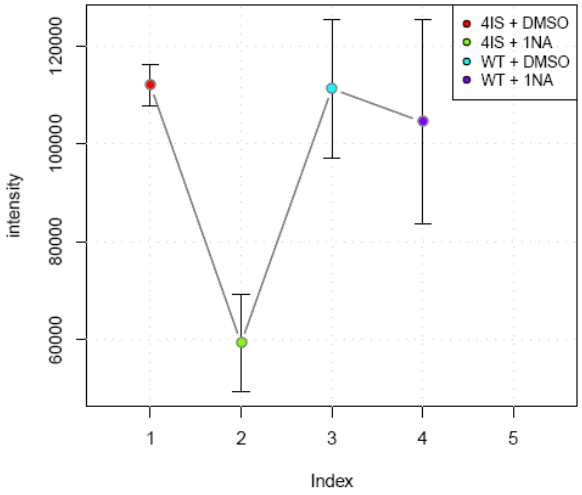

GPI(18:1/1)

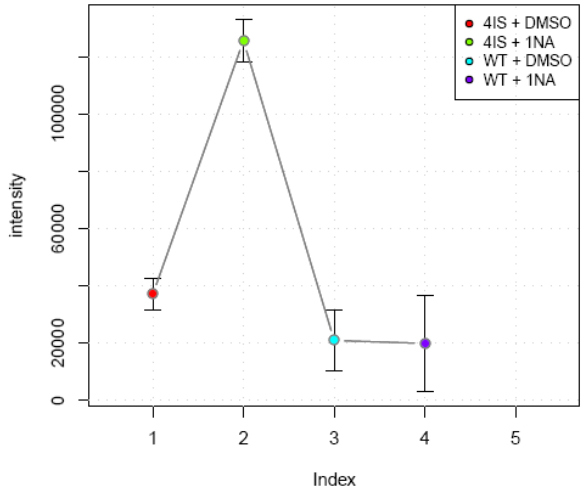

GPE(34:2/1)

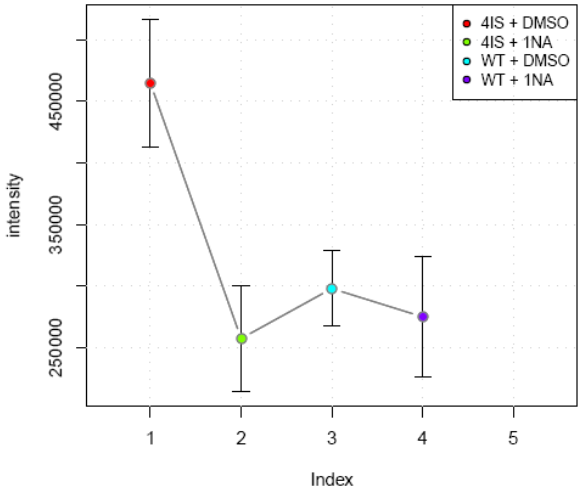

GPC(30:2/2), GPE(33:2/2)

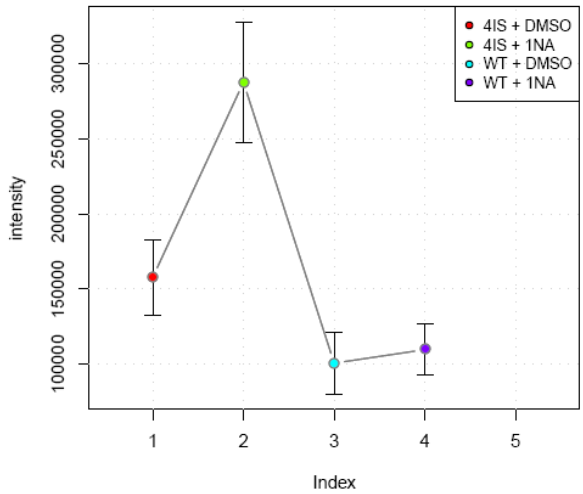

GPnE(34:1/2)

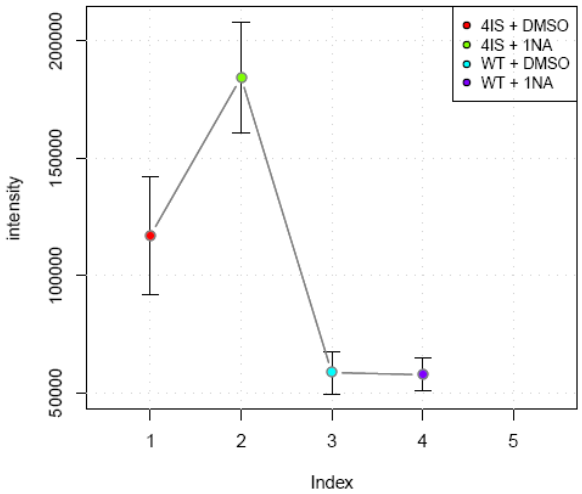

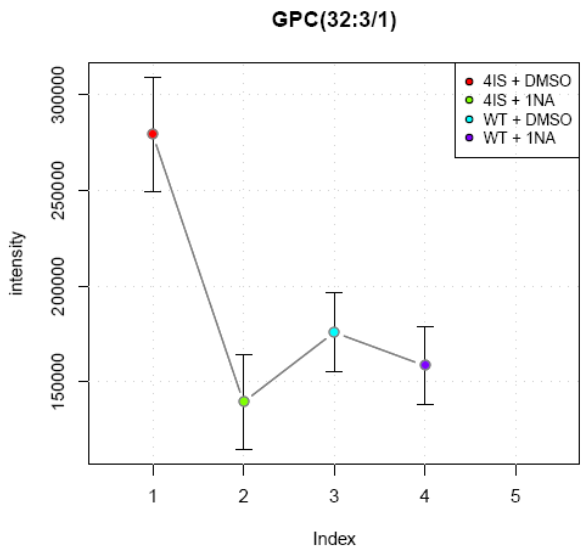
GPC(32:3/1)
intensity
Index
4IS + DMSO
4IS + 1NA
WT + DMSO
WT + 1NA

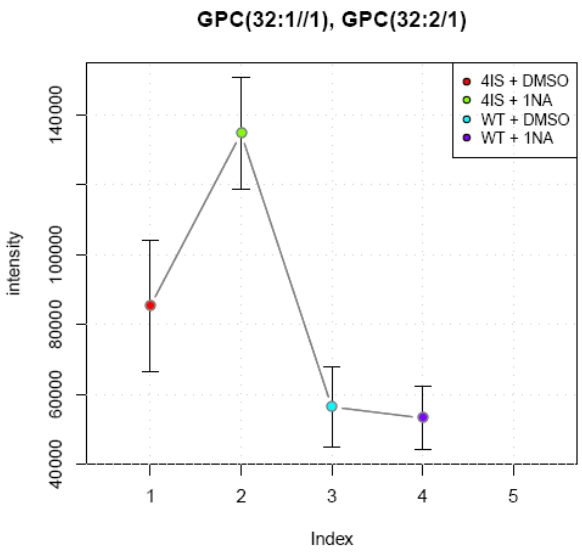
GPC(32:1//1), GPC(32:2/1)
intensity
Index
4IS + DMSO
4IS + 1NA
WT + DMSO
WT + 1NA

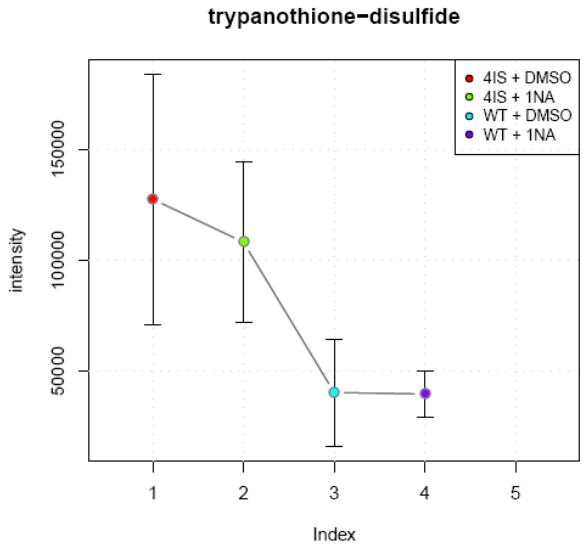
trypanothione−disulfide
intensity
Index
4IS + DMSO
4IS + 1NA
WT + DMSO
WT + 1NA

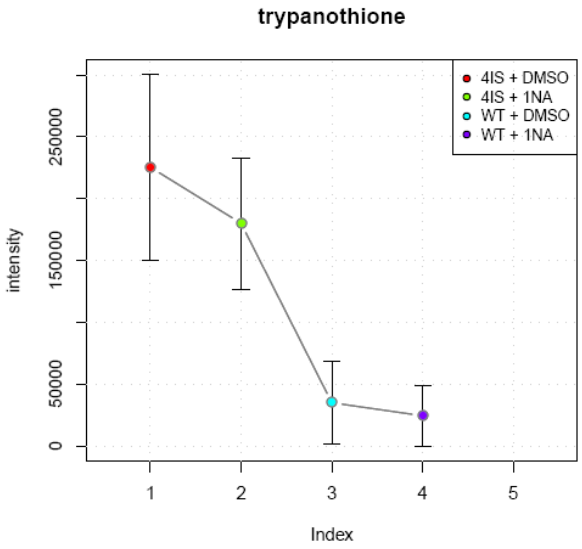
trypanothione
intensity
Index
4IS + DMSO
4IS + 1NA
WT + DMSO
WT + 1NA

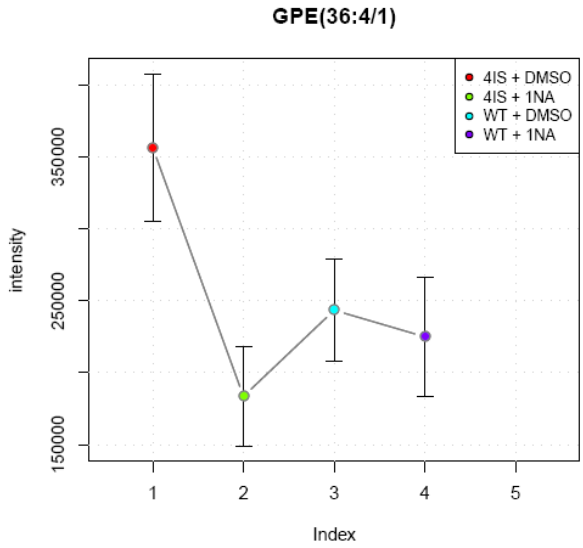
GPE(36:4/1)
intensity
Index
4IS + DMSO
4IS + 1NA
WT + DMSO
WT + 1NA

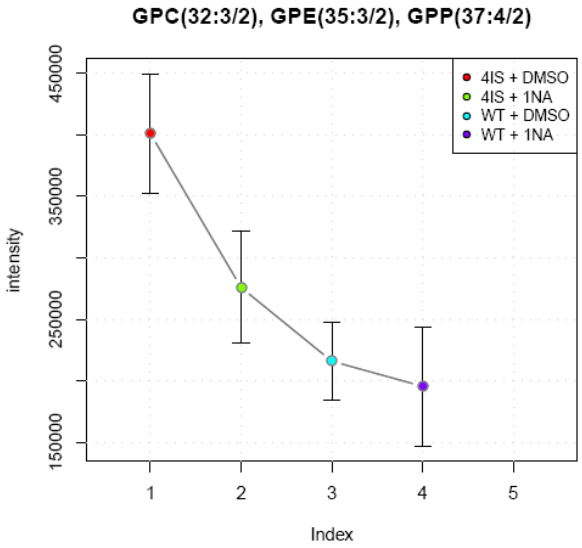
GPC(32:3/2), GPE(35:3/2), GPP(37:4/2)
intensity
Index
4IS + DMSO
4IS + 1NA
WT + DMSO
WT + 1NA

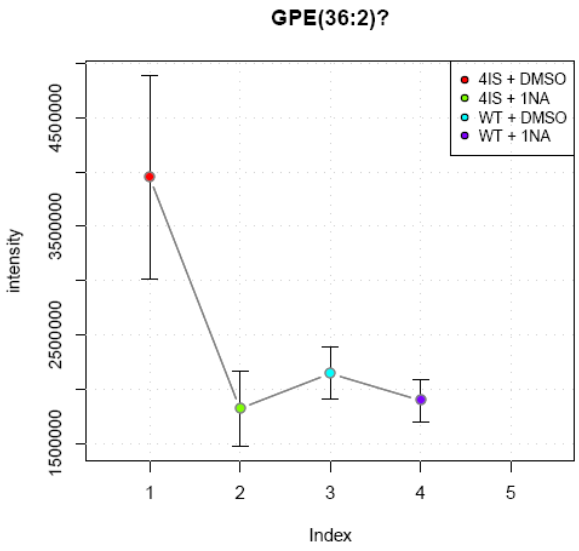
GPE(36:2)?
4IS + DMSO
4IS + 1NA
WT + DMSO
WT + 1NA
intensity
1500000
2500000
3500000
4500000
1
2
3
4
5
Index

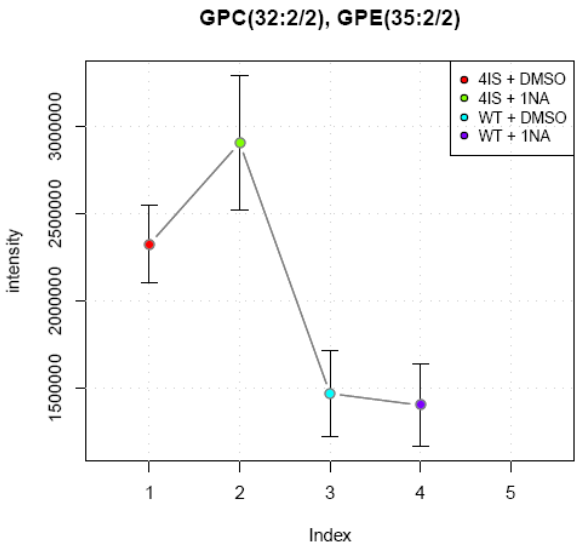
GPC(32:2/2), GPE(35:2/2)
4IS + DMSO
4IS + 1NA
WT + DMSO
WT + 1NA
intensity
1500000
2000000
2500000
3000000
1
2
3
4
5
Index

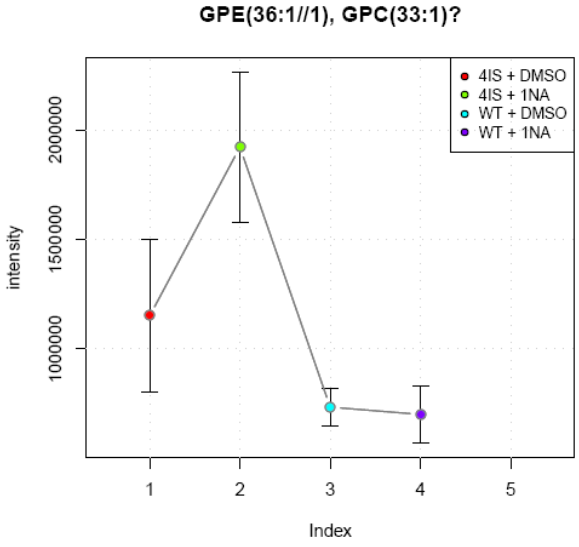
GPE(36:1//1), GPC(33:1)?
4IS + DMSO
4IS + 1NA
WT + DMSO
WT + 1NA
intensity
1000000
1500000
2000000
1
2
3
4
5
Index

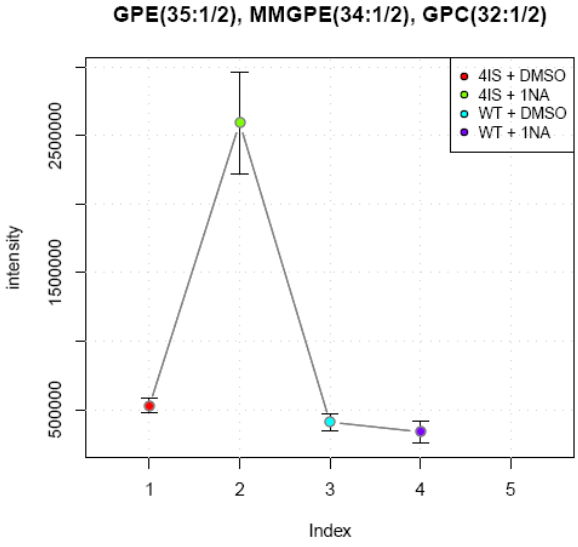
GPE(35:1/2), MMGPE(34:1/2), GPC(32:1/2)
4IS + DMSO
4IS + 1NA
WT + DMSO
WT + 1NA
intensity
500000
1500000
2500000
1
2
3
4
5
Index

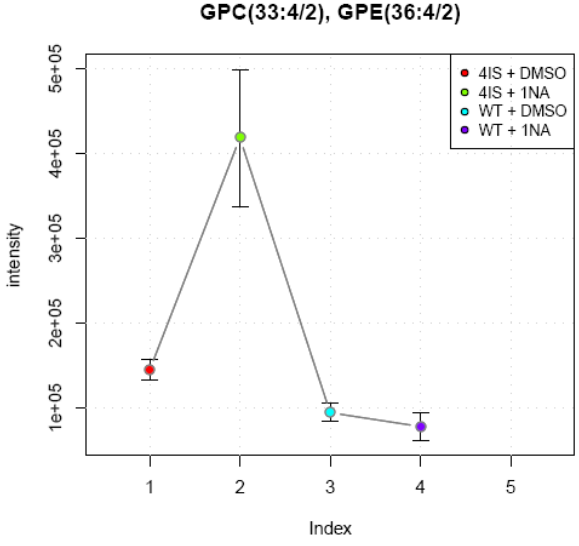
GPC(33:4/2), GPE(36:4/2)
4IS + DMSO
4IS + 1NA
WT + DMSO
WT + 1NA
intensity
1e+05
2e+05
3e+05
4e+05
5e+05
1
2
3
4
5
Index

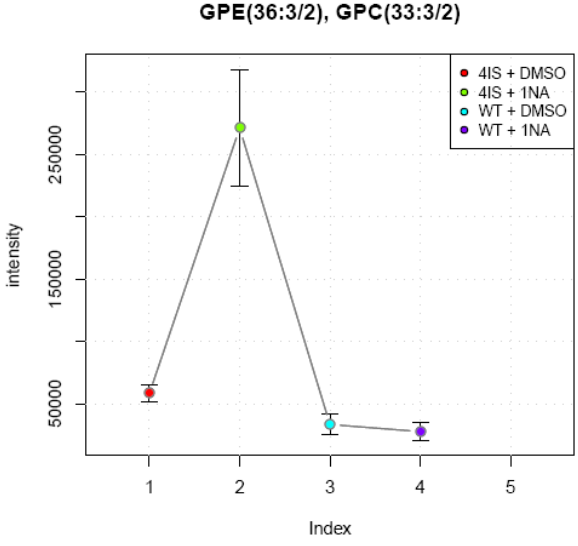
GPE(36:3/2), GPC(33:3/2)
4IS + DMSO
4IS + 1NA
WT + DMSO
WT + 1NA
intensity
50000
150000
250000
1
2
3
4
5
Index

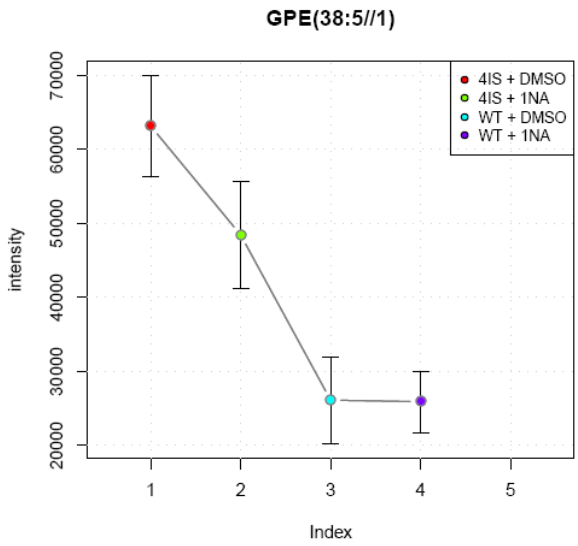
GPE(38:5//1)
intensity
Index
4IS + DMSO
4IS + 1NA
WT + DMSO
WT + 1NA

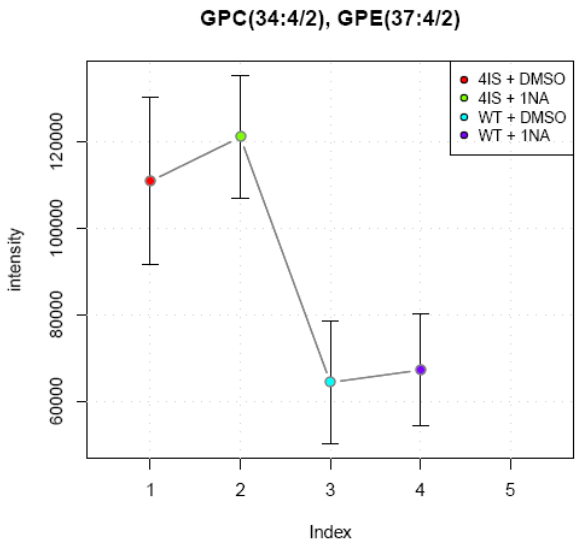
GPC(34:4/2), GPE(37:4/2)
intensity
Index
4IS + DMSO
4IS + 1NA
WT + DMSO
WT + 1NA

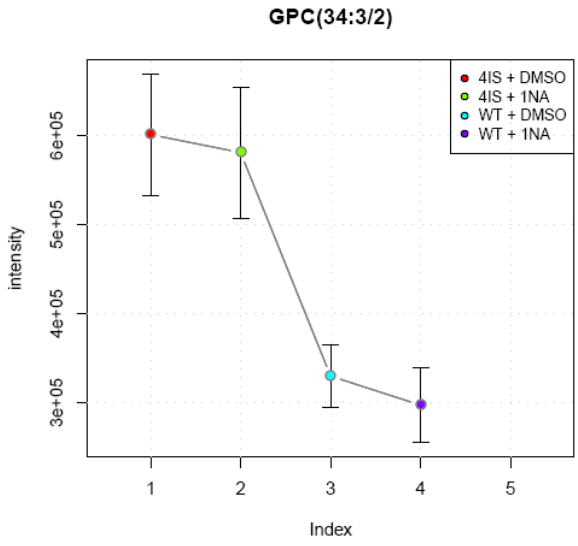
GPC(34:3/2)
intensity
Index
4IS + DMSO
4IS + 1NA
WT + DMSO
WT + 1NA

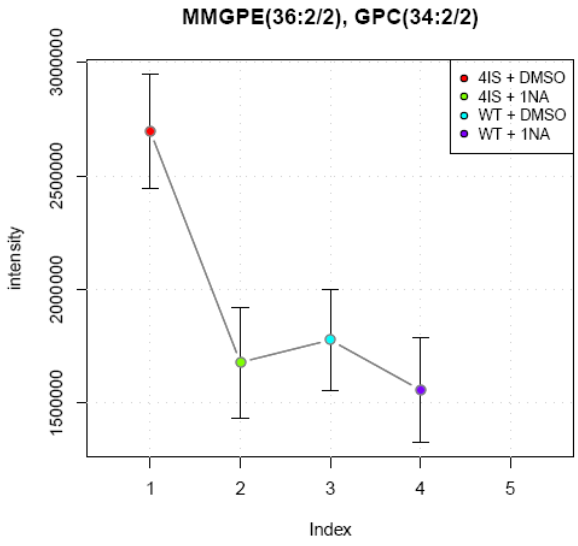
MMGPE(36:2/2), GPC(34:2/2)
intensity
Index
4IS + DMSO
4IS + 1NA
WT + DMSO
WT + 1NA

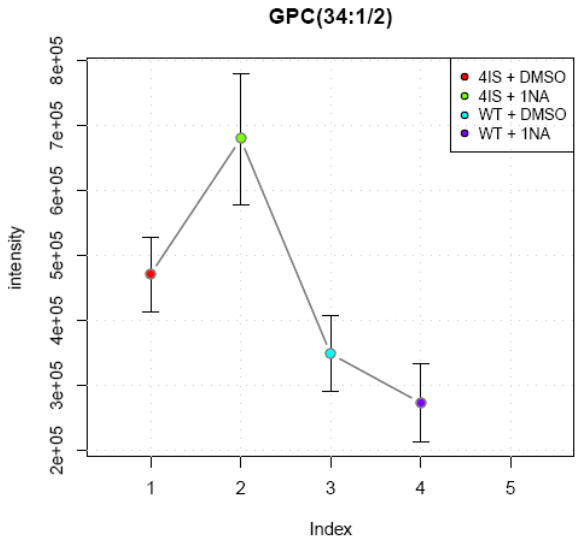
GPC(34:1/2)
intensity
Index
4IS + DMSO
4IS + 1NA
WT + DMSO
WT + 1NA

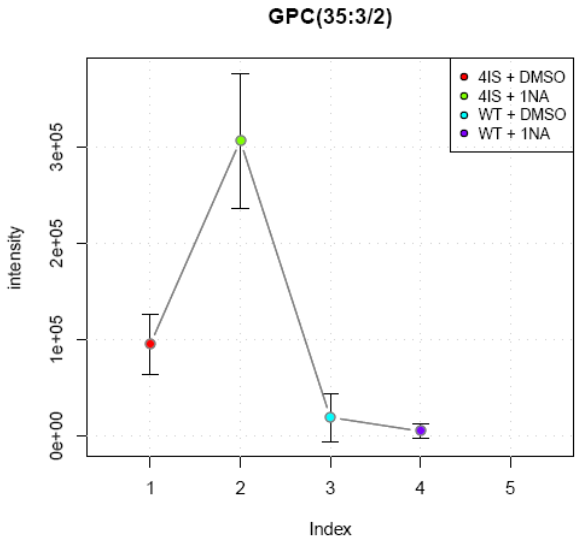
GPC(35:3/2)
intensity
Index
4IS + DMSO
4IS + 1NA
WT + DMSO
WT + 1NA

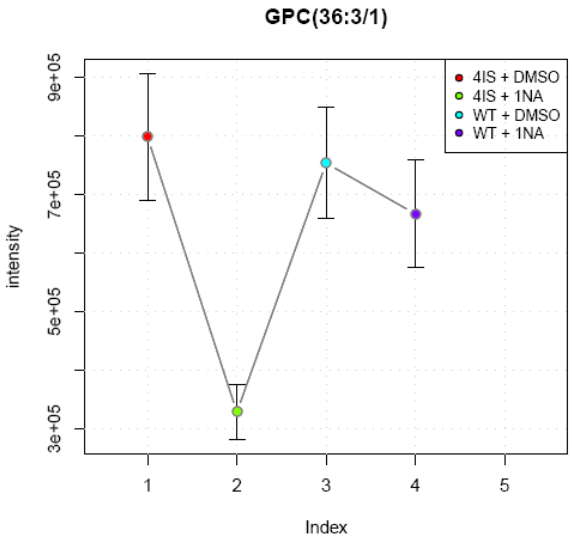
GPC(36:3/1)
intensity
3e+05
5e+05
7e+05
9e+05
1
2
3
4
5
Index
4IS + DMSO
4IS + 1NA
WT + DMSO
WT + 1NA

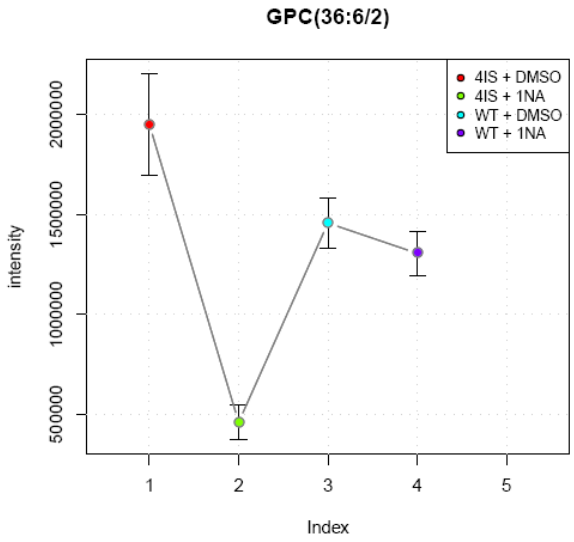
GPC(36:6/2)
intensity
500000
1000000
1500000
2000000
1
2
3
4
5
Index
4IS + DMSO
4IS + 1NA
WT + DMSO
WT + 1NA

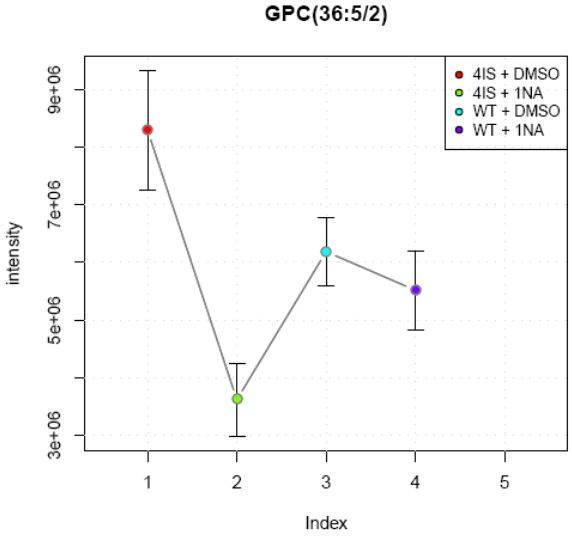
GPC(36:5/2)
intensity
3e+06
5e+06
7e+06
9e+06
1
2
3
4
5
Index
4IS + DMSO
4IS + 1NA
WT + DMSO
WT + 1NA

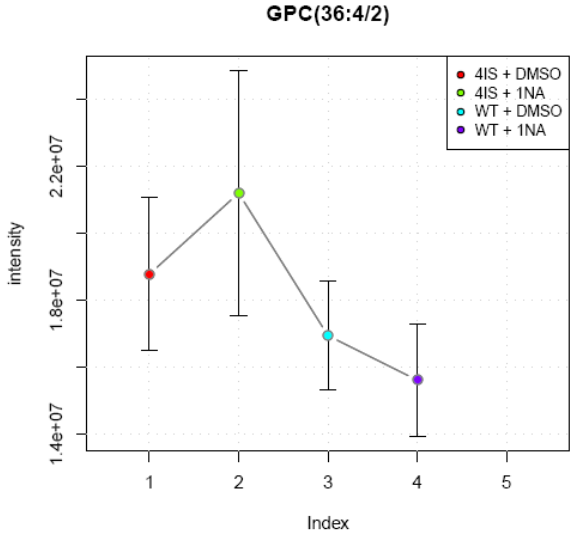
GPC(36:4/2)
intensity
1.4e+07
1.8e+07
2.2e+07
1
2
3
4
5
Index
4IS + DMSO
4IS + 1NA
WT + DMSO
WT + 1NA

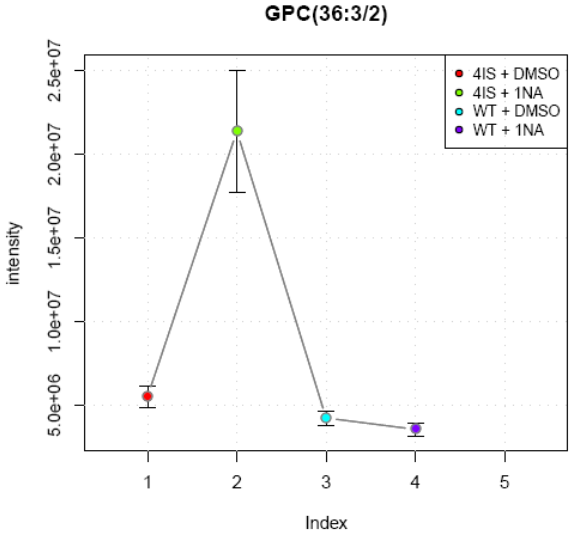
GPC(36:3/2)
intensity
5.0e+06
1.0e+07
1.5e+07
2.0e+07
2.5e+07
1
2
3
4
5
Index
4IS + DMSO
4IS + 1NA
WT + DMSO
WT + 1NA

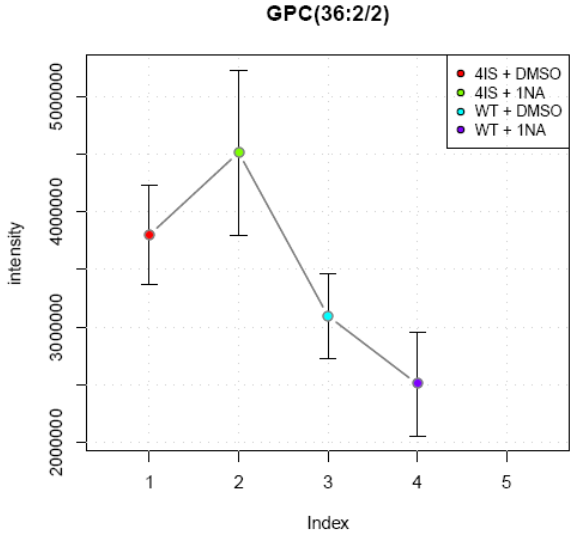
GPC(36:2/2)
intensity
2000000
3000000
4000000
5000000
1
2
3
4
5
Index
4IS + DMSO
4IS + 1NA
WT + DMSO
WT + 1NA

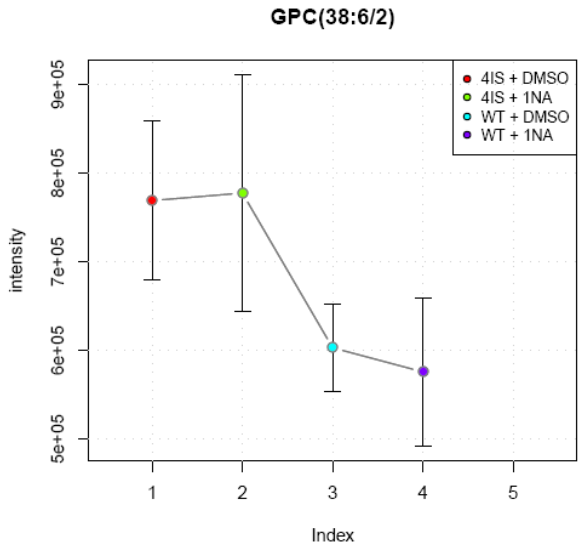
GPC(38:6/2)
intensity
5e+05
6e+05
7e+05
8e+05
9e+05
1
2
3
4
5
Index
4IS + DMSO
4IS + 1NA
WT + DMSO
WT + 1NA

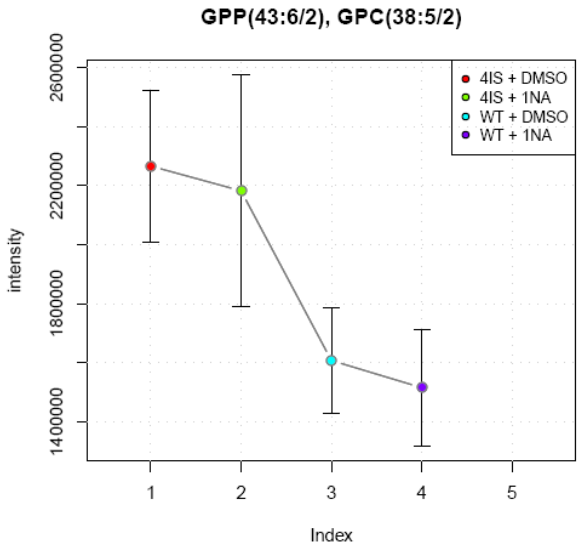
GPP(43:6/2), GPC(38:5/2)
intensity
1400000
1800000
2200000
2600000
1
2
3
4
5
Index
4IS + DMSO
4IS + 1NA
WT + DMSO
WT + 1NA

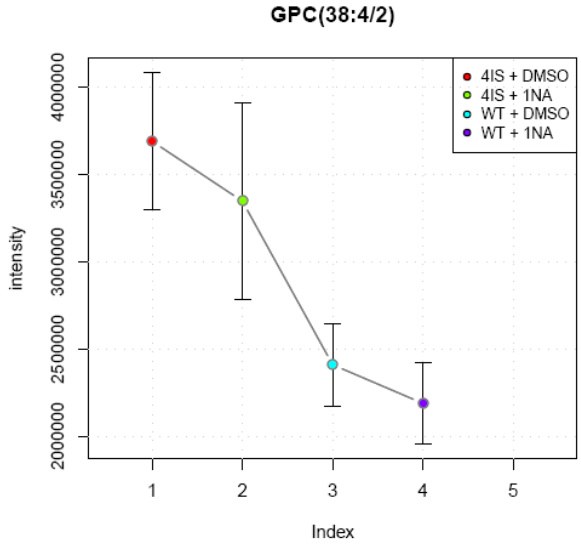
GPC(38:4/2)
intensity
2000000
2500000
3000000
3500000
4000000
1
2
3
4
5
Index
4IS + DMSO
4IS + 1NA
WT + DMSO
WT + 1NA

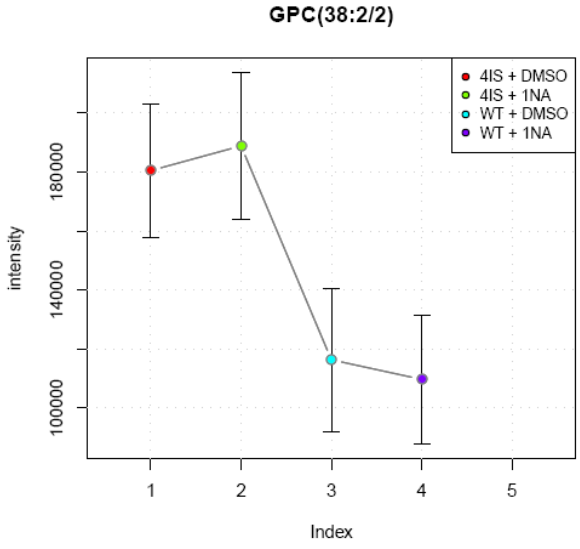
GPC(38:2/2)
intensity
100000
140000
180000
1
2
3
4
5
Index
4IS + DMSO
4IS + 1NA
WT + DMSO
WT + 1NA

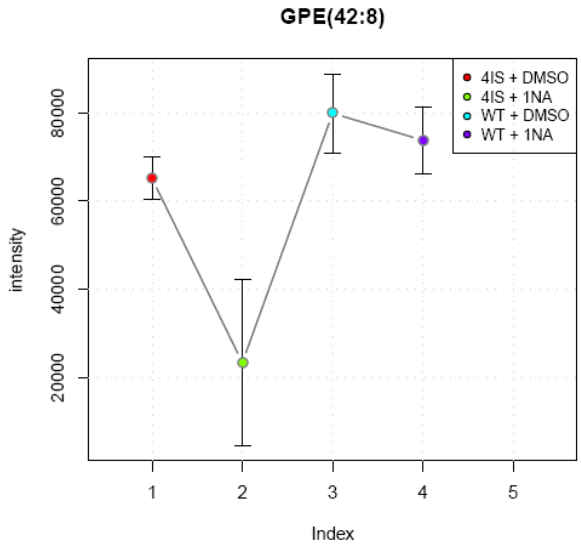
GPE(42:8)
intensity
20000
40000
60000
80000
1
2
3
4
5
Index
4IS + DMSO
4IS + 1NA
WT + DMSO
WT + 1NA

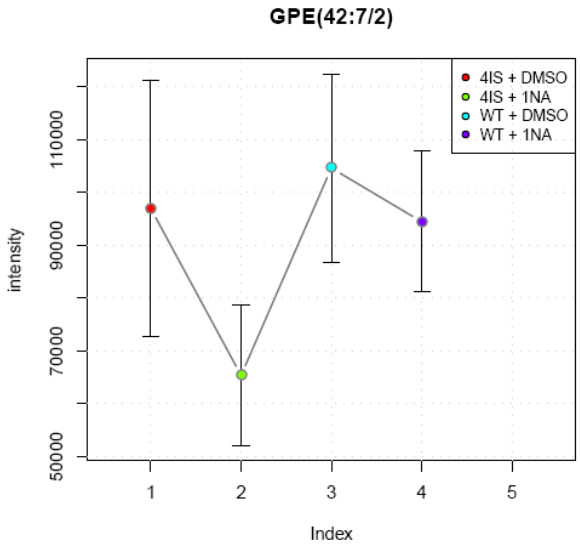
GPE(42:7/2)
intensity
50000
70000
90000
110000
1
2
3
4
5
Index
4IS + DMSO
4IS + 1NA
WT + DMSO
WT + 1NA

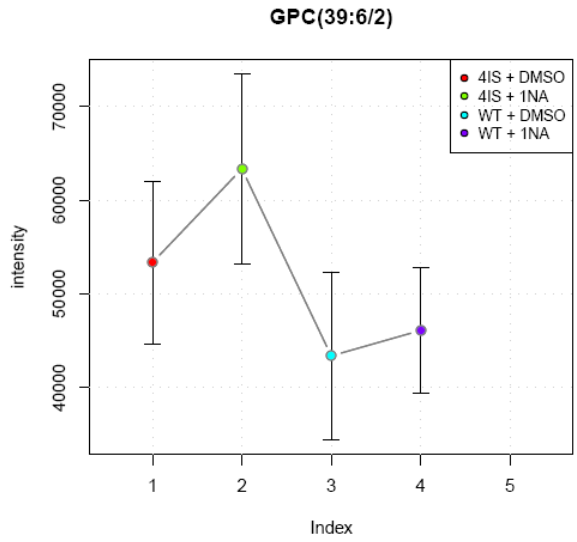
GPC(39:6/2)
intensity
Index
4IS + DMSO
4IS + 1NA
WT + DMSO
WT + 1NA

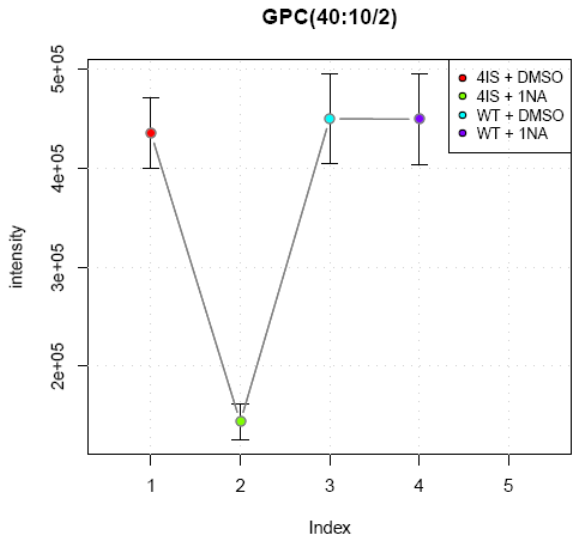
GPC(40:10/2)
intensity
Index
4IS + DMSO
4IS + 1NA
WT + DMSO
WT + 1NA

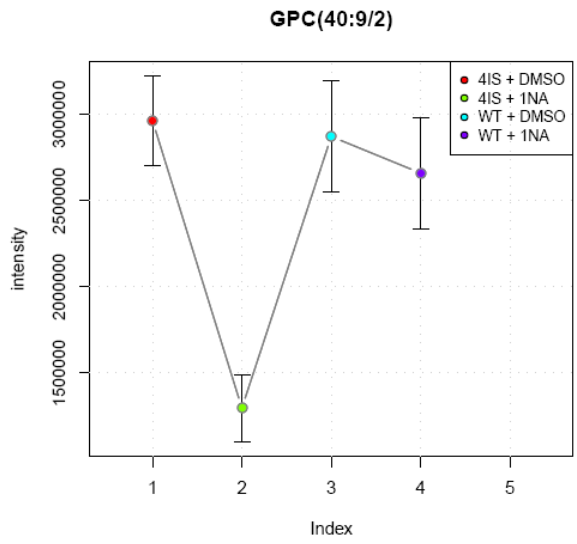
GPC(40:9/2)
intensity
Index
4IS + DMSO
4IS + 1NA
WT + DMSO
WT + 1NA

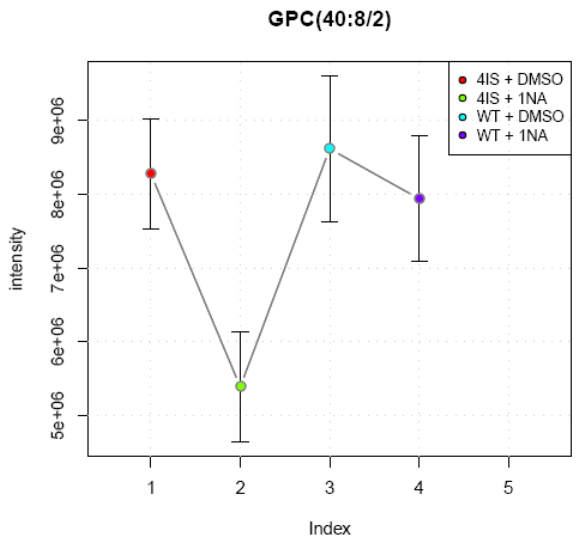
GPC(40:8/2)
intensity
Index
4IS + DMSO
4IS + 1NA
WT + DMSO
WT + 1NA

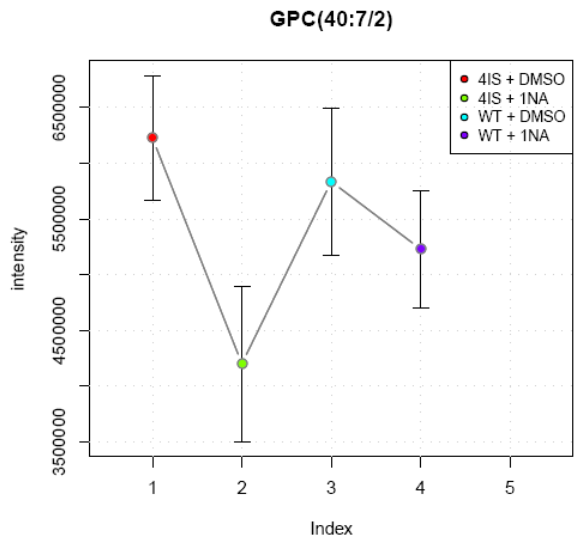
GPC(40:7/2)
intensity
Index
4IS + DMSO
4IS + 1NA
WT + DMSO
WT + 1NA

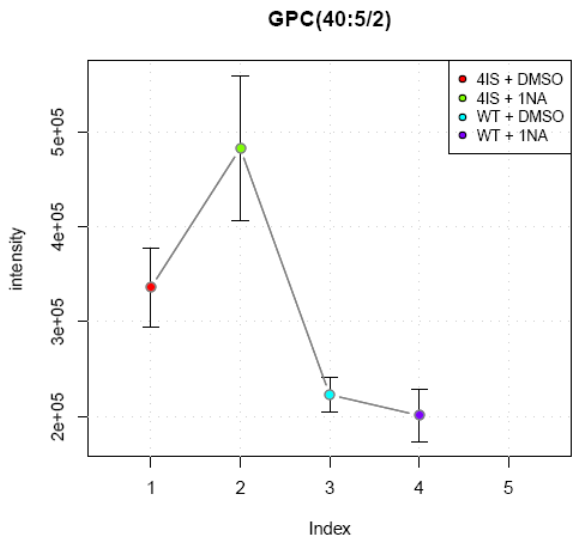
GPC(40:5/2)
intensity
Index
4IS + DMSO
4IS + 1NA
WT + DMSO
WT + 1NA

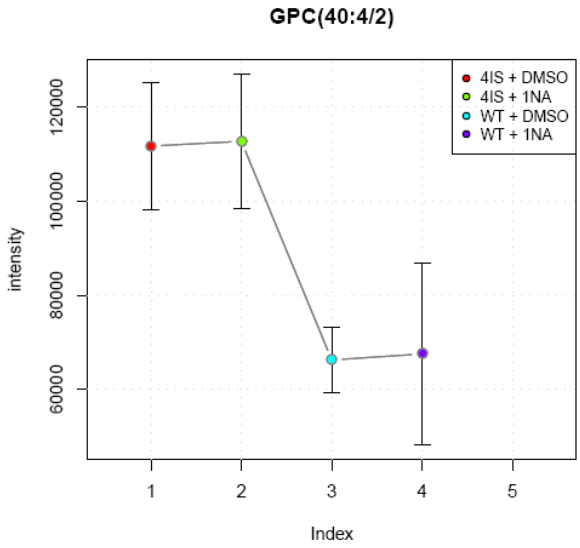
GPC(40:4/2)
4IS + DMSO
4IS + 1NA
WT + DMSO
WT + 1NA
intensity
60000
80000
100000
120000
1
2
3
4
5
Index

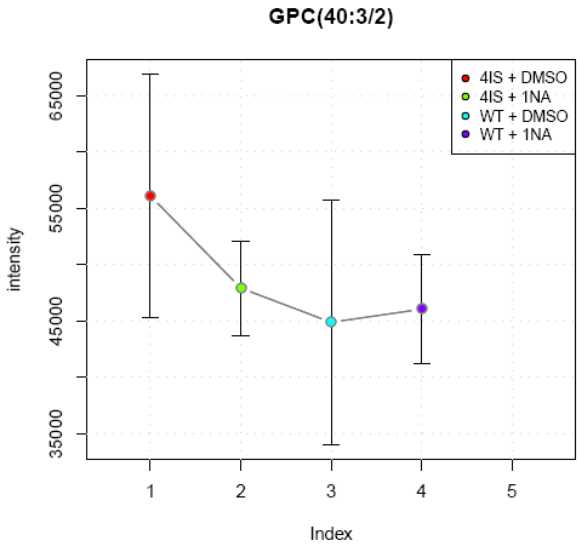
GPC(40:3/2)
4IS + DMSO
4IS + 1NA
WT + DMSO
WT + 1NA
intensity
35000
45000
55000
65000
1
2
3
4
5
Index

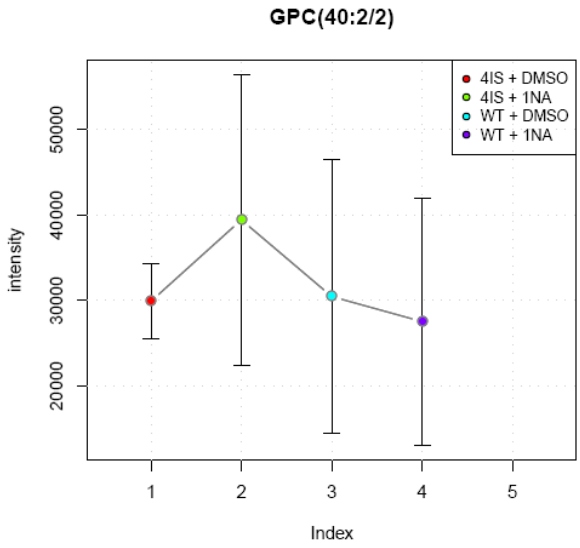
GPC(40:2/2)
4IS + DMSO
4IS + 1NA
WT + DMSO
WT + 1NA
intensity
20000
30000
40000
50000
1
2
3
4
5
Index

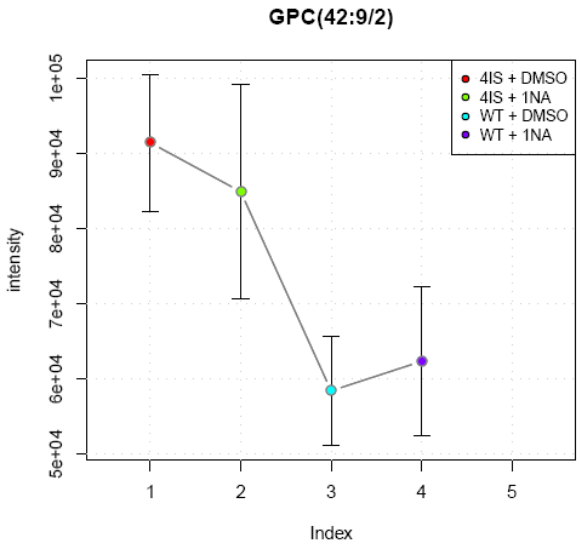
GPC(42:9/2)
4IS + DMSO
4IS + 1NA
WT + DMSO
WT + 1NA
intensity
5e+04
6e+04
7e+04
8e+04
9e+04
1e+05
1
2
3
4
5
Index

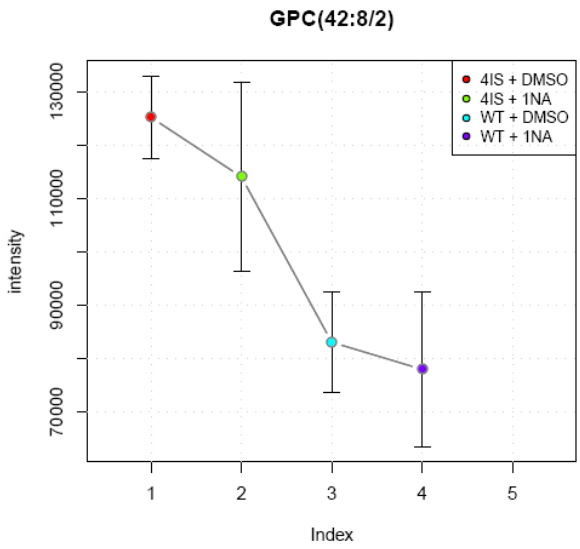
GPC(42:8/2)
4IS + DMSO
4IS + 1NA
WT + DMSO
WT + 1NA
intensity
70000
90000
110000
130000
1
2
3
4
5
Index

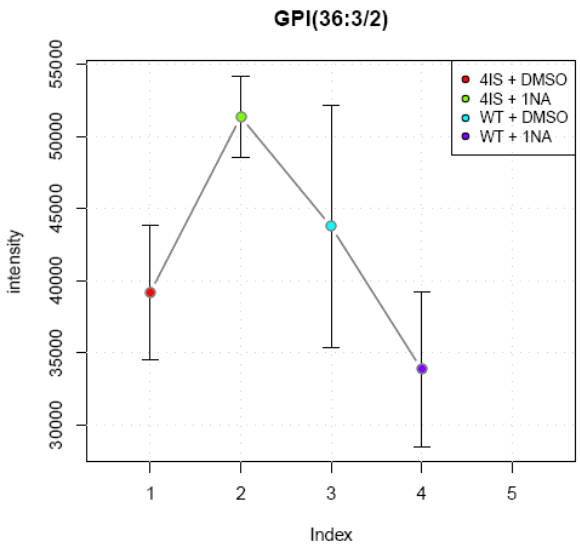
GPI(36:3/2)
4IS + DMSO
4IS + 1NA
WT + DMSO
WT + 1NA
intensity
30000
35000
40000
45000
50000
55000
1
2
3
4
5
Index

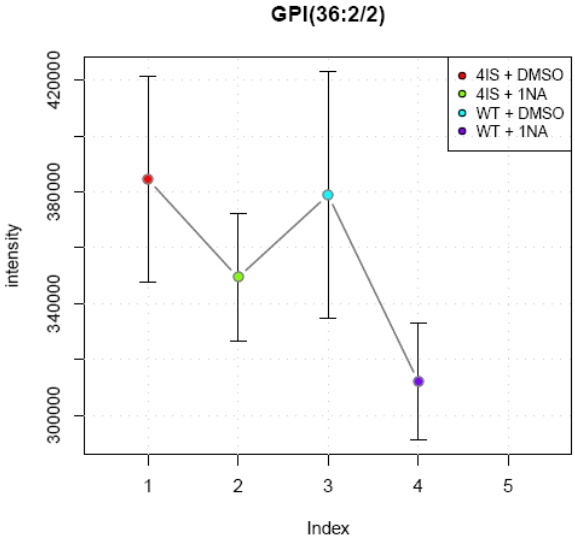
GPI(36:2/2)
intensity
300000
340000
380000
420000
1
2
3
4
5
Index
4IS + DMSO
4IS + 1NA
WT + DMSO
WT + 1NA

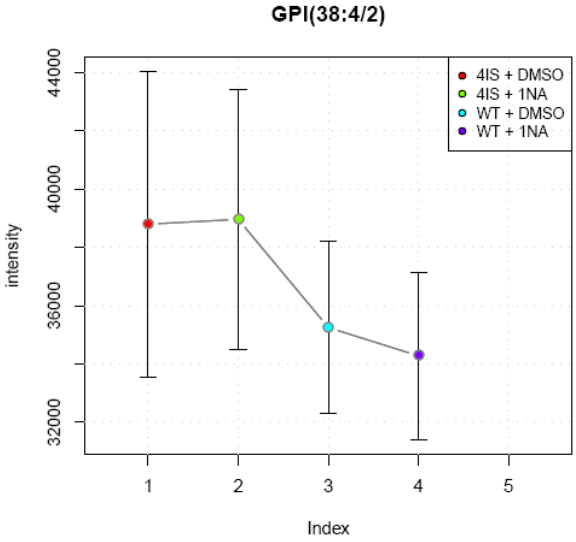
GPI(38:4/2)
intensity
32000
36000
40000
44000
1
2
3
4
5
Index
4IS + DMSO
4IS + 1NA
WT + DMSO
WT + 1NA

Acknowledgements

First and foremost I would like to thank my supervisor PD Dr. Martin Wiese for giving me the opportunity to carry out the research for this thesis in his lab, first in Hamburg and later in Glasgow. You were always approachable and had an abundance of ideas and knowledge to help with all sorts of questions and problems if I needed you, yet you also left me the freedom to find my own solutions and taught me how to be an independent researcher.

I am also very grateful to Iris Bruchhaus for acting as my second supervisor, to Richard Burchmore for conducting the MS analysis of potential LmxMPK4 substrates, to Claudia Sander-Jülch for conducting the FACS experiments, to Kavitah Shah for synthesising the inhibitor 1Na and to Joachim Clos for supplying the pJCduet vector.

Furthermore I would like to thank all members of the Wiese workgroup over the years for their support, advice and most of all for their friendship, which made the lab an enjoyable place to work in. Anne Scholz for many lively and fun discussions and much mentoring during the first year, Inga for conducting much preliminary work on the LmxMPK4 project, Annette for doing the original cloning of the LmxMPK4-LmxMKK5 co-expression construct and the preliminary assays, Anne McDonald for your kindness and much help with tissue culture and general lab work, Heidi Rosenqvist for the conducting of the MS/MS analyses, for your speedy email replies and for many an hour spent patiently explaining data to me. The move to Glasgow during the middle of the thesis was made so much easier by Nadja, Maja and Stefan, so that it was indeed a great experience. Thanks to all of you for tackling everything together, for exploring Glasgow and for raucous laughter in the purple room. Maja, you were a wonderful flatmate and Nadja, you taught me the value of systematic, thorough experiments. Both of you became really good friends and made Glasgow feel like home. A thank you also goes to Patrick that you took the time to proof-read my paper and parts of this thesis. You always cheered me up with your black humour and work was much more fun when accompanied by the most elaborate, passionate discussions about pretty much anything. My thanks also go to everyone in Lab 3. You all welcomed us with open arms when we arrived at Strathclyde and were always happy to help. I have really enjoyed working with you and getting to know you all.

The metabolic profiling analyses would not have been possible without a great amount of help from a number of people. Saskia, you familiarised me with the whole topic, taught me all steps of the extraction process and took a lot of time to introduce me to the principles of the bioinformatic analysis. Your enthusiasm and dedication to your work has been very infectious and inspiring. Ruben, thank you that you ultimately conducted the analysis of

the metabolomics data and that you supplied me with the principal component analysis and the trendplots of metabolites shown in this thesis. You were always really helpful and quick with a smile and it is a shame you were only in Glasgow for a rather short time. Finally, thank you to Leon for tirelessly conducting the LC-MS/MS analyses.

I was very lucky to be able to attend the summer course “Biology of Parasitism” in Woods Hole. Thank you, Martin that you allowed me to go. Also, I am very grateful to all the professors and students taking part in the course for not only giving me a wonderful, albeit exhausting, two months, but especially for inspiring a love for Parasitology.

I have had a great time in Glasgow and made some wonderful friends. Thank you in no particular order to Daniela, Raph, Flo, Flavien, Sara, Stuart, Dave, Tobi, Frank, Johannes, Filip, Nath, Nick, Frøya, Amber, Emily and all the others for many trips to the Highlands, evenings in the pubs, a homely flat to live in, one trip to Chile, afternoons in the park and generally for your support and friendship. A special thank you goes to Daniela, for always being there, many laughs and some great adventures.

Last, but definitely not least, I would like to thank my parents, my sister and my grandmother, for your enthusiastic, tireless and loving support. I am who I am because of you.